APPLICATION OF BIDENTATE N,N′-DONOR EXTRACTANTS IN THE HYDROMETALLURGICAL SEPARATION OF BASE METALS FROM AN ACIDIC SULFATE MEDIUM

A THESIS SUBMITTED IN FULFILMENT OF THE

REQUIREMENTS FOR THE DEGREE OF

DOCTOR OF PHILOSOPHY

IN THE FACULTY OF SCIENCE

OF

RHODES UNIVERSITY

by

ADELEYE ISHOLA OKEWOLE

FEBRUARY 2012

ABSTRACT

Bidentate imidazole-based extractants,1-octylimidazole-2-aldoxime (OIMOX) and 1-octyl-2-(2′-pyridyl)imidazole (OPIM), along with dinonylnaphthalene sulfonic acid (DNNSA) as a synergist, were investigated as p otential selective extractantsfor $Cu^{2+}$and Ni^{2+} respectively from base metals in a solvent extraction system. The study was extended to evaluate the sorption and separation of $Ni^{2+}$from other base metals in a solid-solution system using microspherical Merrifield resins and n anofibers functionalized with 2,2′-pyridylimidazole.

Copper was effectively separated with OIMOX and DNNSA as extractants from nickel with $\Delta pH_{½}$ ≈1.05 and the extraction order of Cu^{2+} > Ni^{2+} > Zn^{2+} > Cd^{2+}> Co^{2+} was achieved as a function of pH. At pH 1.65 the extracted copper, from a synthetic mixture of the base metals reached 90.13(±0.90)%, and through a two-step extraction process 98.22(±0.29)% copper was recovered with negligible nickel and cobalt impurities. Stripping of the copper from the loaded organic phase using TraceSelect sulphuric acid at pH 0.35 yielded 96.60(±0.44)% of the loaded quantity after the second stage of stripping.

The separation of Ni^{2+} from the borderline and hard acids; Co^{2+}, Cu^{2+}, Zn^{2+}, Fe^{2+}, Fe^{3+}, Mn^{2+}, Mg^{2+} and Ca^{2+} at a pH range of 0.5-3.5 with OPIM and D NNSA was acvieved to the tune of a $\Delta pH_{½}$≈ 1.6 with respect to cobalt from a sulfate and sulfate/chloride media. A three-stage counter-current extraction of Ni^{2+}, at the optimized pH of 1.89, from a s ynthetic mixture of Ni^{2+}, Co^{2+} and Cu^{2+}, yielded 99.01(±1.79)%. The total co-extracted Cu^{2+} was 48.72(±0.24)% of the original quantity in the mixture, and it was 19.85(±0.28%) for Co^{2+}. The co-extracted Cu^{2+} was scrubbed off from the loaded organic phase at pH≈8.5 by using an ammonium buffer, while co-extracted Co^{2+} was selectively and quantitatively stripped with H_2SO_4 at pH 1.64. The total recovery of Ni^{2+} by stripping at pH 0.32 was 94.05(±1.70)%.

In the solid-liquid system, Ni^{2+} was separated from Co^{2+}, Cu^{2+}, and $Fe^{2+}$with the microspherical resins funtionalised with 2,2′-pyridylimidazole by a separation factor (β) in the range 22-45. Electrospun nanofibers as sorbents yielded high sorption capacity in the range of 0.97 - 1.45 $mmol.g^{-1}$ for the same metals ions.

Thus, 1-octylimidazole-2-aldoxime (OIMOX), and1-octyl-2-(2′-pyridyl)imidazole (OPIM) can be effectively utilized alongside DNNSA as a co-extractant in the separation of Cu^{2+} and Ni^{2+} respectivelyfrom base metals in acidic sulfate medium in a solvent extraction process, and the latter as a selective ligand in the solid-liquid separation of Ni^{2+} from Co^{2+}, Cu^{2+}, and Fe^{2+}.

Keywords: solvent extraction, chelating ion exchange, imidazole-2-oxime, 2,2′-pyridylimidazole, stereochemistry, stability constants.

ACKNOWLEDGEMENTS

Firstly, thanks to the almighty God for his grace, guidance and provision over me through out the duration of this study.

The role of my supervisor, Dr. Z.R. Tshentu cannot be quantified. He has given me an unequalled kind of leadership that saw me through this study despite the numerous challenges involved. You gave me the room to breathe, but at the same time, I knew your door was always open.

Also, thanks to Prof G. Watkins for his contribution, and the entire Department of Chemistry, Rhodes University for giving me the opportunity to study towards a Doctor of Philosophy (Science) degree in Chemistry. Prof N. Torto, the Head of Department and a renowned analytical chemist in Southern Africa, is acknowledged for encouraging me.

My sincere thanks goes to all the support staff of the Chemistry Department including; A. Adriaan, V. Dondashe,R. Douglas, H. Mcuba, J. Fourie and F. Chindeka, for all their help with the ICP and other instruments.

Dr E. Hosten from the NMMU Chemistry Department is appreciated for his assistance with the solid state UV/Vis studies and ICP-MS analysis.

Thanks to Labs F2, F3, and F5 group members.First and foremost, my thanks to Nomampondo Magwa, my labmate in Lab F2, for all her assistance, Ryan Wamsley for his ready assistance particularly on t he stability constants determination, and Sunday ogunlaja for his assistance with the proofreading of this document. Isaac Gundhla, Omolola Fayemi, Avela Majavu and P humelele Kleyi, you all made my study exciting. Abdullahi Sobola my graduating colleague, you are a wonderful friend, your ready assistance to me is highly appreciated.

Thanks to Tope Olalekan, my brother and friend, Kenny Awokoya and B ridget Moronkola for your inspirational support.

Special thanks go to Pastor A.Adedeji, Pastor S. O. Tella and Deaconess O. Okoh all of the Redeemed Christian Church of God, South Africa for being my encouragers when I needed to vent. Mrs C. K. Idahosa from my host institution, I say thank you. Thanks to Zelalem Shibeshi (my church treasurer) for great friendship. Nelson Oghenekaro (my flat-mate) Siviwe Babane and Rirhandzu Mkhari for their friendship.

I would like to thank Andrew Mellon Scholarship and National Research Foundation for their financial support as well as the Joint Research Council of Rhodes University for funding this research work.

I would also like to thank my employer, Yaba College of Technology, Lagos, Nigeria, for granting me the study leave to undertake this study.

Finally, I would like to gratefully acknowledge my family. Thanks to my wife, Olayinka Okewole, for her patience and love. My children: Grace, Gideon, David, Dominion, and Deborah Okewole, for their sacrifices. My mom and my younger ones; for missing me so much while I was far away in South Africa. You guys are amazing!

TABLE OF CONTENTS

LIST OF TABLES

LIST OF FIGURES

LIST OF SCHEMES

LIST OF ABBREVIATIONS

AC - Alternating Current

Amplats - Anglo American Platinum Corporation Ltd

BC - Before Christ

BET- Brunauer- Emmet-Teller

CFSE - Crystal Field StabilizationEnergy

D - Distribution Ratio

DC - Direct Current

DEPHA - Di-2-Ethyl Hexyl Phosphoric Acid

DIMOX-1-Decylimidazole-2-aldoxime

DMF-Dimethylformamide

DMG - Dimethylglyoxime

DNNSA - Dinonyl Naphthalene Sulfonic Acid

DpH - Decomplexation pH

DPIM -1-Decyl-2-(2′-pyridyl)imidazole

FTIR - Fourier Transform Infrared

GC - Gas Chromatography

HL - Chelating Agent

HPIM -1-Hetyl-2-(2′-pyridyl)imidazole

HSAB- Hard and Soft Acid and Base

ICP-MS- Inductively Coupled plasma-Mass spectrometry

ICP-OES - Inductively Coupled plasma-Optical Omission Spectroscopy

IX - Ion Exchange

KD_{HL}- Distribution coefficients of the extractant (reagent)

K_a - Ionization constant

K_{ex} -Extractive equilibrium constant

K_f - Formation constant

K_{sp}- Solubility product

L - Ligand

logβ - Stability constant

MIMOX -1-Methylimidazole-2-aldoxime

ML - Metal Ligand chelate

N-donor - Nitrogen-donor

NMR - Nuclear Magnetic Resonance

O-donor - Oxygen-donor

O_h- Octahedral

OIMOX-1-Octylimidazole-2-aldoxime

OPIM -1-Octyl-2-(2′-pyridyl)imidazole

PGM- Platinum Group Metals

PIMH - 2,2′-Pyridylimidazole

pK_a - Acid dissociation constant

PLS - Pregnant Liquor Solution

SEM - Scanning Electron Microscopy

SPE - Solid Phase Exctraction

SSX - Synergistic Solvent Extraction

SX - Solvent Extraction

T_d– Tetrahedral

tms - Transition metal series

XPS - X-ray Photoelectron Spectroscopy

β - Separation factor

CHAPTER 1

●●●●

INTRODUCTION

1.1 Base metals

There is an increasing demand for production of metals of high purity in the metallurgical industries in an attempt to meet the corresponding demand for both industrial and domestic applications. This has been the catalyst for the development of simpler and more economical routes for purification of metal ions from their ore solutions. The environmental impact of the processes involved as well as the ultimate goal of cost-saving production has further heightened the decision of would-be investors in the choice of methods of operation. Metallurgical practices involving the beneficiation of metals from their ores dates back to 4000 BC,[1] in which metals were obtained as alloys such as brass or bronze by crude and time-consuming methods of purification. However, developments advanced to a variety of techniques involving processes such as pyrometallurgy, hydrometallurgy, flotation, etc.

Pyrometallurgical routes, though more traditional, are gradually giving way to the hydrometallurgical methods owing to the high cost for high temperature processing and the toxicity of the gases emitted. Hydrometallurgical techniques otherwise known as the wet processes involve the dissolution of metalsfrom their ores (leaching) and the use of chemical reagents for the selective extraction or precipitation of the metals from the aqueous solution at much lower temperatures. Thus fewer environmental problems are involved and are also deemed to be more economical.[2] The birth of modern hydrometallurgy is said to date back to 1887 with the cyanidation process of treating gold ores and the Bayer process for the production of alumina,[3] however more developments are required on this technique in view of its economic benefits and simplicity of operation. Improvements of the

underlying chemical processes of this technique require a thorough knowledge and investigation of the chemistry involved in order to achieve a m eaningful advancement of this technology. Coupled with this, is the major need for best practice in tracking value across all aspects of mining and processing operation so as to make it more economically attractive.[4]

Base metals is a term used informally to refer to metals that oxidize or corrode relatively easily,and metals thatreact variably with hydrochloric acid forming hydrogen.[5] They are common and inexpensive compared with the noble metals, and includemetals like nickel, cobalt, copper, iron, lead, zinc, cadmium, manganese, etc. They are naturally found in the earth's crust. Since most of them constitutethe 3d elements of the transition series they are further classified as the earlier, mid or later 3d metals depending on their position in the periodic table of the elements. An understanding of their coordination chemistry is very important in deriving a successful strategy for their separations.

1.1.1 Nickel

Nickel, the 27th most abundant element and the 7th most abundant transition element, is the major element of interest in this study. It has wide applications in catalysis, coinage, dry-cell, stainless steel, etc. It occurs in an economic deposit in the form of the laterites (oxides or silicate ores) or as sulfides predominantly in more temperate regions such as Canada, Russia and South Africa. Although Russia is the presently known world's leading nickel producer, South Africa is one of the leading nations with deposits in the sulfide form.[6] Nickel sulfides are commonly found in the form of pyrrhotite [$(NiFe)_7S_8$] and pentlandite [$(NiFe)_9S_8$]. Nickel, copper and cobalt are also by-products in the processing of platinum group metal (PGM) ores.They arefound in economic concentrations in the layered reefs associated with the mafic rocks of the Rustenburg layered suite of the bushveld igneous complex of South Africa.[6] South Africa produced 34,000 metric tonnes of nickel in 2009.[7] Out of which Nkomati, a nickel mine located in the Machadodorp area of Mpumalanga, produced 4,495 tonnes of nickel alone by means of underground shaft and open pit mining. Thus, platinum production remains the driving force for nickel and c obalt mining in South Africa. However, beneficiation

from this element along with other base metals had been shown to be very low thus necessitating an improved refining technology.[8]

The coordinationchemistry of nickel(II) reveals its ability to form stable complexes as has been predicted by the Irving-Williams series.[9] However, the nickel(II) ion has been found to adopta wide varieties of coordination numbers(CNs) hence the complicated chemistry of nickel.[10] Although, the octahedral $[Ni(H_2O)_6]^{2+}$ion is predominant in the aqueous state, four coordinate complexes of square-planartype are numerous whilefew tetrahedral geometries have been found. Five coordinate complexes in the form of square-pyramid and trigonal-bipyramid are rarely formed. The significance of the coordination chemistry of each metal ion as a function of its relative stability in the medium under consideration cannot be over emphasized in deciding thechoice of method forits separation. Thus nickel(II) has been shown to form the most stable spin-free six-coordinated complexes of the later 3d transition metal ions,[11] and as such forcing it into this configuration has been a target for its separation from other metal ions in this category in extractive metallurgy. It is also known that nickel(II) forms highly stable complexes that are of square-planar geometry especially with the α,α'-dioximes and other oxime derivatives.[12] Thus ligands of these categories can be exploited as potential nickel specific extractants. However limitations are encountered in the fact that these complexes are only formed at relatively high pH values. Tetrahedral nickel(II) are rather uncommon and relatively unstable.[13]

1.1.2 Cobalt

Cobalt is always closely associated with nickel in occurrence and also shares a lot of similarities with nickel in both physical and chemical properties owing to their adjacent positions in the periodic table of the elements. Hence this poses challenges in the separation of these two metals. Nickel deposits contain cobalt in low concentrations in the form of sulfides, arsenides and carbonates such as linnaeite (Co_3S_4), cobaltite (CoAsS), and sphaerocobaltite ($CoCO_3$). Cobalt is produced in South Africa as a by-product of PGM operations as well as a co-product of a single nickel operation. Commercial operations using solvent extraction for cobalt refining byAnglo Platinum Rustenburg base metal refinery in South Africa dates back to 1979.[14]

The cobalt(II) ion, similarly to nickel(II), exists as hexahydrate ions,$[Co(H_2O)_6]^{2+}$, with octahedral geometry in dilute aqueous solution. However, unlike nickel the rate of water exchange of the cobalt ion is much higher hence the complex formation proceeds with the cobalt divalent ion much faster.[15] The cobalt(III) complexes on the other hand are less labile and form with relative ease compared with nickel(III). Cobalt(II), in a concentrated electrolytic solution,more readily formsa tetrahedral geometry than the octahedral. Square-planar complexes are also formed although they are not numerous. These stereochemical differences can be exploited in the hydrometallurgical separation of nickel from cobalt.

1.1.3Copper

Copper occurs in its commonest form as chalcopyrite, $CuFeS_2$, a bright yellow ore that accounts for 50% of the world's copper deposits.[16] Other forms are malachite, $Cu_2CO_3(OH)_2$, the bright green ore and the red ore cuprite, Cu_2O.The oxide ore of copper occurs less widely than the sulfide ores.

The blue-green aqua ion of copper, $[Cu(H_2O)_6]^{2+}$, showed that two of the axial water molecules are further from the metal ion than the other four equatorial waters due to the Jahn-Teller effect,[13] as such copper does not bind with the 5^{th} and 6^{th} ligands strongly.Multidentate ligands that coordinate through O or N atoms form copper(II) complexes of considerable stability. Copper production received a boost with the introduction of the hydroxyoximes as extractive reagents in the application of solvent extraction in the 1960s.[17] This class of extractants gave rise to the popular commercial LIX reagents produced by General Mills as standard copper extractants. Applications of copper in coinage, electrical, agriculture and even medicinal application underscore the need for improved methods of purification.

1.1.4 Zinc

Zinc is slightly more abundant than copper in the earth's crust with large deposits in the form of its major ore zinc blende in Canada, USA and Australia. About 80% of primary zinc produced is *via* a hydrometallurgical route, that is solvent extraction, however there are two major problems with achieving the successful electrowinning of zinc. Firstly, the presence of traces of organics in the electrolyte solution which may deposit on the cathode resulting on lower current efficiencies which are

detrimental, and secondly, the high purity required of the electrolyte for the successful zinc electrowinning.[18] A process known as the “Zincexprocess” has however been em ployed[18], through which the necessary electrolyte purity is achieved by an elegant two cycle design of the solvent extraction circuit. In the first ‘anionic’ cycle, an amine extractants is used to extract zinc together with some iron from the chloride based leach liquors arising from a c hloride leaching of pyrites cinders. The stripped liquor from the anionic cycle is there after fed into the cationic cycle where di-2-ethyl hexyl phosphoric acid (DEPHA) is used to re-extract zinc from the chloride-containing strip liquor.[19]

1.1.5 Iron

Iron is the most abundant of the base metals in the earth’s crust and is used on the largest scale of any metal. It is also widely distributed, as oxides and carbonates, of which the chiefones are: haematite (Fe_2O_3), magnetite (Fe_3O_4), limonite ($2Fe_2O_3.3H_2O$) and siderite ($FeCO_3$). Iron pyrite (FeS_2) is also common but is not used as a source of iron because of the difficulty in eliminating the sulfur.[16] The deposits in the form of ferric ionhas also been shown to be a major impurity in other metallic ores and i ts removal constitutes one o f the major hurdles in the achievements of successful separation techniques in base metal separation. This borders on its position as a hard acid based on t he HSAB principle of Pearson’s classification.[20] It existsin aqueous solution in its spin-free form (t_{2g}^3 e_g^2), thus it readily forms stable complexes with ligands which coordinate through oxygen. Ferrous ion as a borderline element on t he other hand binds less strongly to o-donors and thus posses less challenges. Removal of ferric ion has however been achieved by selective precipitation prior to separation of the desired metal either by solvent extraction or ion exchange.[21]

1.1.6 Other base metal ions

Other metals in the base metal classification are found at low levels in the pregnant liquor solution (PLS) from leaching of predominantly nickelores. Since they occur as minute and at less desirable level in the context of nickel separations they are often regarded as impurities. These include manganese, cadmium, aluminium, and the alkaline earth metals namely; magnesium and calcium. Removal of these

metals does not pose as much challenges as the erstwhile ions previously discussed.

1.1.7 PGM production

PGM production constitutes a major source of base metals due for separation as shown in Table 1.1. The platinum group metals namely; Os, Ru, Rh, Ir, Pd and Pt are associated with other base metal sulfides and occur in the form of minerals such as braggite, laurite or ferroplatinum. South Africa, for instance, has more than 80% of the worlds platinum reserves and is the world's largest producer of PGMs. These are currently operated by four integrated primary platinum producers. They are Amplats (Anglo American Platinum Corporation Ltd), Impala Platinum, Lonmin Platinum and Northam and their PGM ore bodies contain economic quantities of base metals as by-products.[22] The sulfides are concentrated by the method called floatation and these floatation concentrates are made to undergo smelting and conversion into a PGM-containing nickel-copper matte. Hydrometallurgical treatment of the matte is required to separate the base metals from these precious metals. Table 1.1 shows the analyses of the various PGM concentrates from South African PGM's producers depicting the base metal contents.

Table 1.1: PGM concentrate analyses.[23]

PGM PRODUCERS	Al_2O_3 %	CaO %	Co %	Cr_2O_3 %	Cu %	FeO %	MgO %	Ni %	S %	SiO_2 %	PGM g/t	Total %
Amplats Waterval	3.2	4.7	0.08	0.80	2.1	20	15	3.6	9	34	143	92
Amplats Union	3.8	2.5	0.04	2.59	1.1	15	20	2.2	5	38	142	90
Impala	4.1	2.9	0.06	1.1	1.3	18	18	2.1	5.6	42	138	95
Lonmin Merensky	1.8	2.8	0.08	0.4	2.0	23	18	3.0	9	41	130	101
Lonmin UG2 blend	3.6	2.7	0.06	2.8	1.2	15	21	2.1	4.1	47	340	100
Northam	2.6	3.0	0.05	0.87	1.3	17	18	2.5	5.4	47	132	97

Impala platinum base metal refinery, South Africa, at present produces 17000 t/a nickel, 9000 t/a copper, and 140 t/a cobalt as by-products from a PGM – containing matte.[24] The matte is processed by pressure leaching with the copper electrolyte returned to solubilise the nickel, cobalt, and iron. Thereafter, the residue from this leaching is further leached with sulfuric acid to produce copper sulfate for copper electrowinning and the residue is sent for PGM recovery. The nickel solution is treated with nickel scrap to cement copper and then iron is precipitated. The remaining nickel and cobalt are precipitated as a mixed double salt. In a recent expansion programme, a new refinery to process the mixed nickel cobalt sulfide concentrate that is produced from philnico laterite deposit is planned as illustrated by the flow-sheet in Figure1.1. Although the proposed expansion has not been actualised, this flow-sheet demonstrates the innovative application of solvent extraction technology in nickel/cobalt separation.[24]

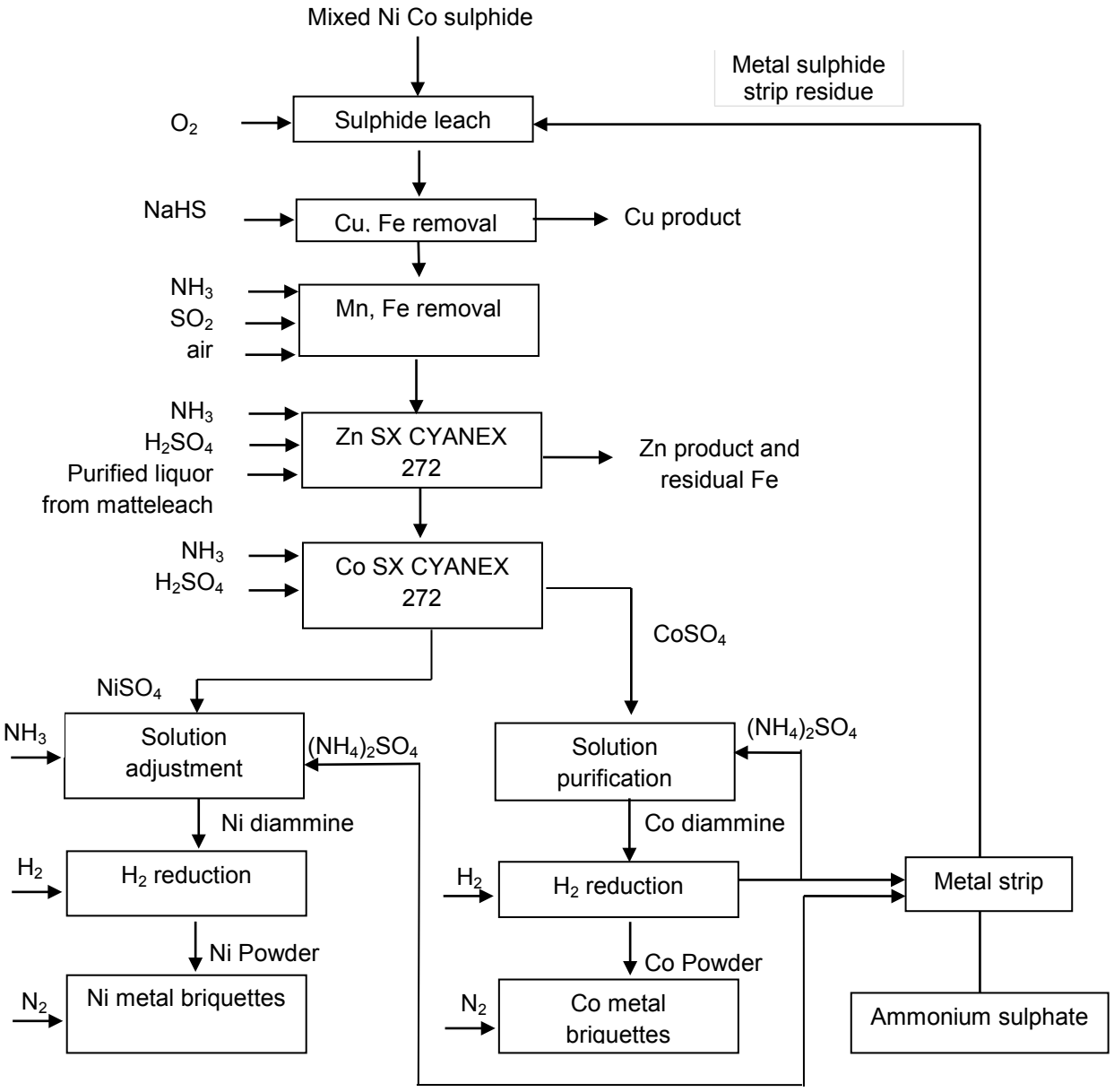

Figure 1.1: Proposed flow sheet for the expanded Impala base metal refinery meant to process mixed nickel cobalt sulfide feed[25]

1.2 Methods of separation

Purification of base metals can be achieved through various techniques ranging from froth floatation, precipitation, distillation, evaporation, and crystallization. However, separation on a l arge scale had always been by high temperature operations (pyrometallurgy) or by the wet methods (hydrometallurgy).

1.2.1 Hydrometallurgical routes

The hydrometallurgical route of metal purification has been commercially applied in the separation of base metals especially in cobalt and nickel separation using the following techniques; sulfide precipitation, precipitation utilizing the oxidation and reduction chemistry, ion exchange (IX) and solvent extraction (SX) processes. Even though each of these processes had proved successful on their own they are not without shortcomings. However, SX has gained wider commercial applications than them all and it still remains a potential route for further development due to its high degree of separation as well as high yield.[26] In addition, it has relatively cheaper operational cost and adaptability of the process to suit the system under consideration is possible. Thus, the initial application in the area of separation of copper from a chloride or ammoniacal solutions have gone further to developing newer extractants and exploiting their application to highly acidic sulfate solution. This became necessary in view of the presence of sulfate ions from oxidation of sulfides as well as sulfuric acid used in acid leaching. Further advancements in the application of SX were achieved with the recent introduction of a synergistic solvent extraction system (SSX), in which two reagents are used in the extraction of a metal ion with enhanced efficiency as compared to an individual extractant.[27,28]

1.2.2 Precipitation

Precipitation in the form of a sulfide has been applied in the separation of cobalt from nickel owing to the difficulty posed by their similar aqueous chemistry. The factor that is being exploited in this case is the lower solubility of the cobalt sulfide compared with nickel sulfide.[15]

Deficiencies are however observed in this technique due to the low cobalt to nickel ratio in the industrial feed solutions which results in cobalt contamination with as much as four parts of nickel thus requiring further processing. A further advance in the application of precipitation as technique is found in selective oxidation/reduction process where, nickel can be selectively reduced at high purity from mixed sulfate solutions by hydrogen under pressure or cobalt is oxidized from mixed sulfides with air under pressure in the presence of ammonia to cobalt(III) state while nickel

remain in solution as nickel(II). Thereafter nickel is precipitated as nickel(II) ammonium sulfate.[29]

1.2.3 Ion exchange

Ion exchange has also been employed in the separation of metals with both anion and cation exchangers, however, they have only enjoyed limited application in commercial sector. In the chloride medium cobalt forms anionic chloro complexes like $[CoCl_3]^-$ and $[CoCl_4]^{2-}$ unlike nickel, and this provides for discrimination between these two metals with anion exchanger. However these complexes are weak and limitations arise from the fact that the stability of these tetrahedral cobalt chloro complexes requires a higher concentration of chloride in which other ions like Fe^{3+}, Cu^{2+}, and Zn^{2+} also form similar chloro complexes, thereby resulting in interference.[30]

Similarly, a cation exchanger had been applied for the removal of nickel in sulfate solutions of high cobalt to nickel ratio but had gained little or no commercially patronage because of the low yield.[29]

Chelating resins based on a microporous polystyrene divinylbenzene matrix with weakly basic functional group have been used in the separation of nickel from cobalt.[31-33] Thus, chelating resins still hold a lot of potential for the application of solid phase extraction methods in base metal ion separation. On this note, this study is further exploiting the application of microporous resins functionalised with 2,2′-pyridylimidazole in the separation of nickel from other base metal ions.

1.2.4 Solvent extraction

Solvent extraction (SX**)** has by far and wide gained much more commercial patronage than the erstwhile methods in hydrometallurgy owing to continuous research in the area of development of extractants, improvement of existing techniques and the economy of the processes involved. SX has been found extremely useful for simple, clean and rapid separation of metal ions. Basically, SX as a separation method involves the transfer of a solute from the aqueous to the organic phase or vice versa. In hydrometallurgical separation, the organic extractant is applied to selectively extract the metal ion of interest from an aqueous

solution and with a favourable distribution ratio the metal ion is thus loaded into the organic phase. The metal can be back extracted in its purer state. Thus the relative distribution ratio of the metal ions present in the solution becomes very important for effective separation factor to be achieved. This can be achieved *via* the chelating system as in the application of hydroxyoximes,[34] in which the neutral metal species is formed through chelating with organic chelating extractants or through ion-association by the formation of dehydrated cationic or anionic metal complex and ion pairing it with a counter ion. The later can be achieved with the use of a synergist which acts as a bulky counter ion. The choice of solvent (diluents with or without a modifier) is also very important hence it is possible to have a solvating system in which the solvent participates in the extractive process.[35]

(a) Quantitative treatment of SX equilibria[36,37]

Consider a chelating agent HL applied in the solvent extraction of a metal ion M^{n+} as shown in equation 1

$$M^{n+} + nL^{-} \rightleftharpoons ML_n \quad (1)$$

The chelating system of the extraction process can be considered as consisting of four equilibrium steps, each with an equilibrium constant.

First, the chelating agent HL distributes between the aqueous and the organic phases;

$$(HL)_a \rightleftharpoons (HL)_o \quad (2)$$

$$K_{D_{HL}} = \frac{[HL]o}{[HL]a} \quad (3)$$

where $K_{D_{HL}}$ is the distribution coefficient of the extractant (reagent)

and the subscripts o and a refer to organic and aqueous phase respectively.

Second, the reagent in the aqueous phase ionizes;

$$HL \rightleftharpoons H^{+} + L^{-} \quad (4)$$

$$K_a = \frac{[H^+][L^-]}{[HL]} \quad (5)$$

where K_a is the ionization constant of the reagent.

Third, the metal ion chelates with the reagent anion to form a neutral molecule;

$$M^{n+} + nL^{-} \rightleftharpoons ML_n \quad (6)$$

$$K_f = \frac{[ML_n]}{[M^{n+}]\,[L^{-}]^n} \quad (7)$$

where K_f is the formation constant of the chelate.

Finally, the chelate distributes itself between the organic and aqueous phases;

$$(ML_n)_a \rightleftharpoons (ML_n)_o \quad (8)$$

$$K_{D_{MLn}} = \frac{[ML_n]_o}{[ML_n]_a} \quad (9)$$

where $K_{D_{MLn}}$ is the distribution coefficients of the chelate.

When all the four equilibria are represented by a single step, we have;

$$M_a^{n+} + nHL_o \rightleftharpoons (ML_n)_o + nH_a^{+} \quad . \quad (10)$$

then an extraction equilibrium constant (K_{ex}) expressed in terms of thermodynamic activities of the reacting species is given by equation 11 below;

$$K_{ex} = \frac{[ML_n]_o \times [H^+]_a^n}{[M^{n+}]_a \times [HL]_o^n} \quad (11)$$

Thus, it is obvious from the terms expressed in equation 11 that the pH as well as the ligand concentration play vital role in determining the extraction efficiency of a given system.

The distribution ratio (D) defined as the ratio of the concentration of the total metal species in the organic phase to that in the aqueous (regardless of its mode)[36] is given by the expression (12), on the assumption that the metal chelate distributes largely in the organic phase and that the metal ion does not hydrolyse in the aqueous phase.

$$D \approx \frac{[ML_n]_o}{[M^{n+}]_a} \quad (12)$$

Substituting all the necessary terms from equations 3-9 and 12 into equation 11 with all the equilibrium constants included, we have the derivation of D in equation 13. Thus, the separation of two metals chelates at a given pH can be predicted from this equation.

$$D = \frac{K_{D_{\mathrm{MLn}}} K_f K_a^n}{K_{D_{\mathrm{HL}}}^n} \cdot \frac{[\mathrm{HL}]_o^n}{[\mathrm{H}^+]_a^n} \qquad (13)$$

The separation factor (β) given as ratio of the individual distribution ratios of the two metal chelates with a given reagent (equation 14) is rather dependent on the relative formation constants (K_f) and on the relative solubilites ($K_{D_{\mathrm{MLn}}}$) of the chelates,[37] and not pH dependent, where n is the same for both M-to-L reactions.

$$\beta = \frac{D_1}{D_2} = \frac{K_{f1} K_{D_{\mathrm{MLn1}}}}{K_{f2} K_{D_{\mathrm{MLn2}}}} \qquad (14)$$

However, where n_1 and n_2 are not the same, separation can be enhanced through stereochemical consideration since pH dependence becomes a factor. Hence, the separation of the metal ions in this study was carried out with the control of the pH for possible formation of different geometrical complexes by these metal ions. Generally the order of extraction may also be predicted by the stability of the complexes, and by the differences in solubilities of the chelates.

(b) Percentage extraction

The fraction of the metal extracted is equal to the moles of metal in the organic layer divided by the total number of moles of metal. The percentage extracted is given by;

$$\%E = \frac{\text{total number of moles in org. phase}}{\text{total number of moles in the system}} \text{ x } 100 \qquad (15)$$

It can be further shown that

$$\%E = \frac{100\,D}{D + \left({}^{V_a}/_{V_o}\right)} \qquad (16)$$

where V_o and V_a represent the volumes of the organic and a queous phases respectively. Thus, the percentage of extraction varies with the volume ratio of the two phases and the distribution ratio (D).[37]

(c) Choice of diluents

The role of diluents in a SX system is accessed by the influence it plays on the distribution ratios of the metal ions in SX.[35] Most diluents are made up of de-aromatized hydrocarbons containing between 17-23% aromatics and about 40% cyclo paraffins. Examples of diluents used in SX of metals include xylene, toluene, kerosene, shellsol of different classifications such as shellsol A, shellsol 2325, etc. A decision on the choice of diluents is made considering its properties such as flash point, boiling point, viscosity as well as its environmental effects. Diluents may influence the selectivity of the organic and as such the aromatic content is guided as it is known to increase the solubility of the metal-extractant complex in the organic phase, acts as equilibrium modifier, and also influences the selectivity of the extractant.[36] In the extraction of copper with oximes, it has been shown that the selectivity for copper over iron increases with the aromatic content of the diluents.[37]

(d) Synergism

Synergistic solvent extraction system (SSX) uses a combination of the extractant and a synergist to enhance metal selectivity. Research to date has indicated that different metals react differently with extractants and synergist in SSX system and that control of the ratio of the synergist to the extractant may be necessary in an extraction to maintain optimum metal ions separation. This would require a fundamental understanding of the type of complexes formed between the extractant/synergist and the different metal ions under certain condition. The use of mixed extractant system in a solvent extraction of metal ions has received significant developments due to the increase in the extraction efficiency caused by the synergistic enhancement.[38] The synergists that can be used as a second extractant include di-nonylnaphthalene sulfonic acid, di-dodecylnaphthalene sulfonic acid, di-n-octylmethyl sulfonic acid.[39] On this note, a similar concept is employed in the present study, with the use of di-nonylnaphthalene sulfonic acid as a synergist in a sulfate medium to facilitate the transfer of the cationic complexes formed through ion-pair formationsince the sulfate ions suffer from lack of phase transferability.

1.3Separating agents

In hydrometallurgy, the development of metal-specific ligands as metal ion extractants applicable for metals separation has been on the increase especially in the solvent extraction processes. This became necessary because of the numerous problems associated with removal of notable impurities, for instance, the presence of iron in base metal ores which is readily oxidized to Fe(III) posses a great challenge since it is preferentially extracted over other divalent ions by the majority of existing extractants since it is astrong Lewis acid.[20] Separating agents that would be feasible for base metals separation in a strongly acidic medium must therefore be able to reject impurities such as Fe(III) in addition to being specific to the metal ion of interest. On this note the donor atom of the ligand becomes a very strong consideration in the choice of extractant for a specific metal ion separation. Also considering the industrial application, from an economic point of view, it must be cheap to manufacture and be stable under the condition employed.[40] Steric effects and the nature of donor atoms are major consideration in the design of metal-specific ligands as well as other operating requirements such as high selectivity, low aqueous solubility, high loading capacity and rapid extraction kinetics.[41,42]

1.3.1 The oxygen donors

The oxygen-donor (O-donor) ligands have been known to be of wide applications in the separation of base metals. In the commercial sector, the oximes in the form of hydroxyoximes, carboxylic acids in form of versatic acids, and the phosphoric acids and derivatives in the form of di-2-ethylhexylphosphoric acids (D2EHPA) (Figure 1.2), etc., have been exploited extensively. However, the major shortcomings lie in their inability to reject the Fe(III) ions hence the practice of the precipitation of this ion prior to extractions.[43] The O-donor extractants in addition do not readily reject the other A-type metal ions such as Mg^{2+}, Mn^{2+} and Ca^{2+}.[44]

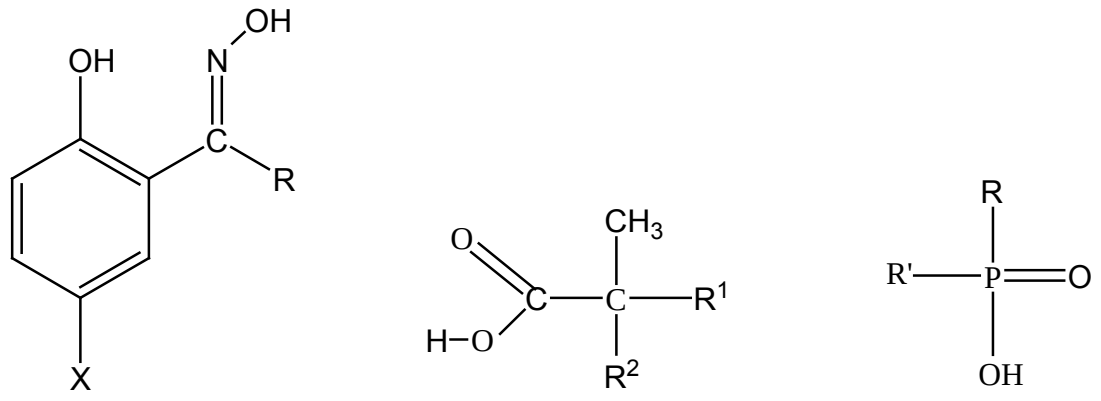

a b c

Figure 1.2: Representative chemical structures of the O-donor extractants. (a) Represents the hydroxyoximes (LIX reagents), (b) the carboxylic acids (Versatic acids), and (c) the phosphoric acid derivatives (CYNEX reagents)

The hydroxyoximes have proved more useful as copper specific extractants owing to the rapid formation of chelate complexes by the acidic functional group with cupric ion in contrast to ferric ion.[45] However, it may also permit the transfer of slowly extracted species as stated by Kordosky.[26] The alkyl phosphoric acid and derivatives have witnessed successful application in the separation of cobalt from nickel in sulfatemedium, and the separation factors follow the order phosphoric < phosphonic < phosphinic acids.[46] Nevertheless they all have proved to be active calcium extractants which is considered as deleterious in sulfate circuits. Versatic acids by virtue of their bulky, highly branched aliphatic structure (thus improving hydrolytic stability), have been used in the extraction of copper and nickel but the selectivity is poor.[47]

1.3.2 The sulfur donors

Sulfur donor ligands, which are soft Lewis baseshave been shown to form more stable complexes with the divalent 3d transition metal ions such as cobalt(II) and nickel(II) than ligands which contain oxygen donor atoms. Thus sulfur derivatives of D2EHPA have been shown to give better extraction of these ions at lower pH values, however, because cobalt is extracted at a very low pH, it requires a very strong acid to be stripped satisfactorily.[48] A previous research study conducted by Chia*et al.*[13] on the coordination chemistry of alkylthiomethylpyridine derivatives shows that six-coordinated complexes are formed for both Ni(II) and Co(II) thus

giving a relative preference for nickel extraction to cobalt. Of important advantage is the fact that S-donor extractants readily reject Fe(III) unlike the O-donors.

1.3.3 The nitrogen donors

It is a known fact that the N-donor ligands form relatively stable complexes with the latter 3d transition metal ions (Co^{2+}, Ni^{2+},Cu^{2+} and Zn^{2+}) compared with the early and middle 3d transition metal ions (TiO^{2+}, VO^{2+}, Cr^{3+}, Mn^{2+},and Fe^{3+}).[49,50] This serves as a potential for the application of N-donor extractants in the separation of base metals into two groups as well as further exploitation in the separation of the individual metal ions from each other. For this reason, there has been an upsurge in research and development into the use of amines as extractants.[51,53]

N-donor extractants have been shown to be more useful in the formation of the six-coordinated species of Ni(II) and since nickel is known to form the most stable spin-free octahedral complexes of all base metal ions, their choice as extractants in the development of nickel specific reagents is a well guided decision. On this note, it is obvious that in the design of a nickel specific N-donor extractant, a ligand that can force six-coordination on nickel would be highly desirable. Cu(II) equally forms stable complexes with the N-donors and often, these are four-coordinated in the form of tetrahedral or square-planar complexes.[54]

1.3.4 Amines as nitrogen donor ligands

Generally, the amines have been shown to have potential as extractants in metal ion separation in the last two decades both in the cationic form and the neutral N-donor form.[55] Consequently, research and development into their application towards metal ions specificity has gone beyond usage as solvent extraction reagents but further into application as functional reagents in an ion exchange technique. The use of alkylated ammonium derivatives as separating agents is engulfed with some notable secondary effects among which are the “perchlorate” effect, the “parent acid effect” and the “secondary cation effect”. The perchlorate effect has been found to cause a lowering of the activity of the bulky cation in the organic phase whilethe secondary cation effect causes a lowering of the activity of the anion to be extracted in the aqueous phase through increasing strong ion paring

with decrease in charge density and increasing the size of the cations in aqueous medium.[56]

Amines in the cationic form as the alkyl ammonium cations which are organic phase compatible can function as counter-cations for the anionic complexes of metal ions such as $CoCl_4^{2-}$, $FeCl_4^{2-}$,$FeCl_4^{-}$, $PtCl_6^{2-}$, etc. These ion-pairs readily phase transfer from the aqueous into organic phase. In this class are the tertiary and the secondary ammonium cations. Thus, these extractants have been successfully used to extract Co(II) from higher chloride concentration and even separate Co(II) from Ni(II) in chloride medium since the latter does not form similar chloro complexes.

Amines as neutral N-donor extractants have been exploited in the separation of Ni(II) from other base metals but not exhaustively. For example, diammines have been developed and studied including aliphatic, aromatic and combinations of these. The studies on the use of N,N,N',N'-tetraoctylethylenediamine, N,N'-dioctylaminomethyl-2-pyridine and 2-(1'-octylthiomethyl)pyridine in dilute acidic media for the separation of base metals have been undertaken.[57] This shows clearly that the bifunctional character of diammines can be used for separating different metals by changing the pH of the aqueous phase since each metal has different affinities for a particular nitrogen donorextractant.[58] It must be emphasized that among all other factors, the choice of a specific amine as extractant must be governed by the phase transferability of the complexes formed with the metal of interest in comparison with that of the protonated species, its organic compatibility and the nature of the metal ion as well as its affinity for the ligand.[59]

Amines, no doubt have received significant attention in the development of N-donor ligands as extractants in base metal separations. In recent times, several studies on the use of amines as neutral donor ligands in the development of separating agents for base metal ions have also been undertaken by researchers such as du Preez and co-workers.[60,61]

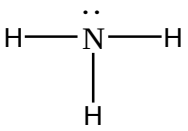

(9.63)

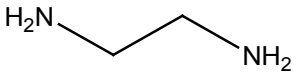

(9.98)

(a) (b)

Figure1.3: Chemical structures of aliphatic amines as possible neutral donor ligands. (a) Ammonia and (b) ethylenediammine (en)

A comparative study on the behaviour of various classes of neutral amines as metal ion extractants shows that alkylated aliphatic amines,e.g. monodentate amine with only sigma donor capability such as ammonia (pK_a= 9.63) (Figure 1.3a) and bidentate amine also with only sigma donor capability, e.g. ethylenediammine(en) (pK_a = 9.89) (Figure 1.3b) have limitations in their applications as metal ion extractant in acidic medium owing to their ease of protonation. When the two are compared, it is obvious that though they both have similar protonation constants, the possibility of "chelate effect" in ethylenediammine would lead to the formation of a stronger metal-ligand bond than with ammonia. However, the σ donor only bonding capability of aliphatic amines cannot discriminate between the later 3d metal ions they can only then best act ascounter cations (as alkylammonium cations) for anionic metal complexes and not as N-donors in metal ion separation even under mild acidic conditons.[62] In addition, the high protonation constants of the aliphatic amines imply that complex formation occurs at high pH values which is not satisfactory for application in strongly acidic solutions. Consequently, the choice of aromatic amines having both σ and π bonding capability suggested an improved metal ion extraction in slightly acidic medium through their N-donor atoms. With this fact, there is need to investigate the aromatic amines with both sigma donicity as well as π interactions in our search for the amine extractant for metal ion separation. A series of possible aromatic N-donor monodentate ligands such as imidazoles (pK_a = 7.31), pyridine (pK_a = 5.31) and pyrazole (pK_a = 2.78) are shown in Figure 1.4.

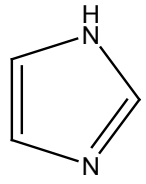

(7.31)

(a)

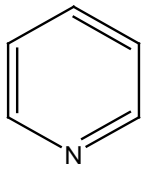

(5.31)

(b)

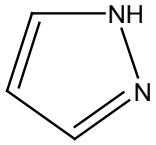

(2.78)

(c)

Figure 1.4: Chemical structures of monodentate aromatic amines. (a) Imidazole, (b) pyridine, and (c) pyrazole

A consideration of the σ donor strength reveals the order as imidazole, pyridine and pyrazole. Therefore, pyrazole followed by pyridine are less readily protonated compared with imidazole due to their lower proton affinity. Thus, application of pyridine as a metal extractant in strongly acidic medium could be performed, but with consideration for the reversibility of the extraction reaction. Pyrazole is limited as a metal extractant by its character as a poor σ donor, challenge of back-extraction inherent from its interaction with metals at low pH, and due to the possibility of steric hindrance arising from alkylation at the α-position to the coordinating nitrogen. Imidazole with stronger σ donicity, smaller cone angle, and less stereochemical crowding, offers more opportunities in the development of separating agents for the later 3d transition metal ions.[63]

Dipyridyl (pK_a = 4.42) (Figure1.5), on the other hand, offers opportunity for the formation of a more stable complex owing to the chelate effect as compared with the monodentate aromatic amine in its potential as 3d tms extractant. However, it's set back as extractant in a strong acidic medium arises from the possible difficulty of back-extraction. It is therefore clear that improvements are obtained if chelates are used for complexation but carefully selected for a higher acid medium.[64]

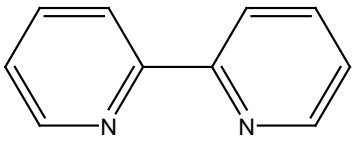

(4.42)

Figure 1.5: Chemical structure of 2,2-bipyridine

The protonation constant of an N-donor as well as its relationship with the stability constant of the metal complexes are of paramount importance in the choice of amine ligand as extractant.[65] Thus, a thorough decision on the choice of a neutral N-donor ligand as a metal ion specific extractantcan best be made if the various equilibrium reactions which are likely to be in competition are carefully considered.[66]

1.4 Ligand design

The choice of a ligand for the application as a specific extractant in metal ion separation is determined primarily by a number of factors whichcentre on the properties of the ligand and the basic coordination chemistry of the metal ion of interest as well as other metal ions, and anions present in the system. Besides the choice of donor atom, it is expected that a ligand must be chemically and physically stable in the SX circuit, so that it can be recycled through the extraction and stripping steps many times without experiencing undue physical loss or chemical breakdown. It must be soluble both in the loaded and stripped form. It must extract the desired metal selectively from the aqueous solution under consideration without formation of crud, and must be able to be stripped to obtain a solution from which the desired metal can be recovered.[67] The extractant must also not transfer deleterious species back from the strip section to the extraction.[68] Of course, meeting all these requirements with one reagents may be challenging and this is why there is a need to design a ligand to meet specific needs of the metal ion under consideration as well as its matrix.

Ligands must be designed such that metal ions are capable of deprotonating it in highly acidic solution to form stable complexes. Selectivity through “stereochemical tailoring” is enhanced by the relative stabilities of these metal complexes, and chelation effect is a key factor in this regard.[69] Since the ability of metals to deprotonate and complex with a ligand respectively not only depends on the donor atom but also on the pH, a determination of the protonation constant (pK_a) and the complex stability constant (log β) can be carried out and the species formed evaluated as a function of pH in the exploitation of these N-donor ligands as extractants. This would give a lead in deriving a pH for the selective extraction of the metal ions of interest by the ligand in an extraction system.

Ligands applied as commercial extractants in the solvent extraction system are required to be inexpensive, easy to synthesise and must form organic-soluble complexes. In addition they are expected to be environmentally friendly.[70]

1.5 Imidazole-based ligands

Structurally, imidazole is a 5-membered planar ring with two nitrogen atoms located at position 1(N-1), otherwise called pyrole-type nitrogen, and position 3 (N-3) known as pyridine-type nitrogen as shown in Figure 1.6. It exists in two equivalent tautomeric forms because the hydrogen atom at N-1 can be located on either of the nitrogen atoms.[71] It owns its aromaticity to the presence of a sextet π electrons made up of the lone pair π electrons at the N-1 and one from each of the remaining four atoms of the ring. Therefore, bonding of a proton or metal-ion at N-1 would be unfavourable. However, N-3 is a modest sigma donor and a good π acceptor of electrons making it favourable to bind a proton or metal ion.

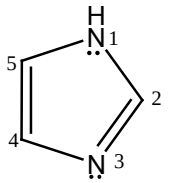

Figure 1.6: The basic chemical structure of imidazole

The protonated species and the metallated structure of imidazole as aromatic cations are better represented as shown in Figure 1.7.

(a) (b)

Figure 1.7: The structures of (a) the imidazolium cation and (b) the metallated imidazole

In acidic and basic medium imidazole can be represented with equation 17 and 18 respectively. These equilibria exclude the deprotonation of the N-1 proton under strongly basic conditions since its pK_a is very high.[72]

$$ImH^+ \rightleftharpoons Im + H^+ \quad (17)$$

$$Im + H_2O \rightleftharpoons ImH^+ + OH^- \quad (18)$$

The protonation constant on imidazole with respect to the N-3 nitrogen is 7.31 (Table 1.2), and in the range of 14.2 to 14.6 with respect to deprotonation at N-1 site. Thus it can form an imidazolium cation in acid medium or deprotonated in very strongly basic solutions to form an anionic imidazole. The basic nature of imidazole which is further improved by the attachment of an alkyl chain at N-1 as well as its ability to bind *via* σ and π bonding as a t ertiary aromatic amine suggests its potential as a metal ion extractant.[73]

For instance, a recent quantitative study done on the possibility of the application of imidazole as base metal ion extractant had shown that by virtue of the protonation constant, imidazole derivatives are able to extract base metals at a pH of about 2 and the back-extraction achieved within a pH range of ≈ 1.5.[64] The pyridine derivatives experience challenges with back extraction since the pK_a is low and formation of the extractible complexes occurs at very low pH. On the other hand, the ammonia derivatives form extractible species at relatively high pH due to the high pK_a values making them unsuitable for extraction at the low pH range. The species distribution plots for the interaction of nickel(II) with ammonia, immidazole and pyridine respectively were generated from the protonation, stability and hydrolysis constants obtained from the literature,[74] and are depicted in Figure 1.8. These plots allow one to glean the pH-metric aspects of coordination of these N-donor ligands as discussed above.

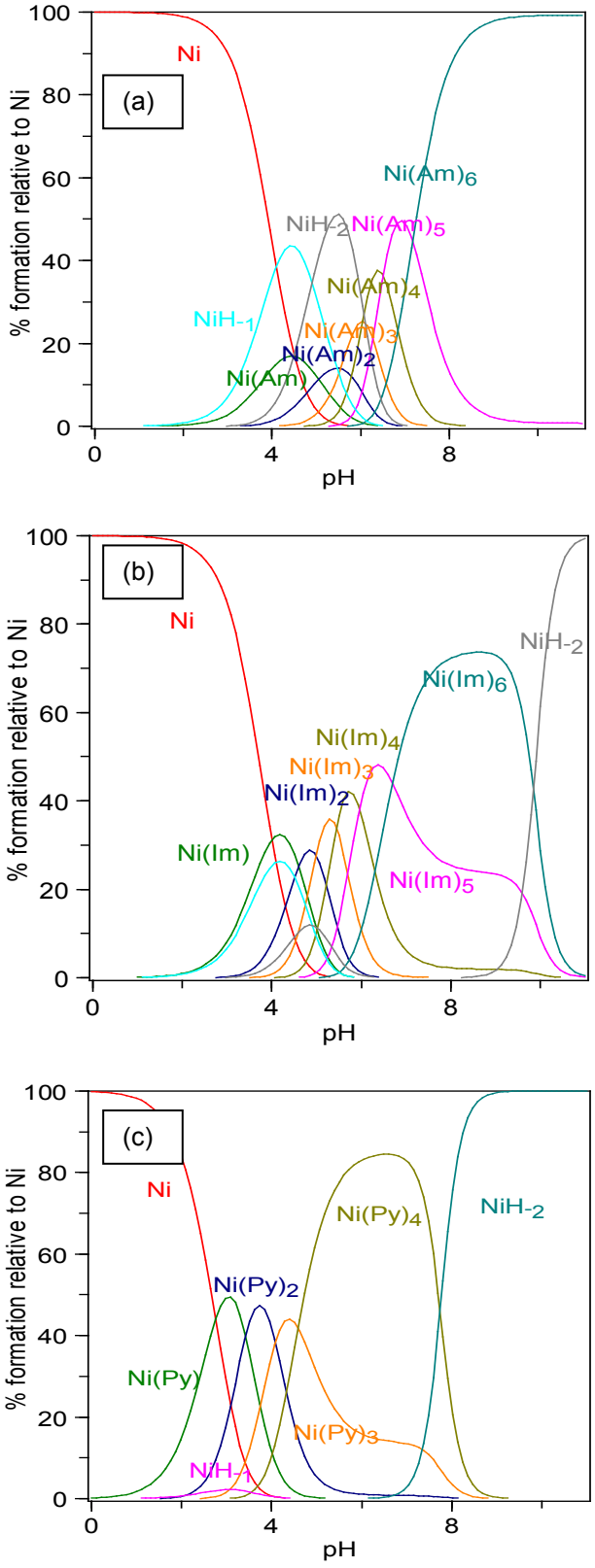

(c)

Figure 1.8: The species distribution plots for the step-wise formation of Ni(II) complexes with (a) ammonia (Am), (b) imidazole (Im), and (c) pyridine (Py).C_{Ni} = 0.001 mol.L^{-1} and c_L = 0.1 mol.L^{-1}. NiH_{-1} = $Ni(OH)^+$, and NiH_{-2} = $Ni(OH)_2$[74]

The degree of association of imidazole extractants with the organic phase are also known to be dependent on the length of the alkyl chain.[75] It is obvious from the above facts that alkylated imidazole-based ligands would be superior extractants due to their stronger σ donor character contributing to the high formation constants of the metal ion complexes.

1.6 Pyridine-basedligands

Pyridine (Figure1.9), a monodentate aromatic amine with both σ and π bonding capability in its neutral state, has a protonation constant value of 5.31 (Table 1.2). In strongly acidic solutions it exists as the pyridinium cation (equation19). Due to its relatively lower proton affinity it is less readily protonated in strongly acidic solutions and this enhances its usage as metal extractant in the low pH range.

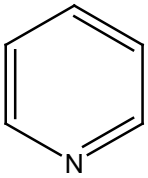

Figure 1.9: The chemical structure of pyridine

$$PyH^{+} \rightleftharpoons Py + H^{+} \qquad (19)$$

Owing to these advances, further exploitation of tertiary amine with the application of pyridine as a neutral N-donor in metal extraction in acidic medium has been carried out. Thus N-alkyl-3-pyridinecarboxamide,[76] and pyridine carboxylate esters[77] were used in concentrated chloride media for the extraction of Cu(II). Also, a potential bidentate pyridine based N-donor extractant, 2-(1'-octylthiomethyl)pyridine was used in the extraction of Cu(II) in a chloride medium and this shows a very high extraction efficiency but stripping of the metal from a loaded organic phase was found to pose a difficult challenge.[58] A number of studies have been carried out with pyridine and pyridine derivatives as metal extractants in acidic media in which the extraction is performed by the pyridinium cation while the metal complex is an anionic species e.g. chloro, thiocyanato, etc.[78-80]

All these results call for a better approach in the optimization of the benefits offered by the pyridine-based ligands in base metals extraction especially in acidic media.

1.7 Nickel specificity and selectivity

Metal ion specificity has been a major goal in the hydrometallurgical separation of base metal ions and this is based primarily on the preference of the applied extractant for the metal ion of interest over others in the medium under consideration. In a solvent extraction system metal ion specificity is known to be determined by a number of factors among which are ligand design, steric hindrances, stability constants and solubility of the metal complexes, however, selectivity of a given extraction system can be enhanced by careful pH control, use of masking agents to remove unwanted species or by "stereochemical tailor-making".[81]

The primary objective of this study was to achieve nickel ion separation from a synthetic nickel ore leach solution containing other metal ions in an acidic sulfate medium. The potential of imidazole-based ligandis explored, and the underlying coordination chemistry of nickel investigated along with that of other metal ions present. As earlier highlighted, nickel is known to form the most stable-spin free octahedral (O_h) complexes of all base metal ions. Exploring the ability of imidazole as an N-donor ligand offersthe advantage of first separating the A-type cations (Fe^{3+}, Ca^{2+}, and Mn^{2+}) from the B-type base metal ions (Cu^{2+}, Co^{2+}, Zn^{2+},etc) as well as discriminating between nickel and the other borderline metal ions namely Co^{2+}, Cu^{2+},Fe^{2+} and Zn^{2+} by forcing a six-coordinated octahedral complex nickel. It is also very well known that though Cu^{2+} forms stable complexes with N-donor ligands, it rarely forms octahedral complexes as compared with nickel, thus this stereochemical difference can be exploited for nickel specificity.[57] Of course, Zn^{2+} would rather form a tetrahedral (T_d) geometry than octahedral, posing a better room for its separation. Cobalt is also expected to show a weaker tendency towards the formation of octahedral (O_h) complexes as compared with Cu^{2+}. It was therefore presumed that carefully designed imidazole-based ligands are worth investigating in the drive towards nickel specificity.

Pyridine-based ligands as earlier mentioned offer some advantages with ease of binding the metal ion in preference to proton in an acidic medium, however, the formation of six-coordinated pyridine complexes of Ni^{2+} is not readily achievable due to the stereochemical overcrowding.[82] Based on the potential advantages offered

by alkyl pyridines such as the metal complexing strength, long-term stability, commercial availability and cost they were successfully applied as a synergist in the separation of nickel from calcium with versatic 10 acids by Preston *et al*.[83] Nickel was stripped in a single stage at an equilibrium pH of 3-4 with 0.25 M sulfuric acid. Table 1.2 illustrates the proton affinity as well as the formation constants of imidazole and pyridine with nickel.

Table 1.2: Literature values of the protonation constants of imidazole and pyridine, and the first formation constants of their nickel(II) complexes.[83] The differences between these constants is also presented.

Ligands (L)	**Log K_H^{+1}**	**Log β_1 Ni(II)**	**Log K_H-log β_1**
Imidazole	7.31	3.02	4.29
Pyridine	5.31	1.88	3.43

Considering these advantages and the disadvantages offered by imidazole and pyridine individually as amine extractants of base metal ions, it would be worthwhile to investigate a ligand that incorporates the properties of these two moieties in the drive towards nickel specificity. On this note, 2,2′-pyridylimidazole was chosen as one of the ligands under this study in the attempt to develop a nickel specific separating agent for an acidic sulfate medium.

1.7.1 Stability of base metal complexes

Relative stabilities of the metal complexes formed between the extractant and each of the metal ions in solution is a very important factor in the separation of the metal ions *via* solvent extraction. It is a measure of the strength of the interaction between the reagents that come together to form the complex. The coordination chemistry of each metal ion still remains a determining factor. Irving and Williams, in their original data on the stability of the high-spin octahedral complexes of bivalent ions of the first row transition metals, proposed the following order;[9] Mn < Fe < Co < Ni < Cu < Zn. This was found to hold for the stability of nearly all the complexes known then. The theoretical background of this order follows the consideration of the

reciprocal of the ionic radii and the second ionisation potentials of the metal as well as the crystal field stabilization energy (CFSE). It was also inferred that variations of the coordination number, stereochemical considerations and entropy factor may affect this stability order. Thus, in the formation of a metal complex denoted by ML_n from a metal (M) and a ligand (L) in a stepwise process the equilibria of the successive stages is denoted by equation 20-22;

$$M + L \rightleftharpoons ML \quad (20)$$

$$ML + L \rightleftharpoons ML_2 \quad (21)$$

$$ML_{n-1} + L \rightleftharpoons ML_n \quad (22)$$

with all the species ML_n in mutual equilibrium and n denoting the maximum coordination number, the equilibrium constants termed as formation constant is given by equation 23;

$$K_n = \frac{[ML_n]}{[ML_{n-1}][L]} \quad (23)$$

The overall stoichiometric stability constant is given as inequation 24;

$$\beta = K_1 . K_2 . K_3 ..... K_n \quad (24)$$

As depicted in Table 1.2, the logarithm value of either K_n or β are often used to denote the extent of the stability of the metal complex or the protonated ligand as the case may be.

In practice, factors contributing to the stability of a given metal complex are; the chelate effect, the geometrical effect, ionic radius of the metal and the classification of the metal ions. The chelate effect predominantly depends on the entropy change while other factors such as solvation changes and ring formation also play a significant role. 5-Membered and 6-membered chelate rings are known to give the most stable complexes[84].

The concentration of free metal ion [M] in solution in a system where the total metal concentration is C_M and the free ligand concentration is [L] can be shown to be

$$[M] = C_M / \sum_o \beta_n [L]^n \quad (25)$$

Thus, with the formation of complexes there is a subsequent change in the concentration of the metal ions and this is considered of great importance in analytical chemistry where the equilibria are shifted to achieve quantitative reactions.[84] This is also fundamental in the discussion of the pH of precipitation of metal hydroxides, sulfides, and organic complexes as well as quantitative treatment of solvent extraction system.[85] In general, since two or more different metals will form complexes of unequal stability with one and the same ligand, possibilities of analytical separations is dependent on the formation of a strong chelate complex with few metal ions or at best with only one of the metal ions by the ligand. This makes the application of a given extractant as a selective or "singular" reagent or better put a truly specific reagent realisable.

It would therefore be expected that in a given metal ion extraction system, to achieve a metal ion specificity, the stability constant (log *β*) of the complex formed between the extractant and the metal ion of interest must not only be higher than the protonated species but must also be significantly higher than that of the other metal ions present. Thus, the position of the extraction curves relative to each other in an extraction isotherm would be in order with the relative formation constants.

1.7.2 The acid-base effect

The presence of acids in a pregnant liquor solution (PLS) is not uncommon; it may be as a result of acid leaching employed prior to separation or some sort of oxidative reaction within the solution. For instance, it is known that the presence of sulfides in ores can be converted to sulfuric acid through oxidative bioleaching processes.[86] Similarly, ammoniacal leaching also result in the presence of alkali in the aqueous solution. The presence of either excessive amounts of acid or base has been known to produce deleterious effect on the extraction system. Thus, the acid loading into the organic phase is known to reduce the loading capacity of the extractants. Consequently, acid loading in a good extraction system must be reduced to the barest minimum. Other effects of acids could be the degradation of the extractant. This is known in the application of oximes as extractant whereby an oxime is degraded into amide through Beckman's rearrangements.[87]

1.7.3 The effect of anions

The nature of the anions in an ex traction systemaffects the complexation and subsequent extractability of the species formed from the aqueous into the organic phase. The relative affinities of the anions to ion-pair with the bulky complex for the formation of a non-polar species that are phase-transferrable is important. Early studies in solvent extraction and ion exchange have shown that this effect is pronounced in the use of amines such as alkylammonium cations, and even also when the N-donors ligand has a higher affinity for the protons. Perchlorate ions exhibit a depressant effect on the extraction of almost all the extracted species.[50] This is due to the large affinity of perchlorate ions for bulky ammonium salts which is shown to manifest in the application of the latter as extractants, resins and even precipitants. This effect was dubbed "the perchlorate effect" by Horne.[88] In a quantitative study on the loading of ClO_4^- and $CoCl_4^{2-}$ on Aliquat-336 resin/extractant, it was found that, due to their lower water content, greater selectivity for both ClO_4^- and $CoCl_4^{2-}$ were observed.[89] The quantitative equilibrium constants (K_{ex} and K_{sp}) values obtained for the loading of common anions for different ammmoniun cations such as aliquat-336, N,N′-dimethyl-N,N,N′,N′-tetraoctyl-1,2-diammonium ethane chloride (dimtetocenCl_2), and N,N,N,N′,N′,N′-hexaoctyl-1,6-diammonium hexanechloride (hexochemCl_2) shows that values for ClO_4^- ($1.37x10^4$, $4.45x10^4$, $1.00x10^6$) are far greater than the common inorganic ions like Cl^-, NO_3^-, SO_4^{2-} and OH^-.[90] This is a reflection of the relative affinities of these anions for the quaternary ammonium extractants (Table 1.3) as reported by du Preez *et al*.[91]

Table1.3: Relative affinities of common anions for some quaternary ammonium extractants (Ionic strength = 0.2 M).

Anion (Y^{n-})	**Aliquat-336 (K*)**	**Dimetocen ($K^{\#}$)**	**Hexochem ($K^{\#}$)**
ClO_4^-	1.37×10^4	4.45×10^4	1.00×10^6
NCS^-	2.00×10^3 (1.7×10^3)	7.70×10^3	6.55×10^4
I^-	7.06×10^2	2.39×10^3	6.53×10^3
NO_3^-	2.77×10^1 (2.4×10^1)	1.79×10^1	3.52×10^1
Br^-	1.34×10^1	1.39×10^1	6.85×10^0
HSO_4^-	6.5×10^{-1} (6.3×10^{-1})	2.2×10^{-3}	6.5×10^{-4}
SO_4^{2-}	4.5×10^{-2} (4.6×10^{-2})	6.0×10^{-3}	1.1×10^{-3}
OH^-	9.5×10^{-3} (2.9×10^{-2})	7.9×10^{-3}	1.6×10^{-4}

Values in parentheses were as reported in a different literature source,[91] while K* and $K^{\#}$ are as depicted in equations 26 and 27 respectively.

$$n\ amCl_{org} + Y_{aq}^{n-} \rightleftharpoons am_n Y_{org} + nCl_{aq}^- \quad (26)$$

$$diamCl_2 + 2/nY_{aq}^- \rightleftharpoons diamY_{2/n\ org} + 2Cl_{aq}^- \quad (27)$$

where Y = anions which compete with the chloride ions.

The magnitude of the charge of the anion is also of consideration due to the electrostatic force that is involved in ion-pairing, thus bulky low charge density cations can be said to have greater affinity for bulky low charged anions. From this order, inference can be drawn to the fact that sulfate ions would have a relatively low affinity for the organic phase which can be attributed to its high hydration energy.[92] Hence it should not be expected to readily phase transfer in an extraction system as the chloride, bromide, iodide, thiocyanate, nitrate and perchlorate ions.

In addition to the above, the donor strength of the counter anion as well as its proton affinity has been shown to play a significant role and as such the one with a lower proton affinity would be better in order to effect an easy pH control in the

extraction process. Sulfate is a much poorer ligand for base metal cations and there are no commercially available solvating reagents which allow the formation of organic soluble [$MLSO_4$] species with the sulfate in the metal's inner coordination sphere.[93] The effect of the donor strength of the anion is better illustrated with equation 28 where X^- = NCS^- extracts higher than $Cl^-$with N,N,N′,N′-tetraoctylethylenediamine(tetocen).[91]

$$M^{2+} + 2\text{tetocen} + 2X^- \rightleftharpoons M\text{tetocen}X_2 \qquad (28)$$

Conclusively, the coordination ability of the anion must be minimised to address this kind of depressant action of the anions on the extractants.

1.8 Extraction on solid adsorbents

Extraction on solid materials in which metal ions are selectively extracted on a solid adsorbent matrix are considered to be superior to the liquid-liquid extraction due to their simplicity, rapidity and the ability to provide a high loading capacity.[94] The characteristic high metal loading capacity they offer provides a high rate of metal extraction and are economical for dilute solutions even when large volume of liquids are involved.[95] The recovery of the metal ion and the ability to regenerate the adsorbent are very important aspect for the successful application of thisprocess. Solid adsorbentsare also useful for pre-concentration of low concentration analytes hence their application for solid phase extraction (SPE) techniques in sample preparation.[96]

1.8.1 Chelating resins

Chelating resins are ion exchangers in which chelating agents have been incorporated.[97] They combine the two analytical processes of ion exchange and complexation reactions. They offer the following advantages over the ordinary type of ion exchangers; high selectivity due to the fact that the affinity for a particular metal ion dependmainly on the chelating group and not on the size of the ion, its charge, or other physical properties. Also the binding is of higher bond strength unlike the ion exchanger whose binding is limited to electrostatic. On the negative side the kinetics in a chelating exchanger is slower and controlled either by a

particle diffusion mechanism or by a second order chemical reaction unlike in ordinary exchanger which is rapid and controlled by diffusion only.[98] The advantages offered by chelating resins as well as their ability to carry out complexing processes in two phase system (solid-liquid) provides a wider scope of research into their application for the separation of metal ions.[99]

Ion exchange with polymer-supported reagents experiences no loss of extractants to the aqueous phase since the ligands are covalently bonded to an insolublepolymer. The aqueous phase is allowed to flow through the polymer in a column while the chelating resin removes the metal through complex formation.[100] After the polymer is loaded and washed, the metal is stripped by the passage of an appropriate solution (often dilute acids) through the bed to regenerate and produce a solution containing the extracted metal. During the acidic elution process, separation of a mixture of metals is achieved by the decomplexation of each metal at a characteristic pH (DpH) which is dependent on the stability constants of the various metals with the chelating resin. The ability of a polymeric resin to be regenerated after recovering the metal ions is considered an important factor for application in a continuous process.

1.8.2 Synthesis of ligand-functionalized polymer beads

Synthesis of the ligand-functionalized polymer as a solid adsorbent can be achieved by either of the following methods:

(a) Ligand-immobilization – This is the attachment of the ligand which has the desired functional group on to the pre-prepared polymeric support which also has an appropriate functional group for the attachment. For instance, Merrifield resin, a chloromethylated polystyrene resin crosslinked with divinylbenzene, which contains the “reactive” chloromethyl groups is made to undergo substitution reactions in the presence of a nucleophile, with a ligand which contains a suitable nucleophilic functional group such as N-H, O-H, S-H, COOH, etc. Through this, the polymer is covalently bonded to the ligand.[100] Scheme 1.1 illustrates a typical immobilization of ethylenediammine on chloromethylated polystyrene.

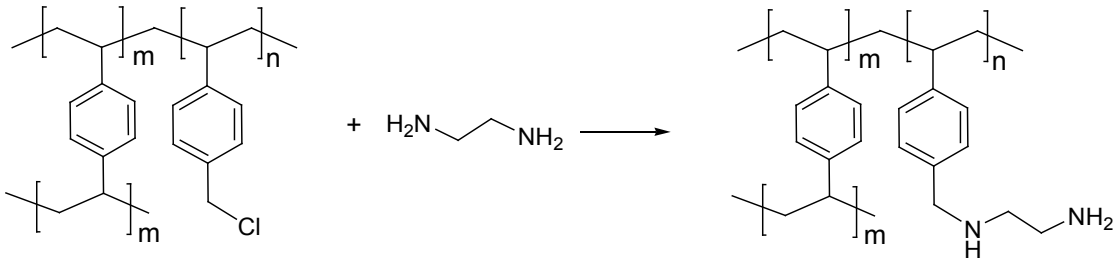

Scheme 1.1: Synthesis scheme for the immobilization of ethylenediammine unto Merrifield resins

(b) Production of cross-linked supports *via* free-radical copolymerization of vinyl monomers with divinyl cross-linking agents.[101] In this method, suspension copolymerization of the monomers is employed to produce the microspherical beads. The copolymerization strategy relies on the availability of a polymerizable ligand. The ligand is first prepared by the process known as monomerization. e.g. alkylating the ligand with a suitable polymerizable precursor. Thus vinylbenzyl chloride (VBC), a commercially available reagent, can be reacted with nucleophiles by a substitution reaction, thereby connecting the ligand to the styryl group. These types of reactions are carried out in polar aprotic solvents such as acetonitrile or DMF in the presence of a base like triethylamine, potassium carbonate, or potassium hydroxide[102] with addition of potassium iodide (KI) as catalyst.[103] An allyl monomer may also be formed by allylation of a diamine under the basic conditions, e.g. the reaction of an allylbromide with a large excess of ethylenediamine to help prevent dialkylation by the Claisen rearrangement to form the corresponding N-allylethylenediamine as shown in Scheme1.2.[104] A rearrangement of this nature is considered beneficial since the amine group remains available for coordination to a metal center.

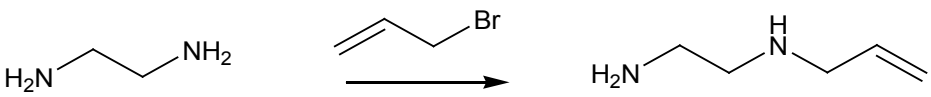

Scheme 1.2 Synthesis of monosubstituted N-allylethylenediamine[105]

(c) The Graft polymerization is known to proceed *via* the connection of a polymerisable ligand that has a vinylic group to the surface of a polymer. Radiation

such as ultraviolet or gamma, is used to introduce the free radicals onto the polymeric surface after which radical polymerisation is employed. This method is not as simple, since it combines both synthetic organic chemistry with polymer chemistry and besides, additional equipment is also required.

1.8.3 Polymer-supported amine ligands

A large number of amine ligands have been used as chelating ligands on polymeric resins in the separation of base metals such as polyethylenediamine on poly(vinylbenzaldehyde) which was found to show high selectivity for Fe^{3+} over Cu^{2+}, Ni^{2+}, Co^{2+}, Fe^{2+}, Zn^{2+} and Mn^{2+}.[106] A chelating resin containing benzoylacetanilide groups was also applied in the separation of Ti^{3+} and Fe^{3+} from Cu^{2+}, Co^{2+}, Ni^{2+}, Na^{+}, K^{+}, Ca^{2+}, Mg^{2+} and Al^{3+} in the pH range 1.3-2.0.[107] Pyridine and imidazole based ligands have been used in studies such as that conducted with polymeric supported picolylamineby Grinstead,[108] and these showed copper selectivity. An acrylic resin containing both sulfur and an imidazole group was found selective for Cu^{2+} over Ni^{2+}, Zn^{2+}, and Cd^{2+}.[109] Although pyridine-type ligands have shown a higher affinity for copper ions, the affinity is dependent on a number of factors among which is the concentration of the hydrogen ion competing for the basic sites. On this note, the use of a chelating ligand, 2,2′-pyridylimidazole, with a slightly higher pK_a value than pyridine alone as a polymer supported ligand, is being investigated in this study in the attempt to separate nickel from other base metal ions. An attempt will also be made to improve the loading capacity of this microscale resin by converting it to nanofibers through employing the electrospinning technique using the linear non-crosslinked polymer counterparts.

1.8.4 Techniques for producing fibers

Fibers can be produced through any of the following methods; drawing, template synthesis, deposition on a substrate, thermally induced phase separation and spinning. The spinning methods include dry, melt, wet and electrospinning.[110] The electrospinning technique allows for fabrication of extremely fine (low nanometer) fibersas discussed below. Each of these methods has its advantages and disadvantages in producing a sorbent for metal ions applications.

Electrospinning is a technique that provides a simple and versatile method for generating ultrathin fibers (diameters less than 1000 nm) from a rich variety of materials which may include polymers, composites and ceramic.[111] It relies on repulsive electrostatic forces in order to draw a viscoelastic solution into nanofibers.[112] Various functional groups can be incorporated prior or post electrospinning thus providing a better means of tuning the nanofibers for the intended application.

Electrospun nanofibers exhibit a range of unique features and properties that distinguish them from nanostructures fabricated using other techniques. For instance, the electrospun nanofiber is highly charged after it has been ejected from the nozzle, making it possible to control its trajectory electro-statically by applying an external electric field. Other features in the context of potential applications of electrospun nanofibers include; extremely long length, thus making it easy for fibers to be assembled into a three-dimensional non-woven mat. The position and spatial orientation of an individual fiber can be easily controlled by moving the collector around. When compared with fibers fabricated using a conventional spinning process electrospun fibers are much thinner in diameter and thus possess higher surface-to-volume ratio. Depending on the fiber diameters, the Brunauer- Emmet-Teller (BET) surface areas of electrospun mats between 9 and 51 $m^2.g^{-1}$ have been identified by Kim and co-workers on the non-woven mat of Nylon-6 nanofibers.[113] The porosity varies from 25% to 80%, and the pore size in the range of 2.737 to 0.167μm. The pores in an electrospun, non-woven mat are relatively large in size and all the pores are fully interconnected making the entire surface fully accessible to chemical species. An outstanding benefit of electrospinningin fabrication of sorbent materials is that it is easy to control the orientation of the nanofibers since the arrangement of the fibers play a significant role in their performance as sorbents.[96]

Other methods of spinning include Drawing, whereby fibers are drawn in a similar way to electrospinning from a micro-droplet of polymer solution. A micropipette is dipped into the droplet and withdrawn at a certain speed. This discontinuous process requires viscoelastic materials and has a lower limit for fiber diameters of 100 nm.[115]

Template Synthesis onthe other hand utilizes a nanoporous template through which the polymer solution is pushed. The resultant polymer fibers solidify in a suitable solvent. The diameter of the fibers is directly related to the diameter of the pores of the template and as such, excellent reproducibility is obtained.[116]

Phase Separation isanother method with variousssteps involved such as; polymer dissolution, gelation, solvent extraction, freezing and freeze drying which finally gives a porous nanofibrous structure. Thus, the formation of fibers occurs due to physical incompatibility.[117] Self Assembly has also been practised. The method provides ultrafine fibers with diameters which are less than 100 nm. Unlike the other methods, this is a 'bottom-up' approach in which atoms and molecules arrange *via* weak non-covalent interactions into well defined structures.[118]

1.8.5 Applications ofelectrospun polymer nanofiber

Applications of electrospun nanofibers are numerous with lots of potential owing to the simplicity and flexibility of their fabrication, remarkable features outlined above, and diverse materials that can be used for electrospinning. For example, it has been used to reinforce composite materials, membranes and smart clothes, as supports for enzymes and catalyst, as solid phase extraction materials, as sensors and electrode materials, etc.[119]

Separation of metal ions by sorption with electrospun nanofibers as adsorbents is a more recent development that holds lots for the future in separation science. This is majorly due to the large surface area to volume ratio they offer as sorbent materials with increased sites for analytes interaction.

1.8.6 Electrospinning setups and mechanisms

A schematic diagram illustrating the basic set up for electrospinning is shown in Figure 1.10.

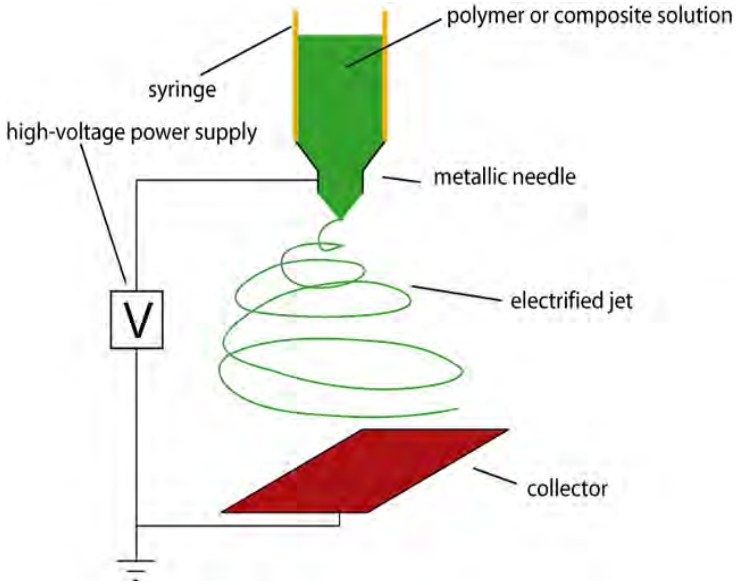

Figure1.10: Schematic illustration of the basic set-up for electrospinning[120]

It is made up three major components namely; a high-voltage power supply, a spinneret (a metallic needle that delivers the polymer solution), and a collector (a grounded fibercollector). A direct current (DC) supply is usually used for electrospinning, though an alternating (AC) current is also feasible.[120-121] The spinneret is usually connected to a syringe which contains the polymer solution. With the application of a syringe pump, the solution is fed through the spinneret at a constant and a controllable rate. A high voltage is applied to the needle tip usually in the range of 1 to 30kv. As the polymer solution drops from the nozzle of the spinneret, it becomes highly electrified and the induced charges are evenly distributed over the surface, thus the drop experiences two major type of electrostatic forces; the electrostatic repulsion between the surface charges and the coulombic force exerted by the external electric field. The liquid drop having been distorted now comes in the form ofa cone usually called Taylor cone. As the applied voltage increases beyond this point, the liquid jet is continuously elongated and the solvent is evaporated while its diameter is greatly reduced from hundreds of micrometers to as small as tens of nanometres. As the jet travels towards the collector, the tensile force brought about by the surface charge repulsion produces a bending motion while the polymer chains within the jet are stretched and oriented.[122]

The following process parametersrequire optimizations; the applied voltage, the polymer solution feed rate, and the tip-to-collector distance.[123-124] This becomes necessary because the applied voltage drives the electrospinning process,and therefore provides the charges necessary to overcome surface tension and subsequently produce the polymer jet. The polymer solution feed rate or flow rate, on the other hand, dictates the speed at which the polymer solution is delivered to the needle tip. It is known that too high flow rate may result in deposition of wet fibers. The flow rate has a definite effect on the resultant fiber diameters. When the tip-to-collector distance is increased it correspondingly increases the flight time of the polymer jet. This provides time for solvent evaporation as well as time for the stretching of the jet. The net result is typically a decrease in diameter of the fibers with an increase in tip-to-collector distance.[125,126] In addition to these variables, ambient parameters of the surroundings such as temperature, humidity, etc., may also play an i mportant role in determining the morphology and di ameter of electrospun nanofibers.

1.8.7 Functionalization of polymer fibers

Modification of the chemical, mechanical and absorbent properties of the fibrous nanostructure could be achieved with the addition of new functionalities without changing the morphology of the original fibers. Chemical modifiers by reactions (e.g., crosslinking or grafting, etc.) could also be c arriedout prio to, during electrospinning or by post-spin treatments. Chemical modification has been shown to be the most versatile route to nanofibers characterised by new functionalities.[127] Liu and Hseish have successfully introduced double-bond units into cellulose fibers *via* deacetylation, followed by reaction with methacrylate chloride.[128] Immobilization of the ligand containing the desired functional group on the nanofibers by alkylation as with Merrifield resins also provides a potential route.

1.9 Extractive metallurgy and the common problems

So far, numerous problems being encountered in the practice of extractive metallurgy for the separation of metal ions ranging from selectivity of an extractant in a SX circuit for a given metal ion to the stripping of a metal product of high purity

suitable for electrowinning operation have been highlighted. These problems and the challenges[129] posed can be summarised as follows:

1. Structural design of the exctractants and the coordination chemistry involved in the exctraction process, since this help to determine the thermodynamic selectivity of one metal ion over other competing metals,
2. The choice and influence of the diluents on the selectivity of the extractant for the preferred metal,
3. The aqueous chemistry of the PLS, bearing in mind the relative concentration of the competing ions present and the speciation of the metal complexes as well as the type of anion present,
4. The differences in the extraction kinetics of the metal ions present,
5. Addressing possible problems such as entrainment, crud effects, degradation of extractants and co-extraction of impurities,
6. The use of scrubbing circuits for the loaded organic,
7. The pH of extraction and stripping, and possibility of selective stripping.

All these challenges point to the fact that there is a wide open door for intensified research and developments in the application of extractive metallurgy for the separation of base metal ions.

1.10 Objectives and scope of this study

1. To synthesize and characterize imidazole-based bidentate (N,N`-donor) ligands; amines and oximes and applytheseas selective extractantsin the development of nickel/copper specific reagents for the separation of base metal ions in an acidic sulfate medium,

2. To apply the concept of synergism in the selective extraction of base metal ions. The use of bulky anion to ion-pair the metal-extractant cationic species would be employed to achieve a transfer of the species formed into the organic phase,

3. To determine the protonation and stability constants for the extractants and M-extractants complexation reactions through pH-metric chemical speciation

modelling of the reactions in the aqueous phase. The stability constants would then be used to explain the extraction isotherms observed,

4. To determine through solid state studies the most probable nature of the extracted species andthe coordination chemistry involved using characterisation techniques such as infrared spectroscopy, electronic spectroscopy, and conductivity measurements,

5. To carry out a comparative study with polymer-anchored 2,2'-pyridylimidazole in the separation of base metal ionsin a similar acidic sulfate medium through the following studies:

(a) Column separation study with a chelating microspherical resins,

(b) Study the sorption properties of functionalised nanofibers as sorbent materials for the selective adsorption of base metal ions.

(c) Determine the loading capacity of the microporous resin and the nanofibers in relation to their properties such as surface area, nitrogen content, etc.

References

[1] D. F. Shriver, P. W. Atkins, C. H. Langford, Inorganic Chemistry, 2nd Ed. W.H. Freeman and Co. New York, 1994, 7.

[2] F. Habashi, A textbook of Hydrometallurgy, Metallurgie Extractive Quebec, Sainte Foy, Quebec.2nd Ed. Laval university Bookstore Zone, 1993, 87.

[3] F. Habashi, Hydrometallurgy 79 (2005) 15-22.

[4] A. Feather, W. Bouwer, A. Swarts, V. Vagel, J. S. Afri.Inst. Min. Metall. (2002) 457- 462.

[5] J. Pearsall, Base metal definition, New Oxford Dictionary of English. Oxford University Press, 1998, 876.

[6] K. C. Sole,A. M. Feather, P. M. Cole, Hydrometallurgy78 (2005) 52-78.

[7] L.A. Meyer, South Africa's Mineral Industry 1996/97, Department of Minerals and Energy-Mineral Economic Directorate Bureau, 14th Ed, 1997.

[8] M. Edwards, M. H. Silk, Platinum in South Africa. Special Publication No. 12, Mintek, Randburg, 1987 12-13.

[9] H.M. Irving, R.J.P. Williams, J. Chem. Soc. (1953) 3192-3210.

[10] K. M. Mackay, R. A. Mackay, Modern Inorganic Chemistry, 3rd Ed. 1972, 220-223.

[11] K. Burger, I Ruff, F. Ruff, J. Inorg. Nucl. Chem. 27 (1965) 179-190.

[12] L. M. Venanzi, Acta Chem. Scand. 10 (1956) 72-93.

[13] P.S.K. Chia, S. E. Livingstone, T.N. Lockyer, Aust. J. Chem. 20 (1967) 239-249.

[14] D.D.J. Clemente, B.I. Dewar, J. Hill, Canadian Inst. of Metal. 10th Annual Hydrometallurgical Meeting, Paper No. 7 Edmonton, Alberta, Canada, 1980.

[15] D. S. Flett, Hydrometallurgy Rev. 12 (2004) 81-91.

[16] F. A. Cotton, G. Wilkinson, P.L. Gaus, B asic Inorganic Chemistry, John Wiley & sons, Inc. 1976, 235-236.

[17] J. A. Marinsky, Y. Marcus, Ion Exchange and Solvent Extraction - A series of advances 8, Marcel Dekker Inc, New York, 1981 29-30.

[18] M. Neira, T.J. O'Keefe and J.L. Watson, Miner. Eng. 5 (1992) 521-534.

[19] J. Monhemius, Chem. Ind. 12 (1981) 410-420.

[20] R. G. Pearson, J. Am. Chem. Soc. 85 (1963) 3533-3543.

[21] S. G. Galbraith, P.A. Tasker, Supramol. Chem.17 (2005) 191-207.

[22] Anglo American Platinum Corporation Limited, Annual Report, South Africa, 1998.

[23] R.T. Jones, Platinum Smelting in South Africa, Mintek, South Africa, 2001.

[24] K.C. Sole, P.M. Cole, In Marcus, Y. Sen, A. Gupta, (Eds.), Ion Exchange and Solvent Extraction, 15 Marcel Dekker, New York, 2001 143-195.

[25] Implats Annual Report, South Africa. 1998.

[26] G. Kordosky, M. Virnig, M. Mackenzie, Solvent Exctraction-Reagents and Selectivity control. Henkel Corp. MID Tucson Arizona, 1988.

[27] M. Cox, D. S. Fleet, Proceedings of ISEC '71. Society of Chemical Industry, London. 34 1971 204-213.

[28] D. S. Fleet, S. Titmuss, J. Inorg. Nucl Chem. 31(1968) 2162-2163.

[29] D.T. Thompson, Insight into Speciality Inorganic Chemicals, RSC., United Kingdom, 1995 17-20.

[30] D. S. Flett, in A.R. Burkin (Ed) Critical Reports in Applied Chemistry, John Wiley & Son. 17 1987 76-78.

[31] K. C. Jones and R. M. Wheaton, U.S. Patent 3998 1976 924.

[32] R. R. Grinstead, W.A. Nasutavicus, U.S. Patent 40098 1978 867.

[33] R. R. Grinstead, A. L. Tsang in: Int. Solvent Extraction conf. Denver,Colorado, American Inst. of Chem. Engnrs. New York, 1983 230.

[34] B. Townsend, K.J. Severs, Min. Eng. 162 (1990) 26-35.

[35] R.R. Blumberg, Liquid-liquid Extraction. Academic Press London, 1988 36-37.

[36] I. Vogel, A Textbook of qualitative chemical analysis. 5th ed. U. K. 1989 161-168.

[37] G. D. Christian, Analytical Chemistry. 6thed John Wiley & Sons Inc U.S. 2003 444-445.

[38] F. Luo, D. Li, P. Wei, Hydrometallurgy 73(2004) 31-40.

[39] J.G.H. du Preez, J. M. Shaeekers, Patent WO 02/101101 A2 2002.

[40] R.Singh, A.R. Kliwaja, B. Gupta. S.N. Tandon, Solvent Extr. Ion Exch. 17 (1997) 367-390.

[41] K. Sole, Barker lecture at Rhodes University, 1995.

[42] R. D. Hankock, A. E. Martell, Chem. Rev.89 (1989) 1875-1886.

[43] L.G. Sillen, Quart. Rev. London 13 (1959) 146-164.

[44] F. A. Cotton, G. Wilkinson, Advanced Inorganic Chemistry. 4thed. Wiley-Interscience publication. New York, 1980 757-759.

[45] J. Monhemius, Bull. Chem. Tech. Mac.13 (1994) 7-12.

[46] W. A. Rickelton, D. S. Flett,D. W. West, Solvent Extr. Ion Exch. 2 (1984) 815-838.

[47] S. Dobson, A. J. van der Zeeuw, Chem. Ind. (1976) 175-181.

[48] K. T. Brian, Hydrometallurgy 32 (1993) 365-372.

[49] J. S. Preston, Hydrometallurgy 10 (1983) 187-202.

[50] Y. Marcous and A. S. Kertes, Ion Exchange and Solvent Extraction of Metal Complexes. Wiley Interscience, New York, 1969 25-26.

[51] S. Kertes, J. Inorg. Nucl. Chem. 26 (1964) 1764-1766.

[52] V.V. Fromin, V. T. Potrapova, Z. N. Kim, J. Chem. Tech. 8 (1965) 990-914.

[53] J.G.H. du Preez, Solvent Extr. Ion Exch. 18 (2000) 679-701.

[54] J. G. H. du Preez, J. Postma, S. Ravindran, B.J.A. M. van Brecht, Solvent Extr. Ion Exch. 15 (1997) 79-96.

[55] Y.Marcus, A.S. Kertes, Ion Exchange and Solvent Extraction of Metal complexes. Wiley Interscience, New York, 1969.

[56] J.G.H. du Preez, D.P. Shillington, E. Herselman, H. E. Rohwer, B.J.A. M. van Brecht and H. Wilke, Solvent Extr. Ion Exch. 13 (1995) 189-214.

[57] J.G.H. du Preez, J. Postma I. A. G. Thomas,W. Edge, V. L. V. Mtotywa, B.J.A.M. van Brecht, Solvent Extr. Ion Exch. 19 (2001) 143-154.

[58] J.G.H. du Preez, S.B. Schanknecht, D.P. Shillington, Solvent Extr. Ion Exch. 5 (1987) 789-809.

[59] J. J.R. Frausto da Silva, J. Chem. Educ. 60 (1983) 39.

[60] J. G. H. du Preez, J. G. H. du Preez, D. P. Shillington, S. B. Schanknecht, Solvent Extr. Ion Exch. 7 (1989) 865-876.

[61] J. G. H. du Preez, N. Sumter, C. Mattheus, S. Ravindran, B. J. A. M. Brecht, Solvent Extr. Ion Exch. 15 (1997) 1007-1021.

[62] J. McMurry, Organic Chemistry, Cornell University, Brookes Cole publishing Co, 4thed. 1996. 56-59.

[63] J.G.H. du Preez, C. Mattteus, N. Sumter, S. Ravindra, C. Pogieter, B.J.A.M. van Brecht, Solvent Extr. Ion Exch. 16 (1998) 565-586.

[64] Haranda and S. Takahashi, J. Chem. Soc., Chem. Comun. (1986) 1229-1243.

[65] R. J. Suberg, R. B. Martin, Chem. Rev. 74 (1974) 511- 523.

[66] J.G.H. du Preez, H.E. Rohwer, D. C. Wantenaar, Solvent Extr. Ion Exch. 5 (1987) 705-718.

[67] R.B. Sudderth, G. Kordosky, Chemical Reagents in the mineral Processing industry. Ed. Malhotra and Riggs. S.M.E. Littleon Colorado, (1986) 181-196.

[68] G. A. Kordosky, W.H. Champion, J.R. Dolegoswki, S. M. Olfason, W. S. Jensen, Min. Eng. (1981) 192-299.

[69] Y. Singh, R. Sharan, R.N. Kapoor, Indian J. Organomet. Chem. 332 (1987) 135-144.

[70] F. C. Liew, Engineering Dept, TES-AMM, Singapore. 2008.

[71] R. Katritzky, J. M. Lagowski, Comprehensive Heterocyclic Chemistry,Oxford Press,1984 469-498.

[72] R. Grimmett, M. Ross, Imidazole and Benzimidazole Synthesis. Academic Press. 1997.

[73] E.G. Brown, Ring Nitrogen and Key Biomolecules. Kluwer Academic Press, 1998.

[74] R. M. Smith, A. E. Martell, Critical Stability constants. Plenum Press, New York. 4, 144 (1976) 207-247.

[75] R. J. Sundeberg, R. B. Martin, Chem. Rev. 74(1974) 511-534.

[76] A. Brorowoiak-Resterna, Solv. Extr. Ion Exch. 5 (1994) 835-945.

[77] K.H. Soldenhoff, Solv. Extr. Ion Exch. 5 (1987) 833-958.

[78] D. Mohammad, T. Mahmood, M. A. Qureshi, M. Ejaz, J. Radioanal. Chem. 42 (1978) 45-59.

[79] S. Mudassar, A. Qureshi,M. Ejaz J. Radioanal. Chem. 44 (1978) 83.

[80] M. Igbal,M. Ejaz, Talanta 22 (1975) 143-158.

[81] L. G. Sillen, Ouartz Revs. London 13 (1959) 146-166.

[82] R.M. Smith, A. E. Martell, Critical stability constants, Plenum Press, New York, 2(1975)36,165 and 235.

[83] J.S. Preston, A.C. du Preez, Hydrometallurgy 58 (2000) 239-250.

[84] G. Gran, Analyst 77 (1952) 813-825.

[85] W. Maeck, G. Booman, M. Kussy, J. Rhein, Anal. Chem. 33 (1961) 1775.

[86] S. Agatzini-Leonardou, P. E. Tsakirdis, P. Oustadakis, T. Karidakis, A. Kastsiapi Min.Eng. 22 (2009) 1181-1192.

[87] R.J. Whewell, H.L. Foakes, M. A. Huughes, Hydrometallurgy 7 (1979) 7-26.

[88] R. A. Horne, R. H. Holm,M. D. Meyers, J. Phys. Chem. 61 (1957) 1661-1674.

[89] J.G.H. du Preez, D.P. Shillington, E. Herselman, H. E. Rohwer, B.J.A.M. van Brecht, H. Wilke, Solv. Extr. Ion Exch. 13(2) (1995) 189-214.

[90] J.G.H. du Preez, D.P. Shillington, B. J. A. M. van Brecht.Solv. Extr. Ion Exch. 2 (1984) 839-858.

[91] F. Helfferich, Ion Exchange, McGraw-Hill Book Company, Inc. U.K. 1962 166-184.

[92] K. A. Allen, J. Phys. Chem. 60 (1956) 943-946.

[93] P.A. Tasker, P.G. Plieger, L.C. West, in: J.A. McCleverty, T.J. Meyer (Eds) Comprehensive Coordination chemistry II, Elsevier, London, 9 1979 245.

[94] N.J.K. Simpson, Solid Phase Extraction, PrinciplesTechniques and Application, Marcel Dekker, New York, 2000.

[95] D.J. Walsh, P. Crosby, R. F. Dalton, Polymer 24(1983) 423-456.

[96] S. Chigome, G. Darko, N. Torto, Analyst 136 (2011) 2879-2889.

[97] G. Schmuckler, Talanta12 (1965) 281-290.

[98] B.S. Garg, R.K. Sharma, N. Bhojak, S. Mittal, Microchem. J. 61 (1999) 94-114.

[99] S.K. Sahni, Reedijk, J. Coord. Chem. Rev. 59 (1984) 1-17.

[100] M. Chanda, G.L. Rempel, React. Polym. 19 (1993) 213-234.

[101] J. Deng, L. Wang, L. Liu, W. Yang, Prog. Polym. Sci. 34 (2009) 156-172.

[102] P.M. Stevens, Polymer Chemistry. An Introduction; Oxford University Press: New York. 1999.

[103] M. Yan, O. Ramstrom, M. Dekker, Molecularly Imprinted Materials. Science and Technology; New York, 2005.

[104] A. Tobiasz, S.Walas, B.Trzewik, P.Grzybek,M. M.Zaitz, M.Gawin, H. Mrowiec, Microchem. J.*93*(2009) 87-99.

[105] F.Linsker, R. L. Evans, J. Am. Chem. Soc. 67 (1945) 1581-1582.

[106] B. B. De, B. B. Lohray, S. Sivaram, P. K. J. Dhal, Polym. Sci. Part A: Polym. Chem. 35 (1997) 1809-1818.

[107] S. Majee, C. Ray, J. Das, Ind. J. Chem. 27A,(1988) 137-140.

[108] R. R. Grinstead, J. Metal.31 (1979) 13-16.

[109] D. Lindsay, D. D. Sherrington, J. A. Greig, R. D. Hancock. React. Polym.12 (1990) 59-73.

[110] J. -H. He, Y. Liu, L.-F. Mo, Y.-Q Wan, L. Xu, Electrospun Nanofibers and Their Applications, Smithers: Shopshire 2008.

[111] D. Li, Yi Xia, Adv. Mater. 16(2004) 1151-1169.

[112] W. E. Teo, S. Ramakrishna, Nanotechnology17 (2006) R89-R106.

[113] Y. J. Ryu, H. Y. Kim, K.H. Lee, H. C. Park, D. R. Lee, Eur. Polym. J. 39 (2003) 1883-1896.

[114] D. C. Sherrington, Chem. Comm.(1998) 2275-2287.

[115] T. Ondarcuhu, C. Joachim, Europhys. Let. 42 (1998) 215-225.

[116] S. Feng, L.Li, H. Zhai, J. Song, Y. Jiang, L. Zhu, D. Angew, Chem. Int. Ed. 41 (2002) 1221-1227.

[117] P. X. Ma, Z. R. J Hang, Biomed. Mat. Res. 46 (1999) 60-72.

[118] G. Liu, L. Qiao, A. Guo, Macromolecules 29 (1996) 5508-5519.

[119] D. H. Reneker, I. Chun, Nanotechnology 7 (1996) 216-230.

[120] A. Frenot, I. S. Chronakis, Curr. Pin. Colloid Interface Sci. 8 (2003) 64-72.

[121] Z.-M. Huang, Y.–Z. Zhang,M. Kotaki, S. Ramakrishna, Compos. Sci. Technol. 63(2003) 2223-2253.

[122] D. H. Reneker, A.L. Yarin, H. Fong, S. Koombhongse, J. Appl. phys. 87 (2000) 4531-4544.

[123] A. Greiner, J. H. Wendorff, Chem. Int. Ed. 46 (2007) 5670-5682.

[124] W. Hai-Sheng, F. Guo-Dong, L. Xin-Song, Rec. Patients Nanotechnol. 3 (2009) 21-31.

[125] Y. Dzenis, Science304 (2004) 1917-1988.

[126] A. Kumar, Nanofibers Intech. (2010) 234-245.

[127] S. Majee, C. Ray, J. Das, Ind. J. Chem. 27A (1988) 137-140.

[128] H. Liu, Y. L. Hseih, J. Polymer Sci. Polym. Phys. 41 (2003) 953-978.

[129] K. Nagapudi, W. T. Brinkman, J. E. Leisen, L. Huang, R. A. McMillan, R.P. Apicarian, V. P. Conticello, E. L. Chaokof, Macromolecules 35 (2002) 1730-1745.

CHAPTER 2

●●●●●

MATERIALS, EXPERIMENTAL TECHNIQUES AND METHODS

2.1 Materials

Table 2.1: List of chemicals and reagents used.

Chemicals	% Purity/Concentration	Supplier
H_2SO_4	98	Merck Chemicals
HCl	0.0364 g/mL	Merck Chemicals
$NiSO_4 \cdot 6H_2O$	98	Merck chemicals
$CuSO_4$ (anhydrous)	99	Merck chemicals
$MgSO_4 \cdot 7H_2O$	99.7	Merck chemicals
$MnSO_4 \cdot H_2O$	99.2	Holpro analytics
$Fe_2(SO_4)_3 \cdot xH_2O$	70	Merck chemicals
$Fe(SO_4) \cdot 7H_2O$	98	Merck chemicals
$CoSO_4 \cdot 7H_2O$	97.5	Fluka
$CaSO_4 \cdot H_2O$	98.5	UniLab
$ZnSO_4 \cdot 7H_2O$	99.5	BDH
$CdSO_4 \cdot H_2O$	98+	BDH
Nitric acid (Trace Select)	≥69	Sigma-Aldrich

$(CH_3)_4NH_4Cl$	97	Sigma-Aldrich
$(CH_3)_4NH_4OH$	10 wt in water	Sigma-Aldrich
DNNSA	50 wt in heptane	Sigma-Aldrich
Shellsol 2325	17-22 v/v aromatic	Shell Chemicals - SA
2-Octanol	98	Sigma-Aldrich
Acetone	98	Sigma-Aldrich
Dimethylglyoxime	97	Sigma-Aldrich
Pyridine-2-aldehyde	99	Sigma-Aldrich
Glyoxal	40 in water	Sigma-Aldrich
Ammonia	28	Merck Chemicals
Methanol	99.9	Sigma-Aldrich
Ethanol	99	Sigma-Aldrich
Diethylether	99	Merck Chemicals
Ethyl acetate	98	Sigma-Aldrich
Alkyl halides	97	Sigma-Aldrich
Imidazole	99.5	Sigma-Aldrich
1-Methylimidazole	99	Sigma-Aldrich
$NH_2OH{\cdot}HCl$	98	Sigma-Aldrich
n-Butyllithium	2.5 M in hexane	Sigma-Aldrich
Toluene-4-sulfonic acid	98	Sigma-Aldrich
DMF	99	Merck Chemicals

KOH	98	Sigma-Aldrich
Na_2CO_3	98	Merck Chemicals
Merrifield resin	1.0% crosslinked, [Cl]: 1.2mmolg^{-1}, 40-60 mesh	Sigma-Aldrich
Azobisisobutyronitrile (AIBN)	98	Sigma-Aldrich
4-Vinylbenzylchloride (VBC)	90	Sigma-Aldrich
Divinylbenzene (DVB)	80	Merck Chemicals
Benzoyl peroxide	75	Sigma-Aldrich
Hydroxyethylcellulose (HEC)	Viscosity: 145 mpa.s 1% in H_2O	Sigma-Aldrich
Gelatine Powder	97	Merck Chemicals

Standard concentrations[1] of the metal ions for ICP calibration were prepared from a 1000 ppm (±0.2%) stock solutions in 0.5 M nitric acid supplied by EC lab services (South Africa). All other chemicals and solvents were purchased from commercial sources and used as received.

2.2 Spectroscopic techniques

2.2.1 NMR Spectrometry

The identity and t he purity of the extractants was determined by ^{1}H NMR spectroscopy on a B ruker AMX 400 NMR MHz spectrometer and reported relative to tetramethylsilane (δ 0.00).

2.2.2 Infrared and Electronic Spectroscopy

The metal complexes were characterised using infrared spectroscopy and recorded on either a Perkin Elmer 400 FTIR spectrometer in the mid-IR range (4000 – 400 cm^{-1}) as KBr pellets or as neat compounds with a Perkin Elmer 100 FTIR-ATR (4000 – 650 cm^{-1}) spectrometer. The solid reflectance spectra of the metal complexes were recorded on a Shimadzu UV-VIS-NIR Spectrophotometer UV-3100 with a MPCF-3100 sample compartment with samples mounted between two quartz discs which fit into a sample holder coated with barium sulfate. The spectra were recorded over the wavelength range of 2000-250 nm, and the scans were conducted at a medium speed using a 20 nm slit width. Solution spectra for the spectrophotometric titrations were recorded on a Varian Cary 1E Spectrophotometer using 1 cm quartz cells. The spectrophotometric titration scans were run 5 minutes after the increment of the ligand ratio. The spectra were recorded in the range 850–350 nm at a scan rate of 200 nm per minute.

2.3 Analytical methods

2.3.1 Elemental analysis

Elemental analysis was carried out with a Vario Elementary ELIII Microcube CHNOS elemental analyser.[2] Calibration of the instrument was done with the use of the following standards in a linear curve adjustment within the total working range.

Standard 1: Sulfanilamide – C; 41.81, H; 4.65, N; 16.25, S; 18.62%

Standard 2: Acetanilide – C; 71.09, H; 0.67, N; 10.36, O; 12.0%

The basic principle of quantitative CHNOS analysis is high temperature combustion of organic and many inorganic solid or liquid samples.[3] The gaseous combustion products are purified, separated into their various components and analyzed with a suitable detector such as thermal conductivity detector (TCD), optional infrared detector (IR) for sulfur, etc.

2.2.2 Inductively coupled plasma (ICP) spectrometry

Metal ion analyses were carried out with a Thermo Electron (iCAP 6000 Series) inductively coupled plasma (ICP) spectrometer equipped with an OES detector. The ICP/AAS metal standards, dissolved in 0.5 M nitric acid, were used to prepare standard solutions for the construction of calibration curves using distilled, deionized, milliQ water for the dilutions. The elements were analysed at the following US-EPA[4] specified wavelengths (nm) for minimal interferences; 231.6 (Ni^{2+}), 237.80 (Co^{2+}), 324.75 (Cu^{2+}), 334.50 (Zn^{2+}), 259.99 (Fe^{2+}, Fe^{3+}), 413.70 (Cd^{2+}), 315.88 (Ca^{2+}), 257.61 (Mn^{2+}), and 279 (Mg^{2+}). The detector type was RACID charge injection device.

The Thermo Electron iCAP 6000 Series-optical emission spectrometer was operated with the parameters in Table 2.2. The elements (atoms) are excited and when they return to low energy status, emission rays are released and the emission rays that correspond to the photon wavelength are measured.[5] The element type is determined based on the position of the photon rays, and the content of each element is further determined based on the rays' intensity.

To generate plasma, first, argon gas is supplied to the torch coil, and high frequency electric current is applied to the work coil at the tip of the torch tube. Using the electromagnetic field created in the torch tube by the high frequency current, argon gas is ionized and plasma is generated. This plasma has high electron density and temperature (10 000K) and this energy is used in the excitation-emission of the sample. Solution samples are introduced into the plasma in an atomized state through the narrow tube in the center of the torch tube.[6]

Table 2.2: ICP-OES method and operating parameters

Parameter	Setting
Applied radio frequency (RF) power	1150 W
Plasma (Ar) gas Flow rate	5.0 L/min
Auxiliary gas flow rate	0.5 L/min
Nebulizer Ar gas flow rate	1.5 L/min
Sampling depth	8.5 mm
Sample pump rate	50 rpm
Time scan acquisition	50 ms/point
Cooled spraying chamber temperature	4 ^{o}C
The camera temperature	46.63^{o}C
Generator temperature	24^{o}C
Optics temperature	36.9^{o}C
Total integration time	30 s per analyte
Sample flush time	30 s
Number of replicates	3

2.3.3 Inductively coupled plasma-mass spectrometry (ICP- MS)

The samples processed from the synthetic mixture of metals were also analysed on a Perkin-Elmer SCIEX ELAN 6100 ICP-MS. The spectrascan SS-028317 multi-element standard was used to prepare the calibration standards and a Sigma-Aldrich (69%) p.a. nitric acid was used to make the sub-boiled acid. The operating parameters are as shown in Table 2.3. The dual detector mode employed was analogue.[7] Isotopes analysed were; Co 59, Ni 60, Cu 65, Zn 66, Fe 56, Cd, 112, Ca

40, Mn 55, and Mg 24. ICP-MS has a superior detection capability in that it combines a hi gh temperature ICP source with a m ass spectrometer. The ICP source coverts the atom of the elements in the sample to ions. These ions are then separated and detected by the mass spectrometer. Thus, it has the ability to obtain isotopic information.[8]

Table 2.3: ICP-MS method and operating parameters

Parameter	**Setting**
Applied radio frequency (RF) power	1100 W
Plasma (Ar) gas Flow rate	5.0 L/min
Auxiliary gas flow rate	0.5 L/min
Nebulizer Ar gas flow rate	0.97 L/min
Dwell time	50.0 ms/analyte mL
Sample pump rate	1.2 mL/min
Total integration time	1000 min
No of replicates	3

2.4 Surface techniques

2.4.1 Scanning electron microscopy

Samples were prepared for scanning electron microscopy (SEM) by mounting them on the SEM stubs using double sided graphite tape and t hen sputter coated with gold using a Balzers' union sputtering device.[9] The samples were viewed using a TESCAN Vega TS 5136LM typically at 20 kV at a working distance of 20 mm.

A scanning electron microscope (SEM) is a f orm of electron microscope used for producing images of a sample by scanning it with a bea m of electrons in form of raster scan patterns. The electrons are made to interact with the atoms of the

samples thereby producing signals that contain information about the sample's surface topography as well as its composition.[10]

An electron beam which posses energy ranging from 0.2 keV to 40 keV, is focused by one or two condenser lenses to a spot about 0.4 nm to 5 nm in diameter. As the beam of electron passes through pairs of scanning coils or pairs of deflector plates in the electron column in thefinal lens, the beam is deflected so that it scans in a raster fashion over a rectangular area of the sample surface. As the primary beam interacts with the sample, the electrons lose energy by repeated random scattering and absorption within a teardrop-shaped volume of the specimen known as the interaction volume, which extends from lessthan 100 nm to around 5 μm into the surface.[11] The electron's landing energy, the atomic number of the specimen and the specimen's density are all determining factors of the size of the interaction volume.[12] The energy exchange between the electron beam and the sample result in the reflection of high-energy electrons each of which can be detected by specialized detectors. The specimen absorbs the beam of current which can be detected and used to create images of the distribution of specimen current.[13] SEM micrograph is known to have magnification of a range of up to six orders of manitude from about 10 to 500,000 times.[14]

2.4.2 X-ray photoelectron spectroscopy

X-ray photoelectron spectroscopy (XPS) is a quantitative spectroscopic technique that measures the elemental composition, empirical formula, chemical state and the electronic state of the the elements that exist on a surface of a material.[15] The design and construction of electron spectroscopy is very complex. The modules necessary for analysis by electron spectroscopy are: a source of primary beam (X-rays or electrons), an electron energy analyser and a detection system, all contained in a vacuum chamber, a data system also forms part of the integral part of the spectroscopy.[16] The analysis and detection of photoelectrons requires that the sample be placed in a high-vacuum chamber, the reason for this is that the analytical signal of low-energy electrons is easily scattered by the residual gas molecules and unless their concentration is kept to an acceptable level, the total spectral intensity will decrease, while the noise level in the spectrum will increase.

The XPS spectra are produced from the irradiation of a material with a beam of X-rays while simultaneously measuring the kinetic enegy and number of electrons that escape from the top 1 to10 nm of the materials that is being analyzed.[16] The basic principle of this technique is based on the irradiation of the sample surface with a monochromatic X-rays. This radiation hits the core electrons of the atoms. The core electrons are targeted because being closer to the nucleus their binding energies are characteristics of their particular elements.[17] By targeting these elements, information on the elements of the particular sample can be obtained.

The kinetic energies of the ejected electrons differ depending on the orbitals from which they originate, these energies are then related to the orbital ionization potential of the molecule or sample atom.[18] Electrons ejected from the surface are energy filtered *via* a Hemispherical Analyser (HSA) before the intensities for a defined energy is recorded by a detector. Since core level electrons in solid state atoms are quantized, the resulting energy spectra exhibit resonance peaks characteristic of the electronic structure for the atom at the sample surface. For each and every element, there will be a characteristic binding energy associated with each core atomic orbital, i.e. each element will give rise to a characteristic set of peaks in the photoelectron spectrum at kinetic energies determined by the photon energy and the respective binding energies. Furthermore, the binding energies differ not only from chemical species to species, but also vary with the bonding conditions in which the element is found. This technique also provides information on the actual compounds present on the surface. The XPS technique is highly surface specific due to the short range of the photoelectrons that are excited from the solid. The energy of the photoelectrons leaving the sample is determined using a Concentric Hemispherical Analyser (CHA), and this gives a spectrum with a series of photoelectron peaks.[19]

2.4.3 Brunauer, Emmett, Teller (BET) surface area analysis

Carbon dioxide adsorption/desorption isotherms were measured at 77K using a Micromeritics ASAP 2020 Surface Area and Porosity Analyzer. Prior to each measurement, samples were degassed for a minimum of one week to ensure complete removal of adsorbed impurities. Degassing was performed at 70°C for the linear polymers and at 150°C for crosslinked polymers, unless mentioned

otherwise. Approximately 0.2 g of sample was used and an equilibration interval of 20 seconds was allowed during the run. The surface area (BET), were calculated from these isotherms.

The theory of BET[20] which explain the physical adsorption of gas molecules on a solid surface provides the basis for the measurement of the specific surface area of a material. The basic concept of the theory is an extension of the Langmuir theory.[19] Langmuir theory deals with monolayer molecular adsorption and multilayer adsorption built on the hypothesis that gas molecules are adsorbed on solid layers infinitely and that there is no interaction between each adsorption layer.

This concept of the BET theory as an extension of Langmuir theory for monolayer molecular adsorption is summarized by equation 29 following these hypotheses listed above.

$$\frac{1}{v[(Po/P-1)]} = \frac{c-1}{v_m\, c}\left(\frac{P}{Po}\right) + \frac{1}{v_m c} \qquad (29)$$

where P and P_0 are the equilibrium and the saturation pressure of adsorbates at the temperature of adsorption,

v is the adsorbed gas quantity (e.g., in volume units),

v_m is the monolayeradsorbed gas quantity.

c is the BET constant, which is expressed by equation (30);

$$c = \exp\left(\frac{E_1 - E_L}{RT}\right) \qquad (30)$$

Equation 29 is an adsorption isotherm and can be plotted as a straight line with $1/v[(P_0 / P-1)]$ on the y-axis and $\varphi = P / P_0$ on the x-axis according to experimental results. This plot is known as BET plot.

The BET method is widely used in surfacescience for the calculation of surface areas of solids by physical adsorption of gas molecules. A total surface area S_{total} and a specific surface area S are evaluated by the following equations 31 and 32:

$$S_{BET,total} = \frac{(v_m Ns)}{V} \quad (31)$$

where v_m is in units of volume which are also the units of the molar volume of the adsorbate gas

$$S_{BET} = \frac{S_{total}}{a} \quad (32)$$

where N is Avogadro's number,

s is adsorption cross section of the adsorbing species,

V is molar volume of adsorbate gas,

and a is mass of adsorbent (g).

2.5 Potentiometry and HYPERQUAD

The protonation and formation constants were determined by potentiometric acid-base titrations using the Metrohm 794 Titrino equipped with a M etrohm LL Ecotrode. The concentration stability constants (β_{pqr}) were calculated using the computer program HYPERQUAD[21] (extension of SUPERQUAD). This program makes use of the following assumptions to calculate the formation constants:

(i) For each of the chemical species $M_pL_qH_r$ in the solution equilibra, there is a chemical constant which is expressed as:

$$\beta_{pqr} = \frac{[M_pL_qH_r]}{[M]^p[L]^q[H]^r} \quad (33)$$

where M, L and H represent a metal, ligand and proton respectively.

(ii) The electrodes used, have a pseudo-Nernstian behaviour.

(iii) Careful calibration of the electrode, accurate standardization of reagents, elimination of weighing and di lution errors, elimination of carbonate impurities, elimination of temperature variance and purity of water minimise the systematic

errors. All statistical tests are based on the assumption that systematic errors are absent.

(iv) The program assumes that the independent variables (such as titre volume) are not subject to errors and that the dependent variables (such as measured potential) have a normal distribution. If this is the case then the calculated residuals should not show systematic trends.

(v) For any equilibrium system, a model exists that will fit the experimental data. All least-square refinements are performed in terms of the assumed model. The model that is found may not be the true model, but it will be the one that fits the observed data. It will have no ill-defined constant and the standard deviation. A constant is considered ill-defined if its standard deviation is more than 33% (such standard deviations are labelled "Excessive") or if its value is negative.

The program calculates the stability constants using a non-linear least-square refinement algorithm based on following the acid concentration in complex acid-base equilibra using the proton sensitive glass electrode. The concentration of the hydrogen ion in solution is related to the potential measured with the electrode by the modified Nernst equation, $E = E^o + RT/F \ln[H^+]$. The standard potential, E^o, must be determined for the specific conditions of operation *via* the calibration of an electrode for a strong acid-base titration using the Gran method.[22]

The concentrations of the chemical species are determined by solving the non-linear simultaneous equations of mass-balance using the Newton-Raphson method. The program allows for up to four reactants and up to 18 species. The equilibra for the specific interactions of the reagents, M (metal) and L (ligand), with H (proton) are

$$M + iH = H_iM; \quad L + jH = H_jL; \tag{34}$$

and the total concentrations (T_M, T_L, T_H) of the species is given by:

$$T_M = [M] + \sum_{pqr} p\beta_{pqr}[M]^p[L]^q[H]^r + \sum_i \beta_{10i}[M][H]^i \tag{35}$$

$$T_L = [L] + \sum_{pqr} q\beta_{pqr}[M]^p[L]^q[H]^r + \sum_j \beta_{10j}[L][H]^j \tag{36}$$

$$T_H = [H] + \sum_{pqr} r\beta_{pqr}[M]^p[L]^q[H]^r + \sum_i \beta_{10i} i[M][H]^i + \sum_j \beta_{10j} j[L][H]^j - [OH^-] \tag{37}$$

Mass-balance equations must be satisfied and hence the total concentration of a reagent is the sum of its concentrations in all the chemical species in the mixture. Once the free reactant concentrations ([M], [L], [H]) have been calculated, the concentrations of the complexes are derived from them and the equilibrium constants (during model fitting, the constants must be estimated). The best fit to the experimental data is determined by minimizing the error square sum of the residuals,

$$U = \sum w_i \, (E_I^{Obs} - E_I^{cal})^2 \qquad (38)$$

where w_i is the weighting factor.

The model adequately accounts for the experimental observations and can be proposed for the equilibrium system. The model is specified by a set of coefficients (p,q,r), one for each species in terms of the assumed model. Choice of the "best" model is based on the statistical value, sigma (σ). Ideally σ should be equal to one but it has been proposed that any fit with $\sigma < 3$ is satisfactory. If σ is large, then the experimental data points with larger residuals must be removed during the refinement if the specified model is a promising fit.

2.6 Other Instruments

2.6.1 pH determinations

The pH measurements were performed on a M etrohm 827 pH meter using a combination electrode with 3 M KCl as electrolyte. Calibration of the electrode was maintained at intervals of two weeks using standard buffer solution of pH 4.0, 7.0 and 9.0 from Metrohm.

2.6.2 Conductivity measurements

The conductivity measurements were carried out on A.W.R. Smith Process Instrumentation cc Laboratory Bench Meter Model AZ 86555. The ABS graphite cell probe was used along with an aqueous standard which has a conductivity value of 135 $ohm^{-1}.cm^{-1}.mole^{-1}$ at 20°C for the calibration. All the complexes were prepared in water as solvent at a concentration of 10^{-3} M for the conductivity measurements.

2.6.3 Melting point determination

The melting points of the solid complexes were determined with the electrothermal IA 9000 digital measuring point apparatus.

2.6.4 Lab Shaker

The Labcon micro-processor controlled orbital platform shaker model SPO-MP 15 was used for contacting the two phases in the solvent extraction experiments.

References

[1] U. S. Environmental protection agency, ICP-OES and AAS Calibration standards, 2007.

[2] Elementar Analysensysteme GmbH, CHNOS Elemental Analyzer Vario Micro operating instruction, 2005.

[3] Elementar.de,Technologia Aplicada Internacionan, San Jose, Costa Rica, America Central, 2000.

[4] U. S. Environmental protection agency, method 200.7 Trace elements in water, solids, and biosolids by ICP-OES, Revision, 2001.

[5] H. J. Van de wiel, Horizontal 19 (2004) 1- 46.

[6] SII Nanotechnology Inc, Product Brochure 2012.

[7] K. G. Heumann, Anal. Bioanal. Chem. 378 (2004) 318-129.

[8] R. E. Wollf, Department of the interior, U.S. Geological Survey, 2005.

[9] Balzers Union Ltd, Sputtering device operating instruction, Accessories for Electron Microscopy, 1988 1-9.

[10] R. Cross, The preparation of material for scanning electron microscopy (SEM) Electron Microscopy Unit, Rhodes University, South Africa, 2001 55-56.

[11] R. Hermann, P. Walther, M, Muller, J. Struct. Biol. 107 (1991) 38-47.

[12] G. M. Hodges, Arch. Histol. Cytol. 55 (1992) 27-38.

[13] T. Osawa, M. Abe, A. Morigami, Y. Nozaka, J. Electron Microsc. 47 (1998) 273-276.

[14] E. Suzuki, J. Microsc. 208 (2002) 153-157.

[15] S. K. Edvarson, K. M. Siegbahn, Nuc. Phys. 1 (1956) 160-169.

[16] K. M. Siegbahn, Physics Nobel Lecture 1981-1990 61-63.

[17] F. J. Watts, J. Wolstenholme, An Introduction to Surface Analysis by XPS and AES, John Wiley, New York, 2 2003.

[18] C. S. Fadley, Electron Spectroscopy: Theory, Techniques and applications. Academic Press, New Yor, 2nded 1978.

[19] I. Langmuir, J. Am. Chem. Soc. 38 (1916) 2221-1195.

[20] S.Brunauer, P. H. Emmett, E. Teller, J. Am. Chem. Soc. 60 (1938) 309-326.

[21] P. Gans A. Sabatini, A. Vacca, Talanta 43 (10), (1996) 1739 -1745.

[22] G. Gran, Analyst, 77 (1952) 661-678.

CHAPTER 3

●●●●●

SOLVENT EXTRACTION WITH DIMETHYLGLYOXIME AND IMIDAZOLE-2-ALDOXIME AS EXTRACTANTS

3.1 Introduction

Oximes, by the nomenclature, are abbreviation of oxy-immines. They are amphiprotic in nature, having a s lightly basic nitrogen atom and a mildly acidic hydroxyl group.[1] Oximes are derived either from an aldehyde group (aldoximes) or the keto group (ketoximes). The structure in Figure 3.1 was much more accepted as being representative of this functional group of all that wereproposed based on a neutron diffraction study of dimethylglyoxime (DMG) which shows the presence of an O−H bond.[2] In the solid state oximes are usually associated to the presence of hydrogen bonding (O−H···N).[3]

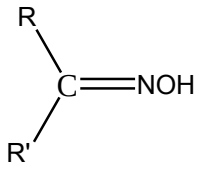

Figure 3.1: The representative structure of oximes. R and R' represent any carbon containing group or hydrogen.

The oxime group may coordinate to the metal through either of the donor atoms, N or O,[4] thus acts as an ambidentate ligand. The mode of coordination of the oxime group is known to be influenced by the other group(s) present in the ligand.[5] The oxime group may be the sole coordinating ligand. Oximes are known in various classifications such as simple oximes, vic-dioximes, carbonyl oximes, hydroxyoximes, etc., depending on other functional groups present and their relative positions to one another.

The application of oximes as separating agents in analytical chemistry dates back to the discovery of DMG (Figure 3.2) as the first selective organic reagent applied in the analysis of metals.[6] In 1905, Tshugaev discovered DMG to be a nickel(II) selective reagent.[7] Ever since, DMG has been applied under certain chemical conditions as a nickel specific reagent. Thus DMG is an ideal reagent for analytical purposes and its structure and behaviour yields principles which may serve as a guide to the discovery and investigation of similar reagents.

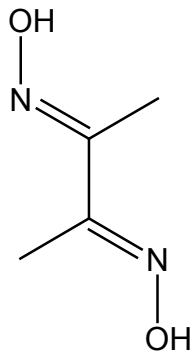

Figure 3.2: The chemical structure of dimethylglyoxime (DMG)

Generally, thevic-oximes through X-ray diffraction and infra-red spectrophotometry[8,9] are known, in accordance with magnetic measurements[10,11] to form square-planar *bis*-chelates with most bivalent ions. The close structures are due to the formation of additional rings by means ofinter ligand hydrogen bridges. These structures are endowed with additional stability provided by the hydrogen bridge.[12-14] The stabilizing effect of the hydrogen bridge is pronounced in dimethylglyoxime complexes of nickel, palladium, copper and cobalt of the composition $M(DMG)_2$, as shown by the structure in Figure 3.3. In addition, the ligand fieldeffect and the presence of metal-metal bond in nickel, palladium and platinum complexes were found responsible for their higher stability.[8]

In further studies, the O−H frequencies indicated the consecutive order of the strength of the hydrogen bridges as Ni ≈ Pd ≈ Pt ≈ Cu » Fe ≈ Co in the complexes of the bivalent metals.[15] Nickel dimethylglyoximate (Figure 3.3) is known to have higher bond strength arising from the symmetrical co-planar structure (the oxime hydrogen in the bridge is equally shared between the two atoms),[16] and the oxygen-oxygen distance (2.44 Å) in nickel complex is the shortest known for hydrogen-

bonded oxygen atoms.[17] However, the stability constants of the dimethylglyoxime complexes of the later 3d transition metals reveals the following order: Cu(II) >Ni(II) >Co(II) >Zn(II).[18] It is therefore clear that if the nickel complex is not the most stable, there must therefore be some other factors involved in the selectivity of DMG for nickel, which may be the difference in the solubility.[19] In analytical chemistry, the solubilities of metal complexes are of vital importance. Thus the analytical selectivity of nickel and palladium with DMG is deemed to have in part arisen from the low solubilities of their complexes whereas other similar transition metal complexes are soluble in water. The strong hydrogen-bonding of the –OH groups in the planar *bis*(dimethylglyoximate)nickel(II) makes it difficult to interact with water molecules and this explains its ready extractability into chloroform.[20] On the other hand, in the corresponding non-planar, cobalt(II) complex, the –OH groups are available for bonding to water molecules, thereby preventing its extraction into chloroform and making possible the separation of nickel from cobalt.[1] On this note, in this study, it was decided primarily to investigate the possible application of DMG as an extractant in the exploitation of oxime for the separation of nickel from cobalt and other base metals. This was carried out in an acidic sulfate medium using Shellsol/2-octanol as the organic solvent.

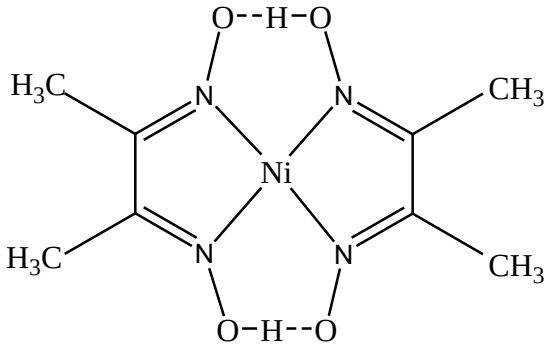

Figure 3.3: The chemical structure of bis(dimethylglyoximate)nickel(II)

Similarly, the hydroxyoximes (LIX reagents) are known to form square planar *bis*-chelates with most bivalent ions. Hydroxyoximes e.g. salicyaldoxime have found useful applications as extractants in the separation of base metals.[21] The chemical structure shown in Figure 3.4 has been widely applied in the commercial solvent extraction of copper from dilute acidic liquors.[22] The stable complexes formed with

the LIX reagents are also due to the formation of a square planar structures characterised with hydrogen bonding.

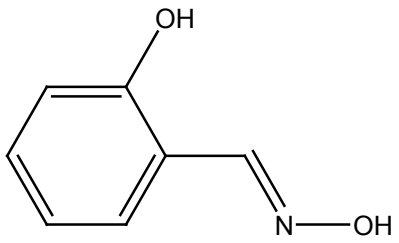

Figure 3.4: The chemical structure of salicyaldoxime

The aromaticity of the benzene ring offers additional stability due to the π bonds involving electron transfer from metal to the ligand. Figure 3.5 shows the respective chelates of a typical hydroxyoxime with the presence of the hydrogen bridges.

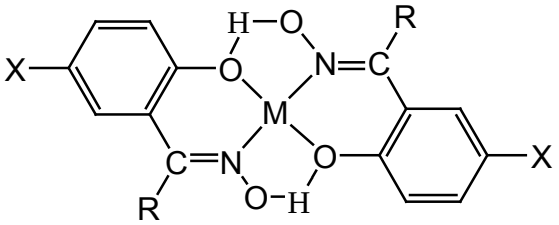

Figure 3.5: The chemical structure of bis(hydroxyoximate)nickel(II)

Furthermore the chelating hydroxyoximes (LIX reagents) have received considerable research activity since the 1970s with several groups engaged in studies related to extraction efficiencies, mechanisms and kinetics of the extraction process. Some representative extractants in this class such as LIX 64 went to commercialization for the extraction of copper in several plants around the world including USA, England, and Southern Africa.[23-25] It has been shown in these studies that these extractants act in an ionised form and that the rate-determining step is the complex formation step. It was further concluded that the rate-controlling step is pH dependent, and that if the reaction took place in a homogeneous aqueous phase then the extraction efficiency would be proportional to the concentration of the extractant in the aqueous phase.[21] These studies invariably

depicted first-order dependence of copper ion concentration for higher oxime concentration and negative first-order kinetics for the hydrogen ion in the pH range 2.8-3.6.[26] These studies, therefore, imply that the ionised oximeextractant must have some water-solubility while the complexed (or chelated) form must be soluble in the organic phase.

In this study, the design of an imidazole-oxime extractantcontaining the imidazole group and the immine group of the oxy imminehas been advanced. The mild-to-good σ-donor and good π-acceptor ability of these donor groups should allow for discrimination in bonding with the base metals. The mildly acidic hydroxyl group of 1-octylimidazole-2-aldoxime could also allow for complex formation in the slightly acidic range, in cooperation with the imidazolyl group, in comparison to the well-established hydroxyimimes and vic-oximes since the overlapping weak dissociation of the phenolic hydroxyl and the oxime hydroxyl in hydroxyoximes[23] shifts the extraction pH range to higher values. This chapter presents a case for the extraction of copper in highly acidic solutions using 1-octylimidazole-2-aldoxime (Figure 3.6) as extractant and dinonlynaphthalenesulfonic acid (DNNSA) (Figure 3.7) as a synergist in Shellsol 2325.

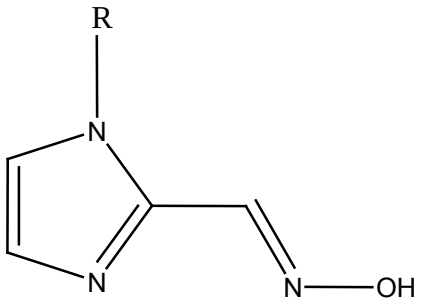

R = octyl and decyl

Figure 3.6: The chemical structures of 1-R-imidazole-2-aldoximes

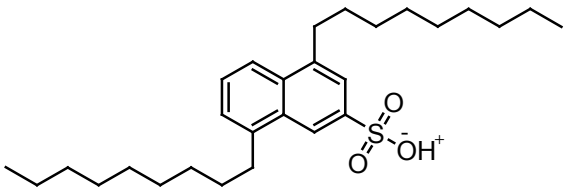

Figure 3.7: The chemical structure of dinonlynaphthalene sulfonic acid (DNNSA)

3.2 Experimental

3.2.1 Preparative work

(a) Synthesis of 1-alkylimidazoles

1-Octylimidazole and 1-decylimidazole were synthesized by alkylation[27] of the imidazole ring with octyland decyl groups respectively.

This was achieved with the addition of 8.65 g (0.15 mol) of potassium hydroxide to a solution of 10 g (0.15 mol) of imidazole in 50 mL acetone. To this, 1-alkylbromide (0.15 mol) was added drop wise. The reaction was allowed to stir for 30 mins and then the mixture was refluxed at 40^{o}C overnight. It was cooled down and followed by vacuum filtration to remove the KBr salt. The resulting solution was concentrated *via* rotary evaporation and then distilled at reduced pressure of 3.0 x 10^{-3} mBar and 110°C to give a yellow coloured oil of 17.04 g of 1-octylimidazole and 16.56 g of 1-decylimidazole respectively.

1-Octylimidazole (OIMZ): Yield = 63%. Anal. Calc. for $C_{11}H_{20}N_2$: C, 73.28; H, 11.18. N, 15.54 % Found: C, 73.89; H, 11.58; N, 15.04 %. ^{1}H NMR (400 MHz, $CDCl_3$) δ (ppm): 6.72, 6.85 and 7.27 (2xd+1xs,3H,Im-H), 3.72 (t,2H,N-$\mathbf{CH_2}$), 1.57 (m,2H,N-CH_2-$\mathbf{CH_2}$), 1.09-1.11 (m,10H,N-$(CH_2)_2\mathbf{(CH_2)_5}CH_3$), 0.71 (t,3H,N$(CH_2)_7\mathbf{CH_3}$). IR ($v_{max}$/cm^{-1}): 665 (s), 810 (m), 1078 (s), 1376 (w), 1465 (m), 1508 (s), 1701(w), 2855 (s) and 2925 (w).

1-Decylimidazole (DIMZ): Yield = 53%. Anal. Calc. for $C_{13}H_{24}N_2$: C, 74.94; H, 11.61; N, 13.45 %. Found: C, 74.89; H, 11.58; N, 13.54 %. ^{1}H NMR (400 MHz, $CDCl_3$) δ (ppm): 6.75, 6.88 and 7.30 (2xd+1xs,3H,Im-H), 3.75(t,2H,N-$\mathbf{CH_2}$), 1.60(m,2H,N-CH_2-$\mathbf{CH_2}$), 1.11 (m,14H,N-$(CH_2)_2\mathbf{(CH_2)_7}CH_3$), 0.74 (t,3H, N$(CH_2)_9\mathbf{CH_3}$).

IR (v_{max}/cm^{-1}): 665 (s), 811 (m), 1077 (s), 1376 (w), 1465 (m), 1508 (s), 1588 (s), 2853 (s) and 2923 (s).

(b) Synthesis of 1-akylimidazole-2-aldehydes

1-Octylimidazole-2-aldehydeand 1-decylimidazole-2-aldehyde were prepared according to the procedure previously published by Inversion and Lund[28] with little modifications. To the suspension of 0.10 mol of the respective 1-alkylimidazole in 150 mL dry diethylether was added 0.10 mol of 2.5 M butyllithium (40.0 mL) under a nitrogen atmosphere at -50°C. The mixture obtained was stirred at this temperature for a period of an hour after which 18 mL of freshly distilled dimethylformamide (DMF) was added. The reaction was left to proceed overnight during which the temperature of the dry ice bath rises to the room temperature. Within a period of 10mins, 10mL of water was carefully added followed by 40mL of 4NHCl. The aqueous layer was separated from the ethereal layers and further washed with portions of the 4 N HCl. The acid extracts werecombined and saturated with potassium carbonate and then extracted with 4 x 20 mL chloroform. The combined chloroform extracts were then dried over magnesium sulfate which was later filtered out. The chloroform was evaporated with rotavapor and the resulting solution was further purified in a chromatographic column filled with silica gel using acetone/chloroform (2:1) as solvent. 13.12 g and 17.26 g of 1-octylimidazole-2-aldehyde and 1-decylimidazole-2-aldehyde were yielded respectively.

11-Octylimidazole-2-aldehyde (OIMDE): Yield = 63%. Anal. Calc. for $C_{12}H_{20}N_2$: C, 69.19; H, 9.68;18 N, 13.45 %. Found: C, 69.12; H, 9.85; N, 12.99 %. ^{1}H NMR (400 MHz, $CDCl_3$) δ (ppm): 9.76 (s,1H,CHO), 7.23,7.12 (2xd,2H,Im-H), 4.34(t,2H,N-**CH_2**), 1.73(m,2H,N-CH_2-**CH_2**) 1.26 (m,10H,N-$(CH_2)_2$**$(CH_2)_5$**CH_3), 0.83 (t,3H, N$(CH_2)_7$**CH_3**). IR (v_{max}/cm^{-1}): 682 (s), 766 (s), 920 (s),1077 (m), 1150 (m), 1218 (m),1289(s),1330 (s), 1380 (s), 1479 (m), 1509 (m), 1532 (w),1671(s), 2835 (m), 2956 (m), 3108 (m).

1-Decylimidazole-2-aldehyde (DIMDE): Yield = 73%. Anal. Calc. for $C_{13}H_{24}N_2$: C, 71.14; H, 10.23; N, 11.85 %. Found: C, 70.94; H, 10.95; N, 11.57 %. ^{1}H NMR (400 MHz, $CDCl_3$) δ (ppm): 9.73 (s,1H,**CHO**), 7.19,7.10 (2xd,2H,Im-H), 4.31(t,2H,N-**CH_2**), 1.70(m,2H,N-CH_2-**CH_2**) 1.18(m,14H,N-$(CH_2)_2$**$(CH_2)_7$**CH_3), 0.80 (t,3H,N$(CH_2)_9$**CH_3**). IR (v_{max}/cm^{-1}): 682 (s), 766 (s), 920 (s),1077(m), 1150 (m), 1218

(m),1289 (s),1330 (s), 1380 (s), 1479 (m), 1509 (m), 1532 (w),1671(s), 2835 (m), 2956 (m), 3108 (m).

(c) Synthesis of 1-Akylimidazole-2-aldoximes

1-Otylimidazole-2-aldoxime (OIMOX) and 1-decylimidazole-2-aldoxime (DIMOX) were prepared according to the method by Gebert *et al.*[29] with slight modifications. A solution of 4.16 g (0.02 mol) of the respective aldehyde in 15 mL of ethanol was added to 1.40 g (0.02 mol) of hydroxylammine hydrochloride. The pH of the resulting mixture was adjusted to between 5.5 and 6.0 with the addition of ice cold solution of sodium carbonate prepared by the addition of 1.06 g (0.01 mol)of the salt into 20 mL of water. This was allowed to stir at room temperature until precipitates were formed. The solvent was removed under rotary evaporation and the product was purified in a c hromatographic column filled with silica gel and acetone/chloroform (2:1) as solvent. The respective yields of 3.25 g and 3.39 g for the octyl and decyl derivatives were obtained.

1-Octylimidazole-2-aldoxime (OIMOX): Yield = 68%. Anal. Calc. for $C_{12}H_{21}N_3O$: C, 64.54; H, 9.48; N, 18.82 %. Found: C, 64.61; H, 9.93; N, 18.69 %. ^{1}H NMR (400 MHz, $CDCl_3$) δ (ppm): 11.53 (s,1H, OH), 8.33(s,1H,C**H**N), 6.97 and 7.12 (2xd,2H, Im**H**), 4.31 (t,2H,N**CH_2**), 1.78 (m,2H,N-CH_2**CH_2**), 1.25-1.29 (m,10H, $N(CH_2)_2$**$(CH_2)_5$**CH_3), 0.89 (t, 3H,$N(CH_2)_7$**CH_3**).IR (v_{max}/cm^{-1}): 710 (s), 751 (s), 837 (s), 909 (m), 985(vs), 1155 (m), 1413 (s), 1466 (s), 1550 (m), 1632 (m), 1714 (br,w), 2679 (s), 2953 (s), 2922 (s), 3116 (s).

1-Decylimidazole-2-aldoxime (DIMOX): Yield = 63%. Anal.Calc. for $C_{14}H_{25}N_3O{\cdot}0.5H_2O$: C, 64.62; H, 10.07; N, 16.15 %. Found: C, 64.80; H, 10.37; N, 15.98 %. ^{1}H NMR (400 MHz, $CDCl_3$) δ (ppm): 11.50 (s,1H,OH), 8.32(s,1H,C**H**N), 6.96 and 7.13 (2xd,2H,Im**H**), 4.29(t,2H,N**CH_2**), 1.94(m,2H,NCH_2**CH_2**), 1.78 (m,2H,$N(CH_2)_2$**CH_2**), 1.25-1.29 (m,12H,$N(CH_2)_3$**$(CH_2)_6$**CH_3) 0.89 (t,3H,$N(CH_2)_9$**CH_3**). IR (v_{max}/cm^{-1}): 672 (m), 726 (s), 758 (s), 835 (s), 986 (vs), 1002 (vs), 1150 (m), 1373 (s), 1428 (s), 1466 (s), 1555 (m), 1636 (m), 1716 (br, w), 2750 (s), 2850 (s), 2918 (s), 3116 (s).

(d) Synthesis of 1-methylimidazole-2-carboxaldehyde

1-Methylimidazole-2-carboxaldehyde was prepared by the same method used in preparing the octyl and decyl derivatives. The only exception is that the chloroform extracts were concentrated and the product was distilled at $3.0x10^{-1}$ mBar to yield a brownish crystalline solid after cooling.

1-Methylimidazole-2-aldehyde (MIMDE): Yield = 76.1%. Anal.Calc. for $C_5H_6N_2O$: C, 54.54; H, 5.49; N, 25.44 %. Found: C, 54.25; H, 5.65; N, 25.19%. ^{1}H NMR (400MHz, $CDCl_3$):δ (ppm): 4.03 (3H, NCH_3), 7.16-7.27 (2H, Im-H), 9.81 (1H, CHO). IR (v_{max}/cm^{-1}): 682 (s), 766 (s), 920 (s), 1077 (m), 1150 (m), 1218 (m), 1289 (s), 1330 (s), 1380 (s), 1479 (m), 1509 (m), 1532 (w), 1671 (s), 2835 (m), 2956 (m), 3108 (m).

(e) Synthesis of 1-methylimidazole-2-aldoxime

1-Methylimidazole-2-aldoxime (MIMOX)was prepared in a similar manner as the octyl and decyl derivatives from 1-methylimidazole-2-aldehyde. A white crystalline solid was obtained and this was further purified by re-crystallization. The characterization data are given below:

1-Methylimidazole-2-aldoxime (MIMOX): Yield 78-80%. M.p. = 175^{o}C (Lit. 176^{o}C). Anal. Calc. for $C_5H_7N_3O$: C, 47.99; H, 5.64; N, 33.58 %. Found: C, 47.82; H, 5.97; N, 33.61 %.^{1}H NMR (400 MHz, $CDCl_3$) δ (ppm): 10.5 (s,1H,OH), 8.10 (s,1H,C**H**N), 6.97 and 7.31 (2xd,2H,Im**H**), 3.90 (s,3H,N**CH_3**). IR (v_{max}/cm^{-1}): 690 (s), 708 (s), 739 (s), 840 (s), 889 (m), 975(vs), 1155 (m), 1413 (s), 1476 (s), 1543 (m), 1634 (m), 1715 (br, w), 2600 (s), 2748 (br, s), 2810 (s).

(f) Synthesis of the metal complexes

1-Methylimidazole-2-aldoxime metal complexes were prepared according to the modified method of Papatriantafyllopoulou *et al*.[30] A mixture of 20 mL of water with 10 mL of methanol was added to a solid mixture containing each of the hydrated metal sulfate salts (0.60 mmol) and 1-methylimidazole-2-aldoxime (MIMOX) (1.80 mmol). The mixture was refluxed for 8 hours. The resulting solution was layered with 60 ml acetone. With slow mixing, crystals of the products were obtained, filtered and washed with acetone. The solid products were air-dried. The cobalt,

nickel, copper and zinc complexes were pink, deep green, green and white, respectively. The characterization data appears below:

$[Co(MIMOX)_3]SO_4 \cdot 4H_2O$: Yield **=** 65%. M.p. = 229°C. Anal.Calc: C, 29.90; H, 4.85; N, 20.92; S, 5.32 %. Found: C, 29.68; H, 4.82; N, 20.40; S, 5.06 %. IR: (v_{max}/cm^{-1}): 678 (w), 755 (m), 860 (m), 978 (m), 1057 (vs), 1221(m), 1294 (m), 1422 (m), 1460 (s), 1520 (m), 1574 (m), 1636 (m), 1701 (m), 3228 (br, s). UV-Vis (λ_{max}/nm):1240, 492. Conductivity (10^{-3}M, $ohm^{-1}.cm^{-1}.mole^{-1}$): 29.

$[Ni(MIMOX)_3]SO_4 \cdot 4H_2O$: Yield **=** 63%. M.p. = 187°C. Anal.Calc: C, 29.92; H, 4.85; N, 20.93; S, 5.32 %. Found: C, 29.85; H, 5.19; N, 20.05; S, 5.07 %. IR: (v_{max}/cm^{-1}):710 (w), 776 (m), 899 (m), 966 (s), 1065 (vs), 1294 (m), 1340 (m), 1431 (s), 1493 (s), 1596 (m), 1665 (m), 1750 (br, w), 3270 (br, s), 3453 (s). UV-Vis (λ_{max}/nm): 1040, 642, 468. Conductivity (10^{-3} M, $ohm^{-1}.cm^{-1}.mole^{-1}$): 55.

$[Cu(MIMOX)_3]SO_4 \cdot 4H_2O$: Yield **=** 60%. M.p. = 222°C.Anal.Calc: C, 29.68; H, 4.82; N, 20.77; S, 5.28 %. Found: C, 29.47; H, 5.11; N, 20.62; S, 4.94 %. IR: (v_{max}/cm^{-1}):743 (m), 847 (m), 980 (m), 999 (s), 1109 (m), 1218 (s), 1375 (m), 1460 (s), 1480 (s), 1547 (m), 1743 (br, s), 2929 (s). UV-Vis (λ_{max}/nm):706. Conductivity (10^{-3} M, $ohm^{-1}.cm^{-1}.mole^{-1}$): 69.

$[Zn(MIMOX)_3]SO_4 \cdot 4H_2O$: Yield **=** 61%. M.p. = 202°C.Anal.Calc: C, 29.59; H, 4.80; N, 20.70; S, 5.27 %. Found: C, 29.15; H, 5.13; N, 20.79; S, 4.89 %. IR: (v_{max}/cm^{-1}):797 (m), 852 (m), 983 (s), 1061 (vs), 1443 (s), 1491 (s), 1640 (s),3182 (br, s).Conductivity (10^{-3} M, $ohm^{-1}.cm^{-1}.mole^{-1}$): 61.

3.2.2 Extraction procedure

All the extractions were carried out in a temperature controlled laboratory at 25(±1)^{o}C. Equal volumes (10 mL) of 0.001 M metal ion solution (aqueous layer) and 80% 2-octanol/shellsol solution (organic layer) were pipette into 50 mL conical separating funnelsin the application of DMG as extractants. 100% shellsol solution (organic layer) was applied in the extraction with 1-alkylimidazole-2-aldoximes. They were shaken with an automated orbital platform shaker for 30 mins at an optimised speed of 200 rpm. A minimum period of 60 mins was observed before harvesting the raffinates. The raffinates were filtered through a 33 mmmillex-HV

Millipore of 0.45 µm and di luted appropriately for analysis by ICP-OES. The percentage extractions (%E) of the metal ions were calculated from the concentrations of the metal ions in the aqueous phase using the equation below:

$$\%E = \left(\frac{C_i - C_s}{C_i}\right) \times 100 \qquad (39)$$

where C_i is the initial solution concentration (mg/L) and C_s is the solution concentration after extraction.

The extraction efficiencies were investigated as a function of pH, and all the extraction curves were plotted with SigmaPlot 11.0.

3.2.3 Potentiometric titrations

The protonation and stability constants for the ligands and the metal complexes were determined by potentiometric titration of approximately 25 mL samples. All solutions were prepared using freshly boiled and degassed deionized milli-Q water to ensure the removal of dissolved oxygen and carbon dioxide. The ligand concentration was 1 mM and metal-to-ligand ratios of 1:1, 1:2,1:3 and 1:4 were used. Titrations were performed over the pH range of 2-11 under a continuous flow of purified nitrogen using HCl and tetramethylammonium hydroxide (TMAOH). The metal stock solutions containing 0.10 M HCl were standardized by metal analysis using ICP-OES. The ionic strength of the titration solutions was kept constant at 0.10 M tetramethylammonium chloride (TMACl). The use of the bulky, non-coordinating cation, tetramethylammonium, was to eliminate the use of the non-innocent potassium and sodium ions in KCl and NaCl with respect to coordination in order to ensure that the model is fitted on accurately collected data. Titrations were controlled using the Tiamo software. The titration rate used was 0.01 ml/min and the pausing time was 60 s. The glass electrode was calibrated for a strong acid-base reaction by the Gran-method[31] using the program GLEE[32], to determine the standard potential, E^o. The ionic product of water (pK_w) of 13.83(1) at 25.0±(0.1) ^oC in 0.10 M TMACl was used in all calculations[33]. The concentration stability constants $\beta_{pqr} = [M_pL_qH_r]/[M]^p[L]^q[H]^r$ were calculated by using the computer program HYPERQUAD[34]. The final values of the constants were obtained from an

average of eight independent titrations using an average of around 400 data points in total for each refinement.

3.3 Results and discussion

3.3.1 Synthesis of extractants

Alkylation of imidazole was achieved under a mild temperature of 40°C with the deprotonation of the pyrrole-type nitrogen of imidazole using potassium hydroxide as a base and subsequent substitution with the alkyl group as illustrated in the reaction Scheme 3.1. This was enhanced by the nature of imidazole as a pi-electron-excessive heterocycle.[35] Purification of the product *via* distillation under reduced pressure proved successful as long as this pressure is maintained. The syntheses of 1-alkylimidazole-2-carboxaldehydes were carried out under argon and in dry diethyl ether. The presence of oxygen and water reduce the yield of 1-alkylimidazole-2-carboxaldehydes since butylithium is deactivated. Care was taken to maintain the temperature at not more than -50°C as higher temperatures also deactivate the butylithium. The 1-alkylimidazole-2-carboxaldehydes may decompose *via* decarboxylation if they stay for more than one week at room temperature before they are converted to 1-alkylimidazole-2-aldoximes.

The 1-alkylimidazole-2-aldoximes were prepared from the corresponding alkylimidazole-2-carboxaldehydes by the condensation reaction with hydroxylamine (H_2NOH) at a controlled pH (see Scheme 3.1). This becomes necessary because the first step of the reaction involves a nucleophilic attack of hydroxylamine at the carbonyl carbon of the aldehyde to give an unstable carbinolamine as intermediate. Since the breakdown of the carbinolamine intermediate to an oxime is acid-catalysed, the rate of this step is enhanced at low pH. However, if the pH is too low, most of the hydroxylamine will be in the non-nucleophilic protonated form (NH_3OH^+), and the rate of the first step will decrease. Thus, in oxime formation, the pH has to be such that there is sufficient free hydroxylamine for the formation of the intermediate and enough acid so that dehydration of the carbinolamine is easily accomplished.[36] This reaction was therefore conducted at an optimum pH range of 5.5-5.8. It requires no heating and water was the only by-product of the

condensation, making it an e nvironmentally friendly option. The necessary purification for 1-alkylimidazole-2-aldoximes was achieved by the removal of residual water *in vacuo*, at a temperature of 45°C and subsequent column chromatographic separation on silica with chloroform:acetone at (2:1) as solvent mixture yielding a pure product. The longer chain 1-alkylimidazole-2-aldoximes solidify into a wax-like transparent product after a while.

The purity of the extractants were ascertained by elemental analysis and ^{1}H NMR characterization (see Figures 3.8-3.10). The alkylation of the imidazole ring by electrophilic substitution at N(1) was successfully achieved as signified by the emergence of the alkyl group peaks as shown in spectra in Figures 3.8(A) and (B). The C(2) position of the 1-alkylimidazoles possesses the most acidic hydrogen, and a carbanion is readily generated at C(2), thus upon treatment with a s trong base, such as butyllithium the nucleophilic substitution at this site with the carbonyl group was achieved (Scheme 3.1). These were confirmed by the appearance of the peak at 9.76 ppm in the ^{1}H NMR spectra of these compounds which signifies the presence of the aldehyde proton (see Figures 3.9(A) and (B)). Similarly, the confirmation of the condensation of 1-alkylimidazole-2-aldehydes to 1-alkylimidazole-2-oximes was exhibited by the disappearance of the aldehyde peaks at 9.76 ppm in their ^{1}H NMR spectra and the appearance of oxime hydroxyl proton peak at 11.50 as depicted by Figures 3.10(A) and (B). The purity of the extractant was further assured by the agreement of the elemental micro-analysis results to the theoretical values.

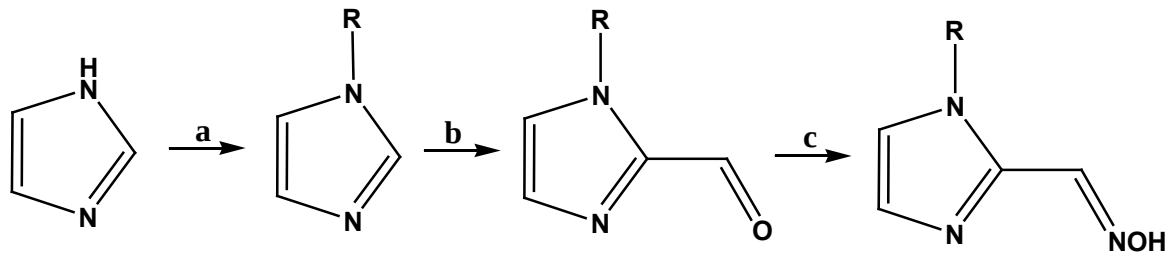

R= Octyl or decyl

Scheme 3.1: Syntheses of 1-alkylimidazole-2-aldoximes. **a.** Alkyl halide, potassium hydroxide **b.** Butyllithium, DMF, diethylether. **c.** Hydroxylamine hydrochloride, sodium carbonate

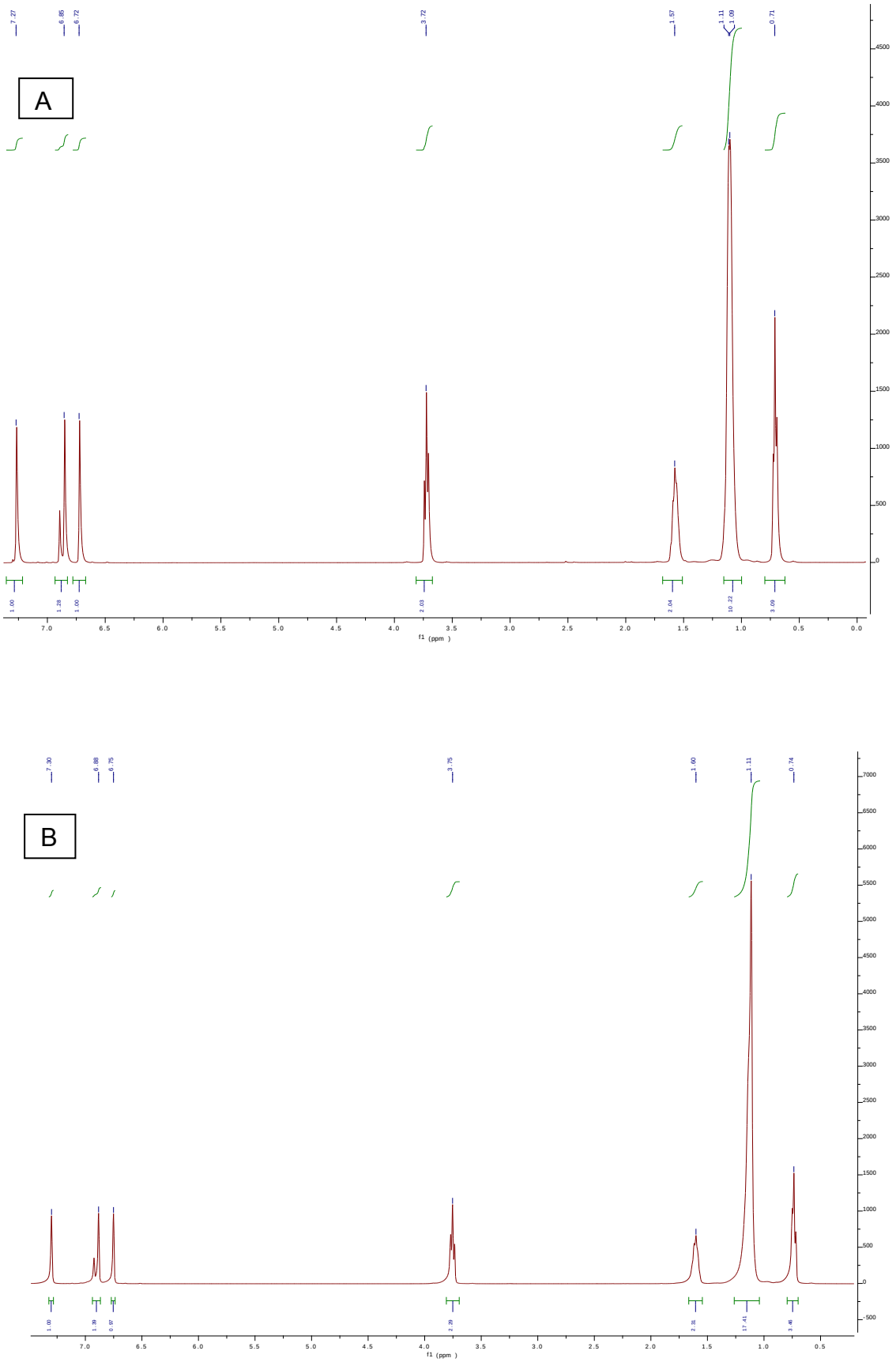

Figure 3.8: The ^{1}H NMR spectra of 1-octylimidazole (A) and 1-decylimidazole (B)

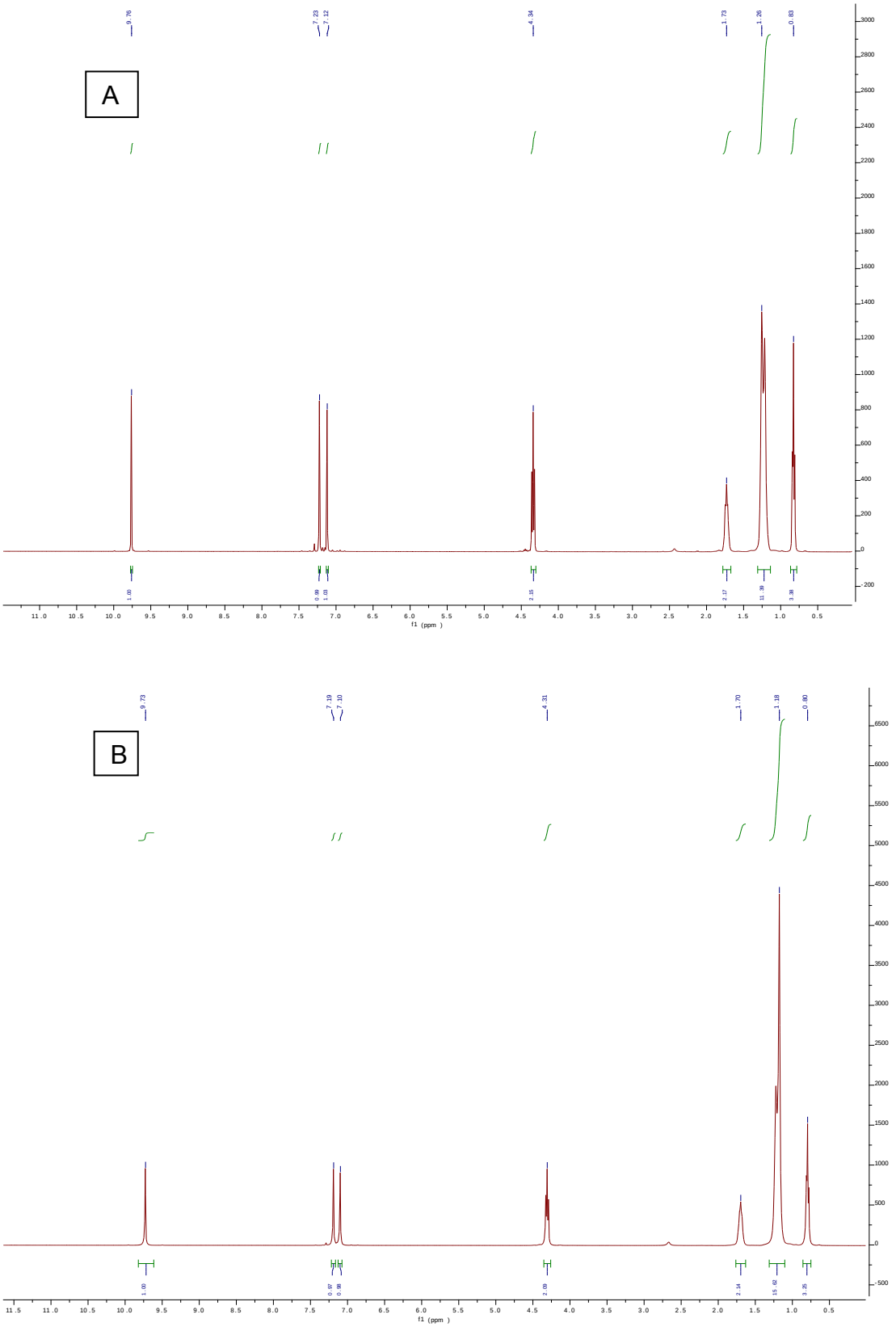

Figure 3.9: The 1H NMR spectra of 1-octylimidazole-2-aldehyde (A) and 1 -decylimidazole-2-aldehyde (B)

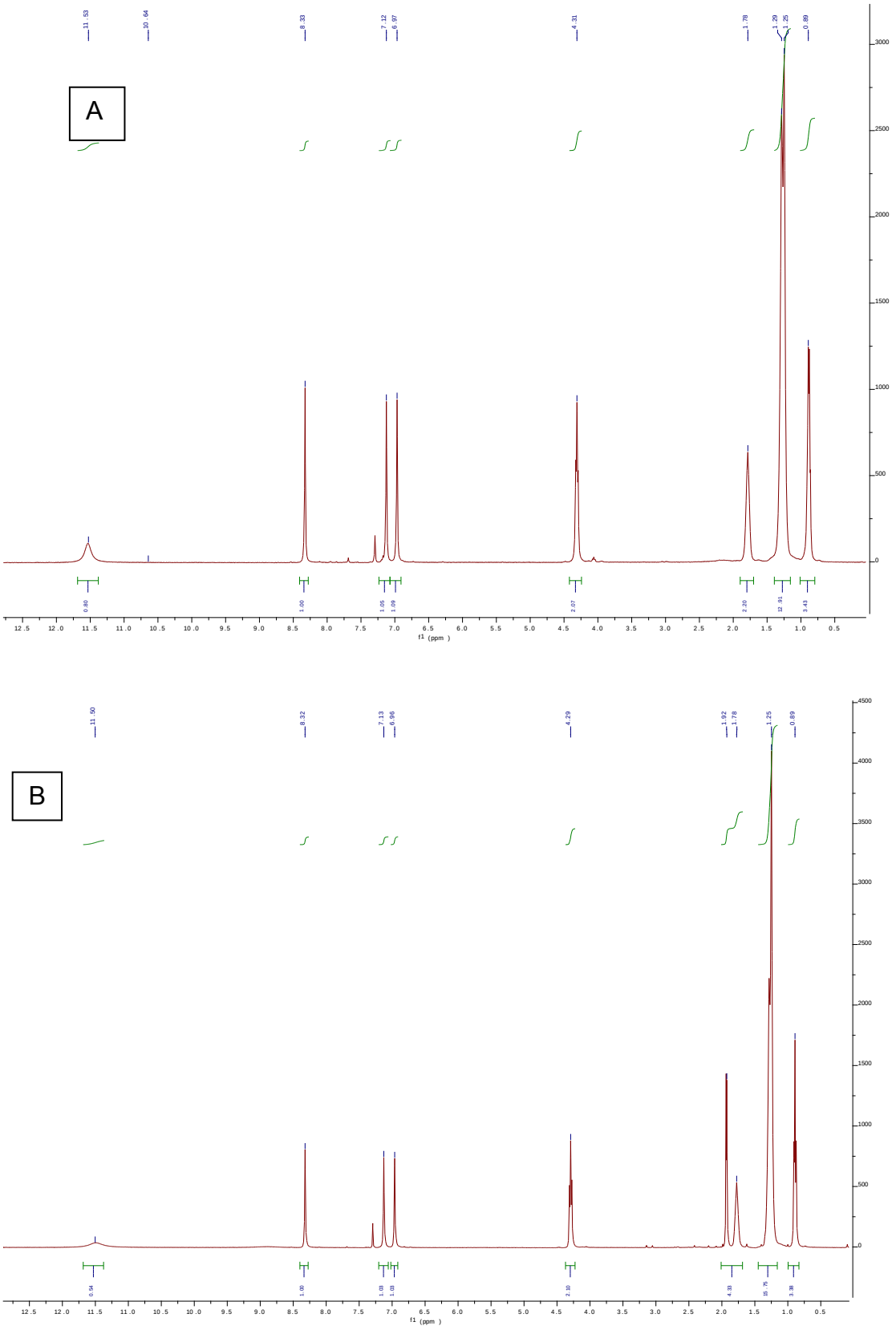

Figure 3.10: The ^{1}H NMR spectra of 1-octylimidazole-2-aldoxime (A) and 1-decylimidazole-2-aldoxime (B)

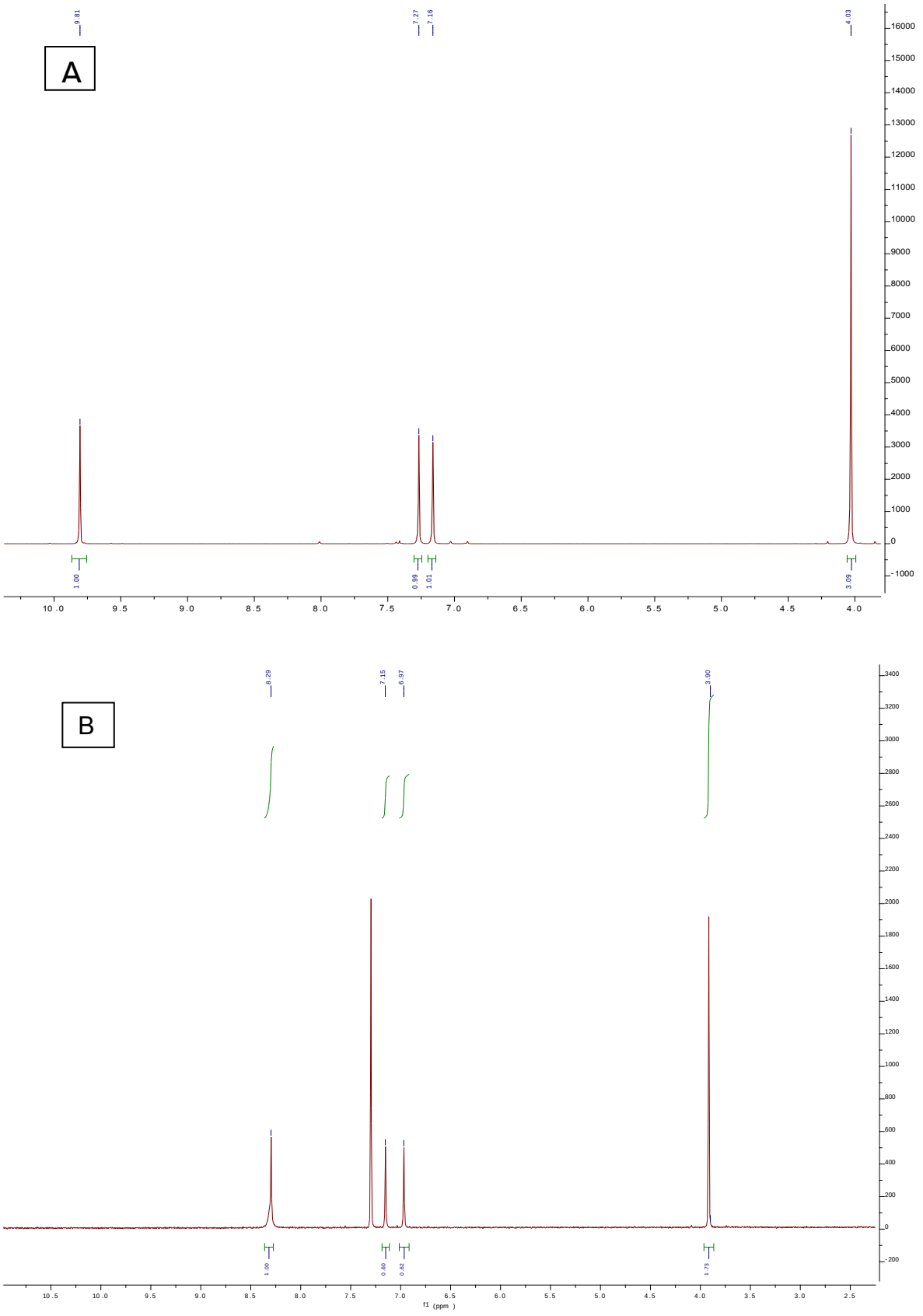

Figure 3.11: The 1H NMR spectra of 1-methylimidazole-2-aldehyde (A) and 1-methylimidazole-2-aldoxime (B)

3.3.2 Extraction studies

(a) Extractions with dimethylglyoxime (DMG)

Preliminary studies involving extractions with DMG as extractant were carried out in dilute sulfate solutions. Conditions tailored towards nickel specificity as compared with extraction of other base metal namely cobalt, copper, zinc, manganese and magnesium were applied. The results obtained in the absence and presence of DNNSA as a synergist in the pH range 0.5-4.0 are illustrated in Tables 3.1 and 3.2, and the corresponding plots in Figures 3.12 and 3.13 respectively. Obviously without DNNSA nickel was extracted at a higher efficiency than other metals, however no meaningful separation was realised. One of the major problem encountered is the formation of visible red precipitate of $Ni(DMG)_2$which is highly undesirable in the context of SX separation of metal ions. The metal complex of interest is not only expected to be readily phase transferred but must equally be soluble in the diluents. The cobalt curve in the absence of DNNSA (Figure 3.12) shows a relatively poor extraction as would be expected compared to nickel. The zinc curve shows a higher extraction percentage suggesting the formation of a different geometry as compared with square-planar expected for nickel. The extraction in the presence of DNNSA was carried out at an optimised concentration of 0.05 M to enhance phase transference of the extracted species. Even though this was achieved, the position of all the curves of the metals examined shows relatively no separation. The concentration of DNNSA couldn't be reduced in order to enhance separation since that resulted in poor extraction. It is therefore clear that DMG only act as a neutral extractant in these highly acid conditions, and that it only begins to function in an ionised form at higher pH values, and early with respect to pH for nickel (Table 3.12).

Lots of reasons could be adduced for this poor performance of DMG along with DNNSA as nickel specific extractants among which are the possibility of acid-catalysed degradation of the oxime into amide through Beckmann's re-arrangements.[37] This aspect was investigated by GC studies and the results did not confirm this. Thus, it can be affirmed that in the low pH range under which this study was carried out, DMG would not be an effective separating agent for nickel from other base metals as depicted by these two plots (Figures 3.12 and 3.13). It is

clear from the results in Figure 3.12 however, that DNNSA is the extractant that is involved in this extraction system because it is well known that it is not a selective extractant.[38] This is further revealed by the plot in Figure 3.14 in which DNNSA alone was applied in a similar extraction. The fact that DMG cannot operate in the traditional dioximate form is due to the fact that the hydroxyl protons are not readily dissociated at the low pH.

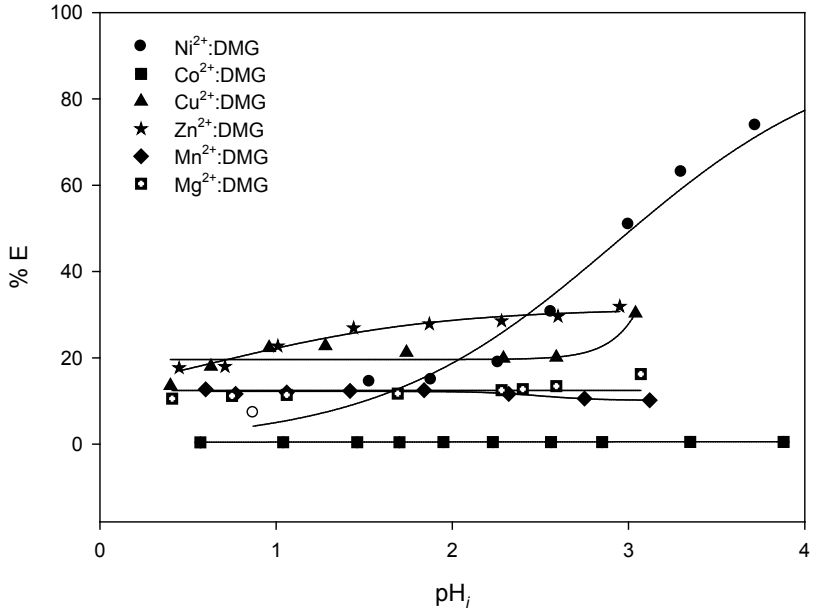

Figure 3.12: A plot of %E vs initial pH in the extraction of 0.001 M Ni^{2+}, Co^{2+}, Cu^{2+}, Zn^{2+}, Mn^{2+} and Mg^{2+} from dilute sulfate medium with DMG at a M:L molar ratio of 1:360 in the absence of DNNSA, in 80% 2-Octanol/Shellsol 2325

Table 3.1: %E vs initial and equilibrium pH in the extraction of 0.001 M Ni^{2+}, Co^{2+}, Cu^{2+}, Zn^{2+}, Mn^{2+} and Mg^{2+} from dilute sulfate medium with DMG at a M:L molar ratio of 1:360 in the absence of DNNSA, in 80% 2-Octanol/Shellsol 2325.

Ni^{2+}									
pH_i	0.87	1.53	1.88	2.26	2.56	3.00	3.30	3.72	4.16
pH_e	0.92	1.63	1.88	2.02	2.94	2.96	2.98	2.99	3.00
% E	7.26	14.46	14.92	18.93	30.66	50.88	63.03	73.85	76.52
Co^{2+}									
pH_i	0.57	1.04	1.46	1.70	1.95	2.23	2.56	2.85	3.35
pH_e	0.69	1.12	1.56	1.82	2.07	2.21	2.43	2.53	3.54
% E	11.52	17.88	17.85	17.96	17.93	17.76	17.55	17.82	18.74
Cu^{2+}									
pH_i	0.40	0.63	0.96	1.28	1.74	2.29	2.59	3.04	
pH_e	0.37	0.64	0.99	1.29	1.75	2.30	2.58	2.87	
% E	13.54	18.00	22.32	22.73	21.21	19.84	20.08	30.32	
Zn^{2+}									
pH_i	0.45	0.71	1.01	1.44	1.87	2.28	2.60	2.95	
pH_e	0.45	0.74	1.01	1.48	1.93	2.37	2.74	3.08	
% E	17.65	17.94	22.69	26.89	27.79	28.50	29.59	31.89	
Mn^{2+}									
pH_i	0.60	0.77	1.06	1.42	1.84	2.32	2.75	3.12	
pH_e	0.58	0.75	1.07	1.72	1.84	2.46	2.67	3.31	
% E	12.67	11.58	11.94	12.29	12.44	11.59	10.52	10.12	
Mg^{2+}									
pH_i	0.41	0.75	1.06	1.69	2.28	2.40	2.59	3.07	
pH_e	0.48	0.78	1.09	1.89	2.39	2.83	2.99	3.26	
% E	10.49	11.12	11.35	11.66	12.44	12.68	13.38	16.18	

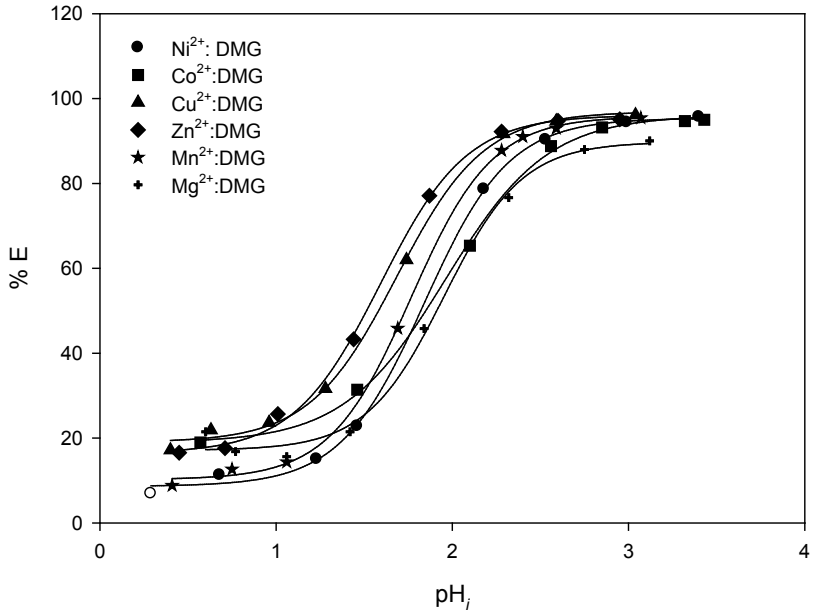

Figure 3.13: A plot of %E vs initial pH in the extraction of 0.001 M Ni^{2+}, Co^{2+}, Cu^{2+}, Zn^{2+}, Mn^{2+} and Mg^{2+} from dilute sulfate medium with DMG at a M:L molar ratio of 1:360 in the presence of 0.05 M DNNSA, in 80% 2-Octanol/Shellsol 2325

Table 3.2: %E vs initial and equilibrium pH in the extraction of 0.001M Ni^{2+},Co^{2+} Cu^{2+}, Zn^{2+} Mn^{2+} and Mg^{2+} from dilute sulfate medium with DMG at a M:L molar ratio of 1:360 and 0.05 M DNNSA, in 80% 2-Octanol Shellsol 2325.

Ni^{2+}								
pH_i	0.29	0.68	1.23	1.46	2.18	2.53	2.99	3.40
pH_e	0.30	0.70	1.26	1.50	2.10	2.28	2.41	2.46
% E	6.88	11.28	15.01	22.78	78.64	90.28	94.38	95.68
Co^{2+}								
pH_i	0.57	1.46	2.10	2.56	2.85	3.32	3.43	
pH_e	0.61	1.53	1.93	2.18	2.30	2.35	3.37	
% E	18.95	31.38	65.31	88.78	93.21	94.69	94.98	
Cu^{2+}								
pH_i	0.40	0.63	0.96	1.28	1.74	2.29	2.59	3.04
pH_e	0.49	0.62	0.91	1.24	1.65	2.01	2.03	2.13
% E	17.17	21.86	23.63	31.63	61.95	91.67	94.66	96.12
Zn^{2+}								
pH_i	0.45	0.71	1.01	1.44	1.87	2.28	2.60	2.95
pH_e	0.46	0.64	1.08	1.88	1.43	1.79	2.14	2.22
% E	16.50	17.58	25.61	43.24	77.05	92.19	94.72	95.09
Mn^{2+}								
pH_i	0.41	0.75	1.06	1.69	2.28	2.40	2.59	3.07
pH_e	0.45	0.76	1.10	1.72	2.14	2.20	2.26	2.33
% E	8.79	12.63	14.32	45.80	87.75	90.98	92.94	95.38
Mg^{2+}								
pH_i	0.60	0.77	1.06	1.42	1.84	2.32	2.75	3.12
pH_e	0.58	0.79	1.06	1.42	1.80	2.10	2.23	2.30
% E	21.42	16.74	15.55	21.41	45.75	76.60	87.93	89.96

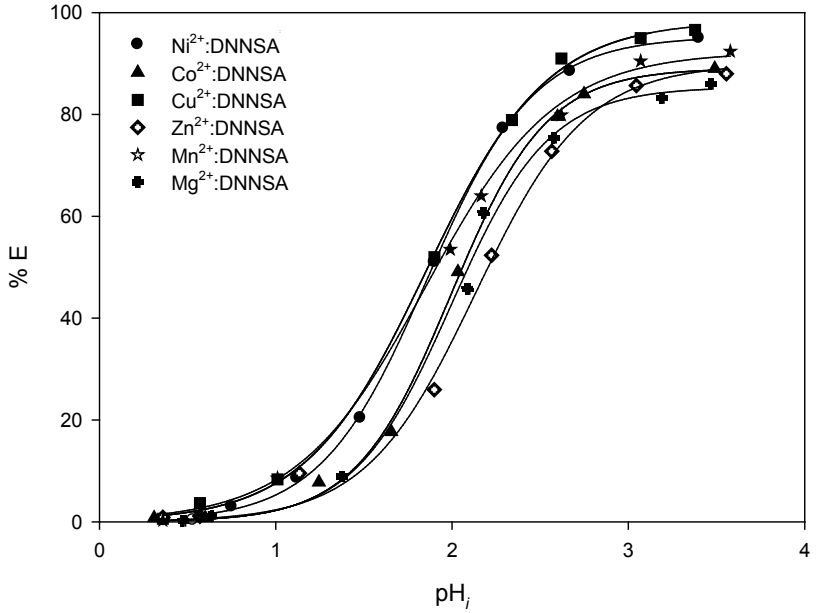

Figure 3.14: A plot of %E vs initial pH in the extraction of 0.001 M Ni^{2+}, Co^{2+}, Cu^{2+}, Zn^{2+}, Mn^{2+} and Mg^{2+} from dilute sulfate medium with 0.05 M DNNSA alone in 80% 2-Octanol/Shellsol 2325

Table 3.3: %E vs initial and equilibrium pH in the extraction of 0.001 M Ni^{2+},Co^{2+} Cu^{2+}, Zn^{2+}, Mn^{2+} and Mg^{2+} from dilute sulfate medium with 0.05 M DNNSA alone in 80% 2-Octanol Shellsol 2325.

Ni^{2+}								
pH_i	0.53	0.75	1.12	1.48	1.90	2.29	2.67	3.07
pH_e	0.53	0.76	1.15	1.47	1.83	2.10	2.25	2.34
% E	0.37	2.97	8.63	20.39	50.98	77.27	88.49	91.87
Co^{2+}								
pH_i	0.31	0.60	1.25	2.03	2.03	2.59	2.75	3.28
pH_e	0.31	0.52	1.03	1.93	1.93	2.28	2.50	2.55
% E	0.95	0.78	12.29	23.32	35.96	62.35	82.78	89.42
Cu^{2+}								
pH_i	0.36	0.57	1.01	1.90	2.34	2.62	3.07	
pH_e	0.31	0.52	1.03	1.93	2.28	2.50	2.55	
% E	6.18	10.29	13.32	13.32	52.35	72.78	79.42	
Zn^{2+}								
pH_i	0.35	0.57	1.13	1.90	2.22	2.78	3.04	3.56
pH_e	0.37	0.52	1.03	1.93	2.28	2.50	2.55	2.64
% E	0.89	1.09	9.57	25.95	52.35	72.77	85.68	88.00
Mn^{2+}								
pH_i	0.36	0.57	1.01	1.99	2.16	2.62	3.07	3.57
pH_e	0.34	0.52	1.00	1.78	2.01	2.33	2.77	2.67
% E	0.26	1.47	8.57	53.50	63.99	79.89	90.48	92.39
Mg^{2+}								
pH_i	0.47	0.63	1.37	2.09	2.18	2.58	3.19	3.47
pH_e	0.46	0.60	1.32	2.00	2.09	2.38	2.79	2.87
% E	0.18	1.09	8.89	45.69	60.68	75.39	83.22	85.99

(b) Extractions with 1-alkylimidazole-2-aldoximes in dilute acidic sulfate medium

In these studies, the conditions for the separation of base metals were optimised through investigating the requisite concentration of the extractant, the use of DNNSA as a synergist, the concentration of the synergist, the diluent/modifier ratio effect, the necessary alkyl chain substituent on imidazole, and the effect of pH.

(i) Effect of the extractant concentration on extraction of nickel

The effect of the concentration of the extractant was studied within the extractible M:L ratio range of 1:40 to 1:80 in the extraction of 0.001 M nickel as shown by the results in Figure 3.15. It is obvious from these curves and the corresponding data on Table 3.3 that the steepest of all the curves is ratio 1:60. This curve unlike others also shows a left leg that would allow for the back extraction of nickel. For these reasons this extractant concentration was chosen for the subsequent studies.

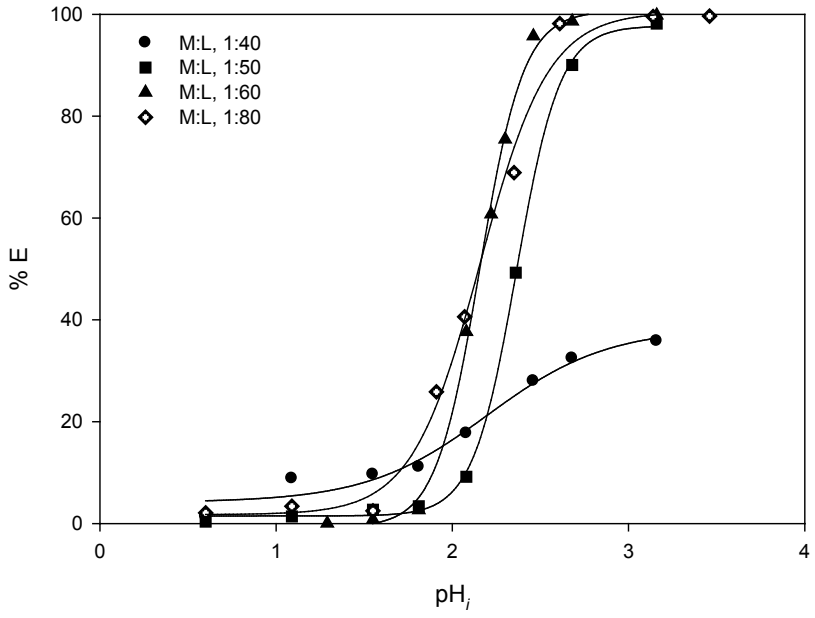

Figure 3.15: A plot of %E vs initial pH in the extraction of 0.001 M nickel from dilute sulfate medium with OIMOX at various M:L molar ratio of 1:40, 1:50, 1:60 and 1:80 with 0.02 M DNNSA in 100% Shellsol 2325

Table 3.4: %E vs initial and equilibrium pH in the extraction of 0.001 M nickel from dilute sulfate medium with OIMOX at various M:L molar ratio of 1:40, 1:50, 1:60 and 1:80 with 0.02 M DNNSA in 100% Shellsol 2325.

Ni^{2+}:L (1:40)									
pH_i	0.60	1.09	1.55	1.81	2.08	2.46	2.68	3.16	
pH_e	0.69	1.16	1.58	1.94	2.18	2.62	2.89	3.37	
% E	1.39	8.85	9.65	11.12	17.69	27.98	32.43	35.82	
Ni^{2+}:L (1:50)									
pH_i	0.60	1.09	1.55	1.81	2.08	2.36	2.68	3.16	
pH_e	0.67	1.14	1.72	1.95	2.62	2.65	2.68	2.69	
% E	0.37	1.39	2.71	3.39	9.20	49.27	90.04	98.18	
Ni^{2+}:L (1:60)									
pH_i	1.29	1.55	1.81	1.91	2.08	2.22	2.30	2.46	3.16
pH_e	1.39	1.77	2.21	2.51	2.78	2.92	3.60	3.66	4.20
% E	0.03	0.76	2.65	18.56	37.66	60.75	75.45	95.71	99.82
Ni^{2+}:L (1:80)									
pH_i	0.60	1.09	1.55	1.91	2.07	2.35	2.61	3.14	3.46
pH_e	0.64	1.75	1.95	2.19	2.60	2.75	2.91	3.24	3.54
% E	2.12	3.39	2.51	25.88	40.59	68.91	98.17	99.56	99.66

(ii) Effect of DNNSA as a synergist on the extraction of nickel and copper

The study on the effect of a synergist was necessitated by the poor extraction of both nickel and copper into the organic phase as depicted in Figures 3.16 and 3.17 and the corresponding Tables 3.5 and 3.6. These depict the poor phase transfer of the

sulfate anion from the aqueous to the organic phase. It is apparent from Figures 3.17-3.19 below that the presence of the bulky anion (DNNSA) as a co-extractant is crucial for the satisfactory extraction of the metals. This has been observed for the other base metals in addition to copper and nickel. This gives credence to a possibility of the species formed being cationic at the low pH region rather than neutral (from the deprotonation of the oxime hydroxyls). However, there is significant extraction with an increase in pH without the presence of DNNSA (Figures 3.16 and 3.17) suggesting a pos sibility of the formation of the neutral species which is extractible at high pH. Therefore, the operation of the extraction system allows for the attainment of significant extraction in a pH range whichis representative of industrial feed solutions. It is therefore likely that the mechanism is based on the ion-association with the imidazolyl and the imine nitrogen of the oxime involved in the coordination sphere while the oxime hydroxyl is not deprotonated.

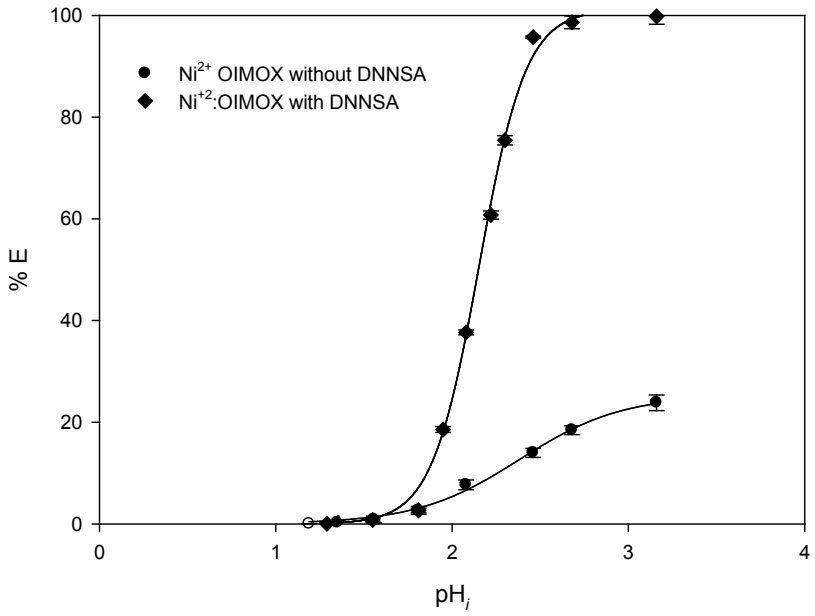

Figure 3.16: A plot of %E vs initial pH in the extraction of 0.001 M nickel from dilute sulfate medium with OIMOX at a M:L molar ratio of 1:60 in the absence of DNNSA, and with 0.02 M DNNSA in 100% Shellsol 2325

Table 3.5: %E vs initial and equilibrium pH in the extraction of 0.001 M nickel from dilute sulfate medium with OIMOX at a M:L molar ratio of 1:60 in the absence of DNNSA, and with 0.02 M DNNSA in 100% Shellsol 2325.

pH_i	pH_e	% E Ni^{2+}(No DNNSA)	pH_i	pH_e	% E Ni^{2+}(with DNNSA)
0.60	0.76	1.39	1.29	1.59	0.03
1.09	1.13	8.85	1.55	1.75	0.77
1.55	1.85	9.65	1.81	1.99	2.66
1.81	1.99	11.12	1.91	2.19	18.57
2.08	2.18	17.69	2.08	2.96	37.67
2.46	2.40	27.98	2.22	3.22	60.75
2.68	3.35	32.43	2.30	3.50	75.45
3.16	3.83	35.82	2.46	3.76	95.71

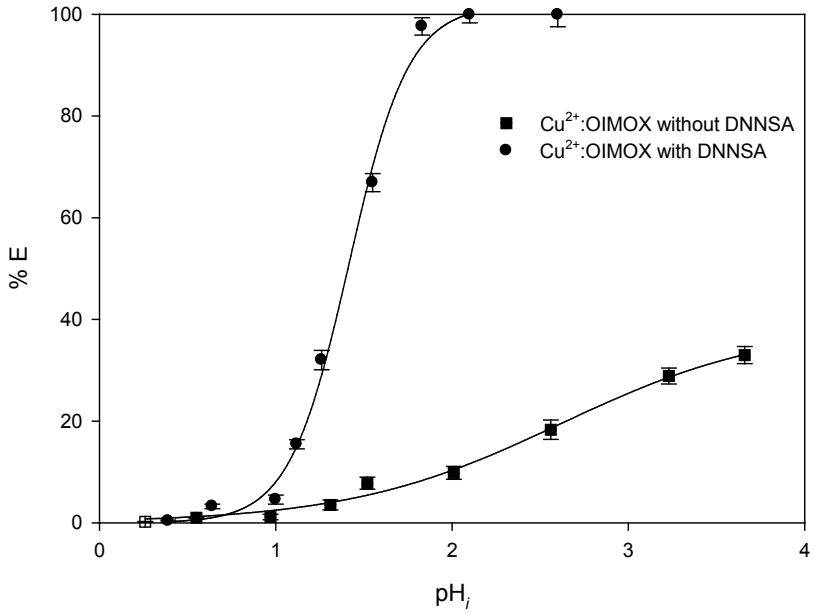

Figure 3.17: A plot of %E vs initial pH in the extraction of 0.001 M copper from dilute sulfate medium with OIMOX at a M:L molar ratio of 1:60 in the absence of DNNSA, and with 0.02 M DNNSA in 100% Shellsol 2325

Table 3.6: %E vs initial and equilibrium pH in the extraction of 0.001 M from copper dilute sulfate medium with OIMOX at a M:L molar ratio of 1:60 in the absence of DNNSA, and with 0.02 M DNNSA in 100% Shellsol 2325.

pH_i	pH_e	% E Cu^{2+}(No DNNSA)	pH_i	pH_e	% E Cu^{2+}(with DNNSA)
0.26	0.29	0.52	0.39	0.47	0.34
0.55	0.69	6.00	0.64	0.77	3.24
0.97	1.07	10.91	1.00	1.70	4.56
1.31	1.51	12.53	1.12	1.91	15.44
1.52	1.82	12.79	1.26	2.34	32.01
2.01	2.61	12.84	1.55	2.45	66.91
2.76	3.06	26.32	1.83	2.73	97.63
3.23	3.83	36.87	2.10	2.90	99.89
3.66	3.96	53.96	2.60	3.20	99.91

(iii) Effect of the synergist concentration on extraction of nickel

The optimised concentration of DNNSA for 100% extraction to complement the extraction of 0.001 M nickel was studied and the results are shown in Figure 3.18 and Table 3.7. It was found out that 0.02 M DNNSA gave the most efficient extraction of the nickel ion as indicated by the plot.

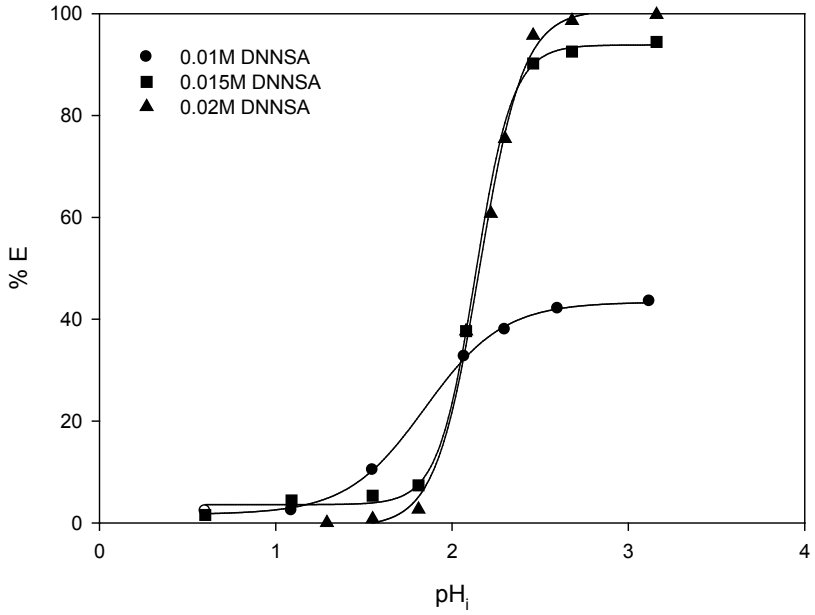

Figure 3.18: A plot of %E vs initial pH in the extraction of 0.001 M nickel from dilute sulfate medium with OIMOX at M:L molar ratio of 1:60 with various DNNSA concentrations of 0.01 M, 0.015 M and 0.02 M in 100% Shellsol 2325

Table 3.7: %E vs initial and equilibrium pH in the extraction of 0.001 M nickel from dilute sulfate medium with OIMOX at M:L molar ratio of 1:60 with various DNNSA concentrations of 0.01 M, 0.015 M and 0.02 M in 100% Shellsol 2325.

pH_i	pH_e	**0.01M DNNSA**	pH_i	pH_e	**0.015M DNNSA**	pH_i	pH_e	**0.02M DNNSA**
0.60	0.66	2.33	0.60	0.67	1.57	1.29	1.55	0.03
1.09	1.12	2.45	1.09	1.14	4.43	1.55	1.81	0.77
1.55	1.75	10.38	1.55	1.72	5.35	1.81	2.08	2.66
2.07	2.27	32.67	1.81	1.91	7.39	2.08	2.22	37.67
2.30	2.44	37.95	2.08	2.62	37.67	2.22	2.30	60.75
2.60	2.84	42.07	2.46	3.26	90.21	2.30	2.76	75.45
3.12	3.32	43.49	2.68	3.68	92.57	2.46	3.58	95.71
						2.68	3.85	98.63

(iv) Effect of the diluent/modifier ratio on extraction of nickel

The role of diluents in the extraction efficiency of a given extraction system, as it has been stressed in Chapter 1 of this thesis, is not only as carrier for the extractant and extracted metal complex but could also be a participant in the extraction process. There is therefore the need to investigate the effect of varying ratio of the duo in an attempt to gain an optimal condition of extraction of the metal ions with this extractant. Results shown in Table 3.8 and the corresponding plots in Figure 3.19 show that 100% Shellsol produced the best results in terms of the percentage extraction, and the steepness of the curve. As observed by Kosamawa *et al*[39] in the use of electron-donor diluents in the extraction of copper with hydroxyoxime, there is likely an interaction of the oxime hydroxyl group, which behave as an electron-acceptor (hydrogen–donor), with the n-donor compound such as alcohols thereby reducing the metal distribution ratio. Thus the presence of isooctanol in the organic phase was found detrimental to the extraction efficiency as indicated by the curves and was therefore eliminated to pave way for 100% Shellsol (a non-polar diluent).

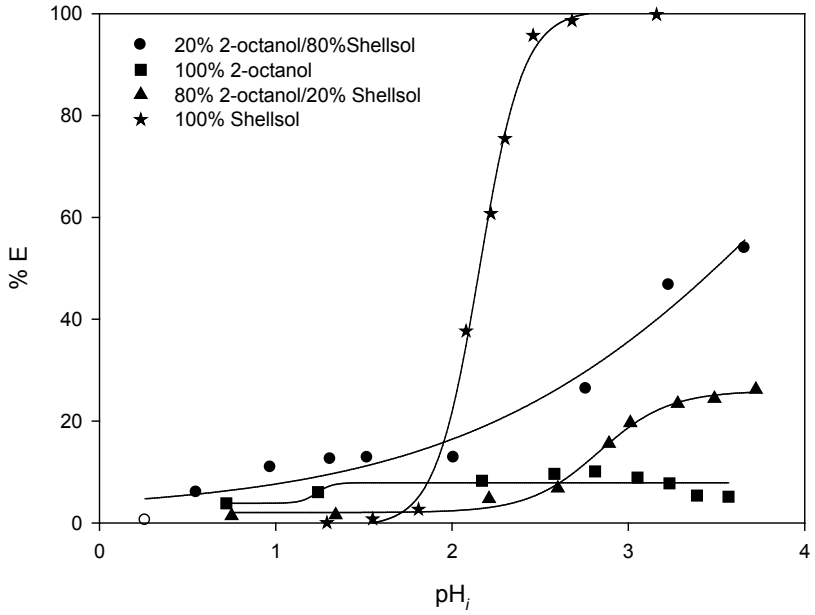

Figure 3.19: A plot of %E vs initial pH in the extraction of 0.001 M nickel from dilute sulfate medium with OIMOX at a M:L molar ratio of 1:60 and 0.02 M DNNSA, with varying ratio of 2-octanol/Shellsol 2325

Table 3.8: %E vs initial and equilibrium pH in the extraction of 0.001 M nickel from dilute sulfate medium with OIMOX at M:L molar ratio of 1:60 and 0.02 M DNNSA concentration using varying ratio of diluent/modifier (Shellsol 2325/2-octanol).

20%2-octanol/80%Shellsol									
pH_i	0.26	0.55	0.97	1.31	1.52	2.01	2.76	3.23	3.60
pH_e	0.29	0.65	1.06	1.41	1.46	1.91	2.36	2.43	2.45
% E	0.51	6.01	10.91	12.53	12.79	12.84	26.32	46.69	53.97
100% Shellsol									
pH_i	1.29	1.55	1.81	2.08	2.22	2.30	2.46	2.68	3.16
pH_e	1.31	1.57	1.90	2.01	2.12	2.22	2,30	2.45	2.48
% E	0.03	0.77	2.66	37.66	60.75	75.45	95.71	98.63	99.81
80% 2-octanol/20%Shellsol									
pH_i	0.75	1.34	2.21	2.60	2.89	3.01	3.28	3.48	3.72
pH_e	0.74	1.32	2.20	2.55	2.78	2.89	2.91	2.92	2.93
% E	1.41	1.56	4.75	6.81	15.60	19.66	23.43	24.41	26.21
100% 2-octanol									
pH_i	0.72	1.24	2.17	2.58	2.81	3.05	3.23	3.39	3.56
pH_e	0.78	1.24	2.17	2.48	2.67	2.89	2.91	2.92	2.92
% E	3.86	6.06	8.28	9.65	10.12	8.91	7.76	5.38	5.15

(v) Effect of the alkyl chain

In order for the extractant to extract significantly, it must be able to have some hydrophilicity to achieve aqueous phase recognition while also compatible with the organic phase to avoid challenges of third phase formation and phase break of the

extracted species. The effect of the alkyl chain length was therefore investigated (using an octyl and decyl group) on imidazole in order to optimise the desired hydrophilicity/hydrophobicity balance of the extractant (Figures 3.20 and 3.21). Both alkyl groups provided good interfacial properties, and the decision to select the octyl derivative was based on the extraction isotherms observed. Looking at the copper extraction curve (Figure 3.20), there is not much gain in extraction pH since the OIMOX curve is slightly steeper than that of DIMOX. However, the real gain in the octyl derivative (OIMOX) is the fact the left leg of the nickel extraction curve is pushed to higher pH values, allowing for a definitive separation of copper from nickel. In addition, the steepness of the nickel extraction curve could allow for separation from cobalt as it could be seen in Figure 3.21. The octyl derivative proved to be a better separating agent of copper from nickel.

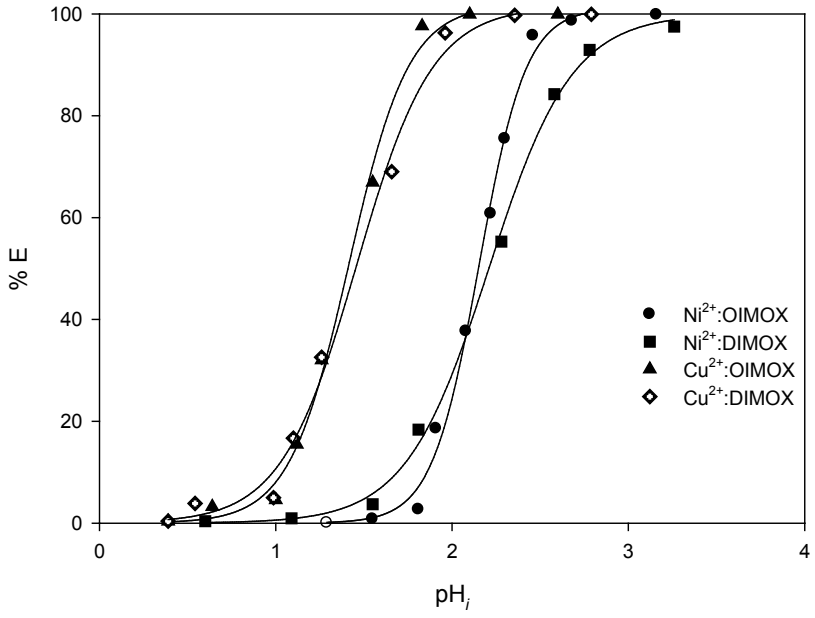

Figure 3.20: A plot of %E vs initial pH for the separation of 0.001 M copper from equimolar concentration of nickel with OIMOX and DIMOX plus 0.02 M DNNSA in 100% Shellsol 2325 from dilute sulfate medium.

Table 3.9: %E vs initial and equilibrium pH for the separation of 0.001 M copper from equimolar concentration of nickel with OIMOX and DIMOX plus 0.02 M DNNSA in 100% Shellsol 2325 from dilute sulfate medium.

$Ni^{2+}$with OIMOX									
pH_i	1.29	1.55	1.91	2.08	2.22	2.30	2.46	2.68	3.16
pH_e	1.39	1.77	2.21	2.51	2.78	2.92	3.60	3.66	4.20
% E	0.03	0.77	2.66	18.57	37.67	60.75	75.45	95.71	99.81
Ni^{2+} with DIMOX									
pH_i	0.60	1.09	1.55	1.81	2.28	2.58	2.78	3.26	
pH_e	0.63	1.20	1.90	2.31	2.80	3.08	3.30	3.46	
% E	0.37	0.94	3.73	18.36	55.29	84.25	92.93	97.49	
$Cu^{2+}$with OIMOX									
pH_i	0.39	0.64	1.00	1.12	1.26	1.55	1.83	2.10	2.60
pH_e	0.35	0.68	1.08	1.23	1.46	1.67	2.57	3.88	3.88
% E	0.34	3.24	4.56	15.44	32.01	66.91	97.63	99.89	99.91
Cu^{2+} with DIMOX									
pH_i	0.39	0.54	0.99	1.10	1.26	1.66	1.96	2.36	2.79
pH_e	0.41	0.60	1.18	1.39	1.56	1.89	2.16	2.87	3.29
% E	0.39	3.84	4.99	16.67	32.56	68.99	96.27	99.69	99.89

The nickel and cobalt separation could not be achieved to the same level with both extractants, however, the octyl derivative (OIMOX) showed better loading ranges with a $\Delta pH_{½} \approx 0.75$ (Figure 3.21).

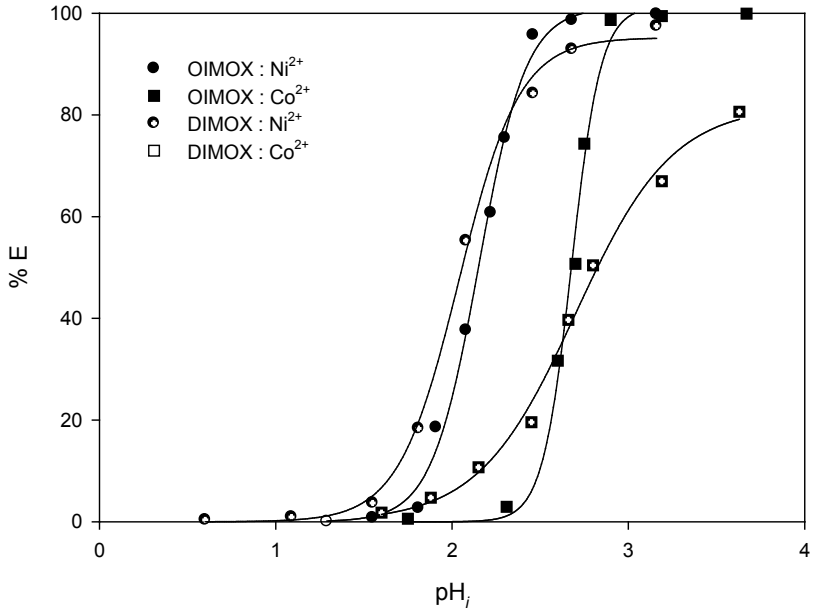

Figure 3.21: A plot of %E vs initial pH for the separation of 0.001 M nickel from equimolar concentration of cobalt with OIMOX and DIMOX plus 0.02 M DNNSA in 100% Shellsol 2325 from dilute sulfate medium

Table 3.10: %E vs initial and equilibrium pH for the separation of 0.001 M nickel from equimolar concentration of cobalt with OIMOX and DIMOX plus 0.02 M DNNSA in 100% Shellsol 2325 from dilute sulfate medium.

% E Ni^{2+}(OIMOX)									
pH_i	1.29	1.55	1.91	2.08	2.22	2.30	2.46	2.68	3.16
pH_e	1.39	1.77	2.21	2.51	2.78	2.92	3.60	3.66	4.20
% E	0.03	0.77	2.66	18.57	37.67	60.75	75.45	95.71	99.81
% E Co^{2+}(OIMOX)									
pH_i	1.75	2.31	2.60	2.70	2.75	2.90	3.19	3.67	
pH_e	1.98	3.31	2.75	3.87	3.95	4.20	4.25	4.39	
% E	0.62	2.94	31.69	50.72	74.37	98.68	99.44	99.92	
% E Ni^{2+}(DIMOX)									
pH_i	0.60	1.09	1.55	1.81	2.28	2.58	2.78	3.26	
pH_e	0.63	1.20	1.90	2.31	2.80	3.08	3.30	3.46	
% E	0.37	0.94	3.73	18.36	55.29	84.25	92.93	97.49	
% E Co^{2+}(DIMOX)									
pH_i	1.60	1.88	2.15	2.45	2.66	2.80	3.19	3.63	
pH_e	1.88	2.55	2.88	3.08	3.31	3.39	3.47	3.42	
% E	1.82	4.77	10.73	19.61	39.73	50.45	66.99	80.66	

(vi) Separation of copper, nickel and cobalt with OIMOX and DNNSA

The optimised conditions for the separation of copper, nickel and c obalt are presented by the extraction curve in Figure 3.22. The $\Delta pH_{½} \approx 1.05$ was achieved for the separation of copper from nickel. The order of the extractions is somewhat

consistent with the Irving-Williams stability order with $Cu^{2+} > Ni^{2+} > Co^{2+}$.[40] This also allows us to glean the fact that the metal-ligand complexes formed could be isostructural.

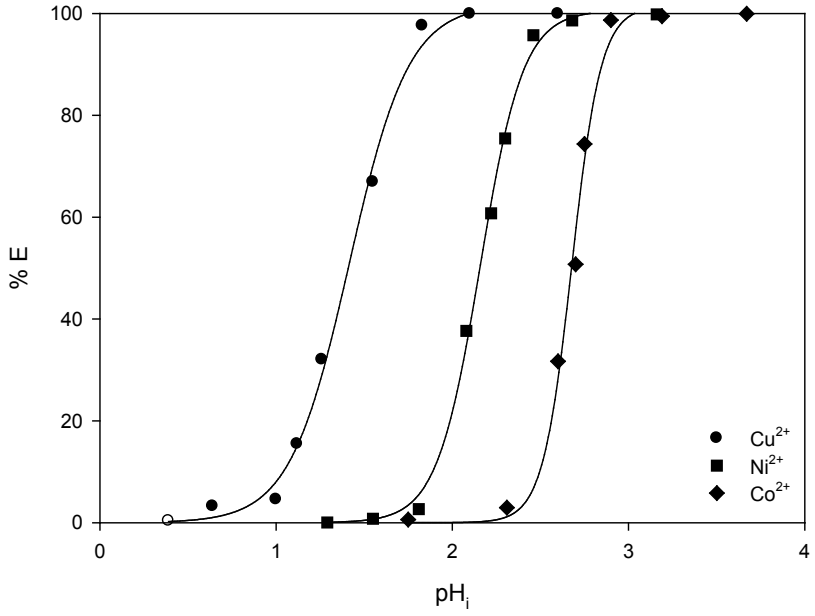

Figure 3.22: A plot of %E vs initial pH in the separation of 0.001 M Cu^{2+}, Ni^{2+}, and Co^{2+} from dilute sulfate medium with OIMOX (M:L ratios of 1:60), and 0.02 M DNNSA in 100% Shellsol 2325

(vii) Separation of copper with OIMOX and DNNSA from other base metals

The effect of the other metal ions including; Fe^{2+}, Fe^{3+}, Zn^{2+}, Cd^{2+} and Mn^{2+} was also included in this extraction system, and Zn^{2+} tended to fall outside the expected order of stability with Cd^{2+} being similar due to their positions in the periodic table (Figure 3.23). The extraction data is presented in Table 3.11. The hard ions Mn^{2+} and Fe^{3+} were extracted mildly at pH above 3, with Fe^{3+} being slightly more extracted possibly due to the operation of the deprotonated oxygen donation property. Therefore, this extraction process provides for an opportunity to remove copper from the other base metals in a highly acidic sulfate medium at a pH around 1.7. Table 3.13 provides some extraction data, and at pH values > 1.7 it is evident that the co-extracted nickel

and cobalt content is higher at these pH values and is consistent with the pH-metric extraction observations in Figure 3.23. This gives assurance that the isolated chemistry of these metals can be applied in a cocktail of the metals to achieve a similar chemistry, and this is simply based on the subtle coordination chemistry of these metals.

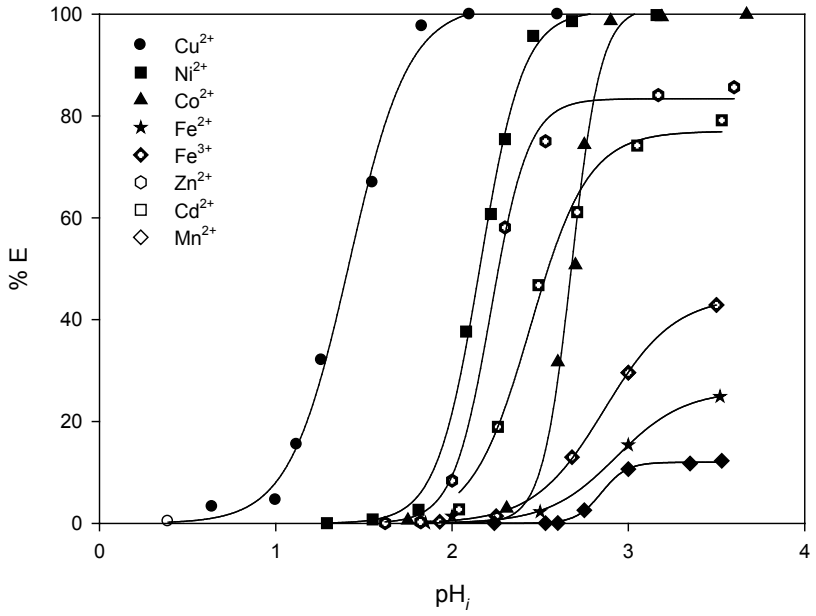

Figure 3.23: A plot of %E vs initial pH in the separation of 0.001 M Cu^{2+}, Ni^{2+},Co^{2+}, Fe^{2+}, Fe^{3+}, Zn^{2+}, Cd^{2+} and Mn^{2+} from dilute sulfate medium with OIMOX (M:L ratios of 1:60), and 0.02 M DNNSA in 100% Shellsol 2325

Table 3.11: A plot of %E vs initial pH in the separation of 0.001 M Cu^{2+}, Ni^{2+},Co^{2+}, Fe^{2+}, Fe^{3+}, Zn^{2+}, Cd^{2+} and Mn^{2+} from dilute sulfate medium with OIMOX (M:L ratios of 1:60), and 0.02 M DNNSA in 100% Shellsol 2325.

Cu^{2+}								
pH_i	0.39	0.64	1.00	1.12	1.26	1.55	1.83	2.10
pH_e	0.35	0.68	1.08	1.23	1.46	1.67	2.57	3.29
% E	0.34	3.24	4.56	15.44	32.01	66.91	97.63	99.89
Ni^{2+}								
pH_i	1.29	1.55	1.81	2.08	2.22	2.30	2.46	2.68
pH_e	1.39	1.77	2.21	2.51	2.78	2.92	3.60	3.66
% E	0.03	0.77	2.66	37.67	60.75	75.45	95.71	98.63
Co^{2+}								
pH_i	1.75	2.31	2.60	2.70	2.75	2.90	3.19	3.67
pH_e	1.98	3.31	2.75	3.87	3.95	4.20	4.25	4.39
% E	0.62	2.94	31.69	50.72	74.37	98.68	99.44	99.92
Fe^{2+}								
pH_i	1.85	2.00	2.50	3.00	3.52			
pH_e	2.01	2.16	2.93	3.63	3.94			
% E	0.08	1.39	2.28	15.39	24.92			
Fe^{3+}								
pH_i	1.93	2.25	2.68	3.00	3.50			
pH_e	1.99	2.35	2.84	3.22	3.71			
% E	0.32	1.42	13.01	29.60	42.90			
Zn^{2+}								
pH_i	1.62	1.82	2.00	2.30	2.53	3.17	3.70	
pH_e	1.80	2.46	3.46	3.90	4.09	4.21	4.29	
% E	0.07	0.27	8.39	58.09	75.03	84.08	85.64	
Cd^{2+}								
pH_i	2.04	2.26	2.49	2.71	3.05	3.53		
pH_e	2.94	3.36	3.76	3.77	3.88	3.90		
% E	2.76	18.96	46.79	61.11	74.19	79.16		
Mn^{2+}								
pH_i	2.24	2.53	2.60	2.75	3.00	3.35	3.53	
pH_e	2.63	2.99	3.07	3.19	3.40	3.49	3.59	
% E	0.03	0.05	0.08	2.59	10.66	11.75	12.29	

Table 3.12: Extraction of copper along with other base metals from a synthetic acidic sulfate solution with OIMOX at three different pH values.

% Extraction of metal ions			
Element	**pH 1.70**	**pH 1.80**	**pH 1.90**
Cu^{2+}	90.06 (0.90)	93.84 (1.98)	98.65 (2.45)
Ni^{2+}	0.55 (0.12)	1.80 (0.27)	6.03 (0.79)
Co^{2+}	0.48 (0.09)	1.54 (0.12)	5.55 (0.28)
Fe^{2+}	0.01 (0.12)	0.01 (0.17)	0.12 (0.04)
Fe^{3+}	0.03 (0.02)	0.05 (0.03)	0.16 (1.08)
Zn^{2+}	0.04 (0.02)	0.05 (0.03)	0.14 (0.07)
Cd^{2+}	0.02 (0.01)	0.10 (0.01)	0.12 (0.04)
Mn^{2+}	0.01 (0.01)	0.04 (0.02)	0.06 (0.02)

Since the co-extracted Ni^{2+}, Co^{2+} were higher at pH 1.80 and 1.90, a loading range around 1.70 was investigated to minimise the effect of the impurities while still maintaining high extraction efficiency. Table 3.13 shows the co-extracted impurities at pH 1.70(± 0.05), and it is clear that pH 1.65 gives a reasonable level of purity of the extracted copper and the efficiency drops slightly to 90.13% compared with 92.49% at pH 1.70. This method requires a two-step extraction process to recover 98.2% copper with negligible nickel and cobalt impurities (Table 3.13).

Table 3.13: Extraction of copper, nickel and cobalt at pH of 1.70 ± 0.05 in a synthetic solution of acidic sulfate with OIMOX.

% Extraction of metal ions			
Element	**pH 1.65**	**pH 1.70**	**pH 1.75**
Cu^{2+}	90.13 (0.90)	92.49 (1.98)	93.65 (3.45)
Ni^{2+}	0.05 (0.02)	0.80 (0.17)	1.03 (0.79)
Co^{2+}	0.02 (0.09)	0.14 (0.10)	1.53 (0.38)

Table 3.14: Two-stage counter-current extraction of copper at pH of 1.65 from a synthetic solution of nickel, cobalt and copper in an acidic sulfate medium with OIMOX.

% Extraction of metal ions			
Stages of extraction	**Cu^{2+}**	**Ni^{2+}**	**Co^{2+}**
1st	90.13 (0.90)	0.05 (0.02)	0.02 (0.09)
2nd	8.09 (0.28)	0.01 (0.17)	0.00 (0.01)

3.3.3 Stripping of copper

The stripping of copper from the loaded organic phase using TraceSelect sulfuric acid at the left leg of the copper extraction curve [pH = 0.40(± 0.05)] gave the results shown in Table 3.15. It is apparent that at pH 0.35, the recovery of copper is more significant to a tune of 96.6% of the loaded quantity after the second stage of stripping compared with 92.5% and 87.5% at the pH values of 0.40 and 0.45 respectively.

Table 3.15: Stripping of copper from the loaded (L.O) organic at pH 0.40 ± 0.05 with H_2SO_4.

pH	**1st Stage % Cu Stripped**	**2nd Stage % Cu Stripped**
0.35	88.50 (1.90)	96.60 (0.98)
0.40	80.31 (1.2)	92.46 (0.17)
0.45	72.68 (2.09)	87.46 (0.10)

3.3.4 Complexation studies

The complex formation reactions in both solution and solid state were investigated using a m ethyl derivative (MIMOX) of the extractant in order to establish the underlying coordination chemistry in this extraction system. This information was then interpreted in line with the extraction curves observed in this separation system.

The methyl derivative simplifies the titrimetric studies and synthesis, respectively, since oils are obtained with the octyl and decyl derivatives. However, MIMOX has the same binding moiety as the extractants with the difference being the presence of the longer alkyl chains to tune organic compability. There is a variety of coordination modes[41,42] which the imidazole-oxime ligand system can have with the metal ions, by inference of the pyridyl-2-oxime system, and these are depicted in Figure 3.24 together with the Harris notation that describes these modes. Both the solution and solid state studies for the complexation which are detailed in sections 3.3.4 (a) and (b) suggest that the coordination in this system follows the common 1.011 mode of a neutral ligand.

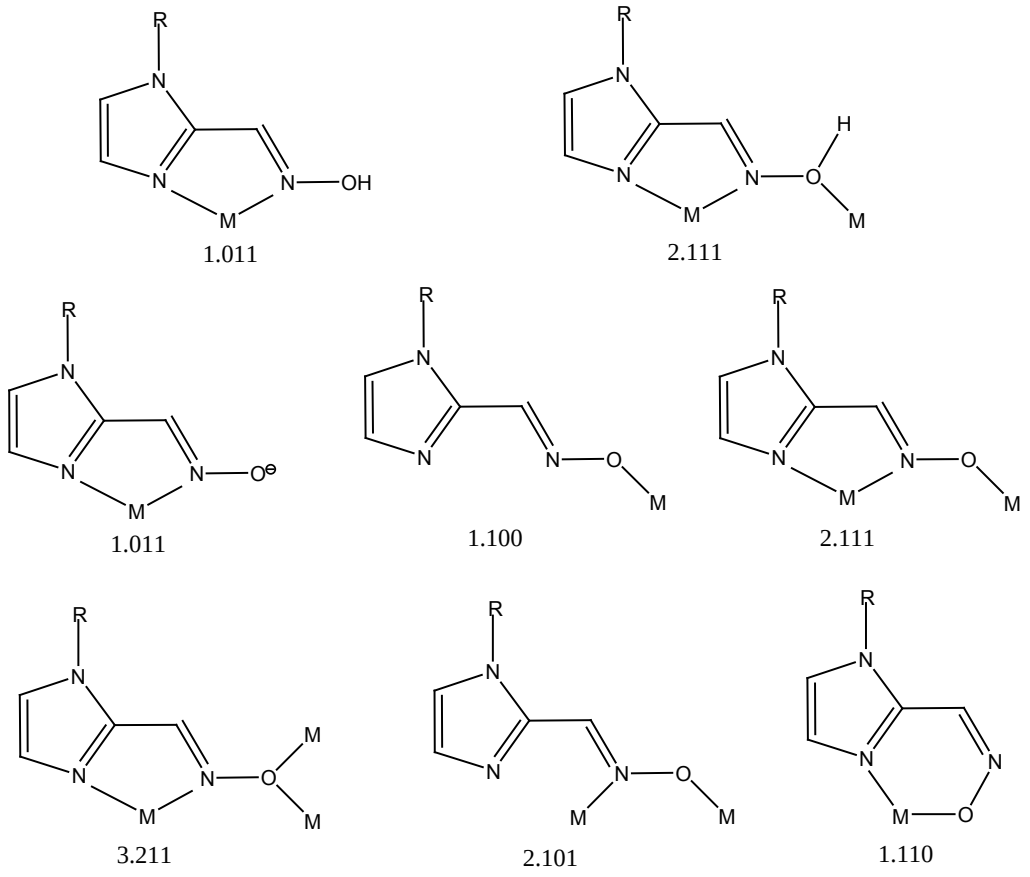

Figure 3.24: The possible coordination modes of the neutral and anionic forms of 1-methylimidazole-2-aldoxime, and the Harris notation that describes these modes

(a) Solid state studies

The microanalyses data of the metal ion complexes of MIMOX are presented in section 3.2.1(f) and they show a similar composition of carbon, hydrogen, nitrogen and sulfur, suggesting that similar compounds are formed with three ligands and one sulfate involved per metal ion. The conductivity measurements are consistent with 1:1 electrolytes in water suggesting a non-coordinated sulfate ion. This is also supported by the presence of a single strong band in the range 1050-1080 cm^{-1} in the spectra of the complexes, which is ascribed to the ν_3 mode of the tetrahedral ion. This band splits in the bidentate (C_{2v}) and monodentate (C_{3v}) coordination modes of the sulfate ion.[43] The azomethine (C=N) stretch of the imidzolyl and the oxime group occur at 1634 and 1543 c m^{-1} respectively (Figure 3.25), and these show coordination-induced shifts in the spectra of the complexes.[44] These shifts also suggest that the ligand binds in a bidentate fashion *via* the two nitrogens. The signals of the oxime hydroxyl in the range 1700-1790 cm^{-1} in the spectra of the complexes suggests that this group remains uncoordinated (Figure 3.26).

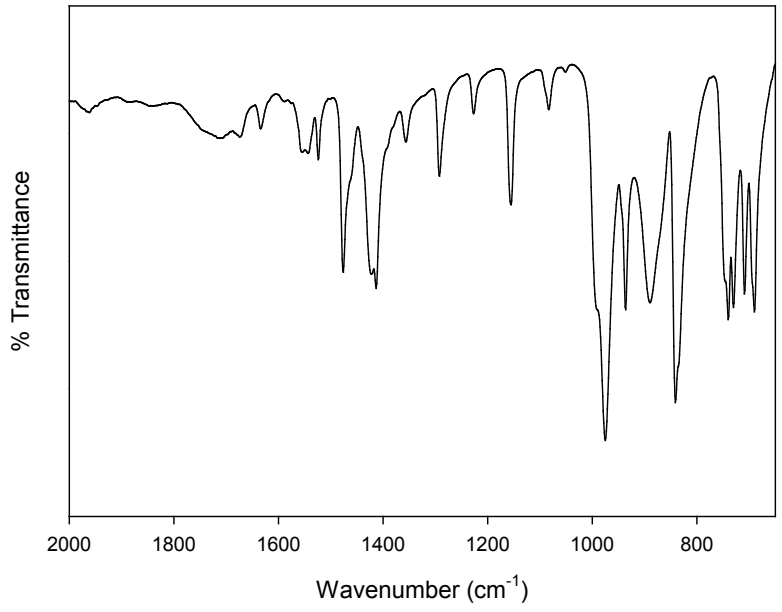

Figure 3.25: The IR spectrum of 1-methylimidazole-2-aldoxime

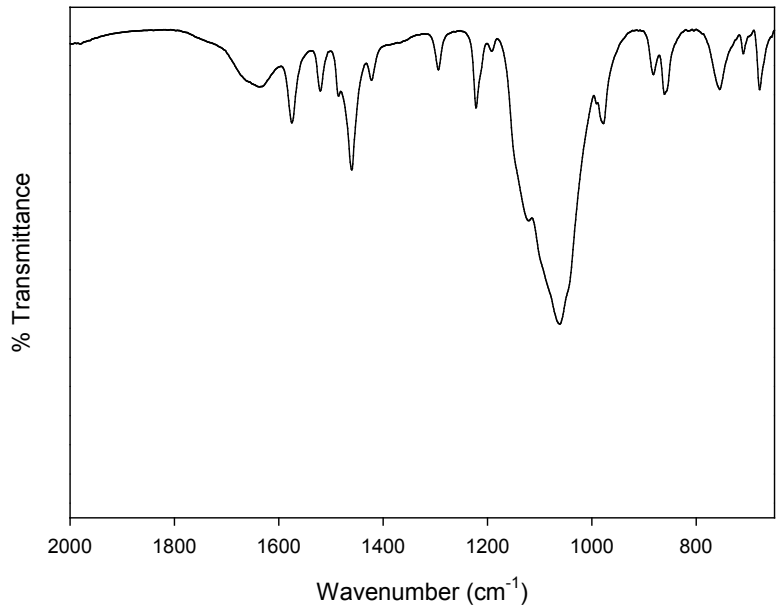

Figure 3.26: The IR spectrum of the cobalt complex of 1-methylimidazole-2-aldoxime

The similarity of the copper, nickel and cobalt complexes is once again supported by the electronic absorption spectroscopic data. The solid reflectance spectra of the complexes are consistent with an octahedral geometry of the complexes (Figure 3.27). The three bands at 1040, 642 and 468 nm correspond to the $^3A_{2g}(F)\rightarrow{}^3T_{2g}(F)$, $^3A_{2g}(F)\rightarrow{}^3T_{1g}(F)$ and $^3A_{2g}(F)\rightarrow{}^3T_{1g}(P)$, respectively, for the octahedral nickel complex while the two bands of cobalt(II) complex at 1240, 492 nm were ascribed to the $^4T_1(F)\rightarrow{}^4T_2(F)$ and $^4T_1(F)\rightarrow{}^4T_1(P)$ transitions.[45] The spectrum of copper(II) complex showed one broad band around 700 nm which correspond to the $^2T_{2g}\rightarrow{}^2E_g$, consistent with an octahedral copper(II) complex.[46] As discussed in section 3.3.4 (b) the thermodynamics of complexation is the main discriminator in this case, and the stereochemical "tailor-making" is absent as a separation driver.

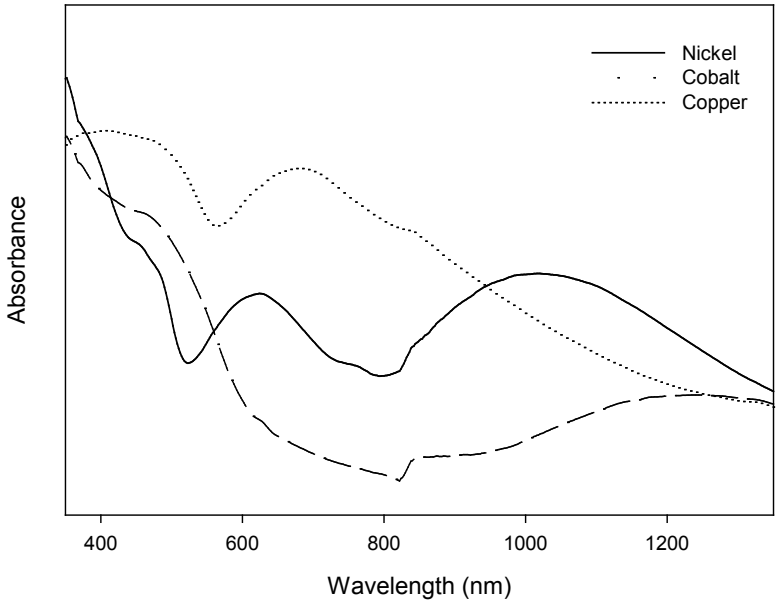

Figure 3.27: The solid reflectance spectra for nickel(II), cobalt(II) and copper(II) complexes of 1-methylimidazole-2-aldoxime

Similar nickel compounds have been isolated and characterized by X-ray crystallography with phenyl(2-pyridyl)ketone oxime and pyridine-2-aldoxime as coordinating ligands,[47,48] in which the three bidentately coordinated units were neutral with the oxime hydroxyl non-deprotonated. It is unfortunate that single crystals which are suitable for X-ray diffraction analysis could not be obtained for the complexes that have been isolated in this study.

(b) Stability constants

The protonation (log *K*) and complex formation (log *β*) constants for 1-methylimidazole-2-aldoxime are presented in Table 3.16 with standard deviations in parenthesis. 1-Methylimidazole-2-aldoxime (MIMOX) was chosen since it presents all the components of the extractant (OIMOX) with the exception of the octyl group which does not play much role in the coordination process since it is away from the coordination environment. The ligand exhibits a two-stage protonation process (Scheme 3.2) with a p K_a value of 9.44 for the oxime hydroxyl, and a single protonation step between the imidazolyl and the imine nitrogen of the oxime with a

constant of 5.25 which is pyridine-like[48] but with a chelating character. The species distribution plot depicted in Figure 3.27 illustrates the species of the ligand as a function of pH. The reaction equilibria involved can be seen in Scheme 3.2. It is evident that at the pH range in which the extractions were carried out the ligand exists in a protonated form and that the metal ions replace the proton that is shared between the imidazolyl and the immine nitrogen of the oxime. However, since it is not strongly held (p*K*a = 5.25) the metal ions are able to compete effectively for this coordination site

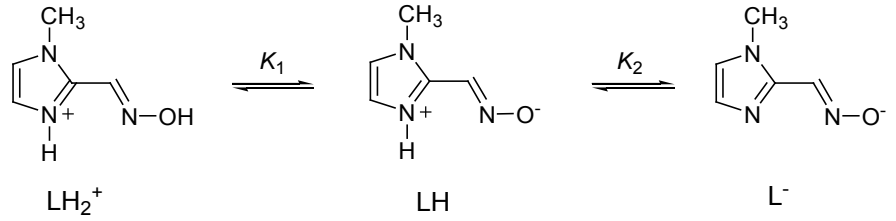

Scheme 3.2: De-protonation steps for the 1-methylimidazole-2-aldoxime (MIMOX). H^+ have been omitted from the equilibria

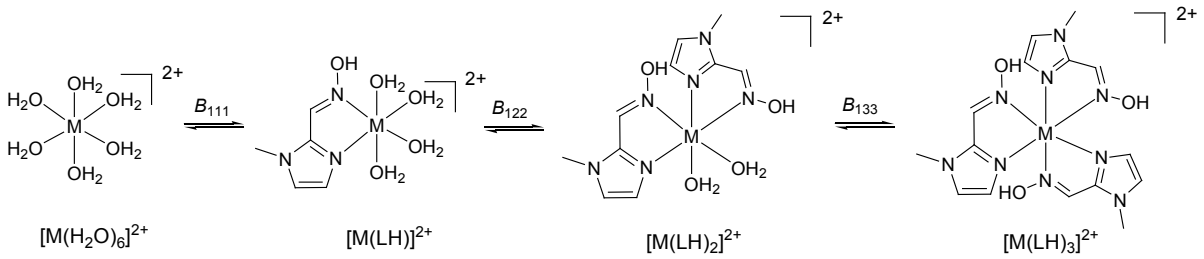

Scheme 3.3: The stepwise formation of base metal ion complexes with 1-methylimidazole-2-aldoxime (MIMOX). LH is omitted in the complexation equilibria

Table 3.16: Protonation (log *K*) and stability (log *β*) constants for the interaction of MIMOX with the base metal ions as determined in 10% ethanol/water at *I* = 0.10 M (TMACl) and 25(±0.1)^{o}C. The standard deviations are reported in parenthesis.

Constant	Reaction	p, q, r	MIMOX	Co^{2+}	Ni^{2+}	Cu^{2+}	Zn^{2+}
pK_1	$LH \rightleftharpoons H^+ + L^-$	0, 1, 2	9.44(0.01)	-	-	-	-
pK_2	$LH_2^+ \rightleftharpoons H^+ + LH$	0, 1, 1	5.25(0.02)	-	-	-	-
logβ_{111}	$M^{2+} + LH \rightleftharpoons [M(LH)]^{2+}$	1, 1, 1	-	4.7(0.1)	7.8(0.1)	10.3(0.1)	4.5(0.1)
logβ_{122}	$M^{2+} + 2LH \rightleftharpoons [M(LH)_2]^{2+}$	1, 2, 2	-	8.7(0.1)	14.4(0.1)	14.9(0.2)	8.8(0.2)
logβ_{133}	$M^{2+} + 3LH \rightleftharpoons [M(LH)_3]^{2+}$	1, 3, 3	-	-	-	-	13.1(0.1)
		Sigma (σ)	0.75	1.03	1.55	0.95	3.18

p,q and r refer to the coefficients of the species in the order of metal, ligand, and proton.

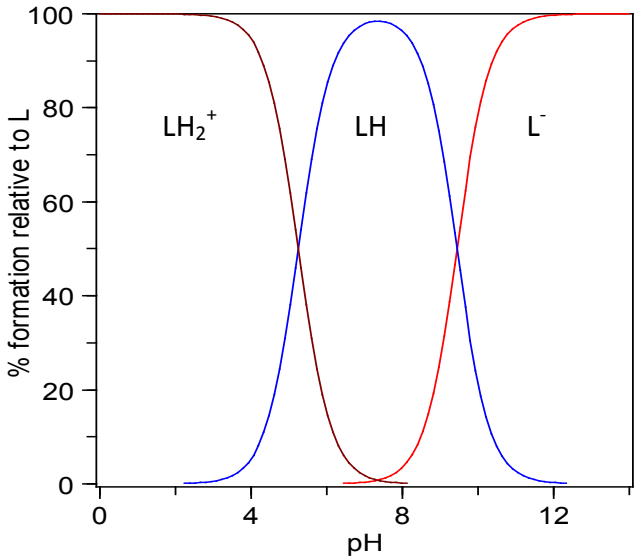

Figure 3.28: Protonation species distribution diagram for 1-methylimidazole-2-aldoxime (MIMOX)

Solution chemistry for the complex formation reactions with the assumption that the hydroxyl group of the oxime remains protonated was the best fitting model for the observed experimental data. The stability constants are presented in Table 3.16 with sigma values for the curve fitting included. The sigma values were satisfactory for this model despite the non-aqueous solvent system (10% ethanol in water) employed. The choice of this solvent system was governed by the solubility of the ligand and the complexes formed. Figure 3.29 shows an experimental potentiometric curve as well as a fitted one based on model fitting on HYPERQUAD by the estimation of the constants followed by their refinement. The closeness of the fit is proof of the reliability of these stability constants determinations.The low sigma values obtained for all these determinations are a further proof of the reliability of the calculated results. The reaction Scheme 3.3 better illustrate the reaction equilibra involved. However, the third constant could only be calculated for zinc due to the precipitation experienced for the other metals but up to the second constant was confidently determined for all the metals.

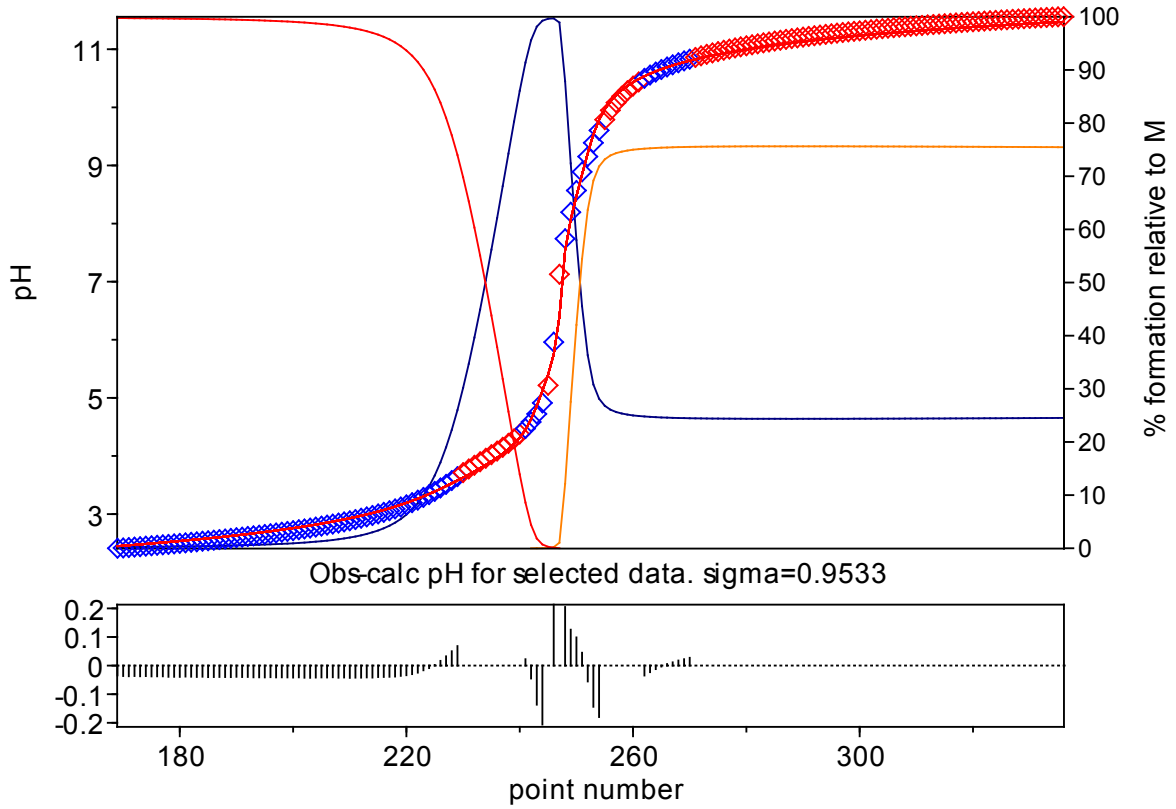

Figure 3.29: Titration and fitted curves of the Cu-MIMOX system. Experimental points are represented by blue squares and the red continuous line is the calculated line based on the fitted constants. The red squares represent the experimental points that have been ignored in the refinement process. The other lines represent the species (not specified)

The bidentate character in coordination was evidenced by the high formation constants that were calculated especially for Cu(II) and Ni(II) (in the pH range 2.5-6.2) for the formation of the metal ion complexes with this coordinating moiety (see Table 3.16). However, the third constant could only be c alculated for zinc since precipitation occurred for the other metal ions above the pH of 6. The overall second stability constants are of the order: Cu^{2+} (14.9) > Ni^{2+} (14.4) > Zn^{2+} (8.8) > Co^{2+} (8.7). This is the same order that is observed in the extraction curves (Figure 3.23), and the stability of the zinc complex is anomalous to the expected Irving-Williams stability order. This result shows that the separation system is driven by the thermodynamics of complexation since the compounds are seemingly isostructural. This stereochemical property was investigated and the findings are presented in section 3.3.4 (a).

3.4 Conclusions

Preliminary extractions of base metal ions conducted with dimthylglyoxime as probable nickel specific extractant in strongly acidic medium did not yield the desired separation of nickel even in the presence of DNNSA. This shows that this reagent was not readily deprotonated for it to bind the metal ions at this low pH. While at the slightly higher pH red precipitate of $Ni(DMG)_2$ were observed due to the poor solubility of the nickel complex formed. The possibility of degradation of DMG in strong acids to amide was not confirmed but raises a strong doubt about the stability of this reagent. With these observations the study on the application of DMG as nickel specific extractant in acidic medium could not proceed further.

The new extractant, 1-octylimidazole-2-aldoxime (OIMOX), was however successfully synthesized and applied in the separation of copper from base metals. The bidentate character of this new extractant imparts high stability of the chelates formed, and this is evident from the low M:L ratio employed in this study compared with the study of the monodentately-operatingextractants.[47,49] This imidazole-oxime with a pyridine-type character allows for the extraction of copper at low pH and with a possibility for stripping to a satisfactory level. The stability constants data gave evidence of the thermodynamics of complexation being the major driver in this separation process. The underlying coordination chemistry was thoroughly studied, and octahedral cationic complexes form upon the interaction of this extractant with the metal ions. The stability of the extractant (OIMOX) under these highly acidic conditions has not been investigated in this account but is recommended for future investigations of this extractant.

References

[1] R. B. Singh, B. S. Garg, R. P. Singh, Talanta 26 (1978) 425-444.

[2] W. C. Hamilton, Acta Crystallog. 14 (1961) 95-100.

[3] J. Donohue, J. Am. Chem. Soc. 78 (1956) 4172-4185.

[4] D. Hall, Acta Crystallog. 18 (1965) 955-980.

[5] D. Mannier, W. Haerdi, Helv. Chim. Acta 41 (1958) 2205-2217.

[6] L. Tshugaev, J. Chem. Soc., Perkin Trans. 1 (1914) 2187-2198.

[7] L. Tshugaev, Z. Anorg. Chem. 46 (1905) 144-154.

[8] R. E. Rundle, M. Parasol, J. Chem. Phys. 20 (1952) 1487-1489.

[9] J. Fujita, A. Nakahara, R. Tsuchida, J. Chem. Phys. 23 (1955) 1541-1559.

[10] R. Blinc, D. Hadzi, J. Chem. Soc. (1958) 4563-4665.

[11] R. Blinc, D Hadzi, Spectrochim. Acta. 16 (1960) 852-865.

[12] D. Dyrssen, F. Krasovec, L. G. Sillen, Acta Chem. Scand. 13 (1959) 50-60.

[13] D. Dyrssen, M. Hennicks, Acta Chem. Scand. 15 (1961) 47-59.

[14] K. Burger, R. Ruff, Talanta 10 (1963) 112-123.

[15] K. Burger, I. Ruff, F. Ruff, J. Inorg. Nucl. Chem. 27 (1965) 179-190.

[16] R. C. Voter, C. V. Banks, V. A. Fassel, P. W. Kebhres, Anal. Chem. 23 (1951) 1730-1736.

[17] L. E. Godycki, R. E. Rundle, R. C. Voter, C. Y. Banks, J. Chem. Phys, 19 (1951) 1205-1221.

[18] R. E. Rundle, M. Parasol, J. Chem. Phys. 20 (1952) 1487 -1498.

[19] R. G. Charles, H. Freiser, Anal. Chim. Acta. 11 (1954) 101-110.

[20] K. Burger, D. Dyrssen, Acta Chem. Scand. 17 (1963) 1489-1499.

[21] A. W. Ashbrook, Coord. Chem. Rev. 16 (1975) 285-307.

[22] D. S. Flett, D. N. Okuhara, D. R. Spink, J. Inorg. Nucl. Chem. 35 (1973) 2471-2487.

[23] A. W. Ashbrook, Hydrometallurgy 1 (1975) 5-17.

[24] K. C. Sole, A. M. Feather, P.M. Cole, Hydrometallurgy 78 (2005) 52-78.

[25] J.S. Preston, Hydrometallurgy 11 (1983) 105-124.

[26] M. Jin, F. C. Michel Jr, R. D. Noble, Ind. Eng. Chem. Res. 28 (1989) 193-198.

[27] M. Haring, Helv. Chim. Acta. 42 6 (1959) 1845-1855.

[28] P. E. Inverson, H. Lund, Acta Chem. Scand. 20 (1966) 2646-2660.

[29] U. Gebert, B. Von Kerekjarto, Leib. Ann. Chem. 718 (1968) 249-256.

[30] C. Papatriantafyllopoulou, C. G. Efthymiou, C. P. Raptopoulou, A. Terzis, E. Manessi-Zoupa, S. P. Perlepes, Spectrochim. Acta Part A: 70 (2008) 718-728.

[31] G. Gran Analyst 77 (1952) 661-669.

[32] P. Gans B. O'Sullivan Talanta 51 (2000) 33-37.

[33] C. Bazzicalupi. A. Bencini, A. Bianchi, A. Danesi, C. Giorgi, B. Valtancoli Inorg. Chem.48 (2009) 2391-2398.

[34] P. Gans A. Sabatini A. Vacca, Talanta 43 (1996) 1739-1753.

[35] B. R. Brown, The organic chemistry of aliphatic compounds, 1994 McGraw-Hills co. 568-572.

[36] A. R. Katrizky, H. Lang, X. Lan, Org. Synth. (1993) 2829-2837.

[37] M. Hashimoto, Y. Obora, S. Sakaguchi, Y. Ishii, J. Org. Chem. (2008)*73* 2894-2897.

[38] K. Osseo-Asare, H. Leaver, J. M. Laferty, M. C. Kuhn, AIME: New York, 1981 195–207.

[39] Komasawa, T. Otake, Y. Ogawa, J. Chem. Eng. Jpn.17 (4) (1984) 410-417.

[40] H. M. Irving, R. J. P. Williams, J. Chem. Soc. (1953) 3192-3210.

[41] C. J. Milios, T. C. Stamatatos and S. P. Perlepes, Polyhedron 25 (2006) 134-194.

[42] G. A. Pearse, P. R. Raithby, C. M. Hay, J. Lewis, Polyhedron 8 (1989) 301-305.

[43] K. Nakamoto, Infrared and Raman Spectra of Inorganic and Coordination Compounds, 3rd ed, John Wiley and Sons, New York, 1978.

[44] T. J. Lane, I. Nakagawa, J. L. Walker, A. J. Kandathil, Inorg.Chem. 1 (1962) 267-279.

[45] D. Nicholls, Complexes and First-Row Transition Elements, Macmillan Press, London, 1974.

[46] A. B. P. Lever, Inorganic Electronic Spectroscopy, 2nd ed., Elsevier, New York, 1984.

[47] J. G. H. du Preez, N. Sumter, C. Matheüs, S. Ravindran, B. J. A. M. van Brecht, Solvent Extr. Ion Exch. 15 (1997) 1007-1021.

[48] L. D. Pettit and K. J. Powell, Stability Constants Database-IUPAC and Academic Software, UK, 2007.

[49] J.G.H. du Preez, T.I.A. Gerber, W. Edge, V.L.V. Mtotywa and B.J.A.M. van Brecht, Solvent Extr. Ion Exch. 19 (2001) 143-154.

CHAPTER 4

●●●●●

SOLVENT EXTRACTION OF NICKEL WITH A 2,2′-PYRIDYLIMIDAZOLE-BASED EXTRACTANT

4.1 Introduction

The basis for metal ion separation has been shown to be a unique property of the coordination chemistry of the particular metal ion. In the development of a metal ion specific reagent, it is necessary to consider the characteristics of the metal ions from which the desired metal ion must be removed as well as its own. In such studies, the nature of the metal ion, the hydrogen ion concentration, the thermodynamics and kinetics of complexation, and the coordinating ability of the anion become important parameters.

Application of amines in their neutral form has not been extensively explored as separating agents for metal ions from a basic bonding viewpoint.[1] The use of the ammonia derivatives (R-NH_2, where R is an alkyl or aryl group) is limited by their high protonation constants which prevent complexation even in weakly acidic solutions thereby resulting in the hydrolysis of metal ions. These strong ligands with σ-donor only character also show lack of relative preference for the metal ions, however, this can be improved if chelates are used for example the alkylated derivatives of ethylenediamine.[1] Aromatic nitrogenous ligands have an app arent relative preference for metal ions which could relate to the possibility of σ and π bonding. Imidazole extractants[2,3] show high formation constants with later 3d-transition metals thereby resulting in high extraction efficiencies, and also interact with these metals in slightly strong to weakly acidic media since their protonation constants lie around 6.5. For example, 1-decylimidazole proved to be a s uitable extractant for Co^{2+}, Ni^{2+}, Cu^{2+} and $Zn^{2+}$from aqueous solutions having pH values above 2.[1] Pyridine derivatives are known to interact strongly with metal ions in strongly acidic media since they have low protonation constants, and are therefore

usually not considered due to the almost irreversible extraction by pH tuning. However, coupling this group with another of higher protonation constant, in the design of a bidentate ligand, should offer three advantages, namely; interaction with metal ions at relatively low pH, higher stability of the chelates, and specificity for metals through stereochemical “tailor-making”.

In this study, a bidentate ligand, 2,2′-pyridylimidazole (Figure 4.1), that incorporates both the pyridyl and the imidazolyl groups for the selective extraction of nickel(II) from base metals has been employed mainly due to the high complex formation offered by the imidazole group and the low protonation constant of the pyridyl group which allows formation of the complex species in a highly acidic medium. The 1-position of imidazole also allows for functionalization with large alkyl groups to tune the compatibility of the extractant with the organic phase. The heptyl (HPIM), octyl (OPIM) and decyl (DPIM) derivatives of pyridylimidazole were initially investigated, (Figure 4.1), along with dinonylnaphthalene sulfonic acid (DNNSA) as a synergist, in a solvent extraction system. The conditions for nickel specificity were designed in extraction studies using these extractants dissolved in 80% 2-octanol and 20% shellsol 2325,[4] as diluent and modifier, respectively.

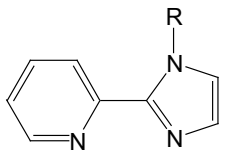

R = heptyl, octyl and decyl

Figure 4.1: The chemical structures of the extractants; 1-Heptyl-2,2′-pyridylimidazole (HPIM), 1-octyl-2,2′-pyridylimidazole (OPIM) and 1-decyl-2,2′-pyridylimidazole (DPIM)

4.2 Experimental

4.2.1 Preparative work

(a) 2,2′-Pyridyl-1*H*-imidazole (PIMH)

The ligand, 2,2′-pyridyl-1*H*-imidazole (PIMH), was prepared as follows according to a method reported in the literature.[5] A solution of 10.70 g of pyridine-2-aldehyde (0.10 moL) in 10 mL ethanol was mixed with 20 mL of a 40% aqueous glyoxal solution at 0°C. Without delay, 30 mL of an ice-cold 20% aqueous ammonia solution was added, and the yellow-brown solution was stirred at 0°C.for 30 min, and then allowed to stand overnight at room temperature. The ethanol was then boiled off, and the residue was extracted several times with 50 mL aliquots of diethyl ether. The ether was evaporated using a rotary evaporator, and the yellow solid crystals were re-crystallized from ethyl acetate. These were filtered and dried under vacuum.

2,2′-Pyridyl-1*H*-imidazole (PIMH): Yield = 71%. M.p. = 133-135°C. Anal. Calc. for $C_8H_6N_3$: C, 66.19; H, 4.86;N, 29.41 %. Found: C, 66.08; H, 4.97;N, 29.11 %.^{1}H NMR ($CDCl_3$) δ(ppm): 7.26-7.29 (d,1H,H5), 7.20-7.30 (m,2H,H4,H5´), 7.81 (t1H, H4´), 8.54 (1d,H,H3´), 8.55 (d,1H,H6´), 11.10 (brs,1H,NH). IR (v_{max}/cm^{-1}):1695, v(C=N_{im}); 3127, v(N-H).

(b) General synthesis of 1-alkyl 2, 2´-pyridyl-1-alkylimidazoles

The alkylated derivatives (extractants) were also prepared according to a literature method.[6]Thus, alkylation of the imidazole ring with heptyl, octyl and decyl group was achieved with the addition of 3.86 g (0.06 mol) of potassium hydroxide to a solution of 10 g (0.06 mol) of PIMH in 50 mL acetone. To this, 0.06 mol of 1-alkylbromide was added drop wise. The reaction was allowed to stir for 30 mins and then the mixture was refluxed at 40°C overnight. It was then cooled and filtered to remove the KBr salt. The resulting solution was concentrated *via* rotary evaporation, and purified using a silica gel chromatographic column with ethyl acetate/methanol (ratio) solvent system. The products were obtained as brown oils with the yields ranging from 41-53%.

1-Heptyl 2,2´-pyridylimidazole: Yield = 53%. Anal. Calc. for $C_8H_6N_3$: C, 74.03; H, 8.70;N, 17.27 %. Found: C, 73.89; H, 8.58; N, 18.54%. ^{1}H NMR (400 MHz, $CDCl_3$) δ

(ppm): δ 0.88 (t,3H,CH_3), 1.27-1.29 (m, 8H,CH_2), 4.56-4.70 (t,2H,CH_2), 7.03 (s,1H,H5), 7.14-7.29 (m,2H,H4,H5´), 7.49 (s, 1H,H4´),8.02 (d,1H,H3´) 8.35-8.43 (d, 1H,H6´). IR (v_{max}/cm^{-1}):1694, v(C=N_{im}); 3127, v(N-H).

1-Octyl 2,2´-pyridylimidazole: Yield = 47%. Anal. Calc. for $C_8H_6N_3$: C, 74.67; H, 9.01;N, 16.33 %. Found: C, 74.18; H, 8.89; N, 17.05 %. ^{1}H NMR (400 MHz, $CDCl_3$) δ (ppm): δ 0.67 (t,3H,CH_3), 1.07-1.27 (m,10H,CH_2), 1.56-1.57 (t,2H,CH_2), 4.37 (t,2H,CH_2), 6.81 (s,1H,H5), 6.96-6.98 (m,2H,H4,H5´), 7.49 (s,1H,H4´),8.02 (d,1H,H3´) 8.35-8.40 (d,1H,H6´). IR (v_{max}/cm^{-1}):1700, v(C=N_{im}); 3135, v(N-H).

1-Decyl 2,2´-pyridylimidazole: Yield =41%. Anal. Calc. for $C_8H_6N_3$: C, 75.74; H, 9.53;N, 14.72 %. Found: C, 76.08; H, 8.65; N, 15.24 %. ^{1}H NMR (400 MHz, $CDCl_3$) δ (ppm): δ 0.90 (t,3H,CH_3), 1.27-1.28 (m, 12H,CH_2), 1.82 (t,2H,CH_2), 4.60-4.64 (t,2H,CH_2), 7.03 (s,1H,H5), 7.14-7.29 (m,2H,H4,H5´), 7.75 (s, 1H,H4´), 8.17 (d,1H,H3´) 8.54-8.60 (d, 1H,H6´).). IR (v_{max}/cm^{-1}):1699, v(C=N_{im}); 3133, v(N-H).

(c) General synthesis ofthe metal complexes

Metal complexes of Ni^{2+}, Co^{2+}, Cu^{2+}, and $Zn^{2+}$with PIMH were prepared by a general method which is outlined below. A hot 20 mL ethanol/water (1:1) solution (60°C) of the appropriate metal sulfate (1 mmol) was added to a hot solution of 2,2´-pyridyl-1*H*-imidazole (3 mmol) in the same solvent. The resulting mixture was stirred under reflux for 1 hr upon which the complexes were precipitated or in some cases crystals were formed upon standing the solution at room temperature. The following colours of the precipitates were observed: purple fornickel, pink for cobalt, green for copper, and white for zinc. These were collected by filtration, washed with ice-cold 1:1 ethanol/water mixture. The characterization data is presented below.

[Ni(PIMH)$_2$]SO_4·4H_2O·½EtOH: Yield=79%. M.p. > 300°C. Anal. Calc: C, 66.19; H, 4.86; N, 28.95; S, 3.31 %. Found: C, 66.08; H, 4.97; N, 29.11; S, 3.33 %. IR: (v_{max}/cm^{-1}) 3146, v(N-H);1492, v(C=N); 1078, $v_3(SO_4^{2-})$; 386, v(M-N). UV-Vis (λ_{max}/nm): 924, 572. Conductivity (10^{-3}M, $ohm^{-1}.cm^{-1}.mole^{-1}$): 60.

[Cu(PIMH)$_2$]SO_4·4H_2O.½EtOH: Yield=71%. M.p. = 295-297°C. Anal. Calc: C, 40.89; H, 4.89; N, 17.34; S, 3.38 %. Found: C, 40.96; H, 4.46; N, 17.78; S, 3.47 %. IR:

(v_{max}/cm^{-1}) 3160, v(N-H); 1492, v(C=N); 1077, $v_3(SO_4^{2-})$; 399, v(M-N). UV-Vis (λ_{max}/nm):800. Conductivity (10^{-3}M, $ohm^{-1}.cm^{-1}.mole^{-1}$): 201.

$[Co(PIMH)_2]SO_4 \cdot H_2O$: Yield=82%. M.p. > 300°C. Anal. Calc: C, 41.48; H, 3.48; N, 18.14; S, 6.92 %. Found: C, 41.16; H, 3.59; N, 17.99; S, 5.89 %. IR: (v_{max}/cm^{-1}) 3140, v(N-H); 1489, v(C=N); 1059, $v_3(SO_4^{2-})$; 384, v(M-N). UV-Vis (λ_{max}/nm):1073, 501. Conductivity (10^{-3}M, $ohm^{-1}.cm^{-1}.mole^{-1}$): 218.

$[Zn(PIMH)_2]SO_4 \cdot H_2O$: Yield=81%. M.p. > 300°C. Anal. Calc: C, 40.91;H, 3.43; N, 17.89; S, 6.83 %. Found: C, 40.96; H, 3.92; N, 17.97; S, 5.77 %. IR: (v_{max}/cm^{-1}) 3140, v(N-H); 1490, v(C=N); 1049, $v_3(SO_4^{2-})$; 385, v(M-N). Conductivity (10^{-3} M, $ohm^{-1}.cm^{-1}.mole^{-1}$): 227.

4.2.2 Extraction studies

(a) Extraction procedure

The extraction studies were carried out in the same manner as that described in Chapter 3.

(b) Scrubbing

The co-extracted metal ion, in particular Cu^{2+}, was scrubbed off the loaded organic phase with NH_3/NH_4Cl buffer at a pH of 8.5 at a v/v phase ratio of 1:1. Two consecutive stages of scrubbing were carried out.

(c) Selective stripping

Selective stripping of $Co^{2+}$and $Ni^{2+}$was quantitatively achieved at pH 1.64 and 0.32 respectively from the loaded organic phase using aTraceSelect sulfuric acid solution at an aqueous-to-organic (A/O) phase ratio of 1:1.

4.2.3 Solution chemistry studies

(a) Potentiometric titrations

The protonation and stability constants were carried out in the same manner as that described in chapter 3.

(b) Spectrophotometric titrations

These titrations were performed manually on a Varian Cary 1E Spectrophotometer by addition of a ligand solution (PIMH) to the nickel solution in a room controlled at 25(±1)°C. This was done by pipetting 1.5 mL of 0.04 M nickel(II) toluene-4-sulfonateaqueous solution into a 1 cm quartz cuvette and adding the increments necessary to achieve the desired mole ratio using 0.4 M PIMH solution in ethanol *via* a micropipette. The solution in the cuvette was well mixed before recording the spectra every 5 mins.The plots were constructed by using the dilution corrected absorbances.

4.3 Results and discussion

4.3.1Synthesis of the ligand and the extractants

The synthesis of 2,2′-pyridyl-1*H*-imidazole (PIMH) from pyridine-2-aldehyde and glyoxal in aqueous ammonia (Scheme 4.1) provides an effective direct route for the preparation of the imidazole ring of the bidentate ligand. This reaction is highly exothermic and must therefore be conducted at a temperature below 5°C. This necessitated the use of ice cold ammonia solution to maintain this temperature. Upon stirring the solution at this temperature for onehour and allowing it to rise overnight to room temperature the colour changes from light yellow to dark brown. A black viscous liquid resulted after evaporating the solvent with a rotary evaporator. Extraction with portions of ethyl acetate was done several times until no visible brown colour remains for an optimum yield. The yielded crystals were further purified by re-crystallization. The percent yield was improved when the crystals were given longer period to grow.

To produce the long chain extractants, considered more compatible with the organic phase, alkylation of the imidazole ring at the pyrole nitrogen was achieved with the

deprotonation of the labile proton by using a base (KOH) and the subsequent substitution with the respective alkyl group of the alkyl halide. The reaction was conducted at a mild temperature of 40°C. Thus, it is considered less hazardous. The two-step reaction is illustrated with reaction Schemes 4.1 and 4.2, and the ^{1}H NMR spectra of 2,2′-pyridyl-1*H*-imidazole (PIMH) and the alkyl derivatives are shown in Figures 4.2 and 4.3(a-c) respectively.

The ^{1}H NMR data as given in section 4.2.1(a) and Figure 4.2 depicts the chemical shift of the pyrole nitrogen proton as 11.10 which is in agreement with literature values.[6] The disappearance of this peak in the spectra in Figures 4.3 (a-c) and the appearance of peaks in the region of 0.50 to 4.5 shows evidence of the connection of the alkyl chain to the imidazole nitrogen.

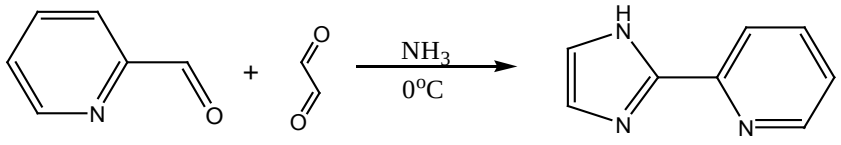

Scheme 4.1: Synthesis of 2,2′-pyridyl-1*H*-imidazole (PIMH**)**

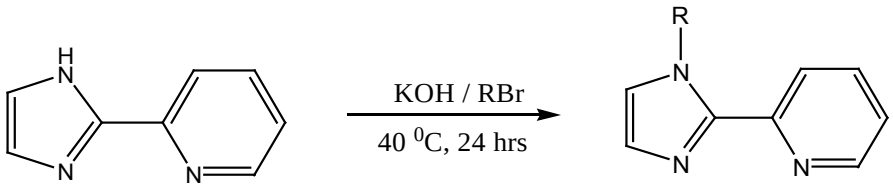

R = heptyl, octyl and decyl

Scheme 4.2: Synthesis of 2,2´-pyridyl-1R-imidazoles

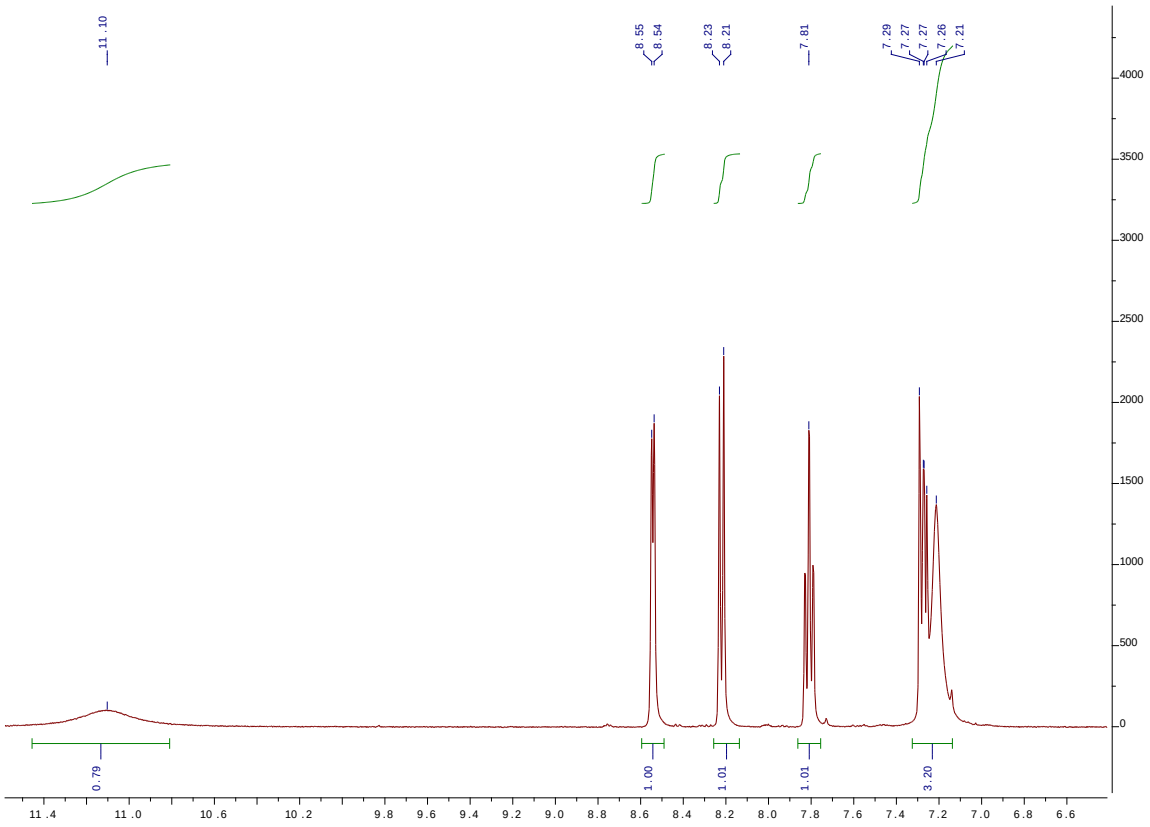

Figure 4.2: ^{1}H NMR spectrum of 2,2′-pyridyl-1H-imidazole (PIMH)

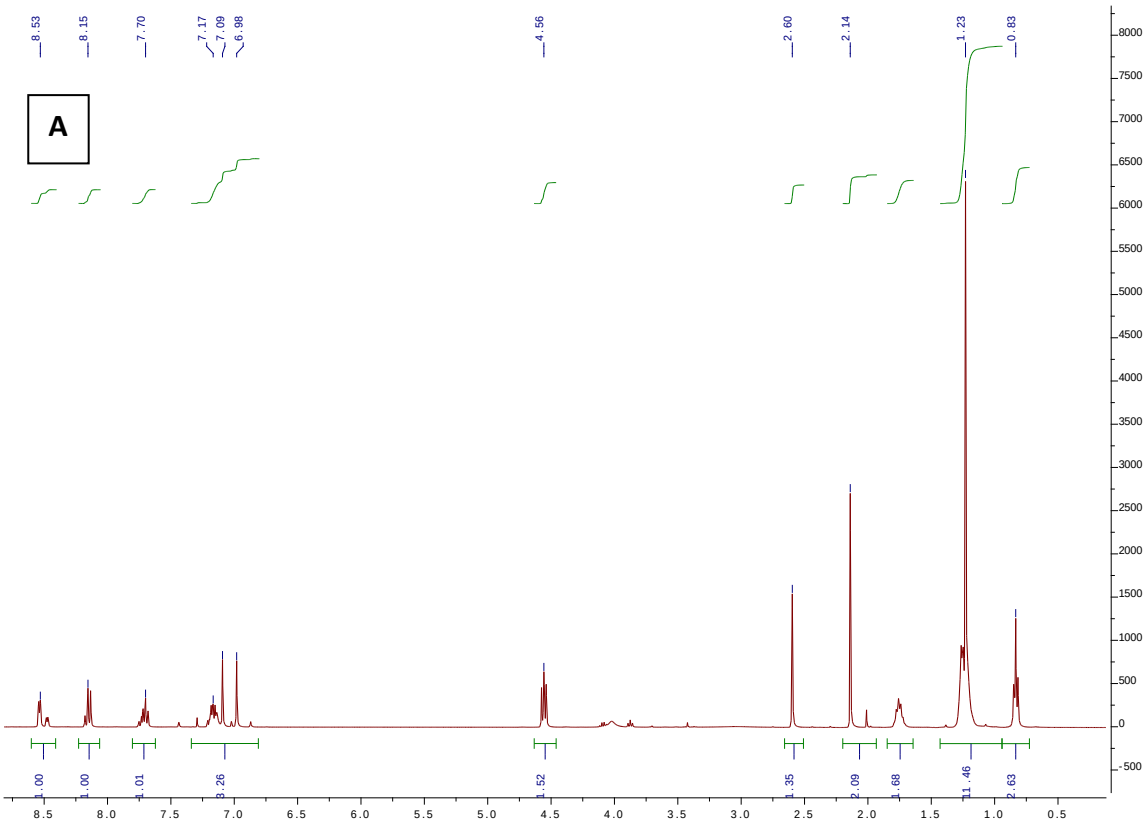
A
8.53
8.15
7.70
7.17
7.09
6.98
4.56
2.60
2.14
1.23
0.83
1.00
1.00
1.01
3.26
1.52
1.35
2.09
1.68
11.46
2.63

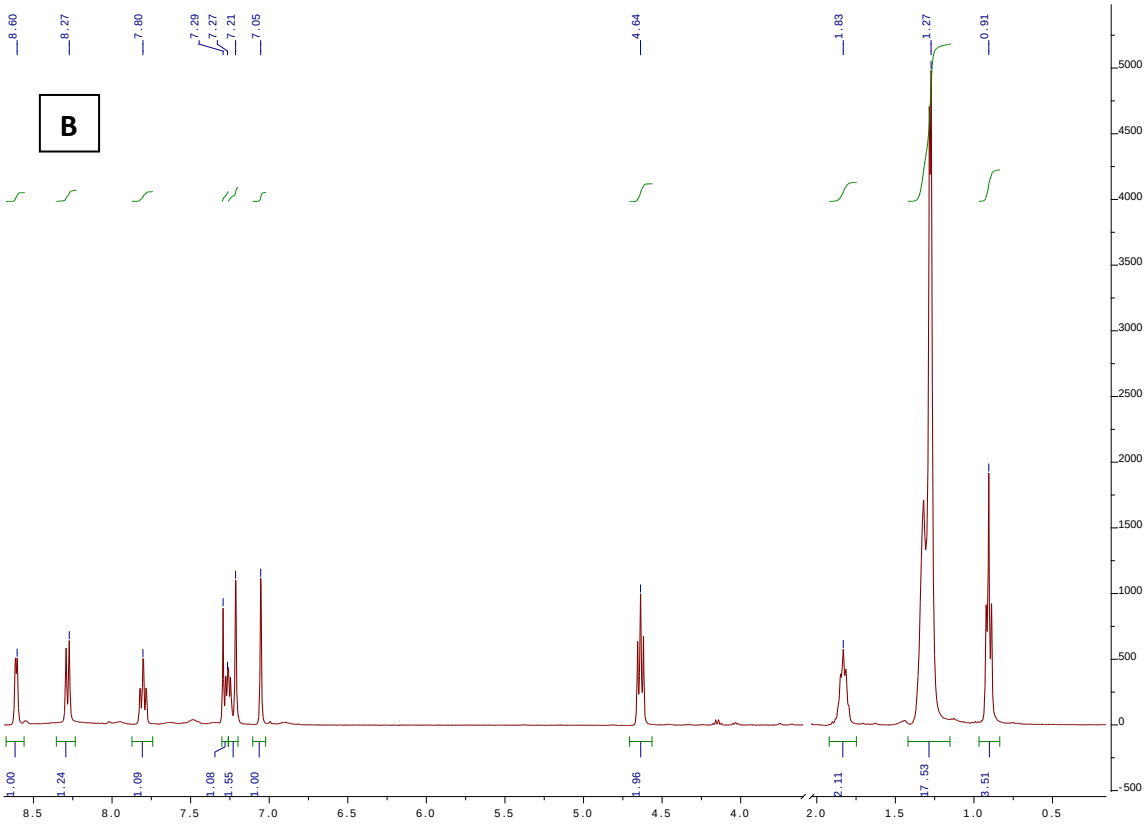
B
8.60
8.27
7.80
7.29
7.27
7.21
7.05
4.64
1.83
1.27
0.91
1.00
1.24
1.09
1.08
1.55
1.00
1.96
2.11
17.53
3.51

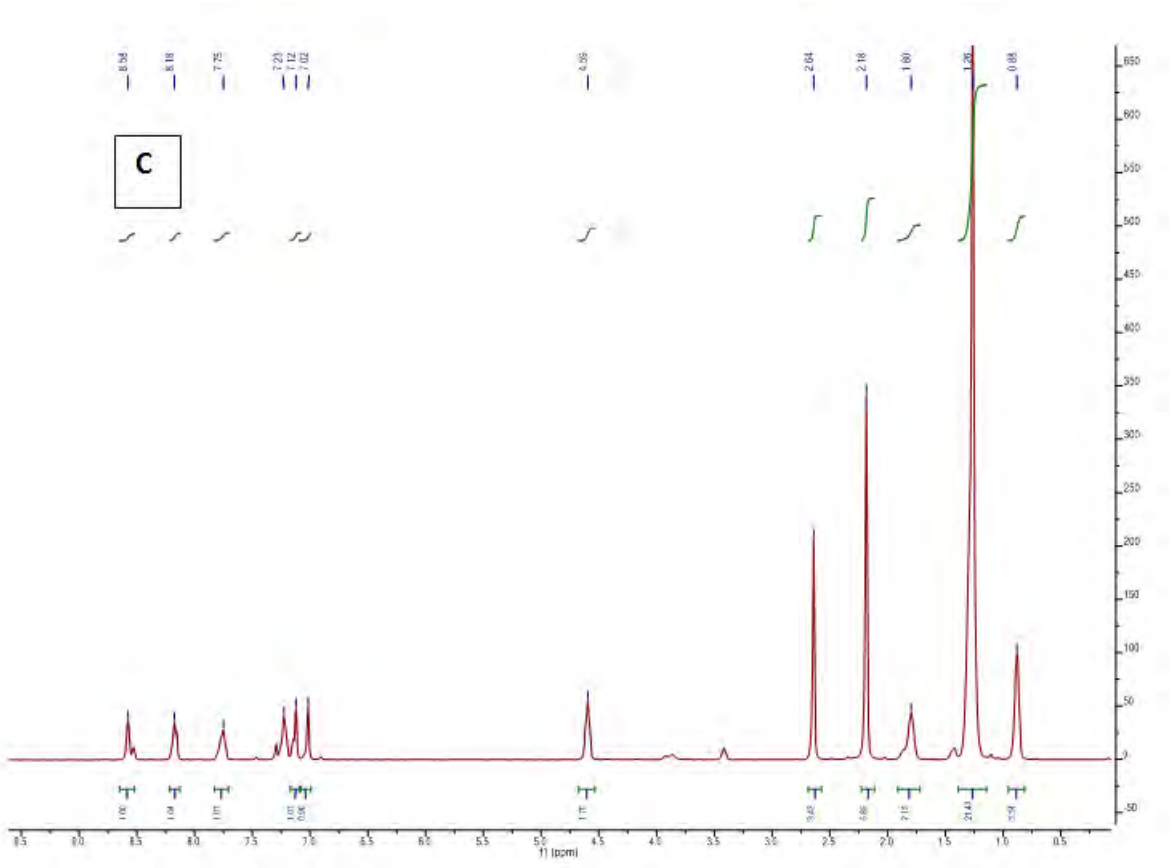

Figure 4.3: The ^{1}H NMR spectra of (a) 1-Heptyl-2,2′-pyridylimidazole, (b) 1-octyl-2,2′-pyridylimidazole and (c) 1-decyl-2,2′-pyridylimidazole respectively

4.3.2 Extraction studies

These studies were carried out in dilute sulfate solutions as well as dilute sulfate/chloride solutions to define optimal conditions for nickel specificity. The subsequent studies involved the use of a synthetic mixture of the metals in dilute sulfate and dilute sulfate/chloride media, as well as the investigation of the effect of the higher sulfate concentration. The scrubbing and stripping steps were also carried out to remove the co-extracted Cu^{2+} and Co^{2+} ions respectively in order to obtainnickel in a pure form.

In these studies, the conditions for the extraction of nickel were optimised through investigating the requisite concentration of the extractant, the concentration of the synergist (DNNSA), the necessary alkyl chain substituent on imidazole, and the effect of pH.

(a) Effect of the extractant concentration

Figure 4.4 shows the effect of various mole ratios of Ni:OPIM examined in the range of 1:15 to 1.45 on n ickel extraction. It is obvious from these curves, and the corresponding data on Table 4.1 that the steepest of all the curves is 1:25. This curve unlike others also shows a left leg that would allow for the back extraction of nickel. For these reasons this metal:extractant molar ratio was chosen for the subsequent studies.

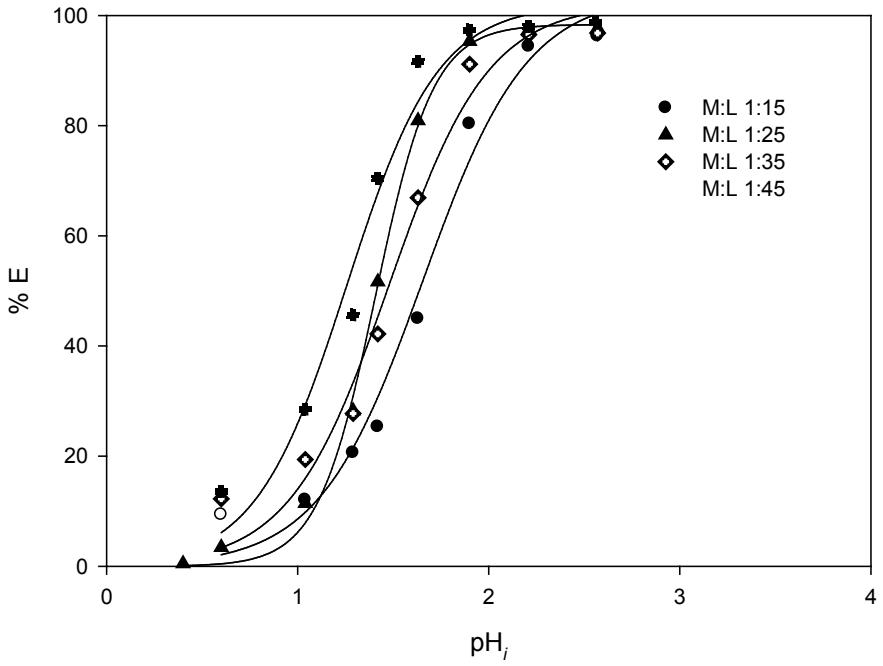

Figure 4.4: A plot of %E vs initial pH of 0.001 M nickel extracted from dilute sulfate medium with M:L ratios, 1:15, 1:25:, 1:35, 1:45 (Ni:OPIM) in 80% 2-octanol/Shellsol 2325

Table 4.1: Data for %E vs initial and the equilibrium pH of 0.001 M nickel extracted from dilute sulfate medium with M:L ratios, 1:15, 1:25:, 1:35, 1:45 (Ni:OPIM) in 80% 2-octanol/Shellsol 2325.

Ni^{2+}:OPIM (1:15)									
pH_i	0.60	1.04	1.29	1.42	1.49	1.90	2.21	2.57	
pH_e	0.62	1.06	1.31	1.43	1.50	1.86	2.21	2.47	
% E	9.36	12.04	20.60	25.31	44.95	80.32	94.36	96.27	
Ni^{2+}: OPIM (1:25)									
pH_i	0.40	0.60	1.04	1.29	1.42	1.63	1.90	2.21	2.57
pH_e	0.47	0.65	1.07	1.34	1.52	1.70	2.10	2.30	2.64
% E	0.50	3.46	11.45	28.24	51.67	80.94	95.33	97.48	97.68
Ni^{2+}: OPIM (1:35)									
pH_i	0.60	1.05	1.29	1.42	1.63	1.90	2.21	2.57	
pH_e	0.65	1.08	1.37	1.49	1.73	1.95	2.32	2.67	
% E	12.25	19.41	27.75	42.22	66.95	91.18	96.55	96.82	
Ni^{2+}: OPIM (1:45)									
pH_i	0.68	1.04	1.29	1.42	1.63	1.90	2.21	2.57	
pH_e	0.68	1.09	1.42	1.57	1.77	1.98	2.30	2.69	
% E	13.57	28.53	45.62	70.38	91.65	97.37	98.03	98.70	

(b) Effect of DNNSA as a synergist on the extraction of nickel

The involvement of DNNSA as a synergist has proven to be vital to this extraction method since there was very low extraction efficiency observed in its absence (Figure 4.5), and this could be attributed to the fact that sulfate ions do not readily phase-transfer the cationic complexes formed in the extraction system from the aqueous to the organic layer.[8] The presence of DNNSA, which is a bulky organic acid with a very low pK_a, provides significant ion pairing with the cationic complex species thus eliminating the hindrance of the sulfate ion.

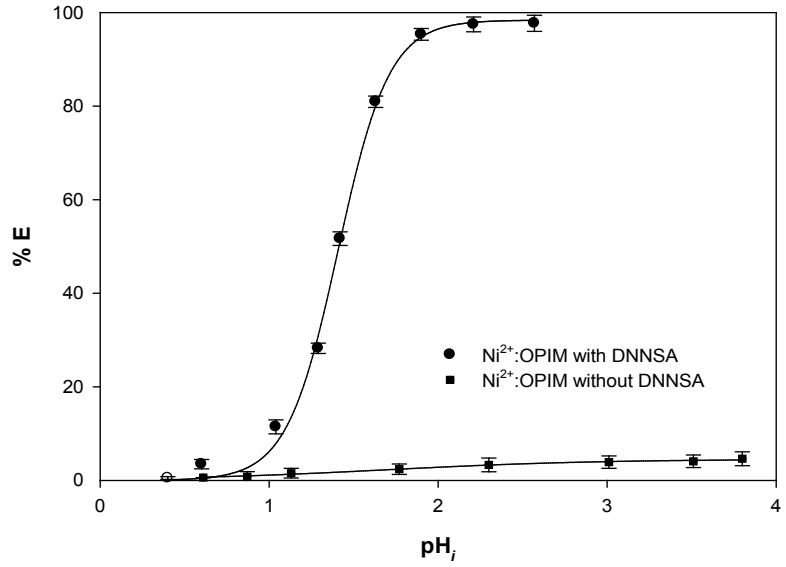

Figure 4.5: A plot of %E vs initial pH in the extraction of 0.001 M nickel from dilute sulfate medium with OPIM at a M:L molar ratio of 1:25 in the absence of DNNSA, and with 0.015 M DNNSA in 80% 2-octanol/Shellsol 2325

Table 4.2: Data for %E vs initial and the equilibrium pH for the extraction of 0.001M nickel from dilute sulfate medium with OPIM at a M:L molar ratio of 1:25 in the absence of DNNSA, and with 0.015 M DNNSA in 80% 2-octanol/Shellsol 2325.

%E Ni^{2+} with DNNSA								
pH$_i$	0.40	0.60	1.29	1.29	1.42	1.63	1.90	2.21
pH$_e$	0.39	0.58	1.31	1.18	1.34	1.56	1.77	2.12
% E	0.50	3.46	11.45	28.24	51.67	80.94	95.33	97.48
%E Ni^{2+}withoutDNNSA								
pH$_i$	0.60	0.87	1.13	1.77	2.30	3.01	3.51	3.80
pH$_e$	0.62	0.88	1.14	1.77	2.29	2.29	3.49	3.79
% E	0.59	0.80	1.55	2.40	3.33	3.33	4.08	4.63

This tentative explanation could be illustrated by considering the following chemical equilibria that are possible under the pH conditions employed with these two extractants:

$$OPIM + H^+ + HSO_4^- \rightleftharpoons (OPIMH^+)(HSO_4^-) \quad (39)$$

$$OPIM + 2H^+ + SO_4^{2-} \rightleftharpoons (OPIMH)_2SO_4 \quad (40)$$

$$OPIM + H^+ + A^- \rightleftharpoons (OPIMH^+)(A^-)\ (A^- = DNNSA) \quad (41)$$

$$Ni^{2+} + xOPIM + 2(OPIMH^+)(HSO_4^-) \rightleftharpoons [Ni(OPIM)_{(x+2)}](HSO_4)_2 + 2H^+ \quad (42)$$

$$Ni^{2+} + xOPIM + (OPIMH)_2SO_4 \rightleftharpoons [Ni(OPIM)_{(x+2)}]SO_4 + 2H^+ \quad (43)$$

$$Ni^{2+} + xOPIM + 2(OPIMH^+)(A^-) \rightleftharpoons [Ni(OPIM)_{(x+2)}]A_2 + 2H^+ \quad (44)$$

Equations 39 and 40 illustrate the functioning chemistry in the absence of DNNSA, while equation 44 depicts the loading of the nickel ions in the presence of DNNSA. The low pK_a of DNNSA and its bulky nature ensures that it acts as a non-coordinating ion pairing agent and an organic compatible anion respectively, thus facilitating an effective transfer of metals ions.

(c) Effect of the synergist concentration on extraction of nickel

The concentration of the synergist (DNNSA), bearing in mind its role as an ion pairing agent for the metal cationic metal ion complexes was also investigated. Table 4.3 gives the percent extraction as a function of pH which is further illustrated with the plot in Figure 4.6.

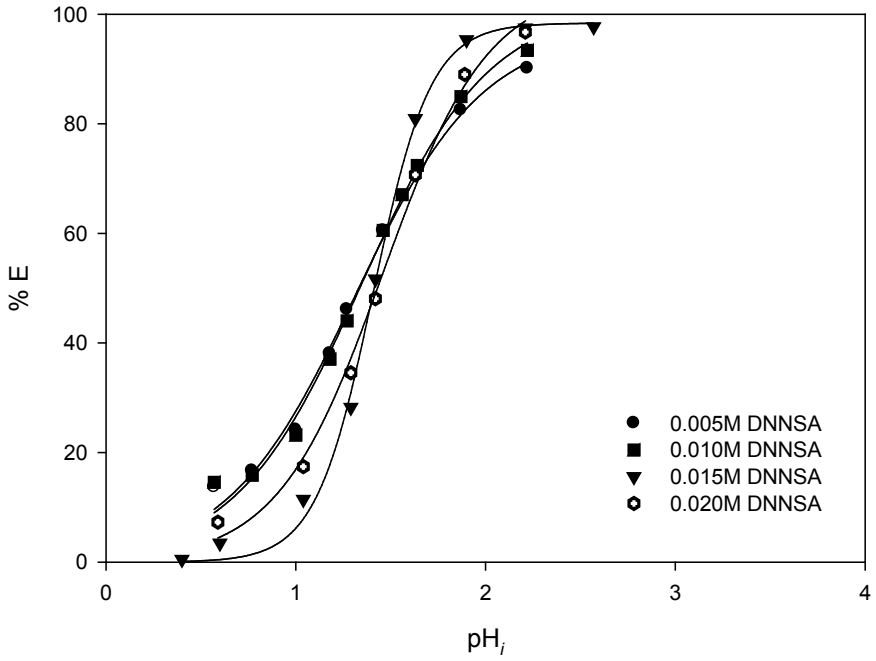

Figure 4.6: A plot of %E vs initial pH of 0.001 M nickel extracted from dilute sulfate medium with varying concentration of DNNSA as a synergist in 80% 2-octanol/Shellsol 2325.

Table 4.3: Data for %E vs initial and the equilibrium pH of nickel from dilute sulfate medium with DNNSA concentration of 0.005 M, 0.010 M, 0.015 M and 0.02 M of Ni:OPIM (1:25) in 80% 2-octanol/Shellsol 2325.

% E 0.005M DNNSA									
pH_i	0.57	0.77	1.00	1.18	1.27	1.49	1.87	2.22	
pH_e	0.59	0.78	1.01	1.87	1.27	1.50	1.87	2.22	
% E	13.71	16.67	24.14	38.06	46.11	60.50	82.49	90.12	
% E 0.010M DNNSA									
pH_i	0.57	0.77	1.00	1.18	1.27	1.46	1.56	1.64	1.87
pH_e	0.60	0.79	1.03	1.21	1.30	1.48	1.57	1.66	1.90
% E	14.57	15.87	23.19	37.04	44.04	60.55	67.07	72.42	84.98
% E 0.015 M DNNSA									
pH_i	0.40	0.60	1.04	1.29	1.42	1.63	1.90	2.21	
pH_e	0.42	0.61	1,05	1.29	1.42	1.63	1.90	2.21	
% E	0.50	3,45	11.45	28.25	51.67	80.94	95.33	97.48	
% E 0.02 M DNNSA									
pH_i	0.59	1.04	1.29	1.42	1.63	1.89	2.21	2.25	
pH_e	0.55	1.07	1.30	1.43	1.63	1.88	2.16	2.20	
% E	7.29	17.42	34.56	48.09	70.70	89.01	96.75	98.07	

The DNNSA on its own, however, does not show selectivity between metal ions since there is no separation observed as a function of pH with this extractant as reported in a patent by du Preez,[11] and as shown in chapter 3 (section 3.3.2).This necessitates the use of a ligand which has been carefully designed to discriminate between the metals ions *via* the bonding preferences with respect to coordination numbers, stereochemistry and type of bonding involved. This effect has been demonstrated in the separation of nickel and cobalt despite their similar coordination chemistry.[12]

(d) Effect of the diluent/modifier ratio on extraction of nickel

The role of the interaction of the diluents and the modifier in the extraction system of OPIM is well revealed in the plots in Figure 4.7. Neither the 100% diluents nor the 100% modifier gave satisfactory extraction efficiency as compared with 80% 2-octanol and 20% Shellsol. The left legs of all other curves are pushed further into the stripping region and some curves are not as steep as that of 80% 2-octanol and 20% Shellsol. Thus the back extraction may not be efficiently achieved. It could be deduced therefore that the 80% 2-octanol and 20% Shellsol plays the expected role of enhancing loading efficiency and avoidance of third phase in this system.

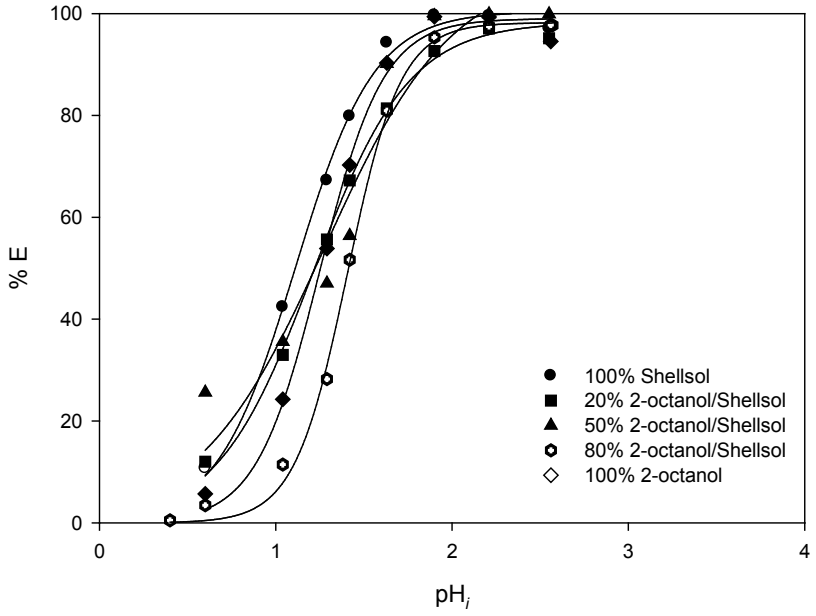

Figure 4.7: A plot of %E vs initial pH in the extraction of 0.001 M nickel from dilute sulfate medium with OPIM at a M:L molar ratio of 1:25 and 0.015 M DNNSA, with varying ratio of 2-octanol/Shellsol 2325

Table 4.4: Data for %E vs initial and the equilibrium pH of 0.001 M nickel from dilute sulfate medium with OPIM at a M:L molar ratio of 1:25 and 0.015 M DNNSA, with varying ratio of 2-octanol/Shellsol 2325.

100 % Shellsol								
pH_i	0.60	1.04	1.29	1.42	1.63	1.90	2.21	2.55
pH_e	0.59	0.65	1.06	1.41	1.56	1.91	2.36	2.03
% E	10.71	42.38	67.21	79.85	94.28	99.68	99.54	97.08
20% 2-octanol/ 80% Shellsol								
pH_i	0.60	1.04	1.29	1.42	1.63	1.90	2.21	2.55
pH_e	0.70	1.38	2.49	2.77	2.99	3.31	3.65	3.88
% E	12.02	32.98	55.66	67.24	81.38	92.65	97.07	95.17
50% 2-octanol/ 50% Shellsol								
pH_i	0.60	1.04	1.29	1.42	1.63	1.90	2.21	2.55
pH_e	0.29	0.65	1.06	1.41	1.46	1.91	2.36	2.03
% E	25.62	35.57	47.04	56.38	90.16	99.53	99.89	99.91
80% 2-octanol/ 20% Shellsol								
pH_i	0.40	0.60	1.04	1.29	1.42	1.63	1.90	2.21
pH_e	0.75	1.38	2.49	2.77	2.99	3.31	3.65	3.88
% E	0.50	3.46	11.45	28.24	51.67	80.94	95.33	97.48
100 % 2-octanol								
pH_i	0.60	1.04	1.29	1.42	1.63	1.90	2.21	
pH_e	0.39	0.65	1.06	1.41	1.46	1.91	2.36	
% E	5.67	24.26	53.86	70.26	90.29	99.33	99.39	

(e) Effect of the length of the alkyl chain

The optimised conditions with respect to the concentrations of the extractant and DNNSA were 0.025 M and 0. 015 M respectively. The extraction efficiencies pertaining to the effect of the alkyl substituent are presented in Figure 4.8. It seems, from this investigation, that the decyl group gives the best extraction as evidenced by the steepness of the curve indicating the definitive loading range of the extractant.

However, a later investigation to achieve separation between nickel and cobalt suggests that the octyl group to be more appropriate (Figure 4.9).

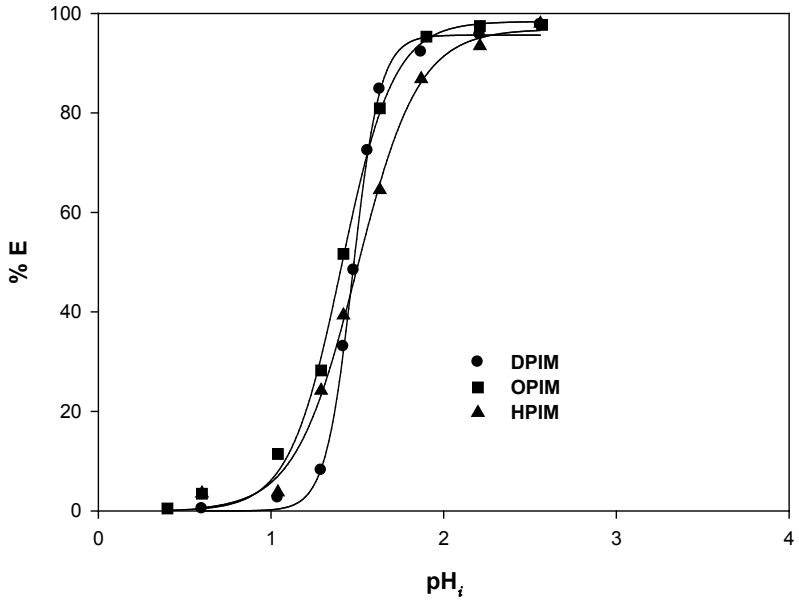

Figure 4.8: A plot of %E vs initial pH of 0.001M nickel extracted from dilute sulfate medium with DPIM, OPIM and HPIM (at Ni:L ratios of 1:25), and 0.015 M DNNSA in 80% 2-octanol/Shellsol 2325

Table 4.5: Data for the extraction of nickel from dilute sulfate medium with DPIM, OPIM and HPIM concentration of Ni:OPIM (1:25) and 0.015 M DNNSA in 80% 2-octanol/Shellsol 2325.

%E Ni^{2+} (DPIM)								
pH_i	0.60	1.04	1.29	1.42	1.48	1.56	1.63	1.87
pH_e	0.56	1.00	1.26	1.39	1.47	1.54	1.62	1.86
% E	0.43	2.65	8.17	33.04	48.39	72.39	84.77	92.26
%E Ni^{2+} OPIM								
pH_i	0.40	0.60	1.04	1.29	1.42	1.63	1.90	2.21
pH_e	0.38	0.58	1.00	1.25	1.38	1.57	1.87	2.07
% E	0.82	3.46	11.45	28.24	51.67	80.94	95.33	97.48
%E Ni^{2+} HPIM								
pH_i	0.60	1.04	1.29	1.42	1.63	1.87	2.21	2.56
pH_e	0.59	1.03	1.28	1.43	1.65	1.94	2.29	2.68
% E	3.63	3.77	24.19	39.33	64.53	86.85	2.56	97.98

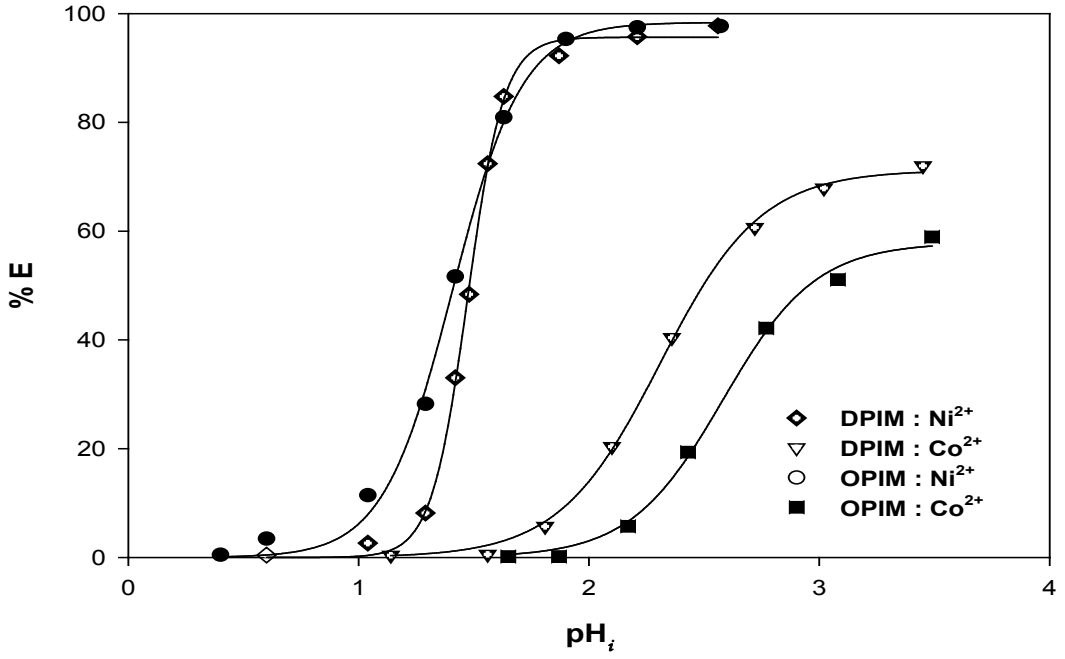

Figure 4.9: A plot of %E vs initial pH for the separation of 0.001 M nickel from equimolar concentration of cobalt with DPIM and OPIM, and 0.015 M DNNSA in 80% 2-octanol/Shellsol 2325 from dilute sulfate medium

A $\Delta pH_{½}$ value ≈ 1.6 was achieved in Ni/Co separation with OPIM as depicted in Figure 4.9 and only $\Delta pH_{½} \approx 1.1$ for DPIM, intimating that OPIM is better at tuning pH-metric selectivity in this system.

Table 4.6: Data for the extraction of equimolar concentration of nickel and cobalt with DPIM and OPIM, and 0.015 M DNNSA in 80% 2-octanol/Shellsol 2325from dilute sulfate medium.

%E Ni (DPIM)								
pH_i	0.60	1.04	1.29	1.42	1.48	1.56	1.63	1.87
pH_e	0.56	1.00	1.26	1.39	1.47	1.54	1.62	1.86
% E	0.43	2.65	8.17	33.04	48.39	72.39	84.77	92.26
%E Co (DPIM)								
pH_i	1.14	1.56	1.81	2.10	2.36	2.72	3.02	3.45
pH_e	1.15	1.58	1.81	2.12	2.33	2.50	2.60	2.67
% E	0.42	0.59	5.72	20.39	40.45	60.68	67.93	72.02
%E Ni (OPIM)								
pH_i	0.40	0.60	1.04	1.29	1.42	1.63	1.90	2.21
pH_e	0.38	0.58	1.00	1.25	1.38	1.57	1.87	2.07
% E	0.50	3.46	11.45	28.24	51.67	8.94	95.33	97.48
%E Co (OPIM)								
pH_i	1.65	1.87	2.17	2.43	2.77	3.08	3.49	
pH_e	1.69	1.89	2.14	2.27	2.42	3.58	3.66	
% E	0.16	0.16	5.71	19.36	42.16	51.07	58.92	

(f) Separation of nickel from other base metals with OPIM and DNNSA

The extraction patterns of the other metal ions typically present in a l each concentrate including Cu^{2+}, Fe^{2+}, Zn^{2+}, Fe^{3+}, Mn^{2+}, Mg^{2+}, Cd^{2+} and Ca^{2+} were investigated under the conditions that were optimized for the separation of nickel and cobalt. The results are presented in Table 4.7 as well as Figure 4.10. Most interestingly; there is a clear rejection of the hard ions (Fe^{3+}, Mn^{2+} and Ca^{2+}) in the pH range under investigation which concurs with our suggestion on t he bonding

nature of the aromatic nitrogenous ligands. The position of the copper extraction curve is rather surprising owing to the relatively higher acidic character of this metal ion which should render it reactive at the lower pH region thereby facilitating high extraction efficiencies. This anomaly could either be due to stability considerations, stereochemical preferences or dissimilar kinetics of complexation with pyridylimidazole when compared with nickel. The same line of thought can be inferred for the nickel and cobalt separation.

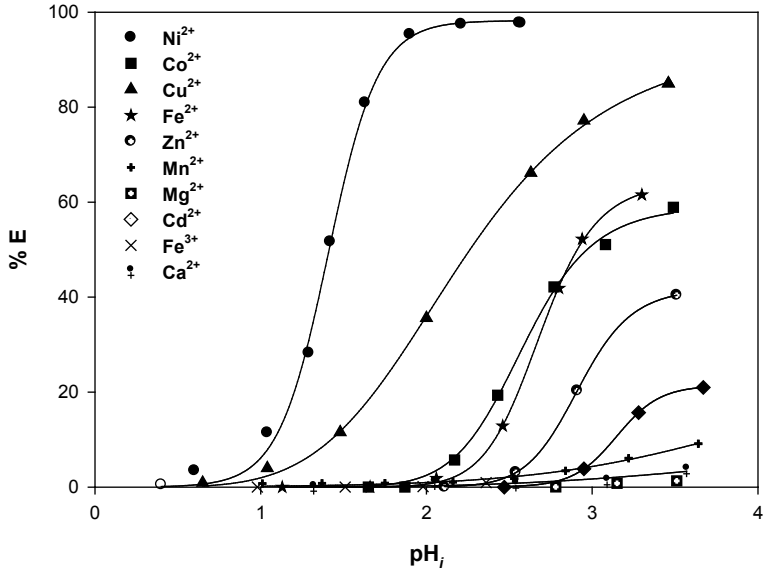

Figure 4.10: A plot of %E vs initial pH of equimolar concentration (0.001 M) of Ni^{2+}, Co^{2+}, Cu^{2+}, Fe^{2+}, Zn^{2+}, Fe^{3+}, Mn^{2+}, Mg^{2+}, Cd^{2+}, and Ca^{2+} extracted with OPIM (at M:L ratio of 1:25) and 0.015 M DNNSA in 80% 2-octanol/Shellsol 2325from dilute sulfate medium

Table 4.7: Data for %E vs initial pH of equimolar concentrations (0.001 M) of Ni^{2+}, Co^{2+}, Cu^{2+}, Fe^{2+}, Zn^{2+}, Fe^{3+}, Mn^{2+}, Mg^{2+}, Cd^{2+}, and Ca^{2+} extracted with OPIM at M:L ratio (1:25) and 0.015 M DNNSA in 80% 2-octanol/Shellsol 2325 from sulfate medium.

% E Ni^{2+}								
pH_i	0.40	0.60	1.04	1.29	1.63	1.90	2.21	2.57
pH_e	0.59	0.78	1.01	1.20	1.27	1.46	1.56	1.64
% E	0.50	3.46	11.45	28.24	80.94	95.33	97.48	97.69
% E Co^{2+}								
pH_i	1.65	1.87	2.17	2.43	2.77	3.08	3.49	
pH_e	1.23	1.33	1.87	2.17	2.43	2.77	3.08	
% E	0.02	0.02	5.71	19.38	42.16	51.07	58.92	
% E Cu^{2+}								
pH_i	0.65	1.04	1.48	2.00	2.63	2.95	1.13	
pH_e	0.62	0.80	1.02	1.50	2.09	2.69	2.95	
% E	0.91	3.99	11.57	35.61	66.18	77.18	0.00	
% E Fe^{2+}								
pH_i	1.13	1.66	2.06	2.46	2.80	2.94	3.30	
pH_e	1.15	1.69	2.05	2.16	2.85	2.87	2.90	
% E	0.00	0.06	1.85	12.87	41.87	52.24	61.54	
% E Zn^{2+}								
pH_i	0.51	1.02	1.44	1.83	2.11	2.54	2.91	
pH_e	0.76	1.05	1.47	1.88	2.25	2.81	3.22	
% E	0.00	0.00	0.00	0.00	0.00	3.08	20.28	
% E Mn^{2+}								
pH_i	1.01	1.37	1.75	2.16	2.53	2.84	3.22	
pH_e	1.02	1.40	1.79	2.30	2.74	3.16	3.57	
% E	0.74	0.80	0.84	1.05	1.79	3.42	6.09	
% E Mg^{2+}								
pH_i	0.52	1.04	1.57	2.12	2.44	2.78	3.15	
pH_e	0.54	1.06	1.60	2.34	2.66	3.10	3.50	
% E	0.00	0.00	0.00	0.00	0.04	0.83	1.31	
% E Cd^{2+}								
pH_i	0.46	0.80	1.21	1.59	1.98	2.47	2.95	
pH_e	0.49	0.86	1.28	1.60	2.05	2.65	3.13	
% E	0.00	0.00	0.00	0.00	3.84	15.69	20.99	
% E Fe^{3+}								
pH_i	0.98	1.51	1.98	2.36				
pH_e	0.85	1.15	1.72	2.19				
% E	0.00	0.00	0.09	0.94				
% E Ca^{2+}								
pH_i	0.41	0.74	1.32	2.05	2.54	3.09	3.57	
pH_e	0.40	0.72	1.22	1.95	2.34	3.89	3.38	
% E	0.00	0.00	0.0	0.94	0.64	1.34	3.67	

A plot of the log D vs pH_e (Figure 4.8) suggests the following order of stabilization with this bidentate N-donor extractant; $Ni^{2+} > Cu^{2+} > Co^{2+} > Fe^{2+} > Zn^{2+} > Mn^{2+}$, and is not consistent with the Irving-Williams order[13] with respect to Cu^{2+} and Zn^{2+}. The stabilization in the Zn^{2+} system may be driven by a four coordinate geometry, and the effect of the π backbonding which is facilitated by the π-acid character of the imidazole and pyridyl rings which is absent in the high-spin Mn^{2+} bonding. As mentioned above, the Cu^{2+} irregularity may be from stereochemical considerations or of kinetic origin. The extraction order of Ni^{2+}, Co^{2+} and Fe^{2+} was as expected as has been observed with this binding moiety in a chloride medium for Ni^{2+} and Co^{2+}.[14] It must be borne in mind, however, that there are a number of equilibria involved in these systems which complicate the chemistry immensely, and that the observed effects may be a combination of several competing equilibria. It must be said, however, that these subtle coordination preferences can seemingly lead to a generalised behaviour of these metals in these extraction systems and provide a conceptual framework in the development of robust methods for their separation that relies purely on the simple principles of coordination chemistry.

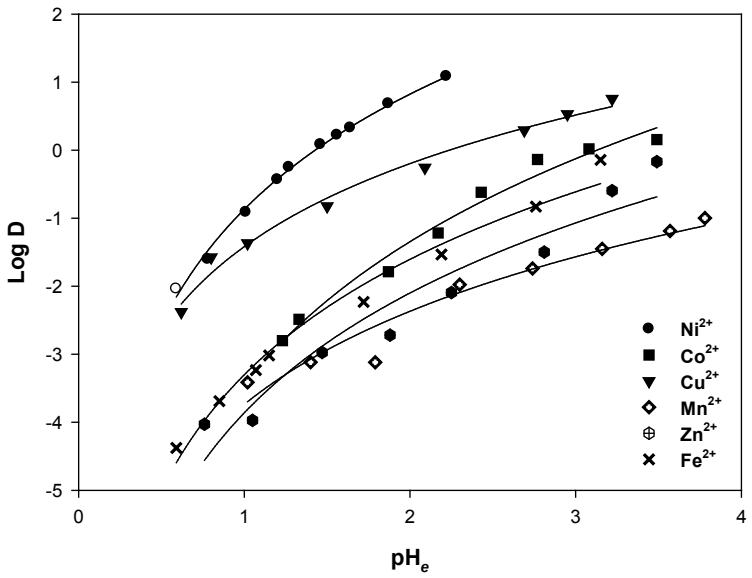

Figure 4.11: A plot of log D vs equilibrium pH for the extraction of 0.001 M M^{2+} (M = Ni^{2+}, Co^{2+}, Cu^{2+}, Mn^{2+}, Zn^{2+} and Fe^{2+}) with OPIM and 0.015 M DNNSA from sulfate medium

Table 4.8: Data for log D vs equilibrium pH for the extraction of 0.001 M Ni^{2+} from equimolar concentration of Co^{2+}, Cu^{2+}, Mn^{2+}, Zn^{2+} and Fe^{3+} with OPIM and 0.015 M DNNSA from sulfate medium.

% E Ni^{2+}								
pH_i	0.40	0.60	1.04	1.29	1.63	1.90	2.21	2.57
pH_e	0.59	0.78	1.01	1.20	1.27	1.46	1.56	1.64
LogD	-2.03	-1.60	-0.91	-0.43	-0.25	0.08	0.22	0.33
% E Co^{2+}								
pH_i	1.65	1.87	2.17	2.43	2.77	3.08	3.49	
pH_e	1.23	1.33	1.87	2.17	2.43	2.77	3.08	
LogD	-2.80	-2.49	-1.78	-1.21	-0.62	-0.14	0.019	
% E Cu^{2+}								
pH_i	0.65	1.04	1.48	2.00	2.63	2.95	1.13	
pH_e	0.62	0.80	1.02	1.50	2.09	2.69	2.95	
LogD	-2.38	-1.57	-1.37	0.82	-0.26	0.29	0.53	
% E Mn^{2+}								
pH_i	1.01	1.37	1.75	2.16	2.53	2.84	3.22	
pH_e	1.02	1.40	1.79	2.30	2.74	3.16	3.57	
LogD	-3.41	-3.11	-3.12	-1.98	-1.74	-1.45	-1.18	
% E Zn^{2+}								
pH_i	0.51	1.02	1.44	1.83	2.11	2.54	2.91	3.31
pH_e	0.76	1.05	1.47	1.88	2.25	2.81	3.22	3.49
LogD	-4.03	-3.97	-2.97	-2.71	-2.09	-1.49	-0.59	-0.17
% E Fe^{3+}								
pH_i	0.98	1.51	1.98	2.36	2,45	2.51	2.89	3.10
pH_e	0.85	1.15	1.72	2.19	1.72	2.19	2.76	3.15
LogD	-4.38	-3.69	-3.23	-3.02	-2.23	-1.53	0.83	-0.14

(g) Extractions in dilute sulfate/chloride solutions

The effect of a dilute chloride medium in the extraction system detailed above was investigated and the results are presented in Table 4.9 and Figure 4.12. The extraction order remained the same. This is a clear indication that the chloride ions played no role in the extraction process, however, the effect could be somewhat different in concentrated chloride solutions and the probability of Zn^{2+}, Cd^{2+} and Co^{2+} extracting significantly at lower pH values as the tetrachloro species (MCl_4^{2-}) through ion pairing with the protonated ligand would be high.[15,1] This method gives confidence for the separation of nickel from Cu^{2+} and Co^{2+} in dilute chloride solutions at a pH ≤ 2.0, without interference from the other metal ions which are rejected in this pH range, especially the ferric ions.

These observations give the assurance that this chemistry can operate in a cocktail of these metals since the principles of the coordination chemistry should not be altered by the metal composition of the leach solution. This was supported through the investigation of the extraction efficiencies at a pH for optimal uptake of nickel and minimal loading of copper and cobalt, and lack of extraction of zinc, iron and manganese in the synthetic cocktail of the base metals (pH 1.8-2.0), and the results presented in Table 4.11 (Stage 1) are in agreement with the chemistry that is demonstrated in the extraction curves (Figures 4.10 and 4.12).

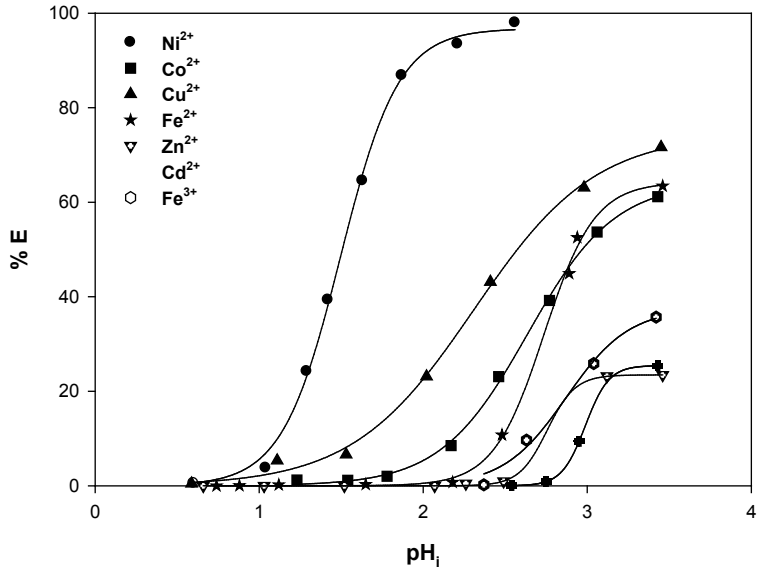

Figure 4.12: A plot of %E vs initial pH of equimolar concentrations (0.001 M) of Ni^{2+}, Co^{2+}, Cu^{2+}, Fe^{2+}, Zn^{2+}, Cd^{2+}, and Fe^{3+} extracted with OPIM (at M:L ratio 1:25) and 0.015 M DNNSA in 80% 2-octanol/Shellsol 2325 from a mixed sulfate/chloridemedium.

Table 4.9: Data for %E vs initial pH of equimolar concentrations (0.001 M) of Ni^{2+}, Co^{2+}, Cu^{2+}, Fe^{2+}, Zn^{2+}, Cd^{2+}, and Fe^{3+} extracted with OPIM at M:L ratio (1:25) and 0.015 M DNNSA in 80% 2-octanol/Shellsol 2325 from a mixed sulfate/chloridemedium.

% E Ni^{2+}								
pH_i	0.60	1.04	1.29	1.42	1.63	1.90	2.21	2.57
pH_e	0.54	0.75	1.07	1.12	1.27	1.52	1.93	2.34
% E	0.53	3.77	24.19	39.34	64.53	88.85	93.48	97.98
% E Co^{2+}								
pH_i	1.23	1.54	1.78	2.17	2.46	2.77	3.06	3.43
pH_e	1.24	1.58	1.85	2.28	2.58	2.78	2.91	3.01
% E	1.24	1.18	2.03	8.52	23.09	39.22	53.69	61.18
% E Cu^{2+}								
pH_i	0.59	1.11	1.53	2.02	2.41	2.98	3.45	
pH_e	0.49	1.12	1.55	2.07	2.45	2.84	3.03	
% E	0.46	5.34	6.62	23.13	43.15	63.10	71.66	
% E Fe^{2+}								
pH_i	0.74	0.88	1.12	1.65	2.18	2.48	2.89	3.46
pH_e	0.75	0.90	1.13	1.70	2.35	2.72	2.90	3.46
% E	0.00	0.03	0.21	0.31	0.74	10.75	44.93	63.44
% E Zn^{2+}								
pH_i	0.66	1.03	1.52	2.07	2.26	2.49	3.12	3.46
pH_e	0.88	1.05	1.54	2.09	2.35	2.58	3.22	3.49
% E	0.00	0.00	0.00	0.00	0.47	0.96	23.18	23.43
% E Fe^{3+}								
pH_i	0.83	1.13	1.36	1.62	2.03	2.37	2.63	3.04
pH_e	0.85	1.11	1.39	1.67	2.13	2.54	2.74	3.04
% E	0.00	0.0	0.0	0.00	0.21	9.67	25.89	35.68

(h) Extractions of nickel from a synthetic mixture of base metals

Studies for maximal uptake of Ni^{2+} in the pH range 1.8-2.0 and the minimal loading of the co-extracted metals (Cu^{2+} and Co^{2+}) were performed in a solution containing the three elements with the results shown in Table 4.10.

Table 4.10: Data for %E vs initial pH of equimolar concentrations (0.001 M) of Ni^{2+}, Co^{2+}, Cu^{2+} in the pH range 1.8-2.0.

pH	Ni^{2+}	Co^{2+}	Cu^{2+}
1.80	70.54	3.19	13.83
1.89	75.26	3.25	16.91
1.99	78.78	6.82	20.35

A solution of pH 1.89 was chosen on a consideration of the pH that would give a minimum number of extraction stages for an optimum extraction of Ni^{2+} and minimum extraction of the co-extracts ($Co^{2+}$and Cu^{2+}). A three stage counter-current batch extraction of nickel was carried out in order to separate it from a synthetic leach solution containing equimolar concentration (0.001 M) of Ni^{2+}, Co^{2+}, Cu^{2+}, Fe^{2+}, Zn^{2+} and Fe^{3+} at pH 1.89 with 0.025 M OPIM and 0.015 M DNNSA, and the results are shown in Table 4.11. A cumulative total of 99.01(±1.79) (ICP-OES) and 99.06(±1.39) (ICP-MS) of nickel was extracted, and 48.72(±0.24) (ICP-OES) and 45.06(±1.82) (ICP-MS), and 19.85(±0.28) (ICP-OES) and 18.06(±0.24) (ICP-MS) of copper and cobalt were co-extracted, respectively, from the initial concentrations. This necessitated a scrubbing stage to remove copper from the organic phase prior to the selective stripping of cobalt and nickel respectively from the loaded organic (L.O.) phase.

Table 4.11: The ICP-OES and ICP-MS data (%E) for the three stage counter-current batch extraction of Ni^{2+}, Cu^{2+}, Co^{2+}, Fe^{2+}, Zn^{2+}, Mn^{2+} and Fe^{3+} at an initial pH of 1.89 from the mixed metal ions solution with 0.025 M OPIM and 0.015 M DNNSA.

Stage of extraction	**1st**		**2nd**		**3rd**	
Method	ICP-OES	ICP-MS	ICPO-ES	ICP-MS	ICP-OES	ICP-MS
Ni^{2+}	78.78 (0.90)	79.79 (0.69)	95.30 (1.27)	95.87 (0.98)	99.01 (1.79)	99.06 (1.39)
Co^{2+}	6.82 (0.09)	6.66 (0.12)	13.05 (0.12)	12.82 (0.17)	19.85 (0.28)	18.06 (0.24)
Cu^{2+}	20.35 (0.12)	18.33(0.72)	35.56 (0.17)	33.30 (1.29)	48.72 (0.24)	45.06 (1.82)
Fe^{2+}	NE	NE	NE	NE	NE	NE
Zn^{2+}	NE	NE	NE	NE	NE	NE
Mn^{2+}	NE	NE	NE	NE	NE	NE
Fe^{3+}	NE	NE	NE	NE	NE	NE

NE = none or negligible extraction, SD are given in parenthesis

(i) Scrubbing and selective stripping

The results for the scrubbing and stripping are presented in Table 4.12. Copper was scrubbed off from the loaded organicphase in two stages with an ammonia/ammonium chloride buffer solution of pH ~ 8.5 at a v:v ratio of 1:1 to the tune of 99.29(±0.18). With this scrubbing step the final co-extracted copper content in the L.O. does not exceed 0.7%, and thus would provide high purity nickel in the final electrowinning step.

Figures 4.10 and 4.12 depict that Co^{2+} can be selectively stripped at pH 1.64 from the loaded organic phase after copper has been scrubbed off. This was achieved quantitatively at a s ingle stage to the level of 98.89(± 0.62) of the co-extracted

amount of cobalt ion. Lastly, the nickel content in the loaded organic phase was back-extracted at pH 0.32 to a satisfactory recovery of 94.05(±1.70) in a single stage. Agarwal *et al*.[16-18] observed from extensive studies that co-extraction, scrubbing and selective stripping of several metals is a more economical and attractive process compared with the selective extraction and stripping technique for individual metal ions. However, in this system it is envisaged that Cu^{2+} and Co^{2+} would be present in very low amounts in a leach solution of an essentially nickel ore.

Table 4.12: Data for the scrubbing of co-extracted Cu^{2+} with NH_3/NH_4Cl buffer at pH ~ 8.5 at a ratio of 1:1, and the selective stripping of Co^{2+} and Ni^{2+} with H_2SO_4 at pH 1.64 and 0.32, respectively, from the loaded organic (L.O.) phase.

Stage of Scrubbing	**%Ni^{2+}**	**%Co^{2+}**	**%Cu^{2+}**
1st	0.29(0.04)	0.53(0.09)	97.03(0.13)
2nd	0.43(0.06)	0.98(0.13)	99.29(0.18)
Selective stripping of Ni $^{2+}$and Co^{2+}			
Stripping pH	**%Ni^{2+}**	**%Co^{2+}**	
1.64	5.54(0.50)	98.89(0.62)	
0.32	94.05(1.70)	0.82(0.12)	

SD are given in parenthesis

(i) Extraction of nickel from a high sulfate medium

In a typical leach solution of an essentially nickel ore the highest metal ion concentration to sulfate ion concentration ratio is around 1:200. The investigation of the effect of high sulfate concentration under the optimised conditions for the uptake of nickel showed that the extraction was not adversely affected by the high sulfate content (Figure 4.12). The %E ~80% at pH 1.89 is consistent with what has been observed in dilute sulfate extractions (Figures 4.10 and 4.12), and the first extraction stage in Table 4.11. This once again suggests the non-coordinating nature of the

sulfate ion in this system and the effective ion pairing nature of DNNSA as discussed in section 4.3.2.

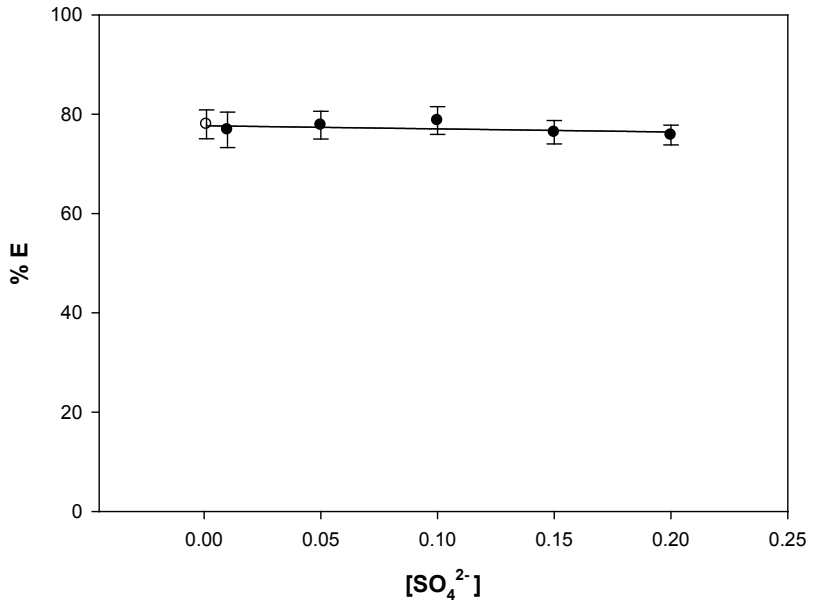

Figure 4.13: A plot of %E vs sulfate ion concentration in the extraction of Ni^{2+} at (0.001 M) with 0.025 M OPIM and 0.015 M DNNSA at pH=1.89

Table 4.13: Data for %E vs sulfate ion concentration in the extraction of Ni^{2+} with OPIM at M:L(1:25) ratio and 0.015 M DNNSA at pH=1.89

$[SO_4^{2-}]$	% E
0.001	87.98 (2.90)
0.005	87.96 (3.57)
0.0100	87.86 (2.79)
0.0500	87.81 (2.80)
0.1000	87.73 (2.40)
0.1500	86.36 (2.35)
0.2000	85.81 (1.98)

SD given in parenthesis

4.3.3 Solid state studies

In an attempt to gain insight into the nature of the extracted complex speciesthe solid state complexes with PIMH as the coordinating moiety to the metal ions Ni^{2+}, Cu^{2+}, Co^{2+} and Zn^{2+}, were prepared and isolated. It is acknowledged, however, that the isolated complexes may not be completely representative of the complex reaction equilibria that operate in the extraction system described but on the basis of the metal ions having a defined preference for this pyridylimidazole moiety the chemistry may be dominant to some extent since excess extractant amounts are used; hence the stereochemical aspects were investigated in the solid state. The data for the full characterization of the complexes has been given in section 4.2.

(a) The Infra-red spectroscopic characterization of the metal complexes

The ligand (Figure 4.14) displays an infrared stretching frequency at 1497 cm^{-1} which can be assigned to the azomethine (C=N) stretch[19], and the coordination of this moiety to the metals was evident from a shift of this stretch to lower frequencies (1489-1492 cm^{-1}).

Table 4.14: Selected Infrared peaks of PIMH and the metal complexes.

Ligand/Complex	Colour	$C=N_{(Py)}$ (cm^{-1})	$C=N_{(Im)}$ (cm^{-1})	N-H (cm^{-1})	SO_4^{2-} (cm^{-1})
PIMH	-	1557	1497	3361	-
$[Ni(PIMH)_2]SO_4.4H_2O.½EtOH$	Blue-green	1573	1492	3140	1078
$[Cu(PIMH)_2]SO_4.4H_2O.½EtOH$	Green	1569	1492	3159	1077
$[Co(PIMH)_2]SO_4.H_2O$	Pink	1571	1489	3142	1059
$[Zn(PIMH)_2]SO_4.H_2O$	White	1572	1490	3136	1050

The appearance of the band around 3140 cm^{-1} (Figures 4.14-4.18) in the spectra of the complexes suggests the protonated nature of the ligand (at the pyrole nitrogen) upon its coordination to the metal ions, and that the observed coordination should represent the same chemistry observed with the alkylated extractant, at least with

respect to the binding groups. The evidence of the non-coordinated nature of the sulfate ion is shown by the presence of the IR band that appears in the range 1050-1080 cm^{-1} in the spectra of the complexes, which is ascribed to the tetrahedral ion while the lowering of symmetry upon coordination (to C_{3v} or C_{2v} for monodentate and bidentate coordination respectively) would result in the splitting of this band.[20] The high conductivity values[21] also infer a cationic character to these complexes which again agrees with the non-coordinated nature of the sulfate ion. The microanalysis data (Table 4.15) suggested a 1:2 metal-to-ligand ratio for all the complexes.

Table 4.15: Microanalysis data of PIMH and the metal complexes.

Ligand/Complex	**% C** **Found(Calc)**	**% H** **Found(Calc)**	**% N** **Found(Calc)**	**% S** **Found(Calc)**
PIMH	66.08(66.19)	4.97(4.86)	29.11(28.95)	0.00
$[Ni(PIMH)_2]SO_4.4H_2O.½EtOH$	40.74(40.89)	4.80(4.89)	17.77(17.34)	3.33(3.31)
$[Cu(PIMH)_2]SO_4.4H_2O.½EtOH$	40.96(40.55)	4.46(4.68)	17.78(17.73)	3.47(3.38)
$[Co(PIMH)_2]SO_4.H_2O$	41.16(41.18)	3.59(3.48)	17.99(18.14)	6.89(6.92)
$[Zn(PIMH)_2]SO_4.H_2O$	40.96(40.91)	3.93(3.43)	17.97(17.89)	6.77(6.93)

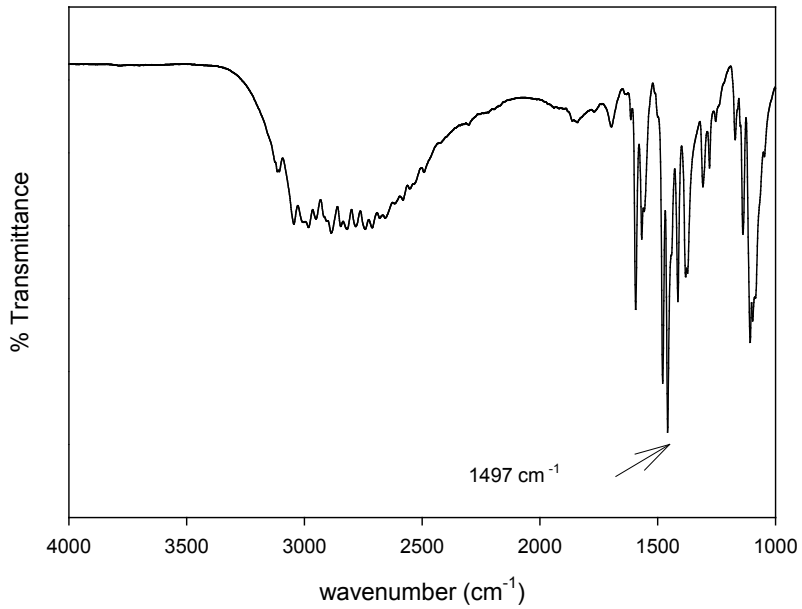

Figure 4.14: The IR spectrum of 2,2′-pyridyl-1H-imidazole (PIMH)

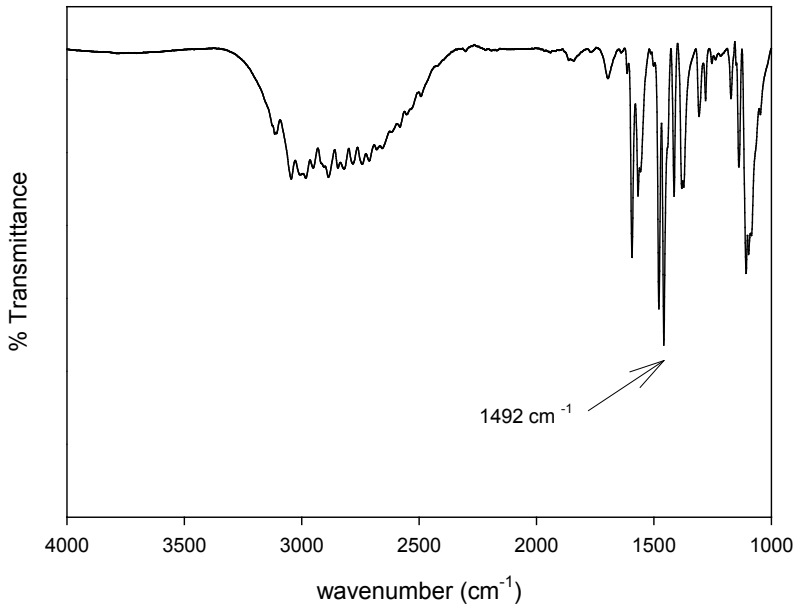

Figure 4.15: The IR spectrum of nickel complex of 2,2′-pyridyl-1H-imidazole $[Ni(PIMH)_2]SO_4.4H_2O.½EtOH$

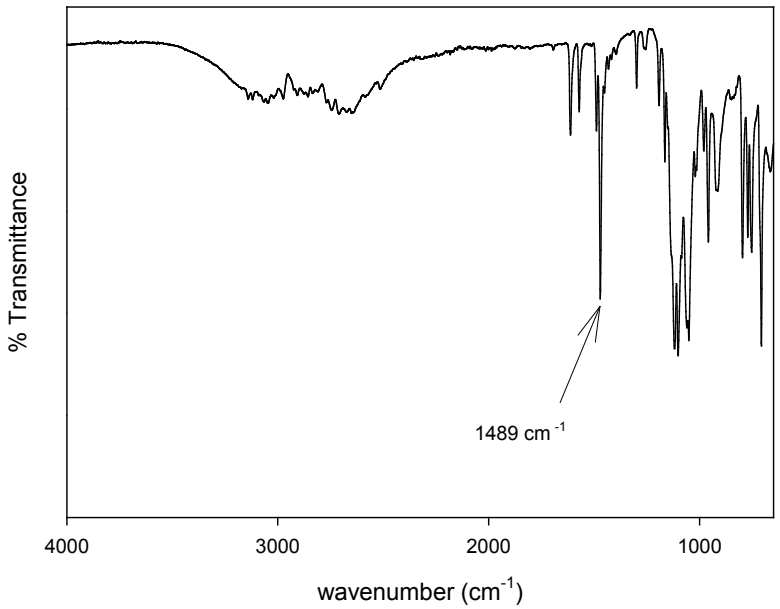

Figure 4.16: The IR spectrum of cobalt complex of 2,2′-pyridyl-1H-imidazole $[Co(PIMH)_2]SO_4.H_2O$

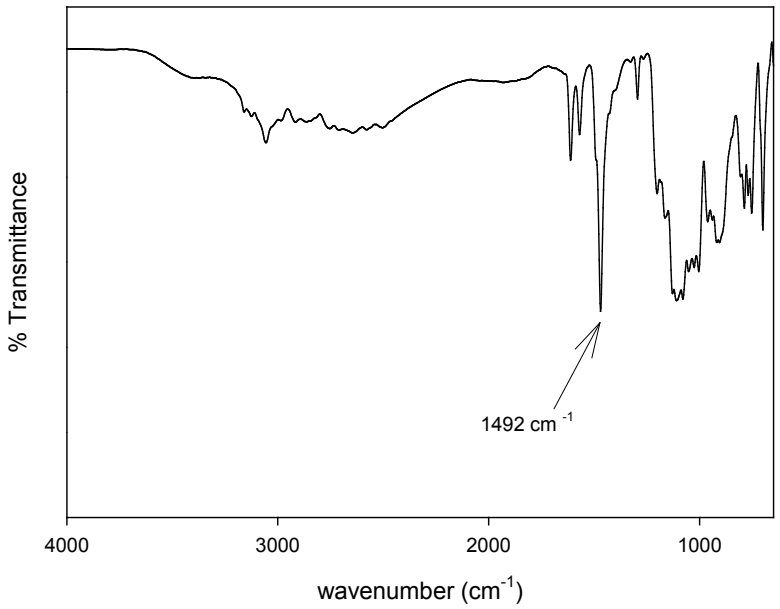

Figure 4.17: The IR spectrum of copper complex of 2,2′-pyridyl-1H-imidazole $[Cu(PIMH)_2]SO_4.4H_2O.½EtOH$

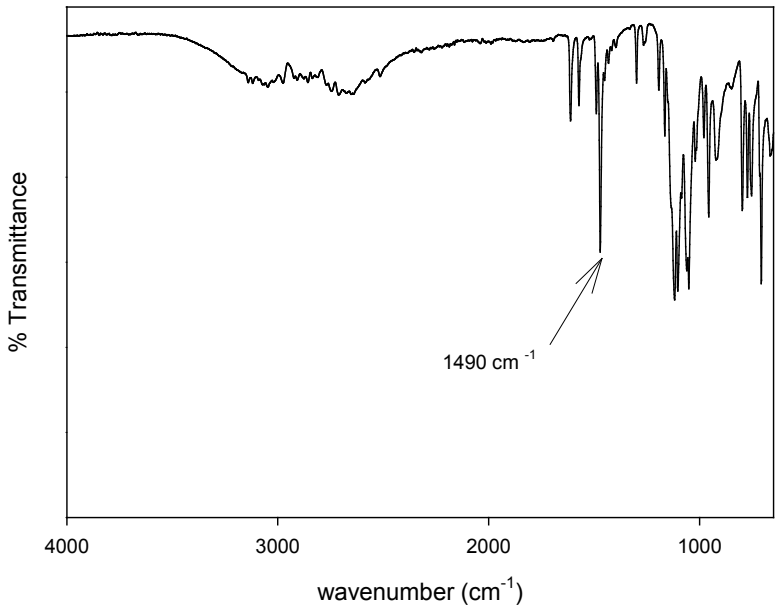

Figure 4.18: The IR spectrum of zinc complex of 2,2′-pyridyl-1H-imidazole $[Zn(PIMH)_2]SO_4.H_2O$

(b) Electronic spectroscopic characterisation of the metal complexes

The electronic absorption spectroscopy studies allowed for some insight to be gained into the possible stereochemistry of these complexes. The solid reflectance spectrum of the nickel complex contained two bands at 924 and 572 nm (Figure 4.19), these bands correspond to the $^3T_1(F) \rightarrow ^3T_2(F)$ $^3T_1(F) \rightarrow ^3A_2(F)$ respectively. The third transition, $^3A_{2g} \rightarrow ^3T_{1g}(P)$, may be masked by the intense intraligand transition between 300-400 nm (Figure 4.19). From this information, the geometry of the nickel complex is suggested to be tetrahedral, since a square planar nickel complex would be expected to have a band at 555–400 nm and a second, more intense band near 434–333 nm.[22,23] The reflectance spectrum of the cobalt(II) complex showed two bands at 1073 and 501 nm, and were ascribed to the $^4A_2 \rightarrow ^4T_2(F)$ and $^4A_2 \rightarrow ^4T_2(P)$ transitions. The observed ligand field transitions are characteristic of a tetrahedral geometry.[22,23] The spectrum of copper(II) complex showed one broad band around 800 nm which correspond to the $^2E \rightarrow ^2T_2$, consistent with a regular tetrahedral copper(II) complex in the absence of splitting due to spin

orbit coupling.[22,23] This lack of stereochemical preference removes this property as a determinant for the separations observed for these metal ions.

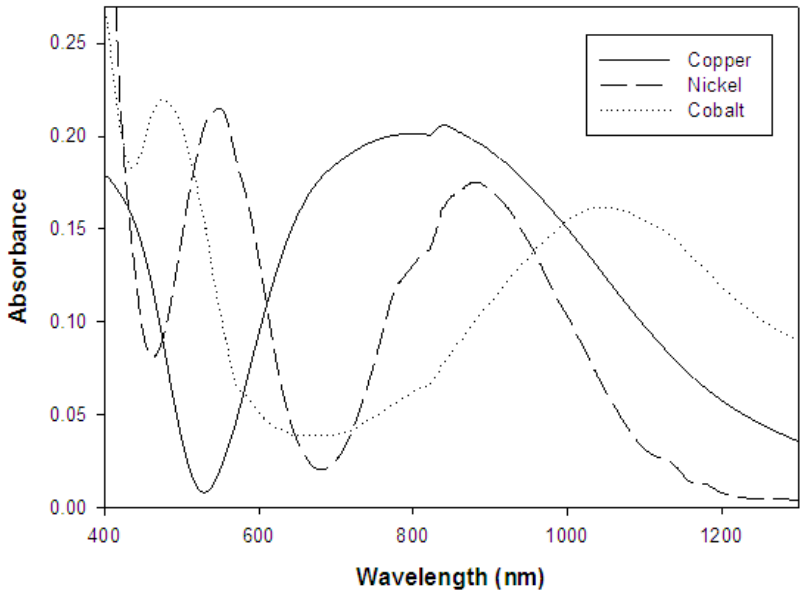

Figure 4.19: The solid reflectance spectra for nickel(II), cobalt(II) and copper(II) pyridylimidazole complexes

4.3.4 Solution studies

(a) Potentiometric titrations

The protonation (log *K*) and stability (log *β*) constants are listed in Tables 4.16 and 4.17 together with standard deviations. The ligand, 2,2′-pyridyl-1*H*-imidazole, exhibits a two-stage protonation process. The pyrole site in this ligand does not dissociate in the pH range measured, hence the data obtained can be viewed as being representative of the aqueous solution interactions of its alkylated derivative (extractant). The log K_1 and log K_2 values are 5.66(±0.04) and 1.23(±0.05) respectively. The model suggests that fraction of the ligand will be doubly protonated in highly acid solutions while the monoprotonated form suggests that the proton will be tightly held between the pyridyl and the imidazolyl nitrogenin both strongly and weakly acidic solutions. This p*K* value is intermediate between that of imidazole (6.95) and pyridine at (5.26),[24] and is closer to that of benzimidazole (5.49).[25]

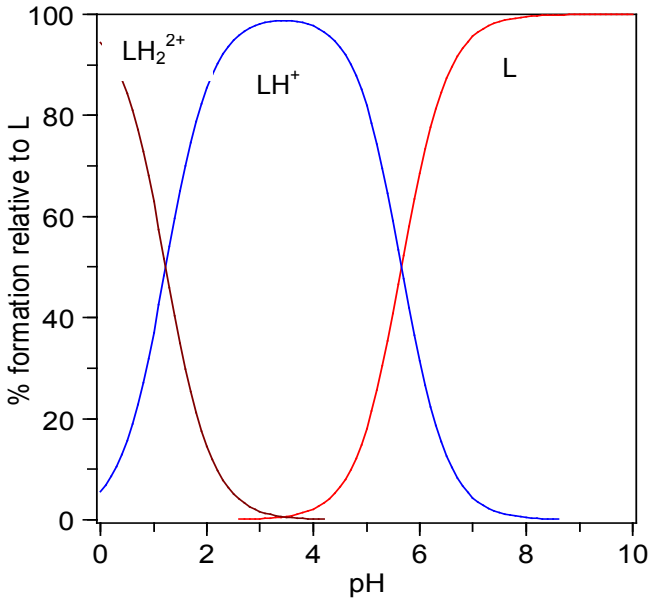

Figure 4.20: Protonation species distribution diagram for 2,2'-pyridylimidazole (PIMH)

The fitting of the protonation and the complexation models could be done to a certain level of satisfaction since enough data points were available for the solution in the refinement process without termination of the calculation (Figure 4.21), However, the sigma values (Table 4.16 and 4.17) were relatively high but this may be attributable to the ethanol/water system which had to be adopted due to the solubility limitations of PIMH in water.

Initially, it was suspected that the use of the metal(II) sulfate solutions complicated the equilibria due t o the involvement of the bisulfate ion hence the experiments werealso carried out in metal(II) chloride solutions. Since the high sigma values were also obtained, the solvent system was therefore deemed the cause for the high sigma values.

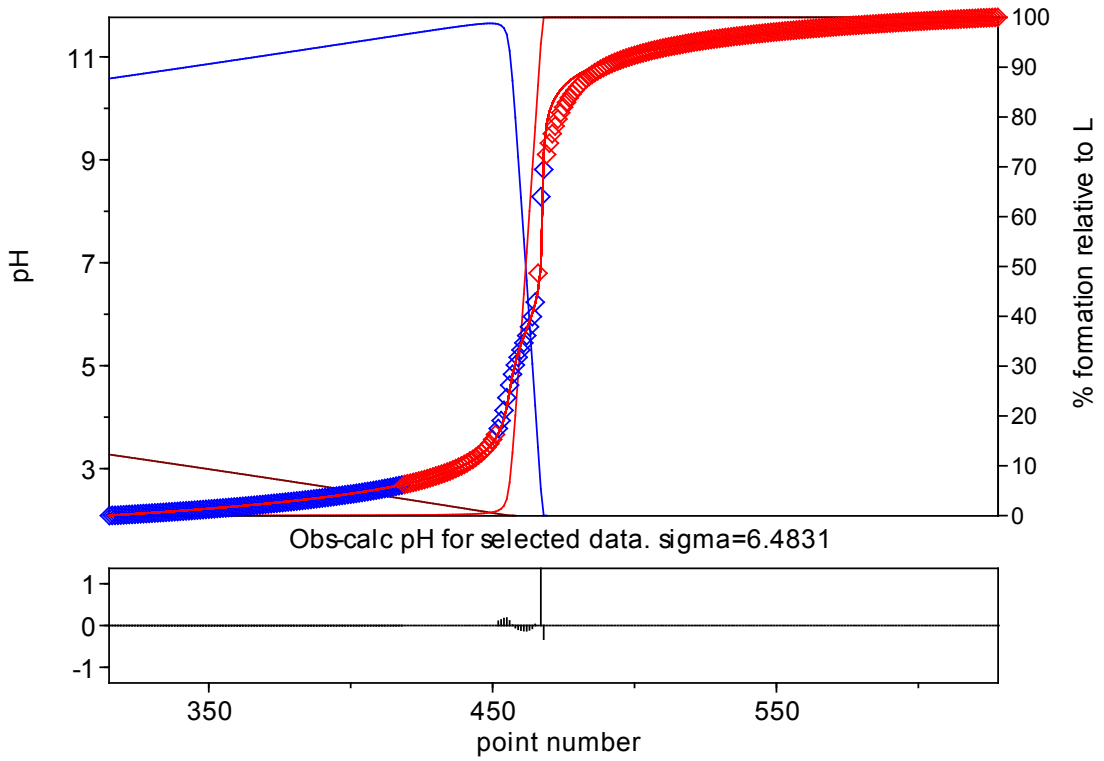

Figure 4.21: Titration and fitted curves PIMH protonation studies. Experimental points are represented by blue squares and the red dotted continuous line is the calculated line based on the fitted protonation constants. The red squares represent the experimental points that have been ignored in the refinement process. The other lines represent the species (not specified)

Table 4.16: Protonation (log *K*) and first stability (log β_1) constants for the interaction of PIMH with the base metal ions (MSO_4 solutions) as determined in 10% ethanol/water at *I* = 0.10 M (TMACl) and 25(±0.1)°C. The standard deviations are reported in parenthesis.

Constant	Reaction	p q r	PIMH	Co^{2+}	Ni^{2+}	Cu^{2+}	Zn^{2+}
pK_1	$LH^+ \rightleftharpoons H^+ + L$	0 1 1	5.66(0.04)	-	-	-	-
pK_2	$LH_2^{2+} \rightleftharpoons 2H^+ + L$	0 1 2	6.89(0.05)	-	-	-	-
logβ_{110}	$M^{2+} + L \rightleftharpoons [ML]^{2+}$	1 1 0	-	6.08(0.02)	5.70(0.03)	5.58(0.04)	6.79(0.04)
logβ_{122}	$M^{2+} + 2L \rightleftharpoons [ML_2]^{2+}$	1 2 0	-	-	-	-	-
		Sigma (σ)	6.48	7.04	11.32	15.80	12.84

p,q and r refer to the coefficients of the species in the order of metal, ligand, and proton.

Table 4.17: Protonation (log *K*) and first stability (log β_1) constants for the interaction of PIMH with the base metal ions (MCl_2 solutions) as determined in 10% ethanol/water at *I* = 0.10 M (TMACl) and 25(±0.1)°C. The standard deviations are reported in parenthesis.

Constant	Reaction	p q r	PIMH	Co^{2+}	Ni^{2+}	Cu^{2+}	Zn^{2+}
pK_1	$LH^+ \rightleftharpoons H^+ + L$	0 1 1	5.66(0.04)	-	-	-	-
pK_2	$LH_2^{2+} \rightleftharpoons 2H^+ + L$	0 1 2	6.89(0.05)	-	-	-	-
$\log\beta_{110}$	$M^{2+} + L \rightleftharpoons [ML]^{2+}$	1 1 0	-	8.2(0.1)	7.5(0.1)	7.07(0.03)	7.8(0.1)
$\log\beta_{122}$	$M^{2+} + 2L \rightleftharpoons [ML_2]^{2+}$	1 2 0	-	-	-	-	-
		Sigma (σ)	6.48	4.23	11.41	7.40	5.35

p,q and r refer to the coefficients of the species in the order of metal, ligand, and proton.

The relatively weak-to-mild σ-donocity and the good π-acceptor capability of this ligand infer interesting coordination chemistries towards the base metal ions to the effect that there is anapparent discrimination in its interaction with these metals as a function of pH. The first stability constants observed allowed one to gain insight into the fact that the thermodynamic aspect of complexation was not very significant in the formation of these tetrahedral species. It is unfortunate that the second stability constants could not be calculated in the pH range where precipitation was experienced since informative data with regards the overall stabilization could have been obtained and evaluated in the line of thought proposed here. The zinc(II) stabilization was consistent with what was observed in Figure 4.18. These results necessitated the exploration of the kinetics of complexation as a likely driving factor for the observed extraction pattern of these base metal ions.

(b) Spectrophotometric titrations

The nickel(II) toluene-4-sulfonate titration with the ligand was carried out to probe into the stereochemical changes that occur upon the interaction of the metal with the ligand as a way of confirming the stereochemistry observed in the solid reflectance studies. These changes also allowed for the evaluation of the kinetic aspects of coordination. The metal(II) toluene-4-sulfonate solutions were used since the extractions are carried out in DNNSA which is an aromatic sulfonate so as to closely mimic the chemistry of the extraction system, with a major difference being the two phases involved in the SX system.

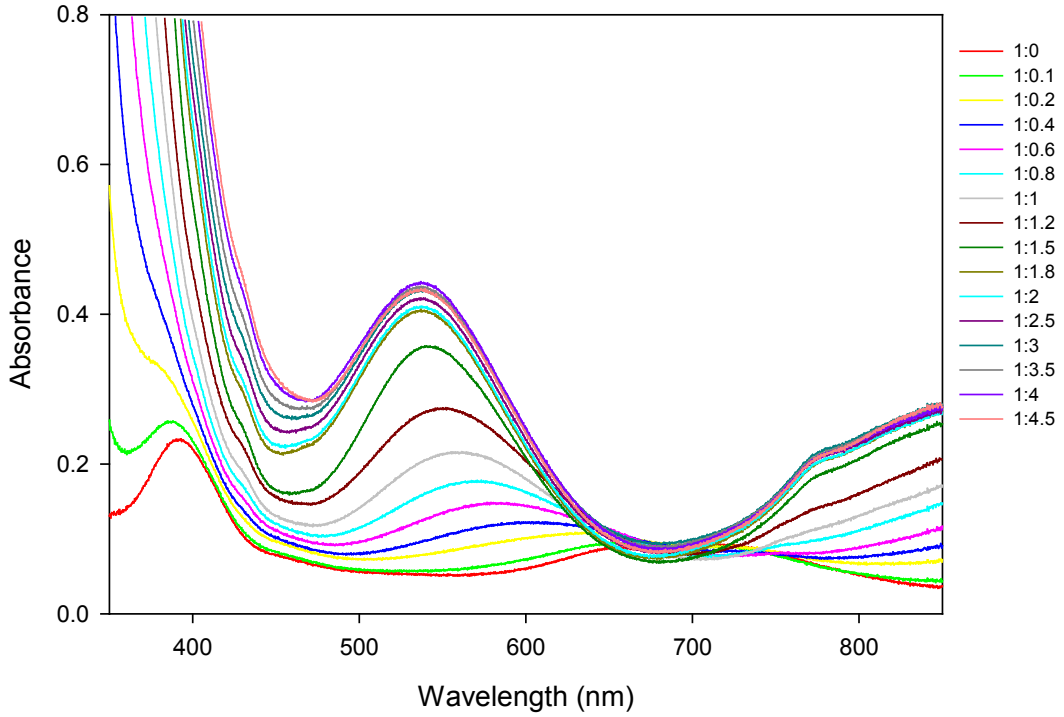

Figure 4.22: A spectrophotometric titration plot of 0.04 M $Ni(RSO_3)_2$ with various mole ratios of PIMH in ethanol and water. The M:L mole ratios are given as legends

The results depicted in Figure 4.22 show a relatively faster change in stereochemistry from the octahedral he xaaquanickel(II) ion to the tetrahedral complex species compared with cobalt(II) (Figure 4.23). Each spectrum was run 5 minutes after the increment of the ligand ratio, and this therefore provided a semi-quatitative kinetic information. Formation of the nickel complex was significant even at low ligand concentrations and becomes complete with ligand-to-metal ratio above 2 while the cobalt complex formation was incomplete and formation progresses even at much higher ratios. The increment of the ligand ratio can be viewed as introducing a constant entropy factor for the complexation and only necessary for the evaluation of the extent of reaction with higher ligand amount. This result gave insight to the separation observed as being of kinetic origin rather than thermodynamic, and the copper anomaly was addressed similarly. A confirmatory study could be done by carrying out a stop-flow kinetic investigation of this complex forming reaction of PIMH with these base metals. The contacting time of 30 minutes used for the extraction

studies was the optimised time for the satisfactory extraction of nickel with least extraction of cobalt.

These results are suprising considering that tetrahedral cobalt(II) and c opper(II) complexes are common and readily obtained while those of nickel are known to form when the ligands do not have enough perturbing power to give compounds of the spin-paired type, and when the stereochemistry is forced by the steric requirements of the ligands.[26]

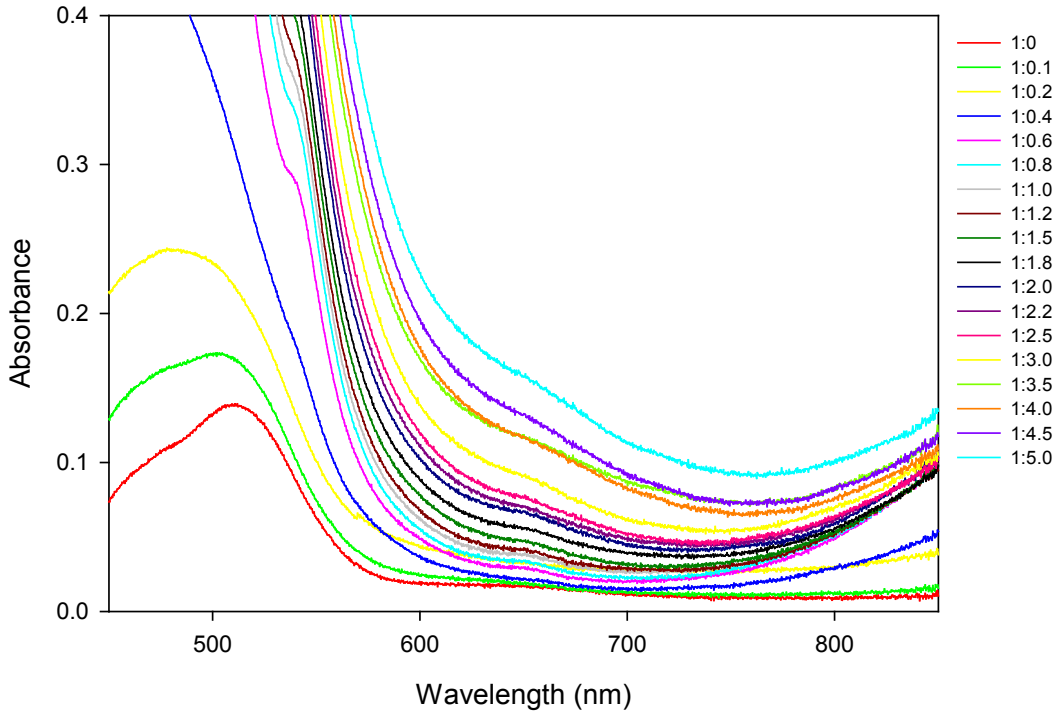

Figure 4.23: A spectrophotometric titration plot of 0.04 M $Co(RSO_3)_2$ with various mole ratios of PIMH in ethanol and water

4.4 Conclusions

This study has proved the applicability of 1-octyl-2,2′-pyridylimidazole as an efficient extractant in the separation of nickel from other base metals from an acidic sulfate medium in the presence of the hard ions which were rejected by this nitrogenous ligand. Most interesting is the ability of this extractant to reject ferrous ions, thus providing a shortened route for the recovery of nickel. It has also been demonstrated

that the dilute chloride and high sulfate content do not affect the extraction patterns and efficiencies observed with pyridylimidazole in dilute sulfate solutions, respectively.

The chemistry that has been demonstrated in this account presents a concept from which the development of innovative, and selective processes based on solvent extraction can be given a renewed impetus. This chemistry-driven approach should also serve as a way of bridging the gap between chemists and engineers in the field of base metal ion separation, and revive the academic approach to research in the hydrometallurgy field. A further investigation in the chemistry presented would be the application of this system to an industrial feed solution, and studies relating to scaling-up to the relevant industrial concentrations.

References

[1] J. G. H. du Preez, Solvent Extr. Ion Exch. 18 (2000) 679-701.

[2] J. G. H. du Preez, J. Postma, S. Ravindran, B. J. A. M. van Brecht, Solvent Extr. Ion Exch. 15 (1997) 79-96.

[3] J. G. H. du Preez, N. Sumter, C. Matheus, S. Ravindran and B. J. A. M. van Brecht, Solvent Extr. Ion Exch. 15 (1997) 1007-1021.

[4] Shell South Africa Energy (pty) Ltd, Certificate of analysis, Batch no 27506 Shellsol 2325 2008.

[5] T.I.A.Gerber, E. Hosten, P. Mayer, Z.R.Tshentu, J. Coord. Chem. 59 (2006) 243-253.

[6] M. Haring, Helv. Chim. Acta 42 (1959) 1845-1850.

[7] G. Gran, Analyst 77 (1952) 661-669.

[8] P. Gans, B. O'Sullivan, Talanta 51 (2000) 33-37.

[9] C. Bazzicalupi, A. Bencini, A. Bianchi, A. Danesi, C. Giorgi, B. Valtancoli, Inorg. Chem. 48 (2009) 2391-2397.

[10] P. Gans, A. Sabatini, A. Vacca, Talanta 43 (1996) 1739-1753.

[11] J. G. H. du Preez, J. M. Shaeekers, Patent WO 02/101101 A2 1-18.

[12] D.S. Flett, J. Organomet. Chem. 690 (2005) 2426-2438.

[13] H.M. Irving, R.J.P. Williams, J. Chem. Soc. (1953) 3192-3210.

[14] J. G. H. du Preez,S.B. Schanknecht, D.P. Shillington, Solvent Extr. Ion Exch. 5 (1987) 789-809.

[15] D.S. Flett, J. Organomet. Chem. 690 (2005) 2426-2438.

[16] J.C. Agarwal, H.E. Barner, N. Beecher, D.S. Davies, R.N. Kust, Miner. Eng. 32 (1979) 1704-1707.

[17] J.C. Agarwal, H.E.N. Beecher, G.L. Hubred, D.L. Natwig, R.R. Skarbo, E/MJ 177, 12 (1976) 74-78.

[18] J. C. Agarwal, N. Beecher, G.L. Hubred, AIChE Symposium series number 192 (1980) 35-38.

[19] T.J. Lane, I. Nakagawa, J.L. Walker, A.J. Kandathil, Inorg. Chem. 1 (1962) 267-276.

[20] Z. Nakamoto, Infrared and Raman Spectra of Inorganic and Coordination Compounds, 3rded, John Wiley and Sons, New York, 1978.

[21] W.J. Geary, Coord. Chem. Rev. 7 (1971) 81-122.

[22] A.B.P. Lever, Inorganic Electronic Spectroscopy, 2nd ed., Elsevier, New York, 1984.

[23] D. Nicholls, Complexes and First-Row Transition Elements, Macmillan Press, London, 1974.

[24] L.D. Pettit, K.J. Powell, Stability Constants Database-IUPAC and Academic Software, UK, 2007.

[25] G. Jerez, G. Kaufman, M. Prystai, S. Schenkeveld, K.K. Donkor, J. Sep. Sci. 32 (2009) 1087-1095.

[26] L.M. Venanzi, J. Inorg. Nucl. Chem. 8 (1958) 137-142.

CHAPTER 5

●●●●●

SORPTION OF BASE METALS WITH CHELATING MICROSPHERICAL RESINS AND ELECTROSPUN NANOFIBERS FUNTIONALIZED WITH 2,2′- PYRIDYLIMIDAZOLE

5.1 Introduction

The application of solvent extraction (SX), no doubt, has yielded to some extent the successful separation of nickel from cobalt and other base metals with the application of di(2-ethylhexyl)phosphoric acid[1,2] and other commercial extractants. Similarly, the oximes have proved to be versatile extractants in the separation of copper with SX technique.[3] It is however known that the application of solvent extraction is limited when the metals are to be separated from pregnant liquor solutions (PLS) of low concentrations.[4] Loss of reagents as a results of entrainment is known to be a further setback in the application of SX as well as difficulty in phase separation.[5] Ion-exchange technique is known to be free from these shortcomings, since it consist of the interchange of ions between a soluble and an insoluble phase.[6] Ion-exchange resins offer numerous advantages among which are their insolubility which renders them environmentally compatible. In addition, the cycle of loading/regeneration/reloading makes them reusable for years owing to the high mechanical strength and toughness of the exchange particles.[7] Ion exchangers have been successfully applied in continuous processes such as columns and chromatographic separations in which the metal ions are removed by sorption on chelating polymers based on their higher adsorption capacities and selectivity as well as physical and chemical stabilities.[8,9]

Chelating ion exchangers have the ability to selectively chelate metal ions of interest through suitable functional groups immobilised on the polymeric structure of the resins or any other adsorbent. Thus, greater selectivity can be achieved among the divalent transition metal ions than with the conventional ion exchange resins.[10] Various polymeric support materials have been used in the design of these chelating

systems such as silica gel, cellulose, functionalised polymers including chloromethylated polystyrene divinybenzene cross-linked resins (Merrifield peptide resins)[11] and more recently electrospun polymeric nanofibers.[12] Fibrous chelating sorbents are characterized by a large surface area and excellent kinetic properties, and are considered superior to granular sorbents.[13] Electrospinning, as a process that produces fibers with nanoscale fibrous structures, offers better options that allow for the control of the diameter, morphology, secondary structure, and the spatial alignment of the electrospun nanofibers.[14] The electrospun nanofibers have proved to be effective metal sorbent materials with high loading capacity owing to their large surface area-to-volume ratio, while microspherical resins are versatile in chelating divalent metal ions due to their numerous pores as shown by Colella *et al*. [15,16]

In the application of chelating resins, the amine containing resins have shown excellent sorption capacity for metal ions and are widely applied in the separation and removal of metal ions. Chanda *et al*[17] found out that polyethylene amine on polyvinylbenzaldehyde has high selectivity for Fe^{3+} over Cu^{2+}, Ni^{2+}, Co^{2+}, Fe^{2+}, Zn^{2+} and Mn^{2+}. Similarly, a chelating resin containing benzoylacetanilide groups was successfully applied in the separation of Ti^{3+} and Fe^{3+} from Cu^{2+}, Co^{2+}, Ni^{2+}, Na^{+}, K^{+}, Ca^{2+}, Mg^{2+} and Al^{3+} in the pH range 1.3-2.0 by Majee *et al*.[18] In all these attempts, not much has been achieved, according to the available literature, on the selective adsorption of nickel in the presence of other base metal ions in a sulfate medium. In an attempt to prepare the functionalized polymer, an approach which involves functionalization of the ligand with a polymerizable group, followed by suspension copolymerization[19] with a suitable cross-linking agent was undertaken. This method is known to offer greater degree of freedom with respect to functional monomer (ligand) content, porosity, degree of cross-linking and bead diameter.

In this study, an attempt to prepare pyridylimidazole functionalized microspherical beads *via* the synthesis of 1-allyl-2,2′-pyridylimidazole and the suspension polymerisation of this monomer is described. Due to the low ratio of the ligand bonded to the polymer unit and the subsequent low binding sites for the metal ions, it was resolved to functionalize the commercial microspheres (Merrifield beads) with 2,2′-pyridylimidazole. The aromatic N-donor ligands like pyridine and derivatives are not so readily protonated at low pH due to their lower proton affinity, and the higher σ

donicity of imidazole moiety should result in an effective chelator for latter 3d transition metal ions. The non-crosslinked poly(vinylbenzylchloride) homopolymer was also prepared by bulk polymerization, electrospun into fibers, and subsequently functionalised with 2,2′-pyridylimidazole. The polymer materials were characterized by scanning electron microscopy (SEM), microanalysis, infrared (IR), X-ray photoelectron spectroscopy (XPS) and other techniques. The sorption capacity of the functionalized Merrifield resins was assessed in the batch study and the selective sorption and separation of nickel, from the synthetic sulfate solution containing cobalt, copper and iron in a column study was investigated in an acidic medium. A comparative batch study was also carried out on the sorption capacity and the sorption rates of the functionalized electrospun nanofibers as sorbent for nickel, cobalt, copper and iron in the synthetic sulfate solution at a pH range 1.0 – 3.0.

5.2 Experimental

5.2.1 Preparative work

(a) Preparation of 2,2′-pyridylimidazole

The ligand, 2,2′-pyridyl-1*H*-imidazole (PIMH), was prepared according to the literature[20] method as reported in Chapter 4 of this thesis.

(b) Attempted synthesis of 2,2′-pyridylimidazole-containing beads

(i) Preparation of 1- allyl-2,2′-pyridylimidazole (APIM)

Allylation of the 2,2′-pyridyl-1*H*-imidazole (PIMH) was achieved by the addition of 0.672 g (0.012 mol) of potassium hydroxide to a solution of 1.76 g (0.012 mol) of PIMH in 50 mL acetone. To this, 1-allylbromide (1.45 g, 0.012 mol) was added drop wise. The reaction was allowed to stir for 30 mins and the mixture was refluxed at 40°C overnight. It was then cooled and filtered to remove the KBr salt. The resulting solution was concentrated *via* rotary evaporation, and purified using a silica gel chromatographic column with ethyl acetate/methanol (3:1) solvent system. The product was obtained as brown oil with the yield ranging from 61-63%.

(ii) Suspension polymerization of 1-allyl-2,2′-pyridylimidazole (APIM)

The organic phase was prepared by dissolving 1.0 g (0.041 mol) of 1-allyl-2,2′-pyridylimidazole in 4.5 mL toluene and 4 mL 80% divinylbenzene (DVB) and 0.125 g of benzoyl peroxide were added and stirred for a while. The aqueous phase was prepared by adding 0.01 g hydroxyethyl cellulose and 0.03 g gelatine as stabilizers to 35.0 mL distilled water. These were allowed to stir for some time until full dissolution after which 3.5 g of sodium chloride was added to make the medium ionic. Unto the aqueous phase, while stirring at a set speed of 360 r.p.m., was added the organic phase dropwise while the temperature was thereafter increased to 70°C. The reaction was allowed to proceed overnight under an argon atmosphere. The resultant yellow beads were filtered, washed several times with water, methanol and finally diethyl ether and dried in an oven at 60°C overnight. Anal. Found: C, 90.12; H, 8.39; N, 0.87%.

(c) Preparation of 2,2′-pyridylimidazole-immobilized microspheres

The commercial microspheres (Merrifield peptide beads) crosslinked with 1% divinyl benzene were functionalized with 2,2′-pyridylimidazole as follows: 10.0 g (0.07 mol) of 2,2′-pyridylimidazole and 5.0 g of the chloromethylated resin matrix in 15.0 mL dry dimethyl formamide (DMF) were refluxed at 70°C under argon for 24 h. Thereafter the resin was washed with excess methanol, filtered and further cleansed with a Soxhlet extraction system using diethylether as solvent. Finally, it was dried in an oven at 60°C overnight. Anal. Found: C, 80.31; H, 7.46; N, 6.52 %.

5.2.2 Procedure for polymerization, electrospinning and functionalization of nanofibers

(a) Synthesis of poly(vinylbenzylchloride)

Bulk polymerisation of the monomer 4-vinylbenzylchloride (5.0 mL, 35 mmol) was achieved by using excess azobisisobutyronitrile (AIBN) (0.04 g, 0.19 mmol) as the initiator in a stoppered flask. Under argon, the mixture was heated to 70°C and stirred overnight. The polymer obtained was washed several times with THF, precipitated with methanol, filtered and air dried.

(b) Fabrication of nanofibers by electrospinning

The polymer [poly(vinylbenzylchloride)] was dissolved in a DMF/THF (1:1) solvent mixture to make a 25% solution (wt/v%). The polymer solution was stirred for 24 hrs to ensure complete dissolution and then loaded into a 20 mL syringe (Figure 5.2).

Electrospinning was conducted under the following parameters. A voltage of 14 kV was applied to the spinneret (needle tip) which had an internal diameter of 1 mm, and the distance between the tip and collector was maintained at 10 cm whilst the rate of the movement of the syringe was maintained at 0.3 $mL.h^{-1}$ using a syringe pump. The resultant dense web of fibers was collected on a grounded piece of aluminium foil.

(c) Post- electrospinning funtionalisation of the nanofibers

A strip of approximately 10 cm x 12 cm of the poly(vinylbenzylchloride) fiber mat measuring 0.1 g was cut and rinsed with water to make the fibers more manageable. These were placed into a 20 mL methanol solution of PIMH (5.0 g, 0.035 mol) in a 50 mL flask along with KOH (3.93 g, 0.07 mol). The content was refluxed and stirred gently at 40 rpm for a period of 5 days at about a temperature of 40°C. Afterwards, the fibres were rinsed in methanol and then filtered. Finally, the fibers were cleansed with diethylether in a Soxhlet extraction system, filtered and dried at room temperature under reduced pressure for 12 hrs. Anal. Found: C, 74.73; H, 6.15; N, 12.56 %.

(d) Surface characterization

The polymer microspheres and the fibers were imaged using a TESCAN Vega TS 5136LM scanning electron microscope (SEM) at 20 Kv and at a working distance of 20 mm.

Surface area analysis was performed using a Micromeritics ASAP 2020. Before analysis the materials (beads and fibers) were degassed; the microspheres were degassed for 7 days 140°C while the fibers were degassed at 70°C for 14 days.Carbon dioxide adsorption/desoprtion isotherms were measured at 273 K using a Micromeritics ASAP 2020. Multiple point BET analysis which helps in determining

the porosity of the materials (beads and fibers) could however not be calculated due to the low relative pressure (P/P_o) of the carbon dioxide in the adsorption/desorption process.

X-ray photoelectron spectroscopy (XPS) measurements were performed with a Kratos Axis Ultra X-ray Photoelectron Spectrometer equipped with a monochromatic Al Kα source (1486.6 eV). The base pressure of the system was below 3 x 10^{-7} Pa. XPS experiments were recorded with 75 W power source using hybrid-slot spectral acquisition mode and an angular acceptance angle of +/- 20°. XPS data analysis was performed with Kratos version 2 program.

5.2.3 Sorption of metal ions with the resins

(a) Batch procedure

5 mL of 0.02 M solution of the metal sulfate at different pH was transferred with a micropipette into each of the five 100 mL flask and diluted to 25 mL with millipore purified water. 0.5 g of the dried resin was weighed into each of the flask and stoppered.

The contents of the flask were shaken with the aid of the Labcon micro-processor controlled orbital platform shaker at a speed of 100 rpm for a period of 5 hrs and 0.5 mL of the solution was taken out at 30 mins interval to determine the optimum time for sorption of the metal ions. Each of the solution was diluted appropriately for analysis by ICP-OES. Thus the distribution coefficient (D) of the metal ions between the resin and the solution at the optimum time was calculated according to equation 45 as follows:

$$D = \frac{\text{Conc. of } M^{n+} \text{ in 1 g of dry resin}}{\text{Conc. of } M^{n+} \text{ in 1 ml of the solution}} \quad (45)$$

Similarly the percent sorption (S_A) of these metal ions were determined as a function of time as given by equation 46:

$$\% S_A = (C_o - C_w)/ C_o \text{ X } 100 \quad (46)$$

where C_w and C_o are the concentrations of the metal ions in the solution after and before adsorption respectively.

(b) Column procedure

The dynamic column studies were carried out using a glass capillary column of 5.0 cm length with an internal diameter of 3.6 mm fitted with an outlet tip of 1.0 mm internal diameter. The column was packed uniformly with 0.4 g of the resin beads by a slurry method and attached to a 5 mL disposable syringe fitted with a programmable syringe pump. The column parameters, namely; breakthrough volume, sample flow rate and loading quantities were optimized prior to the column studies.

5.2.4 The effect of pH on loading capacity of metals on the resin

The capacity of the resin for metal sorption was determined as a function of pH in a column study. A 0.02 M sulfate solution of the metal ion was loaded into the column after conditioning the column at pH 1.0, 1.5, 2.0 and 2.5 respective solution of sulfuric acid. The column was left for 24 hrs after which it was washed with 5 mL millipore water to remove metals that were not adsorbed onto the surface of the resin. The adsorbed metal ions were stripped and eluted from the loaded resin with varying concentration of sulfuric acid solution in the pH range of 0.5-1.5. The eluent was diluted appropriately and analyzed with ICP-OES. The results obtained are hereby presented in Table 5.1, showing the resin sorption capacity for each metal as a function of pH. The resin capacity was calculated as mmol.g^{-1} of the resin as given by equation 47:

$$q_e = \frac{(C_i - C_f)V}{M} \quad (47)$$

where q_e is the sorption capacity (mmol.g^{-1})

C_i and C_f are the initial and final metal ion concentrations (mM) respectively,

V is the solution volume (L) and M is the mass of adsorbent (g) used.

5.2.5 The effect of flow rate on sorption of nickel at pH ≈ 2

In an initial study conducted with 0.02 M $NiSO_4$ solution at about pH 2.0, varying flow rate of the solution of nickel ion on adsorption on the resin was carried out with the aid of syringe pump controlled flow-rate between 0.5 - 3.0 $mL.h^{-1}$. The optimum flow-rate at which the highest kinetics for sorption capacity of the metal ions occur at equilibrium was found to be 1.5 mL/h and was thereon applied for the study of all the metal ions.

5.2.6 Binary separation of nickel from other base metals

The binary separation of nickel from cobalt, nickel from copper, and copper from iron(II) was undertaken by loading the column with a mixed metal solution, containing 0.02 M metal sulfate of the respective metal ions, with a pH value of 2. The column was eluted with sulfuric acid while copper was eluted with 1.0 M ammonium hydroxide solution. The separation factor of nickel from each of the metal ions was calculated as given by equation 48:

$$\beta_{Ni/M} = \frac{[Ni]r[M]s}{[Ni]s[M]r} \quad (48)$$

where $[Ni]_r$ and $[Ni]_s$ or $[M]_r$ and $[M]_s$ refers to the concentration of nickel or the metal ions on the resin and in the solution at equilibrium respectively.

5.2.7 Regeneration of resin

Regeneration of the resin for further usage was examined by loading the column containing 0.4 g of the resin with 0.02 M solution of Ni(II) at a flow rate of 1.5 $mL.h^{-1}$. After reaching the maximum uptake, the resin was washed carefully by running distilled water through the column. The adsorbed Ni(II) ions were stripped and eluted with sulfuric acid solution. After the elution, the resin was thoroughly washed with distilled water to make it ready for re-use for the second run of loading with a solution of Ni(II) ions. The elution efficiency was calculated by dividing the total uptake of the metal ion in the second run by that of the first run as given by equation 49:

$$\% \text{ Regeneration efficiency} = \frac{\text{Uptake of } M^{n+} \text{ in the second run by the resin}}{\text{Uptake of } M^{n+} \text{ in the first run by the resin}} \times 100 \quad (49)$$

5.2.8 Sorption of metals on the PIM-functionalized electrospun nanofibers

(a) Batch study: Effect of time on sorption of metal ions

The optimum time required for the sorption of the metal ions for the attainment of equilibrium condition by the functionalized fiber was determined by the batch method. 10.0 mg of the fiber was inserted into 5.0 mL of the synthetic metal sulfate leach solution (pH ≈ 2) and equilibrated for a period of 5 hrs within which samples of the solution was taken at an hourly interval. The concentration of the metal ions in each of the solution was determined and the amount of metal adsorbed was calculated using equation 46. The amount of the metal ion loaded on the PIM-functionalised fibers at each period was calculated as percent ratio of the total molar concentration of the metal sorbed (see Figure 5.13).

(b) Column study: Effect of pH on the metal sorption capacity of the sorbents in the mixed metal ions solution

Sorption of the metal ions on PIM-functionalised fibers was undertaken to see the dependency of the metal ion sorption capacity on the varying pH values of the synthetic leach sulfate solution under study. The study was carried out by a column technique with optimized amount of dried fiber (25.0 mg) loaded into the column followed by conditioning with pH 1.0, 1.5, 2.0.and 2.5 solution of sulfuric acid. The column was left for 24 hrs after which it was washed with 5 mL of millipore water to remove the unadsorbed metal ions on the fiber. The adsorbed metal ion were stripped and eluted from the loaded resin with varying concentration of sulfuric acid solution in the pH range of 0.5-2.5 through the column. The eluent was diluted. The concentration of the metal ions in solution was determined before and after the adsorption experiment with ICP-OES and the metal sorption/loading capacity at a given pH was calculated as in equation 47.

5.3 Results and Discussion

5.3.1 Synthesis and general considerations

(a) 1-Allyl-2,2′-pyridylimidazole

Introduction of the allyl group to the pyrole nitrogen of the imidazole was readily achieved *via* alkylation reaction under a mild temperature of 40°C with a considerable yield and less cumbersome column chromatographic purification (Scheme 5.1). The brown oily product was concentrated under vacuum with the rotar vapour. This synthesis was easily accomplished with the use of allyl bromide as an alkylating agent and potassium hydroxide as a base.

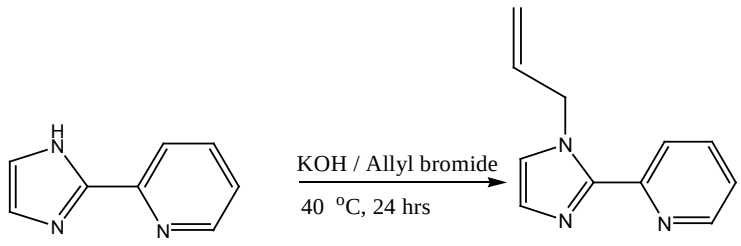

Scheme 5.1: Synthesis of 1-allyl-2,2′-pyridylimidazole

The attachment of the allyl group on t he imidazole ring was confirmed by the disappearance of the peak at 11.10 ppm depicting the pyrole-nitrogen proton in the ^{1}H NMR spectrum of this compound (see Figure 5.1(A)). The confirmation of the allylation of imidazole was further exhibited by the appearance of the peaks corresponding to the allyl group in the range 5.06 – 6.01 ppm in the spectrum as depicted by Figure 5.1(B).

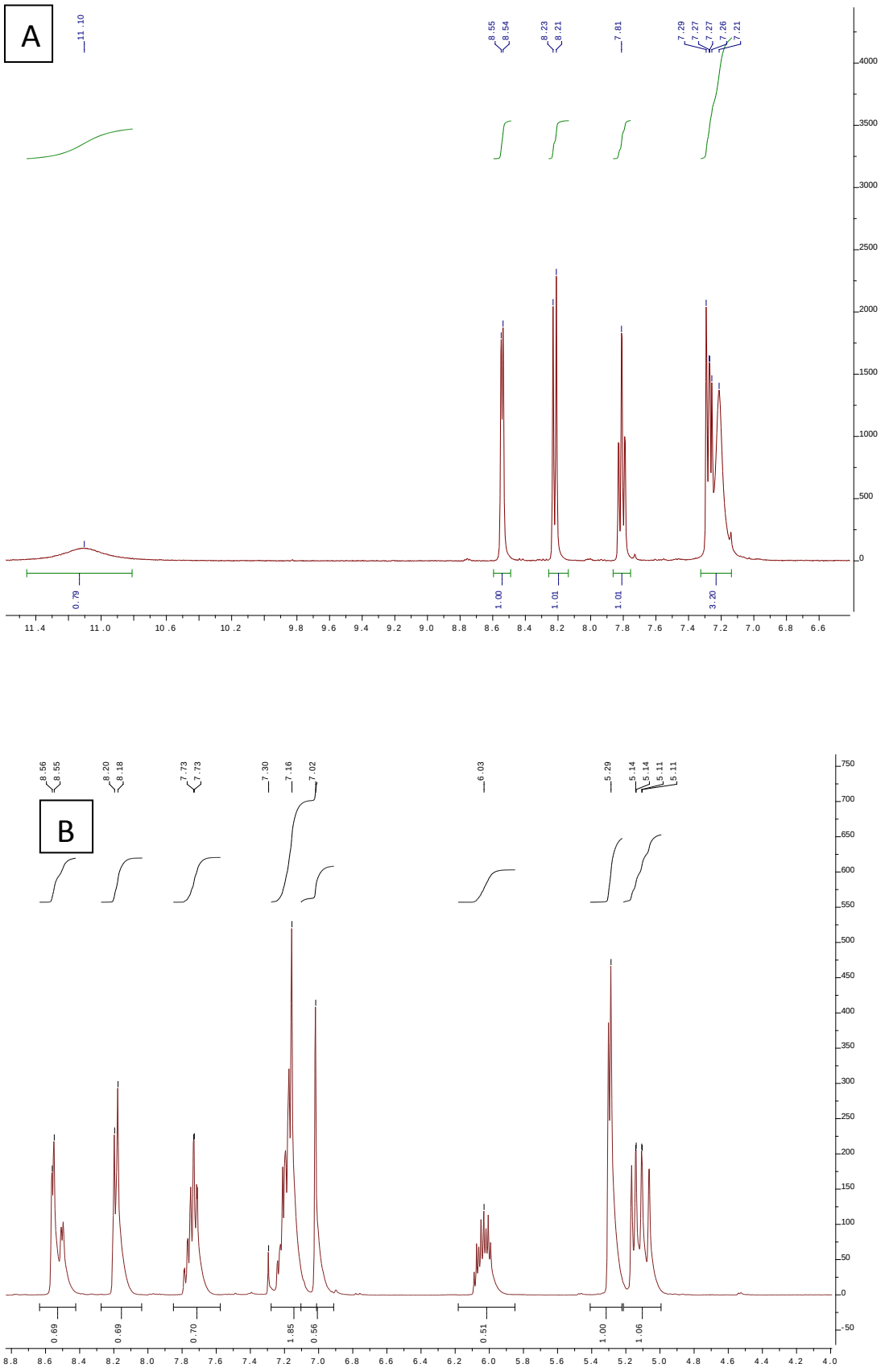

Figure 5.1: ^{1}H NMR spectra of (A) 2,2′-pyridylimidazole and (B) 1-allyl-2,2′-pyridylimidazole

(b) Suspension polymerisation of 1-ally-2,2′-pyridylimidazole (APIM)

The suspension polymerisation of APIM as indicated in the reaction Scheme 5.2 yielded microspherical beads of good sizes as expected. The temperature of the reaction vessel was kept under control and at an optimised stirring speed under an argon atmosphere, a fairly good yield of the desire product was realised. However the microanalysis revealed a low content of the functional groups in the beads (nitrogen content). Several porogens employed in place of toluene as solvent did not however improve the results. The poor incorporation of pyridylimidazole motivated for the immobilization of the functional group on 1% crosslinked Merrified peptide beads as shown in Scheme 5.3.

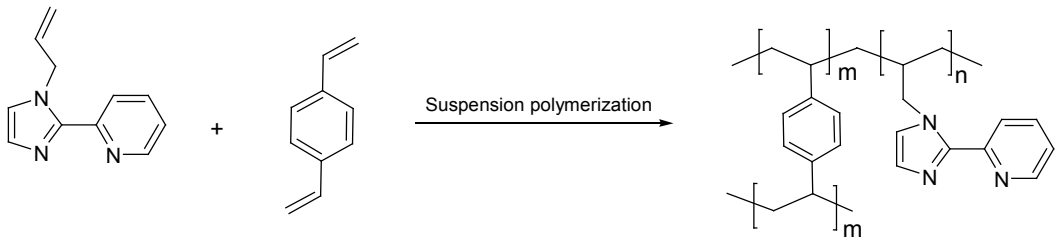

Scheme 5.2: Synthesis scheme for the suspension polymerisation of 1-allyl-2,2′-pyridylimidazole monomer with 1,4-divinylbenzene as crosslinker

(c) Preparation of 2,2′-pyridylimidazole-immobilized microspheres

Functionalization of the Merrrifield resin with 2,2′-pyridylimidazole was successfully accomplished by heating at 70°C in DMF. Care was taken in the choice of the stirring rate to avoid breakage of these beads. The unbound ligand was carefully washed off the beads with the use of methanol, water and Sohxlet extraction with diethyl ether as solvent, and then dried properly before its application. The nitrogen content as revealed by the microanalysis was found to be 6.52%, an indication of a better level of funtionalization of the polymer than was obtained in the suspension polymerisation.

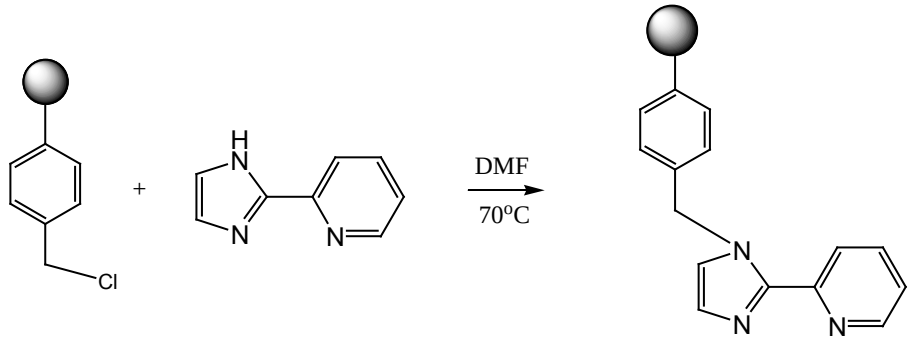

Scheme 5.3: Synthesis scheme for the preparation of 2,2′-pyridylimidazole-immobilized resin

5.3.2 Polymerization, electrospinning and functionalization of nanofibers

(a) Polymerisation

Bulk polymerisation of 4-vinylbenzylchloride monomer was carried out by free radicals reaction in DMF using AIBN as a free radical initiator in DMF (Scheme 5.4). An argon atmosphere was observed in a sealed flask kept in oil bath at 70°C for 24 hrs. The polymer was readily isolated by precipitation in cold water (about 12 times the volume of the reaction mixture). The precipitate was recovered by suction filtration and allowed to air-dry. The poly(vinylbenzylchloride) homopolymer was obtained as a white solid of about 65% yield.

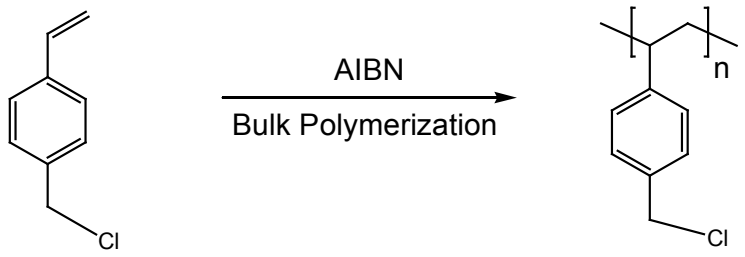

Scheme 5.4: Synthesis scheme for the polymerisation of 4-vinylbenzylchloride

(b) Fabrication of nanofibers by electrospinning

A solution of poly(vinylbenzylchloride) in DMF/THF produced electrospinnable fluid. Electrospinning of this solution was carried out under ambient conditions of temperature and pressure, and the following parameters were optimised: applied voltage, tip-to-collector distance, flow rate, and the collector so as to achieve the smallest diameter fibers. This becomes necessary since the surface area is known to

be proportional to the fiber diameter and the volume is proportional to the square of the diameter, leading to high specific surface areas for small fibres.[22] Thus, this electrostatic processing method uses the high-voltage electric field to form solid fibers from the polymeric fluid stream. Figure 5.2 shows the schematic diagram of the processes involved. The fluid flowing out of the spinneret (syringe) elongates, forming a fine jet. A cone-shaped polymer solution droplet directed to the counter electrode is formed under the high voltage. As the voltage increases, the droplet on the spinneret is slowly stretched, the solution loaded with electrostatic charges undergoes further stretching, and with the evaporation of solvents, the jet eventually solidified on reaching the grounded collector plate in the form of nanofibers.

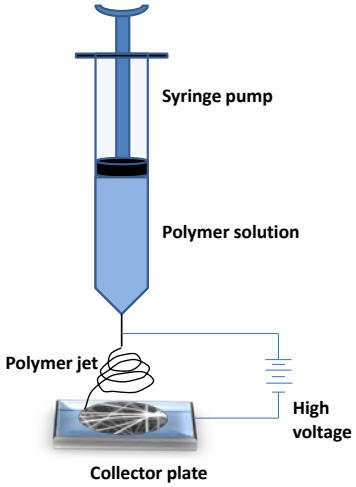

Figure 5.2: Schematic illustration of the basic set-up for electrospinning[22]

(c) Functionalization of nanofibers

The first attempt to prepare a pre-electrospinning functionalized PIM-polymer was unsuccessful owing to the fact that the polymer was insoluble in several solvents and this led to the post-electrospinnig functionalization of the polymer. The functionalization of the polymer with PIMH with the use of KOH as base at a mild temperature of 40°C for a period of 5 days provided a successful binding of PIMH on the fibers as attested by the IR spectra (Figure 5.6) and the XPS data (Figure 5.8).

5.3.3 Characterization of PIM-functionalized microspheres and nanofibers

The SEM micrographs of the corresponding PIM-functionalized beads showed little or no morphological difference from the unfunctionalized beads as depicted by Figure 5.3. The average diameter of the unfunctionalized beads and PIM-functionalized beads as determined by SEM was 223 and 225 µm respectively (n= 25).

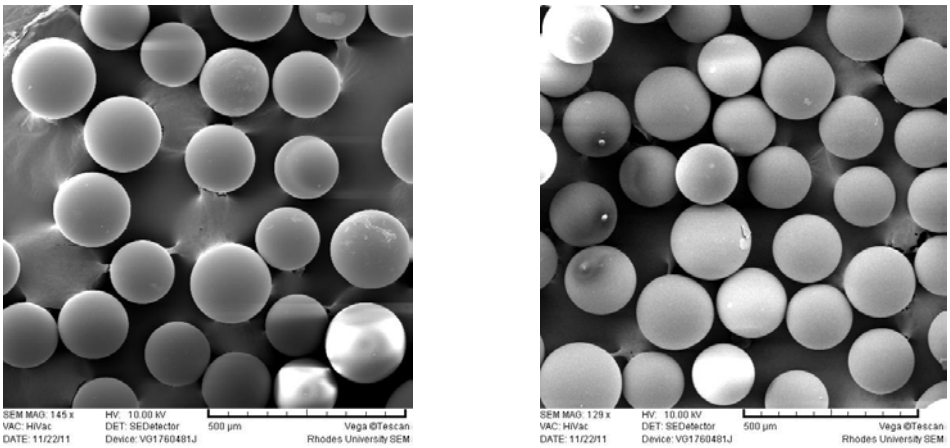

(a) (b)

Figure 5.3: Scanning electron micrographs of (a) unfunctionalized beads; (b) PIM-functionalized beads

The nitrogen content of the PIM-microspheres, which relates directly to the imidazole/pyridine content as determined by microanalysis, was found to be 6.52%.

In contrast, SEM micrographs showed that the PIM-functionalized fibers differ morphologically slightly from the unfunctionalized nanofibers. The diameter distribution range of the PIM-functionalized fibers was 651 – 708 nm (b) while the unfuntionalized fibers were in the range of 620-650 nm (a) (Figure 5.4).

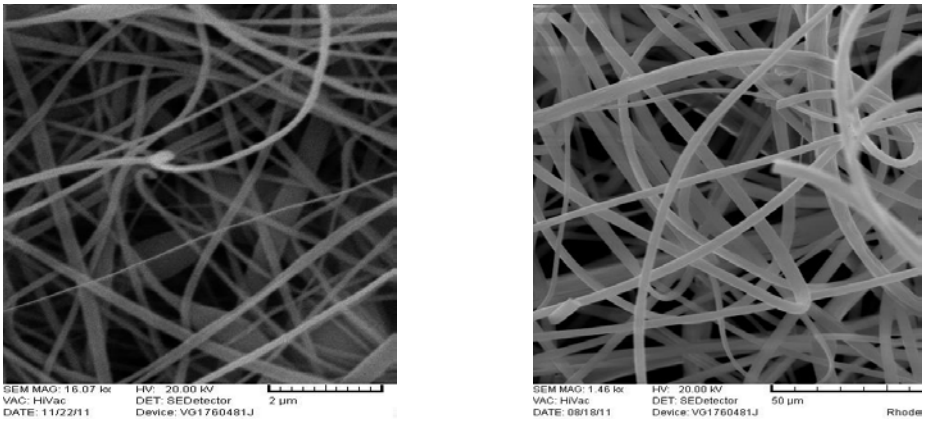

(a) (b)

Figure 5.4: Scanning electron micrographs of (a) unfunctionalized fibers (b) PIM-functionalized fibers

The infrared spectrum (Figure 5.5) confirmed the immobilization of 2,2′-pyridylimidazole on the beads. It is evidenced that the two peaks appearing at 670 cm^{-1} and 1264 cm^{-1} in the unfunctionalized beads corresponding to -CH_2Cl and –CH_2 wagging have completely disappeared.After the reaction, a shift from 1635 cm^{-1} to 1618 cm^{-1} corresponding to C=N in the imidazole ring was observed, confirming the effective anchoring of this functional group. A similar trend was observed on the immobilization on the nanofibers as shown by Figure 5.6. The two peaks at 668 cm^{-1} and 1264 cm^{-1} which were observed in the unfunctionalized fiber corresponding to -CH_2Cl and –CH_2 wagging respectively disappeared while a shift of v(C=N) in the imidazole ring system was observed from 1635 cm^{-1} to 1628 cm^{-1} in the functionalized fiber.

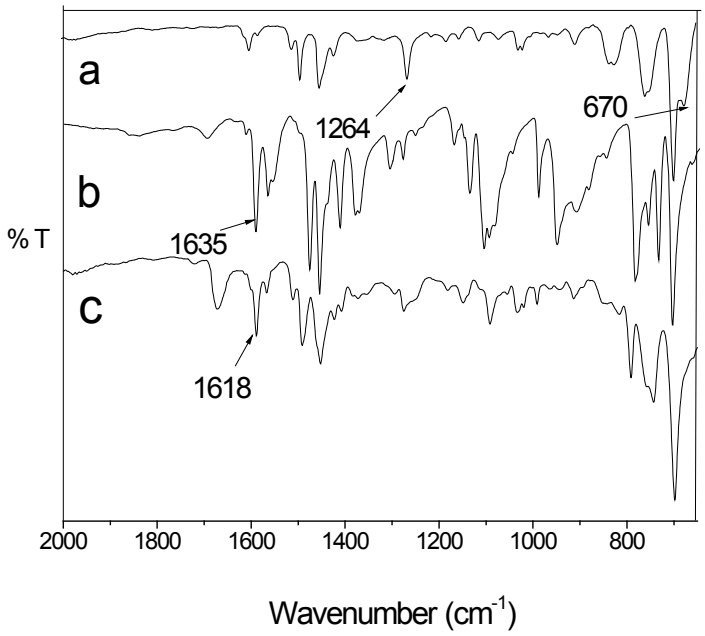

Figure 5.5: Infrared spectra of the beads (a) Unfunctionalized (b) PIMH, and (c) PIM-functionalized beads

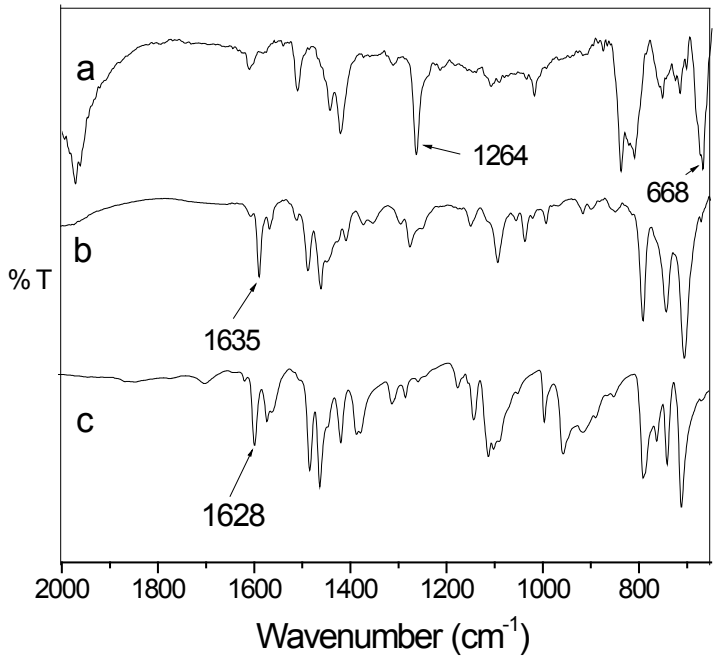

Figure 5.6: Infrared spectra of fibers (a) Unfunctionalized (b) PIMH, and (c) PIM-functionalized fiber

Investigation of the surface chemistry of these adsorbents by XPS also confirmed the presence of nitrogen atoms, along with the other expected elements in these polymers (Figure 5.7). There are N1s peaks appearing at 398 and 399 eV on the beads and the fiber spectra respectively. This confirms the binding of 2,2′-pyridylimidazole to these sorbents surfaces.[21]

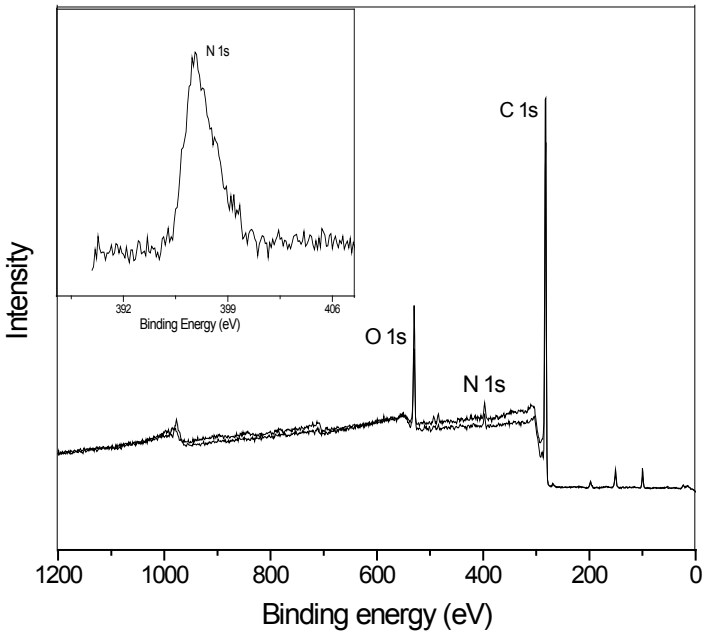

Figure 5.7: Wide scan XPS spectra of PIM-functionalized beads. The insert shows the expanded N1s signal

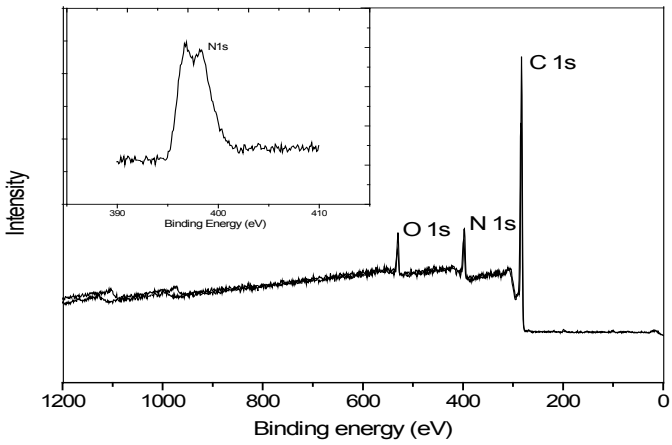

Figure 5.8: Wide scan XPS spectra of PIM-functionalized nanofibers. The insert shows the expanded N1s signal

The specific surface area of the PIM-functionalized beads was determined using the Brunauer-Emmet-Teller (BET) method and was found to be 46.82 $m^2.g^{-1}$ on a single surface area while the average multiple area was determined as 123.34 $m^2.g^{-1}$. The surface area was slightly higher than that of the PIM-functionalized fibers determined under the same condition which on a single surface was found to be 23.79 $m^2.g^{-1}$, while the multiple point is 89.33 $m^2.g^{-1}$. Kara *et al,*[25] reported a surface area of 59.8 $m^2.g^{-1}$ for their 150-200 µM sized beads. The slightly higher surface area observed in the beads could be due to the porous nature of the beads. It may however also be due to the larger amount of crosslinker used, since it has been shown that an increase in crosslinker may result in greater surface area. It is possible however that the internal pores of the beads do not contribute significantly compared to the surface of the beads, and if this is the case, then the highly exposed fiber surfaces will contribute significantly to the adsorption process.

5.3.4 Sorption of metal ions with PIM-functionalized microspheres

(a) Determination of the distribution ratio (D) and sorption capacity as a function of pH

These sorbents with basic properties of aromatic (imidazole and pyridine) amine functional groups are expected to show unique qualities such as selectivity, versatility, and high metal loading capacity of the base metal ions which are pH dependent. On this note, a preliminary assessment of the distribution ratio of the metal ions on the resin was investigated as a function of pH in a batch study prior to determining the loading capacity at the optimum pH values, the result of which is shown in Figure 5.9. This result depicts a higher value of D around pH 1.5 - 2.5 for nickel and copper, hence the column studies were conducted at pH around 2. Furthermore, it can be predicted that nickel would have a higher loading capacity around pH 2.0 than cobalt indicating a possible separation of the two metals which was found to be so in the column studies. Contrarily, a similar batch study conducted with the nanofibers showed less dependence of the distribution ratio on the pH (Figure 5.10).

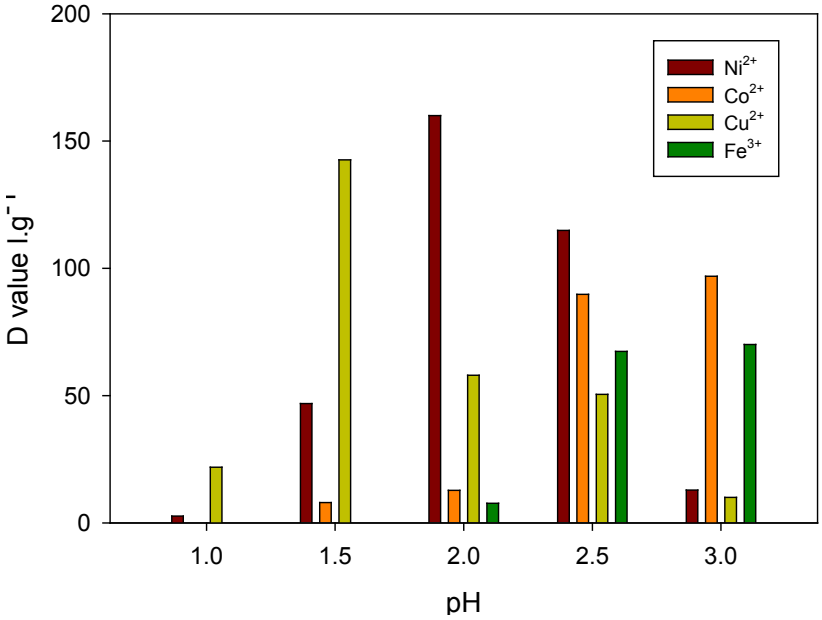

Figure 5.9: Metal ions distribution ratio (D) of the resin as a function of pH conducted in a batch study

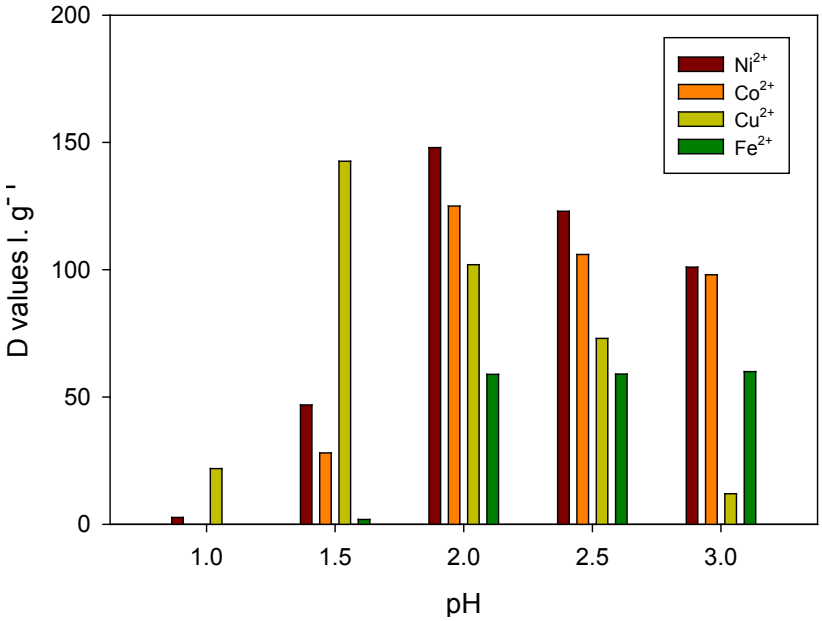

Figure 5.10: Metal ions distribution ratio (D) of the fiber as a function of pH conducted in a batch study

The sorption capacity was found to be pH dependent as depicted by the results shown in Table 5.1. It is also obvious that all the metal ions showed a maximum sorption capacity at about pH 2.0. For this reason, further studies were all carried out

around this pH. On the application of fiber as the sorbent, the results indicate a higher relative sorption capacity, possibly attributable to the higher nitrogen content, but possible lower selectivity of the metal ions compared with the resin.

Table 5.1: Sorption capacity of the sorbent for the metal ions ($mmol.g^{-1}$) as a function of pH.

pH	**1.0**	**1.5**	**2.0**	**2.5**	**3.0**
Nickel(II)					
Resins	0.25	0.28	0.95	0.65	0.23
Fiber	1.0	0.47	1.40	0.88	0.25
Cobalt(II)					
Resins	0.09	0.11	0.55	0.40	0.12
Fiber	0.09	0.31	1.25	0.75	0.22
Copper(II)					
Resins	0.23	0.25	1.20	0.77	0.22
Fiber	0.33	0.55	1.45	0.97	0.52
Iron(II)					
Resin	0.02	0.25	0.05	0.08	ND
Fiber	0.12	0.24	0.95	0.24	ND

ND - Not detectable

(b) Effect of flow rate on the percentage sorption

Optimization of the flow rate with respect to the percentage sorption of the molar content of the metal ions was studied with nickel sulfate solution. This parameter was considered important and was therefore carried out with the use of the auto-control flow rate device of the syringe pump. While over 90% sorption of the metal ions was achieved from 1.5 $mL.h^{-1}$ to 3.0 $mL.h^{-1}$, it is obvious from the plot in Figure 5.11 that the flow rate of 1.5 $mL.h^{-1}$ gives an optimum percent sorption, hence this flow rate was adopted for all the column studies.

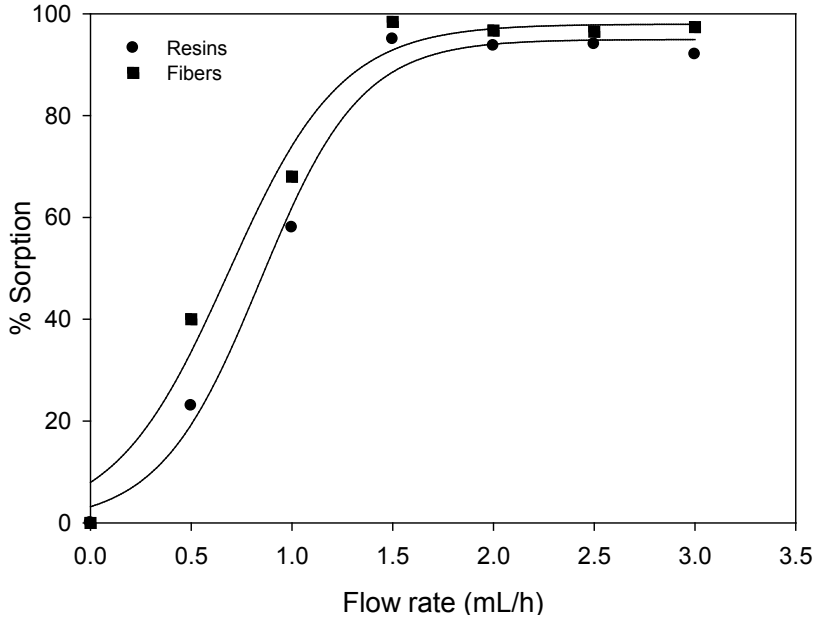

Figure 5.11: Effect of the flow rate on the percent sorption of the sorbents for nickel

(c) Effect of contact time on the percentage sorption

Variations of the contact time show a remarkable effect on the percentage sorption (with respect to total molar content) of the metal ions (Ni^{2+}, Co^{2+}, Cu^{2+} and Fe^{2+}) on the resins as shown in Figure 5.12. For instance, the effect of the contact time on the percent sorption of the four metals under study at pH 2.0 showed that cobalt has the fastest kinetics of uptake of all the metals with the percent sorption reaching as high as 85% within 60 mins. It can also be observed that all the metal ions adsorbed maximally at pH 2.0 and within 3 hrs while iron(II) showed slowest kinetics and was the least adsorbed. Sorption on the fiber was found to proceed at a faster rate than the resin as shown in the two plots (Figure 5.12 and 5.13). On this note the contact time of 3 hrs was chosen for the subsequent batch studies.

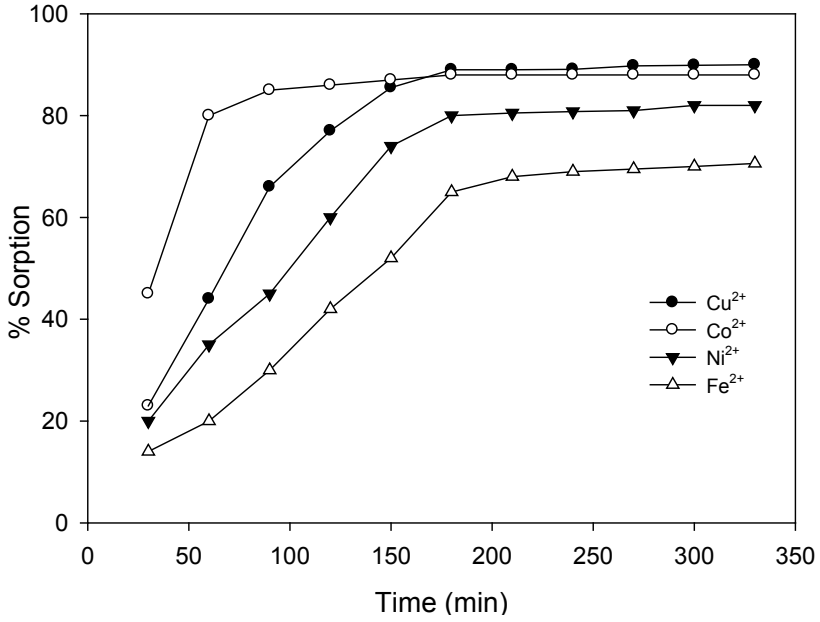

Figure 5.12: Effect of contact time on the percentage sorption of nickel, cobalt, copper and iron by PIM-functionalized beads at pH 2.0

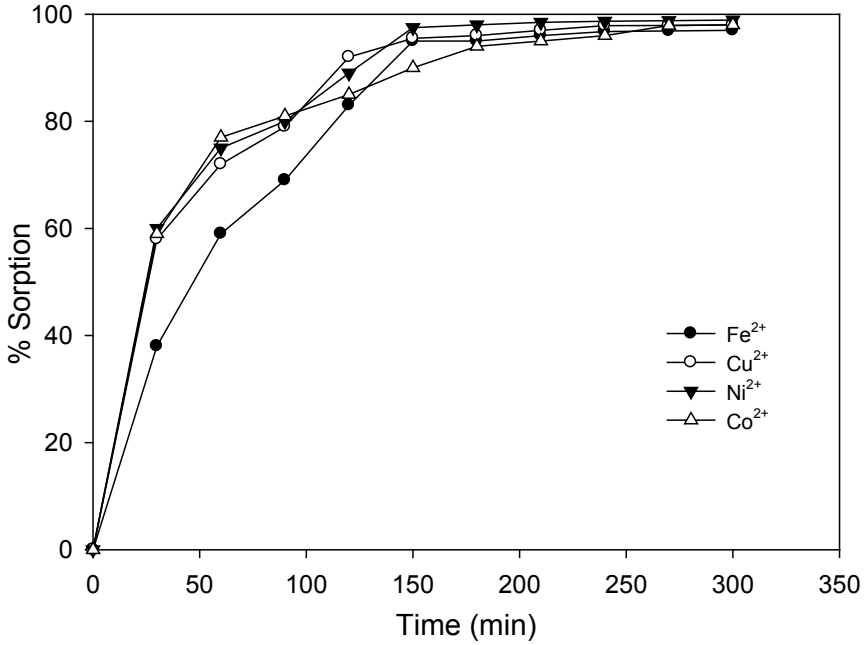

Figure 5.13: Effect of contact time on sorption of metal ions by nanofibers at pH 2.0

5.3.5 Binary separation of nickel from the base metals

Separation of nickel from cobalt was undertaken since the removal of nickel from base metals was the primary focus in this study. This became necessary in view of the limited achievements made thus far in solvent extraction of the duo because of their similar aqueous chemistry. Secondly, the separation of nickel(II) from copper(II) and from iron(II) was also examined.

A binary synthetic solution containing equimolar concentration (0.02 M) of nickel and cobalt as sulfates of each of the metals was loaded sequentially into the pre-conditioned resin in the column. This was allowed for equilibration for a period of 3 hrs. After washing the unadsorbed metal ions off the resins with 20 mL of milli-q water, the resin was eluted by gradientelution with 0.01 - 0.02 M sulfuric acid until complete elution was achieved. Where copper was involved in the separation,1.0 M ammonia solution was applied first as eluent and after washing with water, the pH was adjusted to pH of 2 with sulfuric acid, elution and stripping of the second metal ions was thereafter carried out. The metal ions were determined upon appropriate dilution with milli-q water and analysed with the ICP-OES. The resins were removed from the column after elution, washed and dried for the next determination.

Table 5.2 gives the calculated separation factors according to equation 48. The data were obtained after the optimum contact time of about 3 hrs. The separation factor are fairly good with respect to Ni^{2+}/Co^{2+}, however a better selectivity is required for Ni^{2+}/Cu^{2+} and Ni/Fe^{2+} binary system.

Table 5.2: Selective sorption of the metal ions ($mmol.g^{-1}$) by the resin in a binary separation at pH 2.0 under the column study

Binary pair	Ni^{2+}/ Co^{2+}	Ni^{2+}/Cu^{2+}	Ni^{2+}/Fe^{2+}
Separation factor (β)	22	5	15

The corresponding plots on Figures 5.14 – 5.16 gives the respective elution profile of Ni^{2+}/Co^{2+}, Ni^{2+}/Cu^{2+} and Ni^{2+}/Fe^{2+} illustrated by the plots of concentration of the metal ions as a function of the fraction number collected during elution. The separation of nickel from cobalt with PIM-functionalized resin as shown in Figure 5.14 proved a

better selective adsorbent for this pair. The first nine fractions of the eluent collected contain cobalt ions predominantly while fractions 11-19 are dominantly nickel contained. The break observed in the elution profile in fractions 9-11 give credence to the effective separation of nickel and cobalt by this system and the high level of purity of the separated metals. The results obtained are further backed-up with highest separation factor of 22 obtained for Ni^{2+}/Co^{2+} (Table 5.2).

Separation of nickel from copper however shows a lower separating factor of 5 in Ni^{2+}/Cu^{2+} and the elution profile in Figure 5.15 buttresses this results. Separation of nickel from iron gave a separation factor of 15 which is a better value for this pair. This result further suggests that nickel can be separated from a synthetic leach solution containing these four metals ions since it is retained in the column due to its higher affinity for pyridylimidazole.

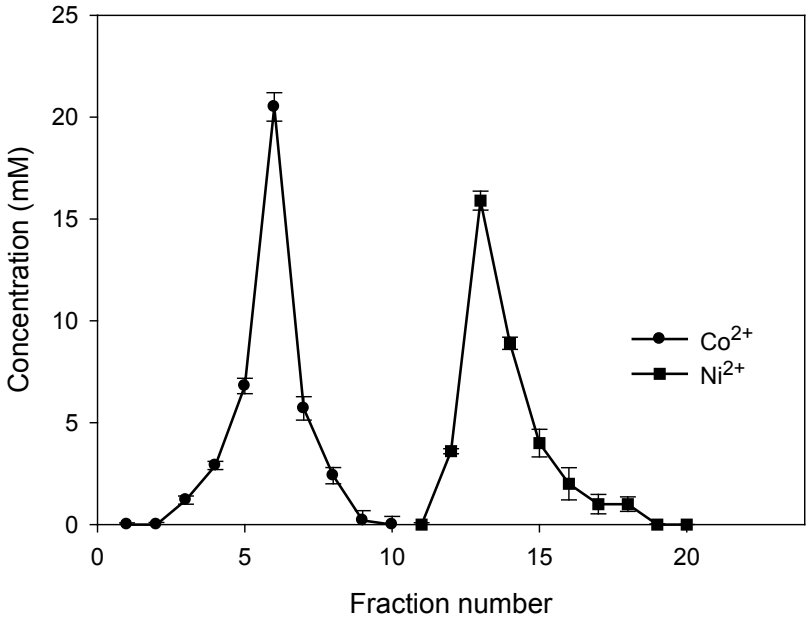

Figure 5.14: Elution profile of mixed sulfate solution of 0.02 M nickel and cobalt eluted with sulfuric acid in a binary column study

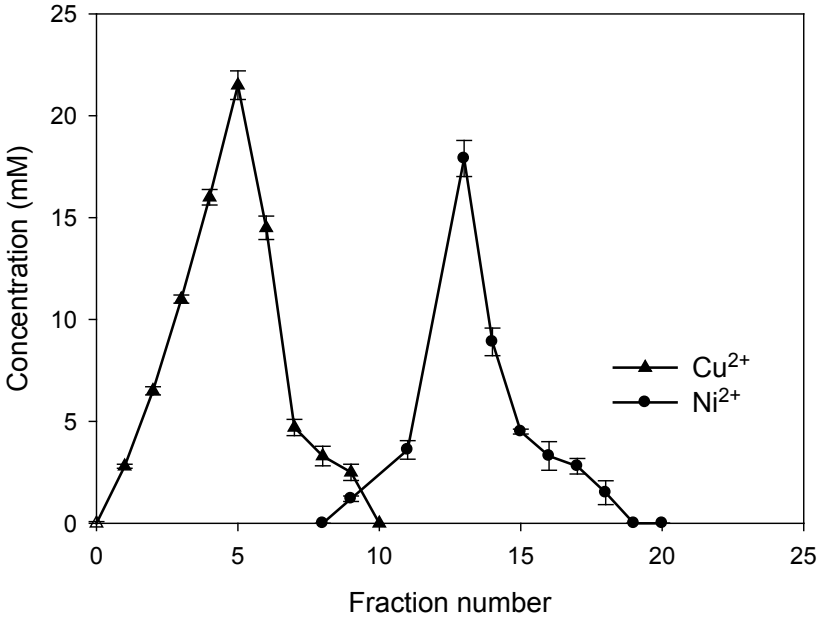

Figure 5.15: Elution profile of mixed sulfate solution of 0.02 M nickel and copper eluted with sulfuric acid in a binary column study

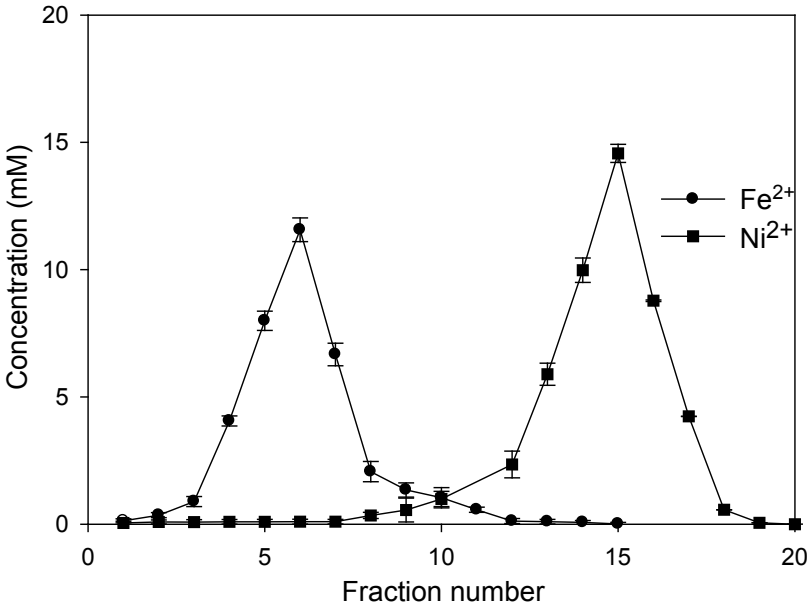

Figure 5.16: Elution profile of mixed sulfate solution of 0.02 M nickel and iron eluted with sulfuric acid in a binary column study

5.3.6 Regeneration of the resin

Regeneration efficiency was studied to determine the durability of the resin for more separations by the method of loading/regeneration/reloading for several usage. The separating efficiency of the resin was retained even after repeated processes and this was quantified as 94% efficiency of the initial capacity according to equation 49. This proves the resins to be more economical in its application as a separating material.

5.4 Conclusions

The two polymeric materials examined under this study were both found to be versatile adsorbents for the sorption of base metals owing to their high sorption capacity. The higher sorption capacity for nickel at pH of about 2 underscore the fact that even in highly acidic sulfate solution, these adsorbent can perform at reasonably high efficiency.The solid-solution system also addresses the problem of poor phase transference of the sulfate ion experienced in the solvent extraction system (discussed in Chapter 4 of this thesis). Also the separation of nickel from cobalt of the magnitude recorded in the application of the PIM-functionalized resin is considered good for this system. The high regeneration efficiency of the resin proves this process as not only economical but also environmentally friendly. Higher kinetics of cobalt ions in its sorption on the two polymers under consideration was observed. The higher surface area-to-volume ratio of the fibres as manifested in its higher loading capacity of the metals under study can be further exploited in fine tuning better separating conditions with the fibers.

References

[1] D. S. Flett, S. Afr. Patent 78/0161.

[2] J. S. Preston, J. S. Afr. Inst. Min. Metall. 83 (1983) 126-132.

[3] A. J. Monhemius, Bull. Chem. Tech. Mac.13 (1994) 7-12.

[4] A. R. Green, R. D. Hancock, J. S. Afr. Inst. Min. Metall. (1982) 303-307.

[5] L. R. Morris, R. A. Mock, C. A. Marshall, J. H. Howe, J. Am. Chem. Soc. 81 (1959) 377-389.

[6] S. D. Alexandratos, Ind. Eng. Chem. Res. (2009) 388-398.

[7] B. S. Garg, R. K. Sharma, N. Bhojak, S. Mittal, Microchem. J. 61 (1999) 94-114.

[8] B. A. Boto, L. Pawlowski, Waste Water Treatment by Ion Exchange, Chapman & Hall, New York. 1987.

[9] D. C. Sherrington, P. Hoge, Syntheses and Separations using Functional Polymers, John Wiley, Chinchester, 1988.

[10] H. P. Gregor, M. Taifer, L. Citarel, E. I. Becker, Ind. Eng. Chem. 44 (1952) 1796-1880.

[11] R. B. Merrifield, J. Am. Chem. Soc. 85 (1963) 2149-2160.

[12] K. Jinno, M. Ogawa, I. Ueta, Y. Saito, Trends Anal. Chem. 26 (2007) 27-35.

[13] D. Bilba, D. Bejan, L. Tofan, Croat. Chem. Acta 71 (1998) 155-178.

[14] Z. M. Huang, Y. Z. Zhang, M. Kotaki, S. Ramakrishna, Compos. Sc. Technol. 63 (2007) 2223-2253.

[15] M. B. Colella,S. Siggia, R. M. Barnes, Anal. Chem. 52 (1980) 967-980.

[16] C. Y. Liu, P. J. Sun, Anal. Chim. Acta 132 (1981) 353-372.

[17] M. Chanda, G. L. Rempel, React. Polym. 19 (1993) 213-225.

[18] S. Majee, C. Ray, J. Das, Ind. J. Chem. 27A (1988) 137-145.

[19] F. Helferich, Ion Exchange, McGraw-Hill. New-York, 1952.

[20] T. I. A. Gerber, E. Hosten, P. Mayer, Z. R. Tshentu, J. Coord. Chem. 59 (2006) 243-253.

[21] E. Uguzdogan, E. B. Denkbas, E. Öztürk, S. A. Tuncel, O. S. Kabasakal, J.Hazard. Mater. 162 (2009) 1073.

[22] L. Young-Seak, J. S. Im, Nanofibres (2010) 121-138.

CHAPTER 6

●●●●●

CONCLUSIONS AND FUTUREWORK

6.1 Conclusions

Bidentate N,N′-donor imidazole-based extractants in the classes of oximes and aromatic amines have been synthesised, characterised and applied as extractants for the separation of nickel and copper from other base metal ions in an acidic sulfate medium. Hydrometallurgical methods including solvent extraction, chelating ion exchange of metals on Merrifield beads and el ectrospun nanofibers were exploited in the achievement of this goal.

Dimethylglyoxime, an established nickel selective reagent was exploited in a preliminary study on the investigation of oximes as nickel selective extractant from base metals in a highly acidic sulfate medium. The study was undertaken with the extractant alone and in the presence of DNNSA as a s ynergist. The presence of highly hydrated sulfate ions prevented a meaningful extraction of the cationic complex formed with the extractant in the former case while in the latter the desired separation was not obtained.This scenario of non-selective extraction was attributed to the dominant role of DNNSA. From the results obtained in this study, it could be inferred that dimethylglyoxime is not a relevant reagent for the separation of nickel from other base metals at the low pH.

1-Octylimidazole-2-aldoxime (OIMOX), a representative of bidentate N,N′-donor imidazole based extractant was applied in the exploitation of oximes for the separation of base metal ionsfrom acidic sulfate solution. It was observed that the bidentate character of this new extractant imparts high stability of the chelates formed, and this is evident from the low M:L ratio employed in this study compared with the studies of the monodentately-operatingextractants.This imidazole-oxime with a pyridine-type character allows for the extraction of copper at low pH and with a

possibility for stripping to a satisfactory level. The extractant also readily rejects the extraction of ferric ions and other base metal impurities in the pH range of interest. The stability constants data gave evidence of the thermodynamics of complexationbeing the major driver in this separation process. The underlying coordination chemistry was thoroughly studied, and octahedral cationic complexes formed upon the interaction of this extractant with the metal ions were inferred. The stability of the extractant under these highly acidic conditions has not been investigated in this account but is recommended for future investigations of this extractant.

In an attempt to address the traditional limitations on the application of aliphatic and monodentate aromatic amines as base metal ions extractants, the application of 1-octyl-2-(2′-pyridyl)imidazole (OPIM) as a representative of bidentate N,N′ donor aromatic amine was investigated in the separation of nickel from base metal ions. These extractions were conducted in a similar synthetic acidic sulfate solution. Thus, with the approach of a synergistic solvent extraction system employed and the use of DNNSA as synergist, this study has established empirical evidence for the successful recovery of nickel from other base metals in a solvent extraction process. Contrary to the arguments that appear in the literature to the effect that the pyridyl moiety should be rendered inappropriate for these kinds of studies (due to the lack of back-extraction experienced even using highly acid solutions), it has been demonstrated that coupling this moiety with an imidazole group results in a pseudo-benzimidazole but with a chelating character that results in successful pH-metric selectivity between the metals. The relatively faster reaction of the nickel(II) ion with the pyridylimidazole moiety renders the process nickel-specific to some extent. This proves the applicability of OPIM as an efficient extractant in the separation of nickel from other base metals from an acidic sulfate medium in the presence of the hard ions which were rejected by this nitrogenous ligand. Most interesting is the ability of this extractant to reject ferrous ions, thus providing a shortened route for the recovery of nickel. It has also been demonstrated that the dilute chloride and high sulfate content do not affect the extraction patterns and efficiencies observed with pyridylimidazole in dilute sulfate solutions, respectively.

The complexation of the ligand with the metal ions Ni^{2+}, Co^{2+}, Cu^{2+} and Zn^{2+} was investigated in order to understand the underlying coordination chemistry in this

extractionsystem. The spectral analysis of the isolated complexes revealed the formation of tetrahedral complexes which was rather unusual for nickel(II). Insight was gained through time-monitored spectrophotometric titrations that the separation of nickel was kinetically driven as opposed to being influenced by stereochemichal “tailor-making”. The thermodynamic stability constants were also determined, and the pH-metric orders of the metal extraction curves were not in agreement with the order of the calculated constants thereby eliminating the thermodynamics as a driver in these separations.

Chelating ion exchange resins and electrospun nanofibers functionalized with 2,2′-pyridylimidazole were employed in the selective adsorption of base metal ions.The characterization methods employed for these adsorbents viz; scanning electron microscopy (SEM), microanalysis, infrared (IR), X-ray photoelectron spectroscopy (XPS) and Brunauer-Emmet-Teller (BET) method confirm the originality of these sorbents as funtionalized with 2,2′-pyridylimidazole.

The separation of nickel from cobalt was achieved with the resin around the pH range of 2. Other base metals including copper and iron were separated from nickel with this resin. The process was found less solvent dependent and so the phase problem as known in the solvent extraction process was never experienced. The separations obtained in the solvent extraction and the chelating ion exchange technique with with 2,2′-pyridylimidazole show a similar trend with respect to the separation of nickel from cobalt at around pH 2. Also as observed in the extraction plot in Chapter 4 (Figure 4.10) copper was not readily separated as much from nickel.

This study has successfully unravelled the potential of imidazole-basedbidentate N,N′-donor ligands as separating agents for base metals in both the liquid-liquid and solid-liquid state applications and has therefore open a wider door for further work in the design of new extactants for consideration as base metal ions separating agents.

6.2 Suggestions for future work

These imidazole-based bidentate N,N′-donor ligands (amines and oximes) employed in this study as separating agents for base metal ions in an acidic sulfate medium have proved to be efficient separating agent for nickel and copper respectively. These extractions were applied to dilute metal sulfate solutions and not upscaled to more concentrated solutions but this could be explored in future. The methods can also be applied to real industrial solutions since the study focused on developing the methods using synthetic solutions of the metals that mimic the industrial solutions.

The imidazolyl group has been successfully applied for the selective extraction of nickel(II) from base metals mainly due to the high complex formation offered by the imidazole group and it would be worthwhile to further investigate newly designed imidazole-based ligands in the search and development of separating agents for base metal ions separation. Thus, 2,2′-biimidazole (Figure 6.1a) is worth investigating as a bidentate N,N′-donor. Also a combination of a low pK_a benzimidazole with a high pK_a aliphatic amine would also be desirable for low pH interaction with the metals and higher formation constants respectively (Figure 6.1b). Another combination of imidazole with benzimidazole would also be expected to yield a similar results to 2,2′-pyridylimidazole but the difference in the π bonding capability of pyridine and benzimidazole may results in some differencies (Figure 6.1c). These combinations with differences in σ and π bonding of the nitrogenous groups should result in a systematic study for the necessary amines for these separations.

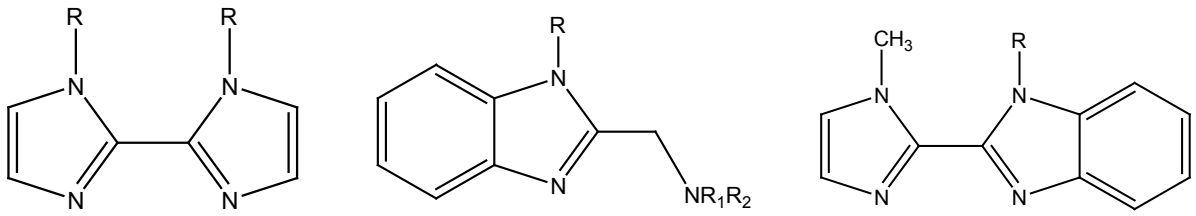

(a) (b) (c)

Figure 6.1: The chemical structures of the proposed imidazole-based extractants for future study. (a) 1,1-R,R-2,2′-biimidazole (b) 2-aminomethyl-1-R-benzimidazole, and (c) 2-(1-methylimidazol-2-yl)-1-R-benzimidazole